

SERI/CP--213-4079

DE91 002120

PHOTOVOLTAIC MODULE

RELIABILITY WORKSHOP

October 25-26, 1990

Sheraton Inn Lakewood/Lakewood, Colorado

Edited by: Laxmi Mrig (SERI)

Sponsored by
Solar Energy Research Institute
under contract to the
U.S. Department of Energy

MASTER *db*
DISTRIBUTION OF THIS DOCUMENT IS UNLIMITED

PREFACE

The papers and presentations compiled in this volume form the Proceedings of the fourth in a series of Workshops sponsored by SERI/DOE under the general theme of photovoltaic module reliability during the period 1986-1990.

The reliability of PV modules/systems is exceedingly important along with the initial cost and efficiency of modules if the PV technology has to make a major impact in the power generation market, and for it to compete with the conventional electricity producing technologies. The reliability of photovoltaic modules has progressed significantly in the last few years as evidenced by warranties available on commercial modules of as long as 12 years. However, there is still need for substantial research and testing required to improve module field reliability to levels of 30 years or more.

Several small groups of researchers are involved in this research, development, and monitoring activity around the world. In the U.S., PV manufacturers, DOE laboratories, electric utilities and others are engaged in the photovoltaic reliability research and testing. This group of researchers and others interested in this field were brought together under SERI/DOE sponsorship to exchange the technical knowledge and field experience as related to current information in this important field. The papers presented here reflect this effort.

Laxmi Mrig
Workshop Chairman
SERI

TABLE OF CONTENTS

	<u>Page</u>
Session 1: Module Performance and Field Experience	
An Update on Performance Trends at PVUSA Tim Townsend and Paul Hutchinson, Endecon; Steve Hester, PG&E	1
Module Field Experience With Austin's PV Plants John Hoffner, City of Austin Electric Utility Department	17
Performance and Reliability of a 15 KWp Amorphous Silicon Photovoltaic Array in Florida Gobind Atmaram and Bill Marion, Florida Solar Energy Center; Christy Herig, Florida Power Corporation	25
Early Experiences of the 15 kW NMPC Demand-Side Management Photovoltaic Project Bruce Bailey, Richard Perez, John Doty, Kurt Elsholz and Ronald Stewart, Associated Weather Services, Inc.; William Huse, Niagara Mohawk Power Corporation	47
Three Year Performance and Reliability Analysis of a 4kW Amorphous-Silicon Photovoltaic System in Michigan Robert Pratt, The Detroit Edison Company	53
Photovoltaic Concentrator Module Reliability: Failure Modes and Qualification Elizabeth Richards, Sandia National Laboratories	61
The World is Ready for PV but is PV Ready for the World? John Schaefer, Electric Power Research Institute	73
Session 2: Module Research and Testing	
The Use of Indoor Light Soak Data to Project End of Life Output Power of Hydrogenated Amorphous Silicon Solar Modules Dennis Cunningham and J. Morris, Solarex	79
CuInSe ₂ Module Environmental Reliability Dale Tarrant, Robert Gay, Jean Hummel, Cynthia Jensen and Al Ramos, Siemens Solar Industries	93
Reliability Studies of Eureka Modules J. Grez, J. Kolesar and Frank Kampas, Chronar Corporation	107
Encapsulation and Termination Processes for High Reliability of Thin Film Modules Gilbert Duran, UPG	121

	<u>Page</u>
Photovoltaic Power Systems and The National Electric Code John Wiles, New Mexico State University	123
Stability Results on CdS/CdTe Submodules Scot Albright and Rhodes Chamberlin, Photon Energy, Inc.	137
Factory and Field Test Experience From PVUSA Steve Hester, PG&E; Walt Stolte and Bill Clements, Bechtel; Tim Townsend and Paul Hutchinson, Endecon	145
Session 3: Module Design and Encapsulation Research	
Possible Causes of EVA Degradation in PV Modules Al Czanderna, Solar Energy Research Institute	159
Field Test Results for the 6-MW Carrizo Solar Photovoltaic Power Plant Andrew Rosenthal and Cary Lane, New Mexico State University	217
Mirror Madness John Kusianovich, Carrizo Solar Corp.	241
Solarex Experience with EVA Encapsulation John Wohlgemuth and Raymond Petersen, Solarex Corporation	247
Spire's Experience with EVA Lamination/Curing Mike Nowlan, Spire Corporation	259
Recent Generic Studies of Ethylene Vinyl Acetate (EVA) Degradation John Pern, Solar Energy Research Institute	279

Session 1:
Module Performance and Field Experience



An Update on Performance Trends at PVUSA

• **Tim Townsend and Paul Hutchinson, Endecon**
Steve Hester, PG&E

**SERI Photovoltaic Module
Reliability Workshop**

October 25, 1990



- **Background**
- **Status**
- **Performance**



PVUSA Project Objectives

- **Compare and evaluate PV systems (modules and balance of systems) for performance and reliability.**
- **Assess PV operation and maintenance costs within a utility setting.**
- **Evaluate PV systems in differing geographic areas.**
- **Provide utilities with hand-on experience.**
- **Document and disseminate the data.**



PVUSA Participants

U.S. Department of Energy

SANDIA National Laboratory

Solar Energy Research Institute

Jet Propulsion Laboratory

California Energy Commission

Electric Power Research Institute

Pacific Gas and Electric Company

**Virginia Power/Commonwealth
of Virginia**

State of Hawaii/Maui Electric

San Diego Gas and Electric

Salt River Project

New York State Energy R & D Authority

Niagara Mohawk Power Corp.

City of Austin Electric Utility Department

EMERGING TECHNOLOGY (EMT) SELECTIONS

Nominal 20 kW PV arrays

COMPANY PV MODULE TECHNOLOGY

Siemens Solar	Microgridded Crystalline Silicon
Solarex	Bifacial Poly-Crystalline Silicon
Sovonics	Tandem Junction Amorphous Silicon
UPG	Tandem Junction Amorphous Silicon
ENTECH	Linear Concentrator, Silicon Cells
Siemens Solar	Copper Indium Diselenide (CIS)
AstroPower	Polycrystalline Silicon film on ceramic substrate
Photon Energy	Cadmium Sulfide/Cadmium Telluride (Cds/CdTe)

PCU's (DC/AC Inverters) from DECC/HELIONETICS

UTILITY SCALABLE-1 PV SYSTEM SELECTIONS

<u>COMPANY</u>	<u>PV SYSTEM DESCRIPTION</u>
----------------	------------------------------

200 kW Systems:

Siemens Solar

1-Axis Passive Tracking, Flat-Plate
Siemens Crystalline Silicon
Modules, with a Dickerson Inverter
Turnkey Price = \$ 9.34/watt

Integrated Power
Corp. (IPC)

1-Axis Active Tracking, Flat-Plate
Mobil Solar Ribbon Silicon Modules,
with an Omnion 3200 Inverter
Turnkey Price = \$ 9.64/watt

400 kW System:

Chronar

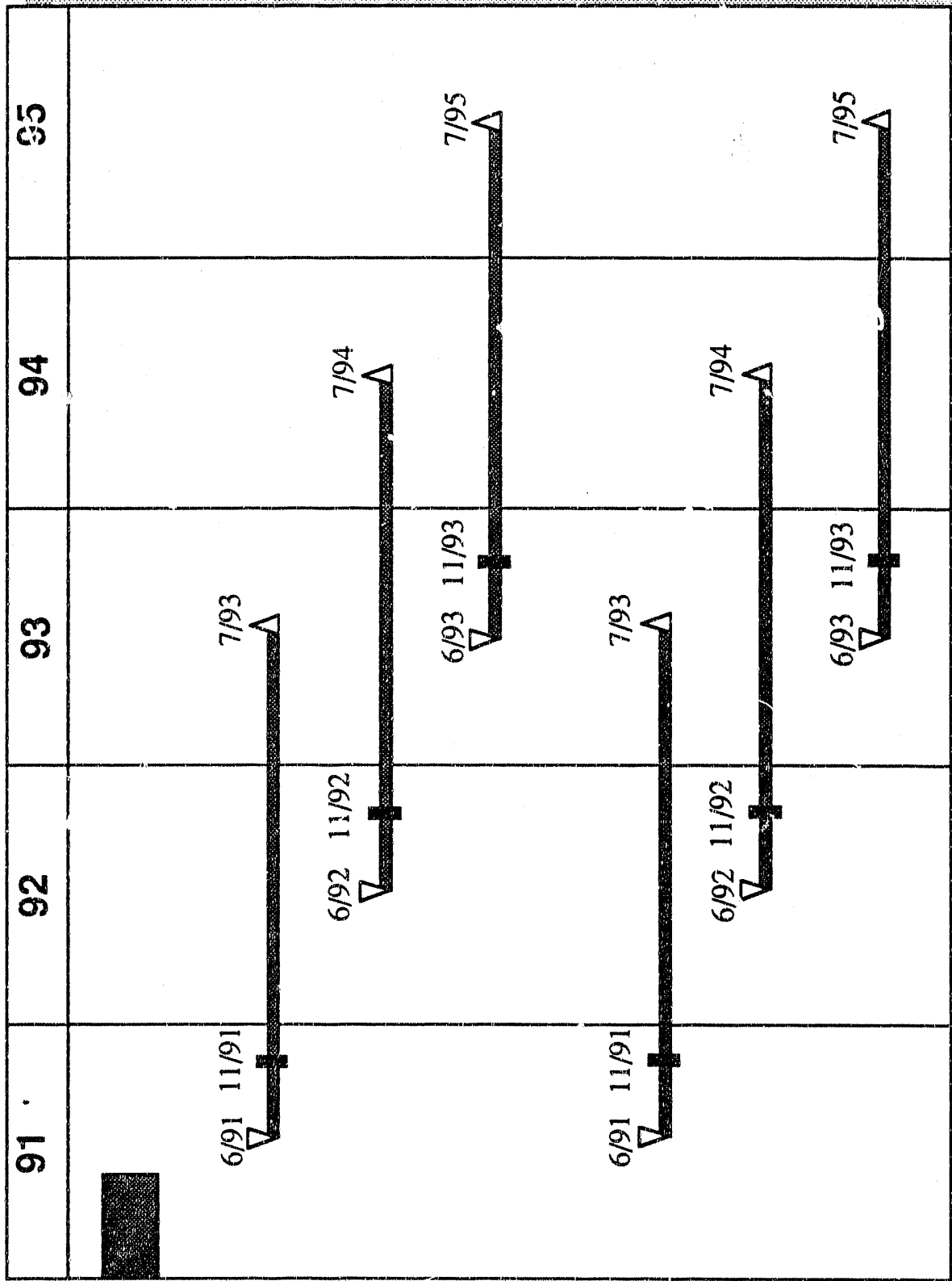
Fixed Flat-Plate, 30 degree Tilt
Amorphous Silicon Modules with
a Chronar Inverter
Turnkey Price = \$ 4.72/watt

PVUSA SCHEDULE

	1988	1989	1990	1991
4TH QTR '87	.			
PHASE ONE
EMERGING TECH SEG 1	[]	[]	[]	[]
EMERGING TECH SEG 2	[]	[]	[]	[]
DAVIS UTIL-SCAL SEG 1	[]	[]	[]	[]

----- Indicates Forecast

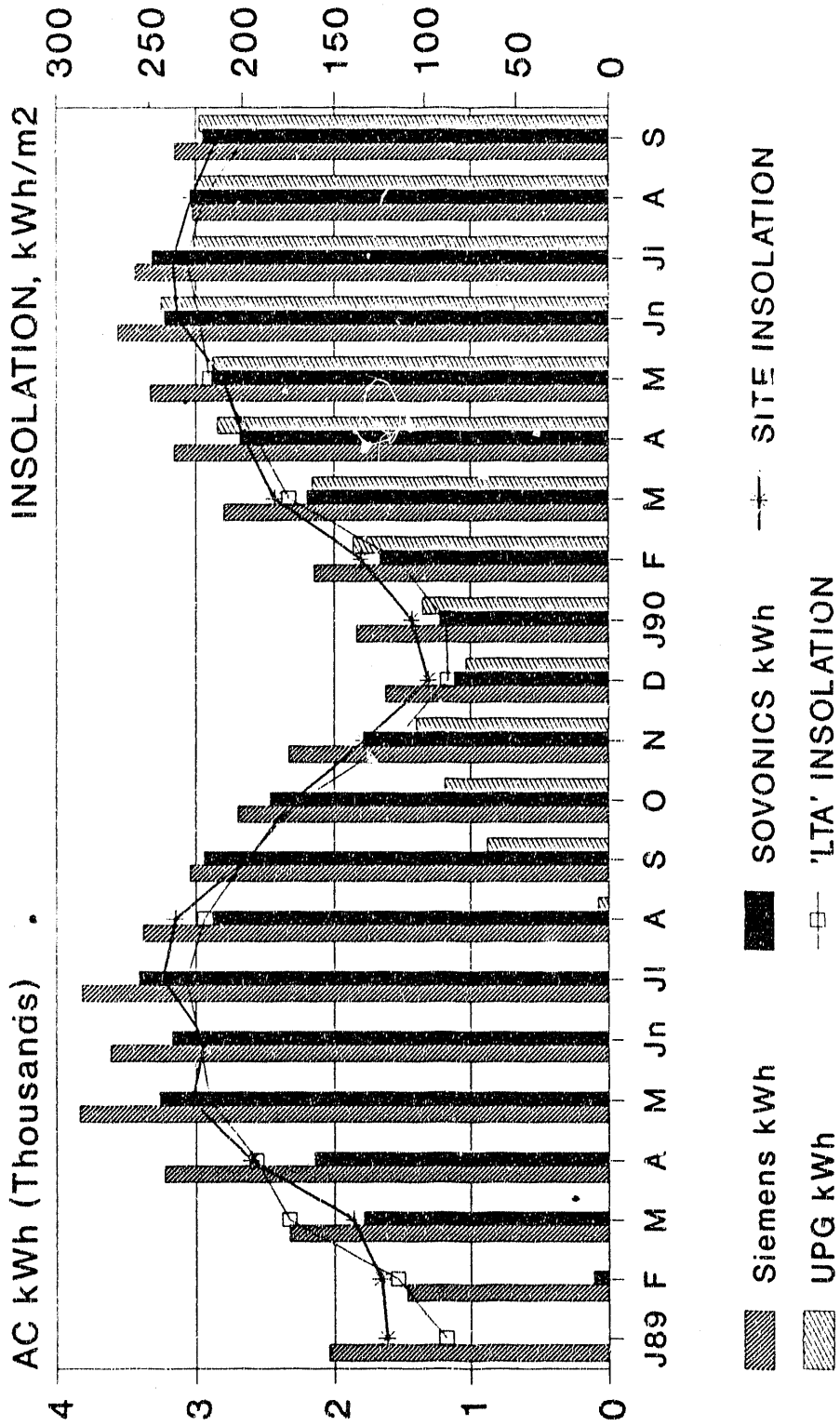
ANUSA Second Phase Schedule



▽ Issue RFP ■ Award Contract Δ Complete Installation

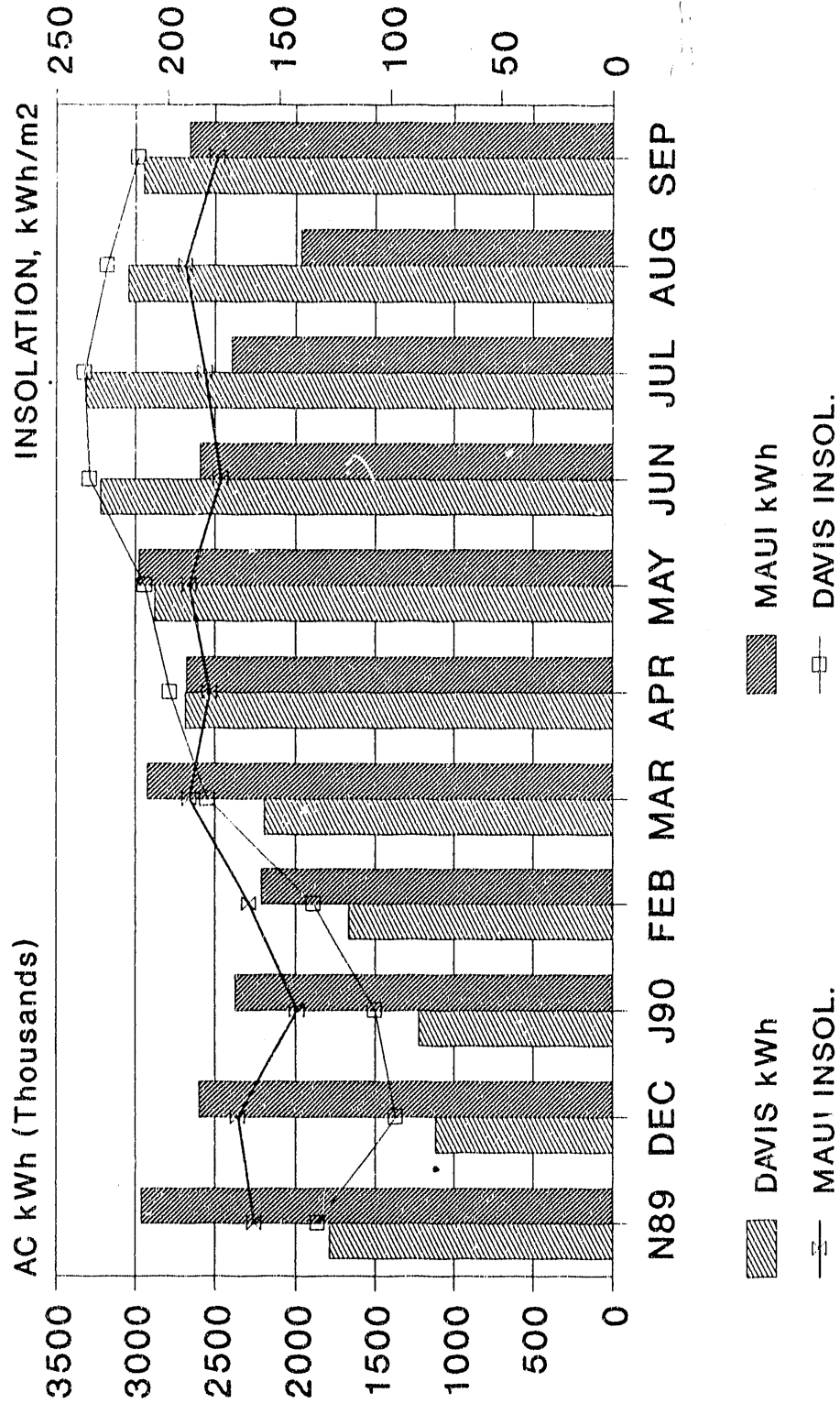
PVUSA DAVIS AC kWh AND INSOLATION

1989-90 EMT OUTPUT



'LTA': Long-Term Average
 Insolation: 30 deg. south facing surface

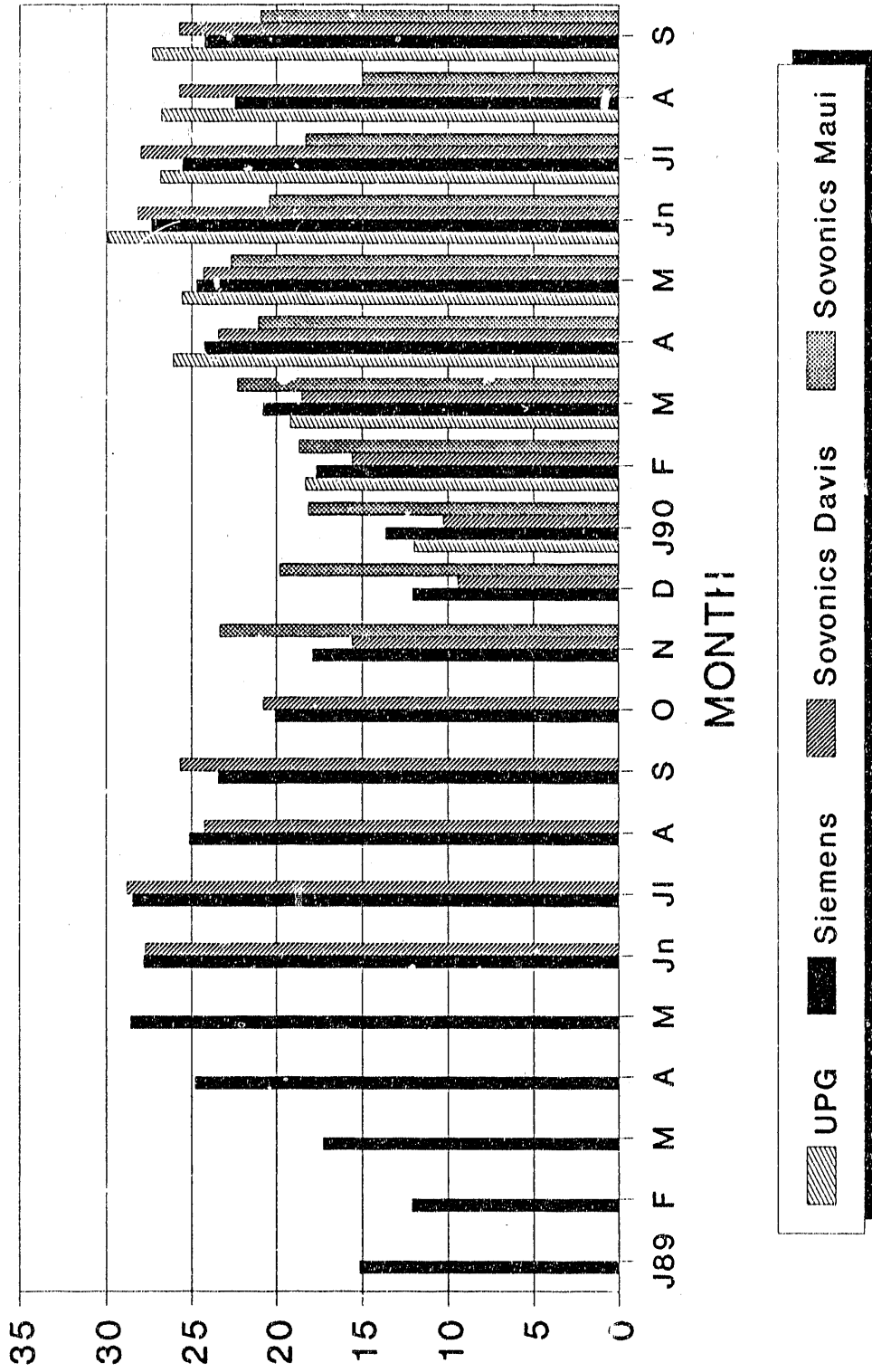
PVUSA MAUI & DAVIS SOVONICS EMT AC kWh AND POA INSOLATION



POA = Plane of Array
Tilt = 30 deg., Davis; 22 deg., Maui

PVUSA CAPACITY FACTORS

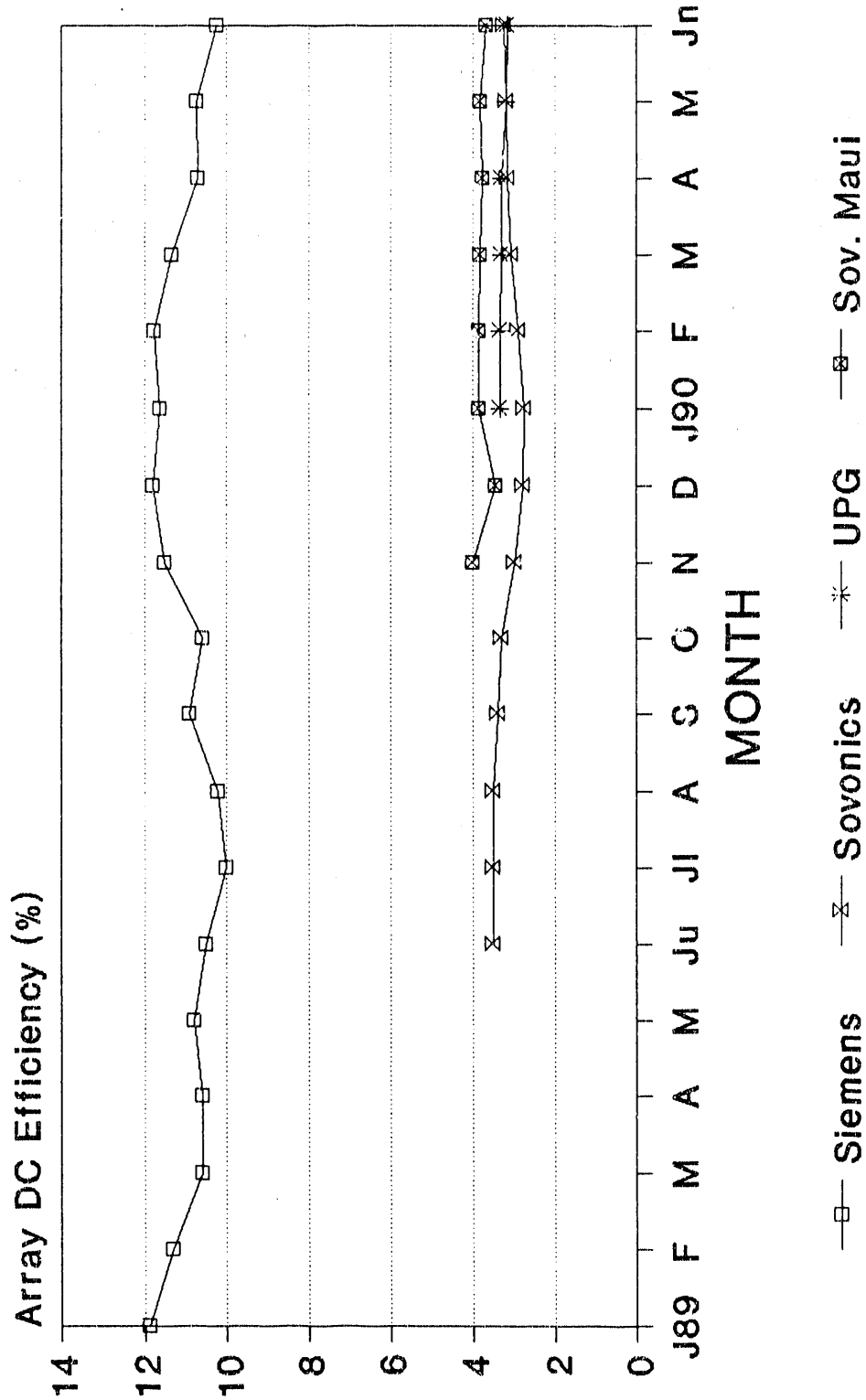
DAVIS and MAUI SITES: 1989-90



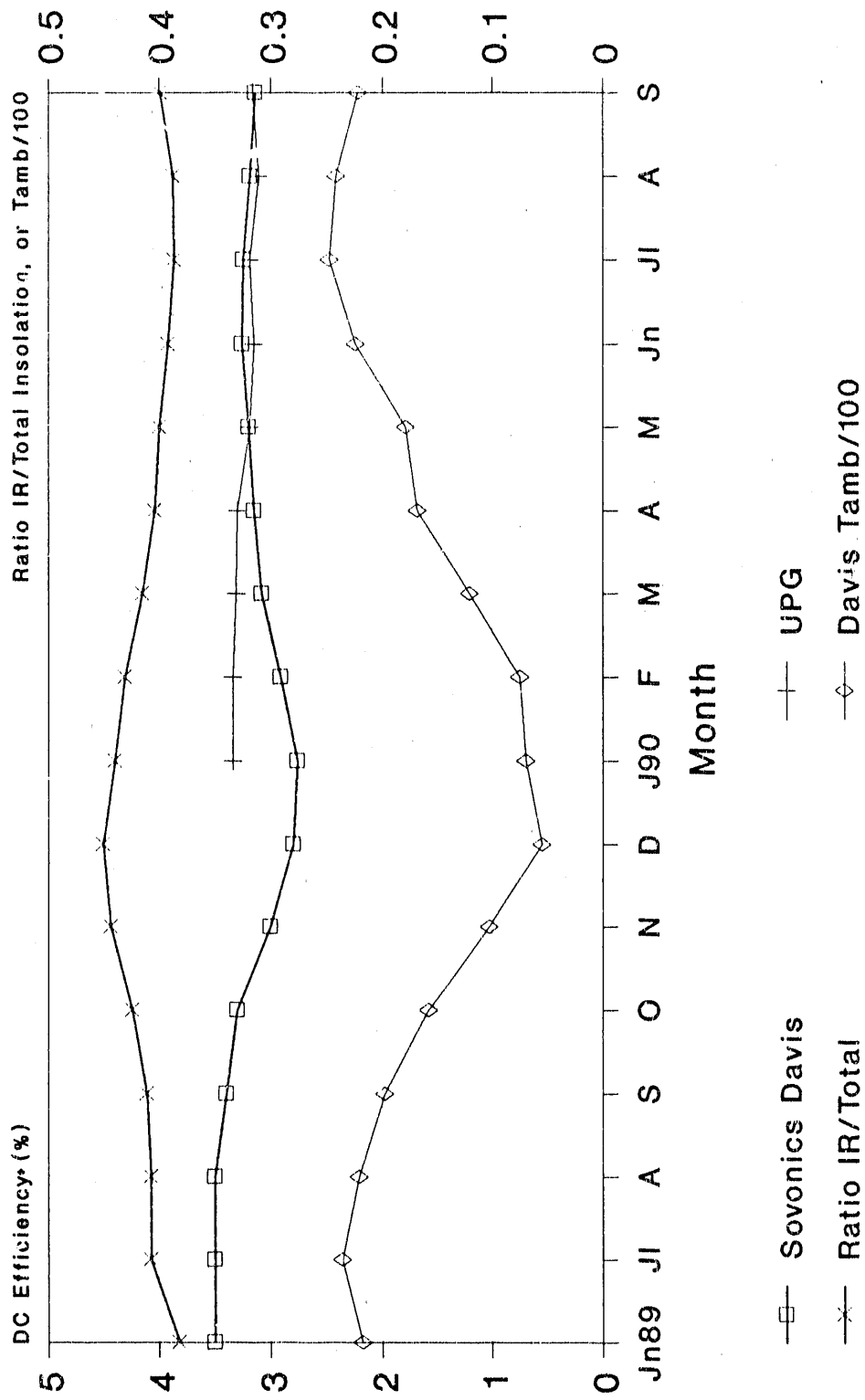
Cap.Factor= Actual Output/24hrs @ rated

PVUSA DC EFFICIENCIES

1989-90



PVUSA Davis amorphous-Si efficiency, temperature, & infrared/total insolation

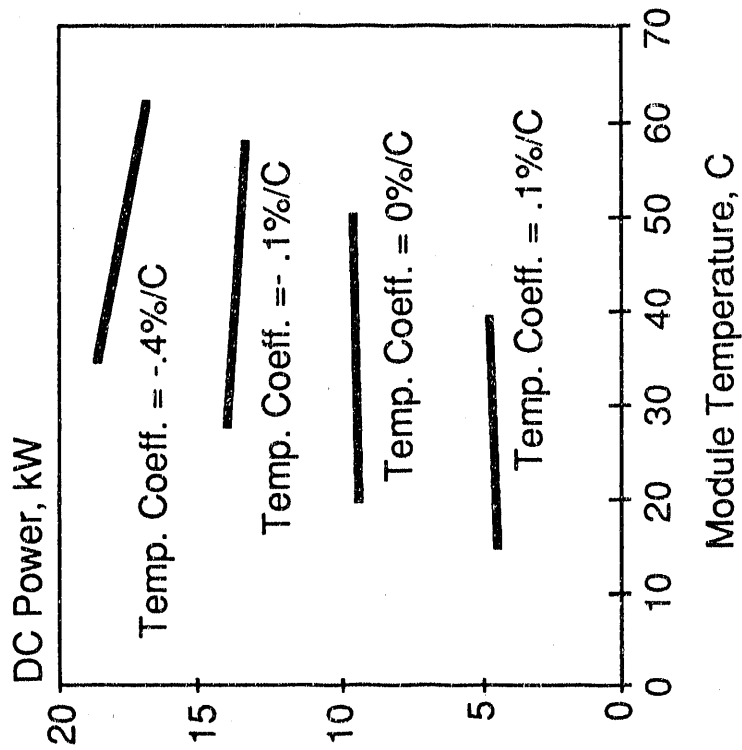


X Data	ARCO Solar	Sovonics Davis	UPG	Ratio IR/Total
J89	11.9			0.434
F	11.3			0.435
M	10.6			0.403
A	10.6			0.412
M	10.8			0.405
Jn89	10.5	3.5		0.382
J1	10	3.5		0.407
A	10.2	3.5		0.407
S	10.9	3.4		0.411
O	10.6	3.3		0.424
N	11.5	3		0.444
D	11.8	2.8		0.451
J90	11.63	2.76	3.34	0.44
F	11.76	2.91	3.34	0.431
M	11.35	3.08	3.31	0.415
A	10.69	3.15	3.3	0.404
M	10.73	3.2	3.19	0.4
Jn	10.24	3.26	3.15	0.392
J1	9.88	3.25	3.19	0.387
A	9.5	3.19	3.11	0.388
S	10.05	3.14	3.16	0.399

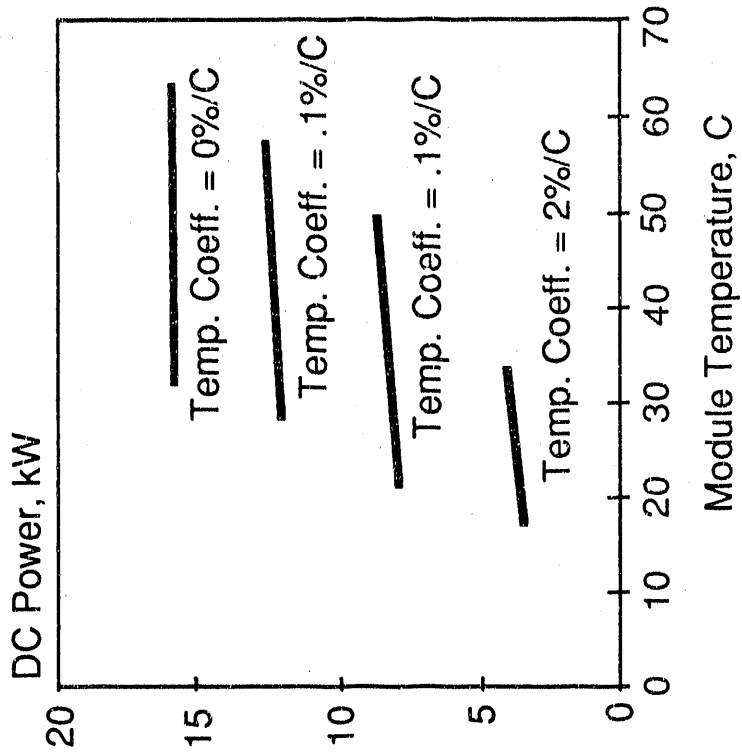
X Data	Davis Tamb/100
J89	0.06
F	0.074
M	0.121
A	0.163
M	0.186
Jn89	0.218
J1	0.236
A	0.221
S	0.198
O	0.158
N	0.103
D	0.055
J90	0.07
F	0.075
M	0.121
A	0.168
M	0.179
Jn	0.224
J1	0.248
A	0.242
S	0.222

Power vs. Module Temperature

Siemens EMT-1, May 1990



Sovonics EMT-1, May 1990

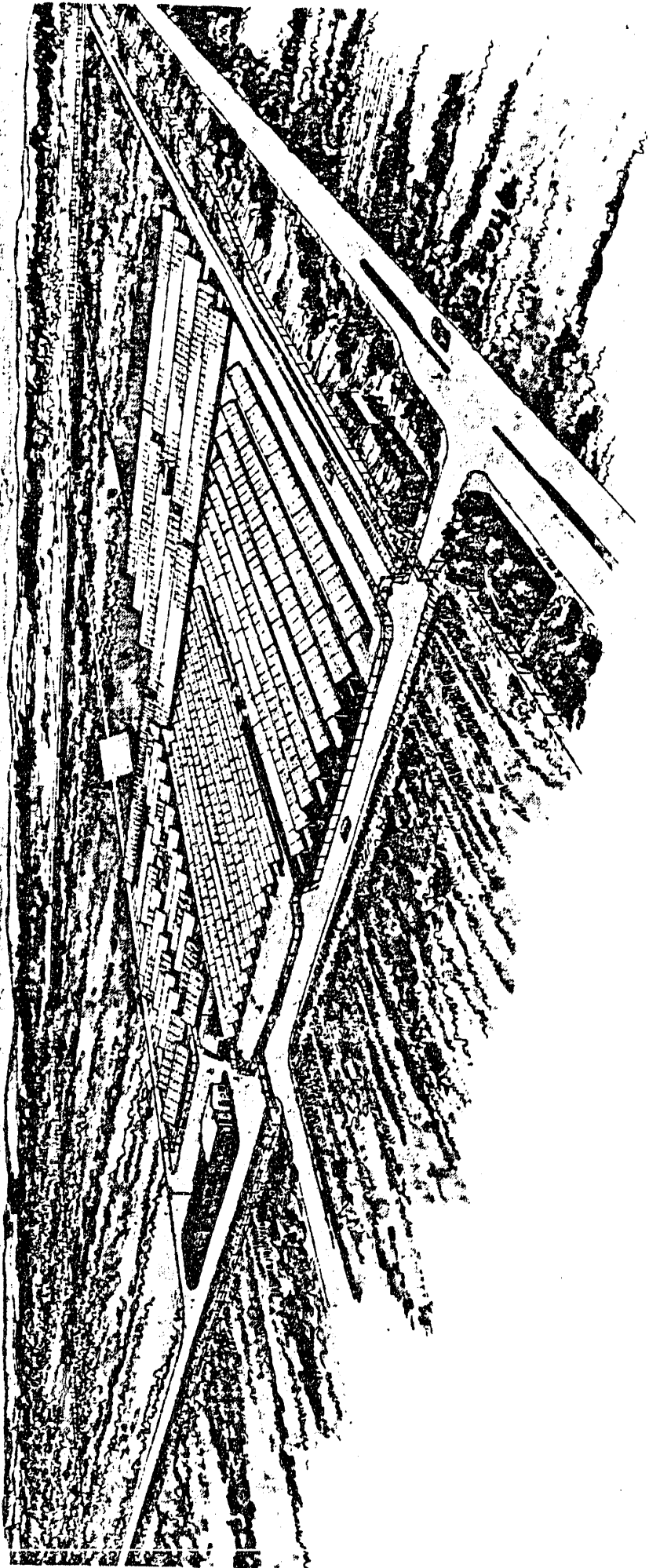


1 sun 3/4 sun

1/2 sun

1/4 sun

All irradiances are +/- 3%



PHOTOVOLTAICS FOR UTILITY SCALE APPLICATIONS (PVUSA)

(ARTIST'S CONCEPT) DAVIS SITE

PACIFIC GAS AND ELECTRIC COMPANY

Module Field Experience With Austin's PV Plants

John E. Hoffner
City of Austin Electric
Utility Department
721 Barton Springs Road
Austin, Texas 78704

1. Background

The City of Austin Electric Utility Department (The City here after) has installed two, nominal 300-kilowatt photovoltaic plants which are now being monitored and tested. The flat-plate system (PV300) was put into commercial operation in July of 1987 and it has now been monitored for three years. The concentrating system (The 3M Austin Center PV Plant) was recently dedicated in March of 1990 and is still going through adjustments and start-up procedures. The flat-plate system is fully owned by the City while the concentrator is owned 69% by 3M and 31% by the City. A comparison of the specifications and plant features is shown in Table 1. Further details on plant specifics can be found in references 1,2 and 3. The two photovoltaic (PV) plants are similar in their peak ratings, therefore it will be an interesting testing ground for comparing two, similar sized photovoltaic plants with widely varying technologies operating in one City.

The following paper discusses some of the module reliability issues that have been observed during the first three years of operation for the 300-kilowatt flat-plate system. At the time of this presentation the concentrator plant had not been fully tested and monitored for a reasonable period of time. Therefore, module reliability issues related to the concentrator plant are not discussed in this paper.

2. Description

2.1 PV300 Modules (laminates)

After all the modules (sometimes referred to as laminates because they are unframed) had been installed at the PV300 flat-plate installation in February 1987, all 6160 modules were tested using a method developed by the New Mexico Solar Energy Institute (ref 4). The objective of the tests was to identify non-producing modules in the array field. The test procedure consisted of shading up to three modules and measuring the current through the group by-pass diode, while the inverter was operating at a fixed voltage. The testing procedure identified 39 non-producing modules or a little over 1/2 percent of the modules. The low failure rate did not raise great concern, because of the low percentage compared to the field of 6160 modules. However, in

the following three months (March, April and May 1987) tests were carried out again and over 100 non-producing modules were identified, or over 1% of the field were non-functioning. Therefore, the number of failed modules appeared to be growing, and the manufacturer ARCO Solar (now Siemens Solar) assigned a task force from its factory to identify the cause for the failures and to develop a solution for avoiding future failures.

ARCO staff attributed the module failures to differential expansion of a the copper busbar which the modules were attached to and the plastic cover over the busbar. Small ribbons which exit from the (+) and (-) end of the modules, are spot welded to a copper busbar. A plastic cover is then glued to over the busbar to protect it from the elements and to prevent personnel from touching it. During manufacturing the glue that was used to attach the plastic busbar covers squeezed over the ribbons which bonded the copper busbar, the plastic cover and the ribbon all together in a continuous fashion. When the system was exposed to the heat of the sun, the copper and plastic expanded at different rates and the ribbons either sheared, or were sheared-off at the point of the spot welds. The module (laminated) then became open-circuited making it a non-producing part of the array field.

ARCO offered the solution of cutting each plastic cover to create an expansion joint therefore reducing the potential for differential expansion. By June 1987 all non-producing modules were replaced, or repaired and the expansion joints were installed. In July of 1987 when the plant was put into commercial operation it appeared that the module problem had been solved. Since that time all modules have been tested at regular intervals and it appears that the number of ribbon failures has been decreasing as shown in Figure 2. Only further testing and monitoring over the next few years will verify that the problem has been solved.

It is important to note that the failures never affected the integrity of the modules themselves, merely the exterior connection point to the busbar. Thus, the modules have been highly reliable for the first three years of operation. As noted in an earlier paper (ref 2) the plant has had an availability of greater than 99% for the first two years of operation and an average capacity factor greater than 55% during Austin's peak demand periods for electricity.

2.2 PV300 Tracking System

The flat-plate installation is fitted with a passive tracking system that utilizes 42 Robbin's Engineering tracking actuators. The actuators consist of a closed-loop system of freon and oil which tracks the sun from east to west on a daily basis. The panels are installed horizontally and rotate around a north-south axis. The trackers were installed to increase yearly output and to increase power output in the late afternoons (5 or 6 PM) in summer when the City's peak demand period occurs.

Several preliminary tests were conducted to examine the tracking accuracy of the passive actuators. A protractor was used to measure the angle of the sun's image that projected through the cracks between the modules over the course of the day. The angle measured was the angle of incidence of the sun with respect to the normal of the flat-plate panels from east to west. The incident angle with respect to the sun's azimuth angle is ignored because the panels only track in one axis.

Tracking accuracy tests were conducted on two different sunny days - August 11, 1987 and July 19, 1990 shown in Figures 3 and 4 respectively. As can be seen, the angle of incidence with respect to the normal of the panels is 10 degrees during the peak sunlight hours from 9:00 AM to 6:00 PM (CDT). This is considered to be highly effective since at 10 degrees or less only 1 to 2 percent of the sun's energy is lost due to reflected energy (cosine 10 degrees = .98). Therefore, the passive actuators are considered to be reliable for flat-plate, single-axis tracking PV systems.

During initial start-up and over the first year of operation, several tracking actuators experienced blow-outs through the cylinder seals. The problem was attributed to incorrectly installed O-rings by the manufacturer. After the first year it appeared that the problem had diminished as shown in Figure 5. However, several more failures have occurred over that past year causing some concern. The actuators will be examined and monitored over the next few years to evaluate their reliability.

Concluding Remarks

- o The reliability of the flat-plate modules has been very high with a plant availability of greater than 99% for the first two years of operation.
- o The problem of differential expansion of the busbars and plastic covers appears to have been solved due to the downward trend of module failures.
- o The integrity of the modules has been maintained throughout the plant operation.
- o Tests on the passive trackers indicate that they are capable of tracking within 10 degrees of the sun (from east to west) on sunny days during peak sunlight hours 9:00 AM to 6:00 PM.
- o The failures of the O-rings associated with the passive trackers appear to be increasing. The actuators will be closely monitored over the next few years.

References

1. J.E. Hoffner, "Analysis of the 1988 Performance of Austin's 300-Kilowatt Photovoltaic Plant", Proceedings of the 1989 Annual Meeting of the American Solar Energy Society, Denver, Co., June 19-24, 1989.
2. J.E. Hoffner, "The First Two Years of Operations for Austin's 300-Kilowatt Photovoltaic Plant", Proceedings of the 25th Intersociety Energy Conversion Engineering Conference (IECEC), Reno, Nevada, August 12-17, 1990.
3. J.E. Hoffner, C. Garcia-Velez, "Construction and Start-up of the 3M/Austin Concentrating Photovoltaic Plant", Proceedings of the 25th Intersociety Energy Conversion Engineering Conference (IECEC), Reno, Nevada, August 12-17, 1990.
4. New Mexico Solar Energy Institute, Internal report to the City of Austin Electric Utility Department, "Testing of PV300 Solar Photovoltaic Project", Testing Performed Feb. 16 and 17, 1987.

TABLE 1 COMPARISON OF PLANT SPECIFICATIONS

	<u>PV300 PLANT</u>	<u>3M/AUSTIN PLANT</u>
SYSTEM TYPE	flat-plate	linear fresnel concentrator
CELLS	single-crystal	single-crystal w/prism covers
CELL EFFICIENCY	14.5 %	17.5 %
ARRAY AREA	2620 sq. M	2006 sq. M
TRACKING	single-axis	two-axis
DESIGN RATING	272 kw AC at SOC (NOCT=46.7 C)	273 kw AC at project conditions (cell temp=60 C, 1000 w/sq M)
FIELD TEST RATING	250 kw AC at SOC	250 kw DC at project test

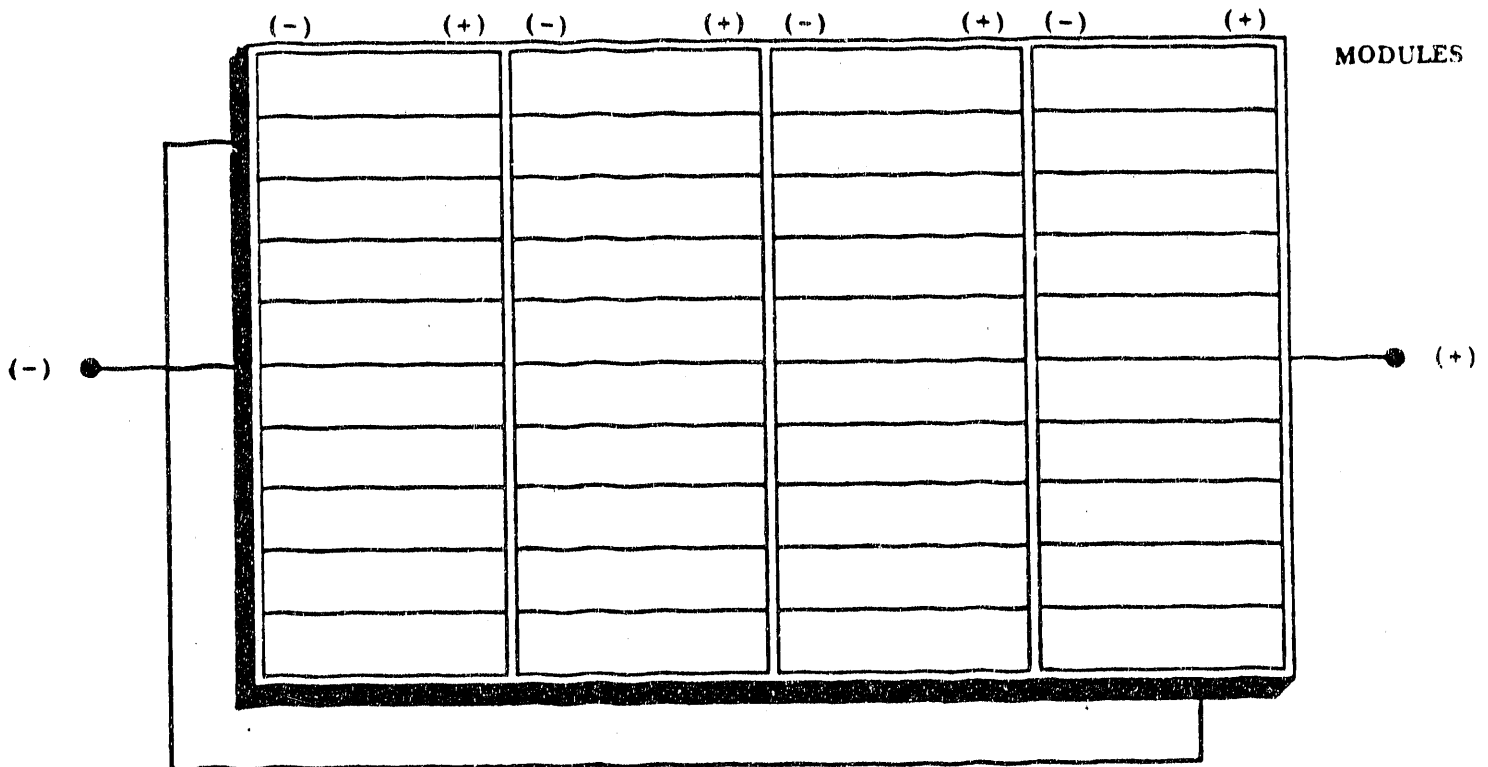


FIGURE 1 SCHEMATIC OF SOLAR PANELS

4 SETS OF 10 MODULES
IN SERIES

Forty modules, each at 53 watts, are wired together to produce the desired voltage and current. Ten modules are wired in parallel. Then 4 sets of 10 modules are wired in series to form the solar panel.

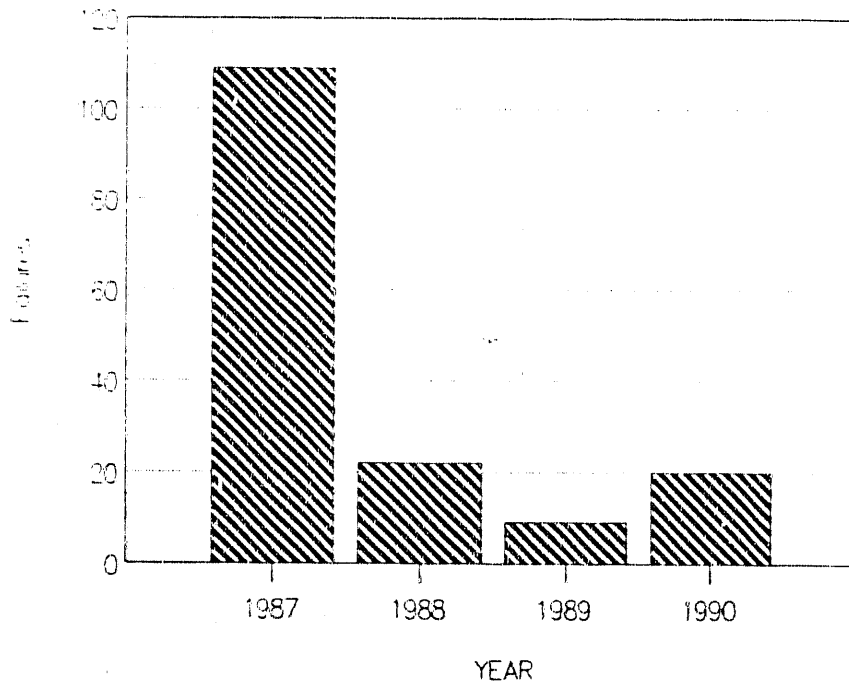


FIGURE 2 - Number of module (laminates) failures for the flat-plate system, PV300. Years 1987-1990. Total field consists of 6160 modules.

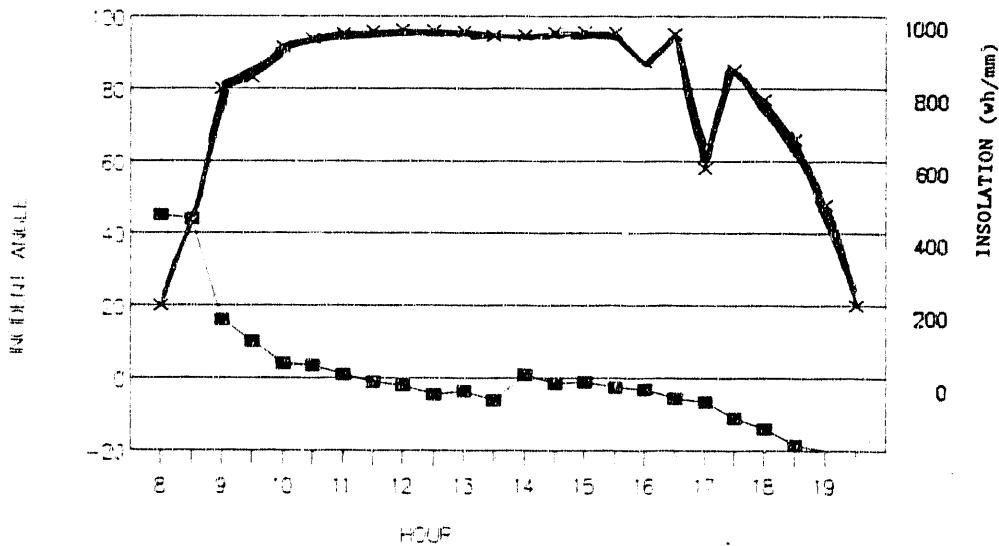


FIGURE 3 - Results of passive tracking accuracy test on flat-plate system, PV300. Test date Aug. 11, 1987.

- Incident angle (tracking accuracy angle, 0 = normal)
- x— Insolation

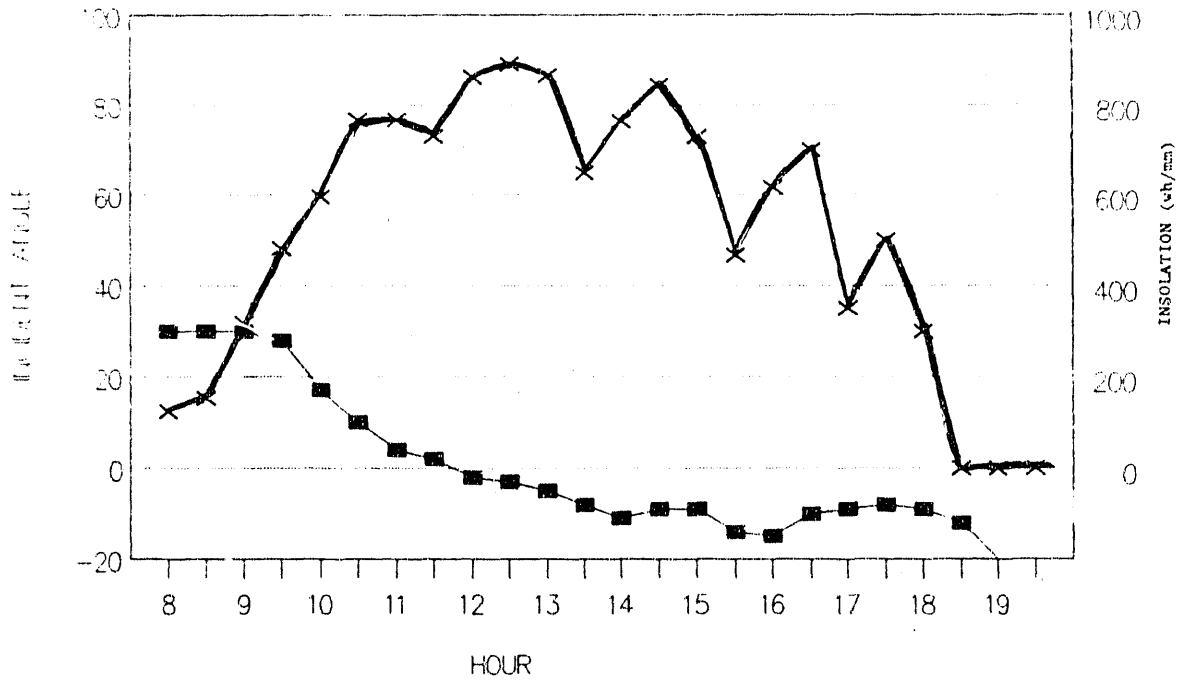


FIGURE 4 - Results of passive tracking accuracy test on flat-plate system, PV300. Test date July 19, 1989.

- Incident angle (tracking accuracy angle, 0 = normal)
- ×— Insolation

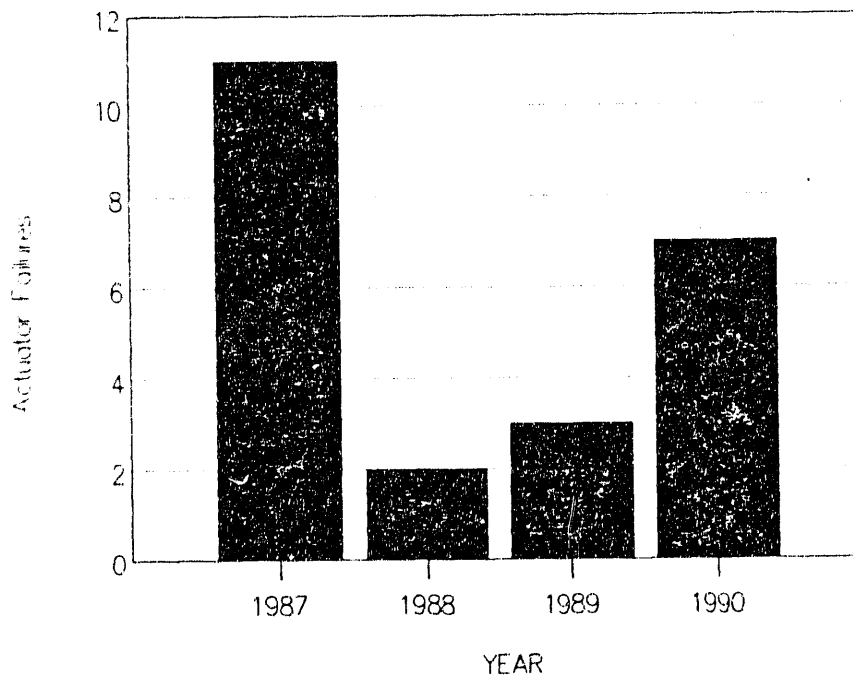
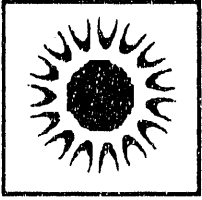


FIGURE 5 - Number of passive actuator failures for the flat-plate system, PV300. Years 1987-1990. Field consists of 42 passive actuators.



Performance and Reliability of a 15 kWp Amorphous Silicon Photovoltaic Array in Florida

**Gobind H. Atmaram, Ph.D
and Bill Marion, P.E.
Florida Solar Energy Center**

**Christy Herig
Florida Power Corporation**

Scope

- Project and system description
- Array power degradation and efficiency variation for two year period
- Module failures
- Leakage currents
- Module corrosion
- Further tests for leakage currents
- Conclusions

Objectives

- **To evaluate performance, power degradation and reliability of amorphous silicon in a grid-connected system representative of a utility scaleable application.**
- **To provide Florida Power Corporation with first hand experience on photovoltaic system installation, operation and maintenance.**
- **To implement low-cost array installation techniques, and fault protection and fault-tolerant features in the system electrical design.**



Project participants and roles

- **Florida Power Corporation**
 - System owner.
 - System installation and operation.
 - Grid interconnection design.
 - Provided funds for purchase of modules.
- **Florida Solar Energy Center**
 - System design.
 - Technical assistance in module selection and procurement.
 - Balance of system (BOS) components procurement and integration in system design.
 - Instrumentation, system monitoring and diagnostics.



Project participants and roles cont.

- **Sandia National Laboratories**
 - Provided power conditioners and data acquisition system.
 - Provided funding for BOS components.
 - Provided project review.
- **Electric Power Research Institute**
 - Provided funding for instrumentation, system monitoring and diagnostics.

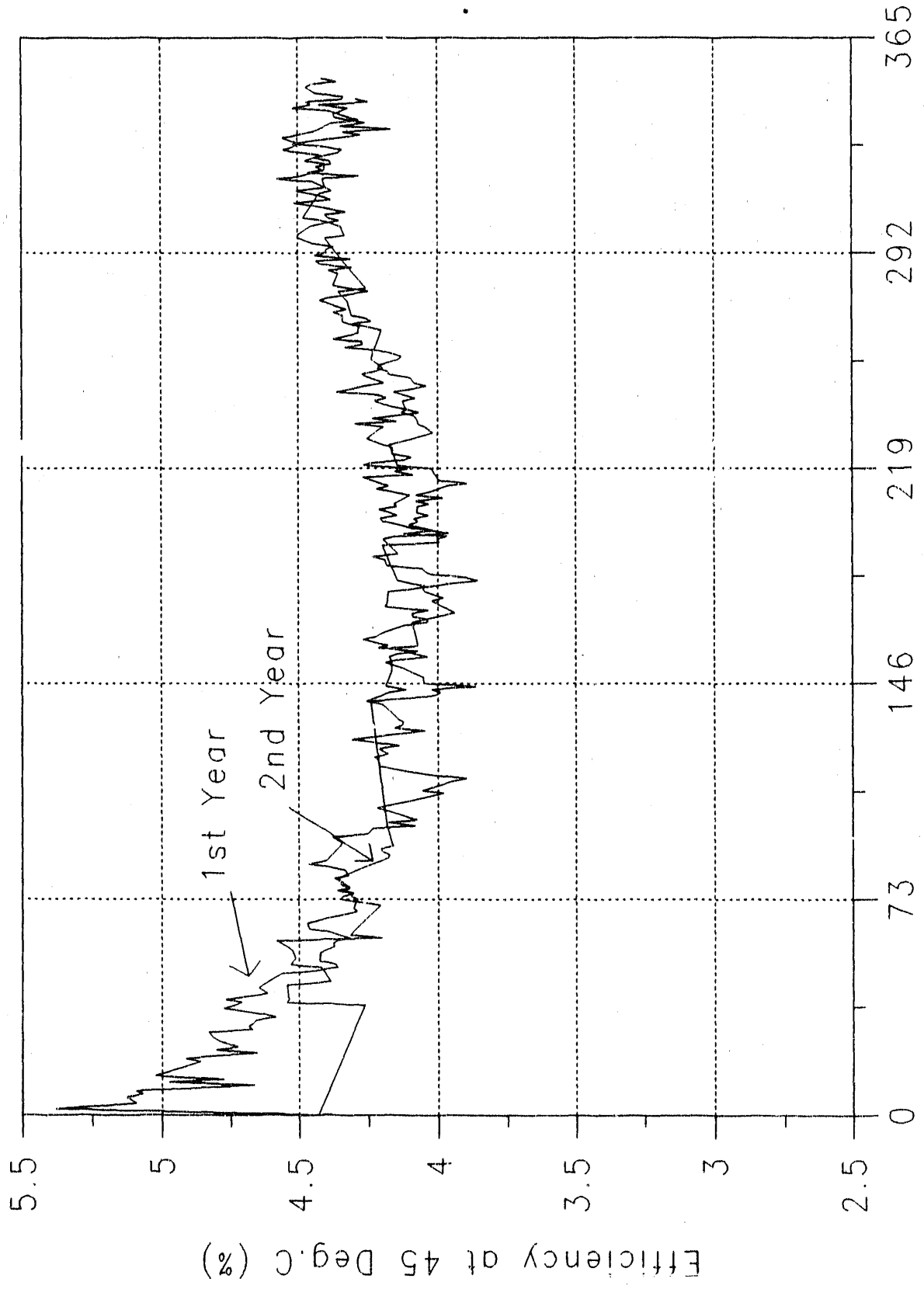
Solar progress system characteristics

First year's configuration	Second year's configuration
<ul style="list-style-type: none"> • Ground mounted fixed array at 25° tilt in five rows. • Three arrays with total 14.6 kWp, 624 ARCO G4000 modules. • Six source circuits, each with 13 panels in series. Two source circuits per array. • Three single-phase power conditioners, 5 kW each. • Grid-interactive system. 	<ul style="list-style-type: none"> • No change. • One array 15 kWp, 640 ARCO G4000 modules. • Five source circuits, each with 16 panels in series. • One three-phase 15 kW power conditioner. • No change.



Data analysis

- Hourly data between 10:00 AM and 2:00 PM EST used.
- Data only with irradiance greater than 800 Watts/m² used.
- For each day hourly data quantities corresponding to array temperature closest to 45° C selected.
- Selected data normalized to 1000 Watts /m² irradiance and 45° C array temperature.



Exposure Time (Days)

Efficiency at 45 Deg.C (%)

Array performance determined from I-V curve measurements

Date	Number of days of exposure	Array power rating P_p (kilowatts)*	Fill factor	Power degradation (%)	Peak power efficiency (%)*
Array configuration with 624 modules					
08/23/88	1	17.4	0.63	—	5.3
10/14/88	53	14.5	0.56	16.5	4.4
11/10/88	80	14.4	0.56	17	4.4
12/06/88	106	14.0	0.55	19.5	4.3
02/03/89	165	13.9	0.56	20	4.3
04/28/89	249	13.9	0.55	20	4.3
08/03/89	346	14.6	0.56	16	4.5
Array configuration with 640 modules					
08/17/89	360	15.0	0.55	16	4.5
11/02/89	437	14.3	0.55	20	4.3
12/15/89	480	13.6	0.53	24	4.1
04/04/90	590	13.3	0.53	25	4.0

* Values are calculated at Standard operating Conditions of 1000 Watts/m² irradiance and 45°C array temperature. No corrections are made for spectral distribution of solar irradiance.



Replacement of Modules

Number of Modules	Cause	Replacement Date
1	High leakage current	August 23, 1988
4	Hairline cracks	October 6, 1988
2	Shattered glass cover	February 3, 1989
1	Broken glass cover	October 31, 1989



Module corrosion

Source circuits/row	Number of corroded modules
1	8
2	8
3	2
4	1
5	5



Measured leakage currents of source circuits

Source circuit	A. Dry conditions (Measurements on 11/08/89)		B. Wet conditions (Measurements on 02/28/90)	
	Positive lead to ground (milli-amperes)	Negative lead to ground (milli-amperes)	Positive lead to ground (milli-amperes)	Negative lead to ground (milli-amperes)
1	0.35	-0.36	16.0	-15.5
2	0.27	-0.49	2.8	-8.4
3	0.30	-0.10	1.2	-0.32
4	0.08	-0.02	0.18	-3.5
5	0.28	-0.19	2.3	-5.2



Wet insulation resistance test Method

- Similar to SERI Interim Qual. Test 4.5 modified for field application
- Conducted on 16 panels and 8 individual modules
- Meggar applied voltage of 300 VDC



Wet insulation resistance test Method cont.

- Module wetted with tap water containing 0.1 percent Triton X-100 surfactant
- Simulates conditions for high leakage current, when modules wetted
- Resistance measured between panel/module terminal leads and frame



Wet insulation resistance test Results

Panels

- Measured resistance values under wet condition: $6.0k\Omega$ to $50M\Omega$
- Recommended value is $12M\Omega$ or higher
- 3 panels out of 16 showed an acceptable resistance under wet condition



FSEC

Wet insulation resistance test

Results cont.

Panels

- 6 panels indicated lower resistances even under dry condition than the recommended value
- Panels with corroded modules generally showed lower resistances

GA-590



Wet insulation resistance test Results cont.

Modules

- Measured resistance values under wet conditions: 1.0 M Ω to 300 M Ω
- Recommended value is 100 M Ω or higher



Conclusions



Array performance

- Array power degraded by 25% during 20 months of exposure, with majority of degradation due to decrease of fill factor.
- Light-induced degradation appears to be nearly stabilized within 6 months of exposure.
- In addition to the light-induced degradation array peak power varies due to seasonal, spectral, and dirt accumulation effects, which are temporary and reversible.



Module reliability

- **Out of 640 modules, only 3 modules have actually failed.**
- **Significant problems are high leakage currents and corrosion of modules. Out of 640 modules, 24 have shown corrosion build-up.**



Acknowledgements

**This work was supported by
Electric Power Research Institute
Palo Alto, CA**

**and
Sandia National Laboratories
Albuquerque, NM**



Early Experiences of the 15 kW NMPC Demand-Side Management Photovoltaic Project

Bruce Bailey, Richard Perez, John Doty, Kurt Elsholz, Ronald Stewart
Associated Weather Services, Inc.
55 Colvin Avenue
Albany, New York 12206

and

William Huse
Niagara Mohawk Power Corporation
300 Erie Boulevard West
Syracuse, New York 13202

Summary - The Niagara Mohawk Power Corporation has begun operation of a photovoltaic system in upstate New York to study the summer peak load reduction capability of grid-connected PV systems serving commercial buildings. The roof-retrofitted system consists of 151 m² of polycrystalline silicon module area rated at 15.4 kW DC, three one-axis trackers, and a high efficiency power conditioning unit. Preliminary results from the first two months of operation indicate PV system output is at a high fraction of capacity when the building experiences its electrical demand peaks. Ongoing studies are evaluating a cross-section of commercial customer load profiles in terms of the probability of peak demand reduction.

Introduction

The Niagara Mohawk Power Corporation (NMPC) has designed and installed a roof retrofitted 15.4 kW (DC) PV system in upstate New York for the purpose of evaluating the summer peak load reduction capability of grid-connected PV systems serving commercial buildings. Theoretically, photovoltaics are well-suited to demand-side management (DSM) because the availability of insolation coincides well with the typical daily electrical demand curve of commercial customers. For a minimum 15-month period, the project will study the practical and technical aspects of PV system operation, including issues dealing with reliability, power quality, load matching, need for storage, and maintenance. Ultimately, the potential benefits of PV-based DSM systems, both to the utility and to the customer, are to be evaluated for various types of commercial customers and for other areas of the NMPC service territory where weather conditions may vary from those at the project site. This paper presents preliminary performance results from the first two months of operation, July and August 1990.

System Description

The PV system consists of: 70 Mobil Solar Ra180 modules (151 m² collector area) having a combined rating of 15.4 kW DC at standard test conditions, three single-axis tracking frames (with horizontal N-S axis) each with a SunSeeker tracker drive made by Robbins Engineering, and the new high-efficiency Series 3200 Omnion power conditioning unit (PCU) which features automatic maximum power point tracking. The PCU outputs to an existing 480V 3-phase electrical distribution panel within the host building.

A dedicated PC-based data acquisition system, which includes a Campbell Scientific 21X datalogger and two multiplexers, polls 50 sensors every 10 seconds, stores 10-minute averages and runs preliminary data validation routines. Measurement parameters include: array output, array temperature and orientation, PCU performance, customer demand, and weather and insolation conditions. A harmonics measurement system capable of recording up to the 100th harmonic measures inverter voltage and current output for one cycle every 10 minutes.

The host building is the headquarters of the New York State Division of Military and Naval Affairs located adjacent to the Albany County Airport. This state-owned facility is primarily an office building that experiences a Monday to Friday midday electrical demand peak. The facility's peak demand is approximately 560 kW compared to a base load of about 325 kW. The PV system capacity was determined prior to building selection and thus represents a scale model of what this particular facility could accept.

Early Results

Acceptance tests were conducted to verify that minimum system specifications were met. The specifications included the following:

- a) 15 kW DC output ($\pm 5\%$) at 1000 W/sq. m. at 25°C panel temperature.
- b) Total system efficiency near full load $\geq 90\%$.
- c) PCU power factor ≥ 0.95 under rated array output conditions and ≥ 0.85 at 25% of rated output.
- d) Total harmonic distortion (THD) for current $\leq 5\%$; Individual harmonic distortion $\leq 3\%$; THD voltage $\leq 3\%$; Single frequency distortion $\leq 1\%$.

These and other tests (e.g., inverter start-up, stand-by operation, maximum power point tracking) found the system to be in compliance with original specifications. The stability of system and component performance will be monitored for the duration of the project. PV system availability during the first two months of operation exceeded 90 percent.

Five Ra30 Mobil Solar panels underwent indoor and outdoor performance tests at SERI's PV Module Testing and Performance Facility. The purpose for testing was to establish benchmark module performance characteristics prior to extended exposure tests at the project site. The Ra30 modules, one-sixth the size in aperture area of the Ra180 modules, are being used for testing purposes

because of the logistical constraints posed by the larger Ra180 modules in shipping and indoor testing.

Figure 1 illustrates average diurnal system output for July-August in terms of theoretical DC, measured DC, and measured AC. The theoretical DC power (top curve) is calculated from measured plane of array insolation and manufacturer's output specifications adjusted for operating panel temperature. The actual DC output (middle curve) is measured at the PCU. This curve's lower value relative to the theoretical curve is attributed to several factors, including measurement uncertainty, line losses, module mismatching, and imperfect maximum power point tracking by the PCU. The last factor is found to be the dominant effect for low insolation conditions; Figure 2 shows that the ratio of measured to theoretical DC deteriorates markedly at low insolation levels. The lower curve in Figure 1 reflects the DC-AC conversion efficiency of the PCU. Near full load conditions, the PCU efficiency is approximately 93%.

The average demand reduction during the day for the July-August period as a result of the PV system is depicted in Figure 3. The upper curve defines the building's diurnal demand on the utility without the PV system while the lower curve shows building demand with the addition of the PV system sized 10 times larger than the present scale model system. The difference between the two curves represents the average demand reduction value of the PV system.

Perhaps of greater interest is PV system performance at the times of the building's peak loads. To the user, a DSM PV system offers the benefits of demand charge savings which are a function of the system's output when the peaks occur. A comparison of PV system performance with peak building loads is shown in Figure 4. PV system output expressed as a fraction of its rated AC capacity is shown for the times when the top 5, 10, 25, 50 and 100 building loads (10-min. average) occurred in July and August. This analysis shows that PV system output is consistently high when it is most needed. Future analyses will be evaluating PV system output during the utility grid's demand peaks. Figure 4 also illustrates the importance of the selected system rating reference. System availability at peak times is shown in terms of 1) AC output vs. estimated system capacity at 30°C ambient temperature and 1000 W/m² insolation, 2) AC output vs. estimated AC capacity at standard conditions (25°C panel temperature, 1000 W/m²), and 3) AC output vs. DC rated capacity at standard conditions. For the present type of summer peak shaving application, the first rating may be the most appropriate measure because the ambient temperature is around 30°C when the building's highest peaks occur.

Future Plans

The results presented here are based on only the first two months of a planned 15-month monitoring program and thus are preliminary. Pending analyses will address overall system and individual component performance, maintenance requirements, power quality, and the probability of peak demand reduction. The value and sizing of storage will also be evaluated for maximizing the probability of energy availability at peak demand. An actual battery storage system may be added to the project. We also intend to validate widely used PV simulation programs such as PVFORM and evaluate their suitability for system design within NMPC's service area.

Whereas this project is sited at one individual building, the objective is to evaluate the DSM value of PV systems used by the commercial customer sector in general. Therefore, time series load data are being obtained from a cross-section of commercial customer types and geographical areas within NMPC's service territory (comprising half of New York State's total land area). We intend to evaluate the value of distributed PV systems to the utility in terms of net demand reduction during peak periods.

Acknowledgement: This project is sponsored by the Niagara Mohawk Power Corporation (Contract No. EW73889ABR) and the Empire State Electric Power Research Institute.

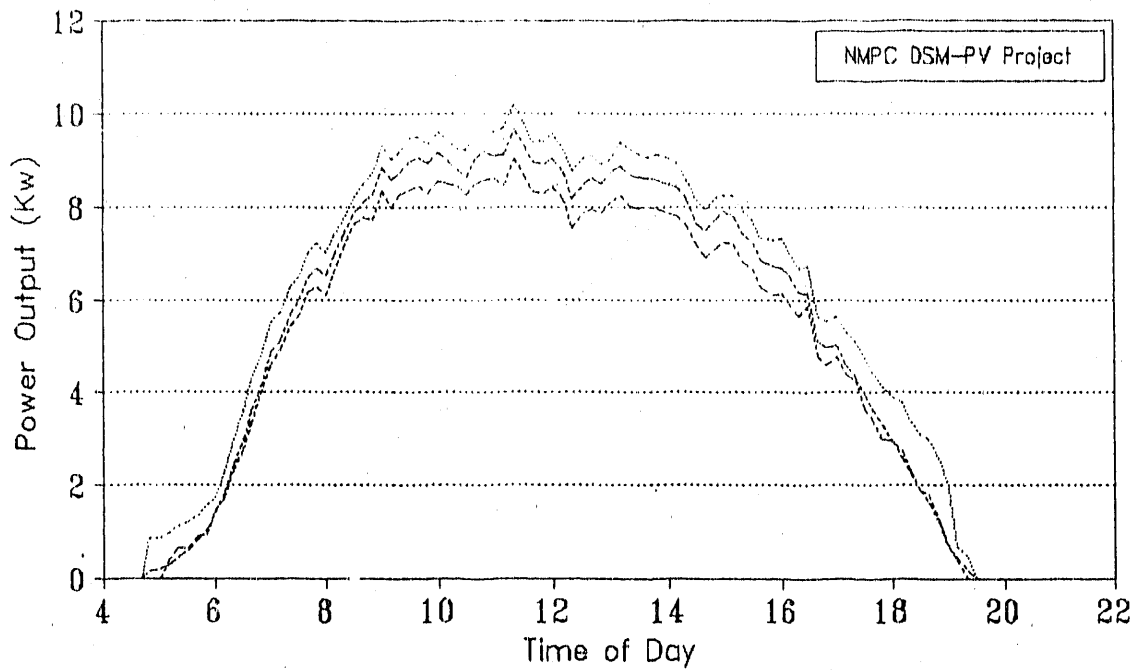


Figure 1 - Average PV system power output for July-August 1990 expressed as 1) theoretical DC determined from plane of array insolation and adjustments for panel temperature (top curve), 2) measured DC (middle curve), and 3) measured AC (bottom curve).

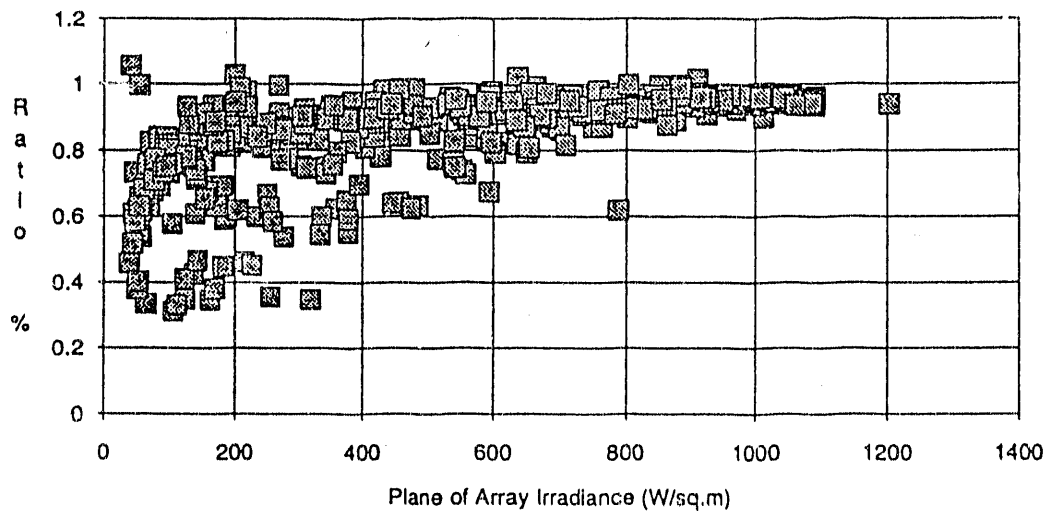


Figure 2 - Ratios of measured to theoretical DC power output based on 10-min. averages in July 1990.

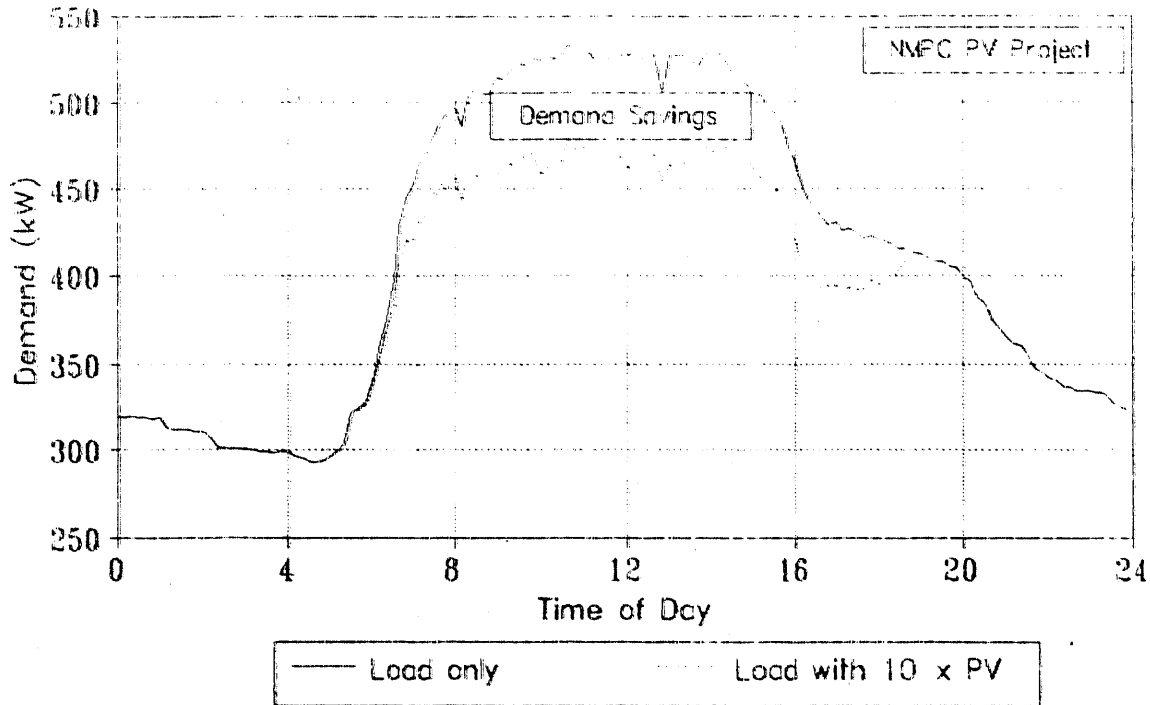


Figure 3 - Average building demand reduction for July-August 1990 due to the addition of PV system scaled 10 times larger in capacity than existing system. Upper curve defines building demand on the utility grid without the PV system; lower curve defines building demand with the PV system.

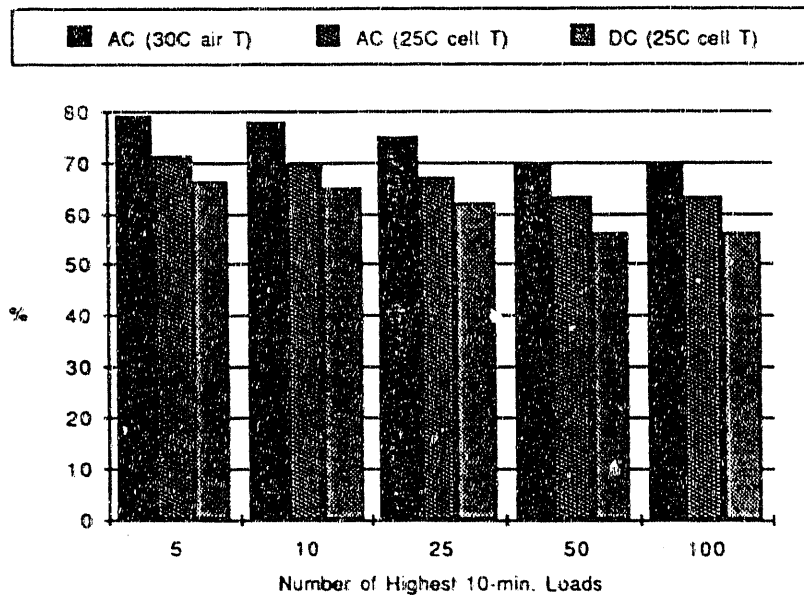


Figure 4 - PV system capacity ratios (%) for three reference ratings during the building's highest 5, 10, 25, 50 and 100 10-min. loads in July-August 1990. Reference ratings are 1) AC output vs. estimated system AC capacity at 30°C ambient temperature and 1000 W/m² insolation, 2) AC output vs. estimated AC capacity at 25°C panel temperature and 1000 W/m², and 3) AC output vs. 15.4 kW DC rated capacity at standard conditions.

THREE YEAR PERFORMANCE AND RELIABILITY ANALYSIS OF A 4 kW AMORPHOUS-SILICON PHOTOVOLTAIC SYSTEM IN MICHIGAN

ROBERT G. PRATT

The Detroit Edison Company
2000 Second Avenue
Detroit, Michigan 48226
U.S.A.

Presented at
Photovoltaic Module Reliability Workshop
Lakewood, Colorado

October 25, 1990

SUMMARY

A 4 kW photovoltaic power system composed of 144 Sovonics R100 amorphous-silicon alloy modules was constructed in southeastern Michigan in early 1987. During more than three years of continuous operation, the system and its components have been reliable and durable. Analysis of array performance has shown initial degradation, followed by stabilization. Cyclic efficiency variations have been found to be related to solar spectrum, ambient temperature and past history of temperature.

INTRODUCTION

This project was initiated as a joint venture between three electric utilities, a photovoltaic manufacturing company, two research oriented organizations and an educational institution specializing in alternate energy technologies. The Consortium, led by The Detroit Edison Company (Detroit, MI), also consists of Consumers Power (Jackson, MI), The Board of Water and Light (Lansing, MI), Energy Conversion Devices/Sovonics Solar Systems (Troy, MI), Oakland Community College (Auburn Hills, MI), Michigan Energy Resource and Research

Association (Detroit, MI) and the Electric Power Research Institute (Palo Alto, CA).

The project was developed as a learning tool for the utilities involved and as a public demonstration of the capabilities and realities of photovoltaic energy production. Toward those ends, the participants have profited greatly from the experience and knowledge gained.

Amorphous PV materials are uniquely different in their operating characteristics from crystalline and polycrystalline cells. They are sensitive to a different part of the solar spectrum, they exhibit strong seasonal efficiency variations and are annealed by the long summer heat soak. Another significant difference is that amorphous silicon is subject to an initial efficiency degradation (the Staebler-Wronski Effect) [1].

The 4 kW amorphous-silicon PV facility studied in this project was constructed at the Auburn Hills Campus of Oakland Community College north of Detroit, Michigan. It was first energized on May 6, 1987 and has been in continuous operation since that time. During the 40 months since system start-up, considerable data have been collected and analyzed. Conclusions have been reached with regard to

efficiency variations caused by temperature, solar spectrum, material degradation and annealing. Data are also available to evaluate long term energy production from this system in the Michigan environment. Extrapolations of this data should yield performance predictions in other solar regimes. This paper presents the details of these conclusions and shows much of the data used in their discovery.

THE PHOTOVOLTAIC SYSTEM

The PV system evaluated in this paper consists of 144 model R100 amorphous-silicon alloy modules manufactured by Sovonics Solar Systems, Inc of Troy, Michigan in late 1986. The cells are dual tandem construction designed for enhanced light capturing capability. Each module contains 420 cells, resulting in module ratings of approximately 30 Watts. The array is organized into nine strings of 16 modules each. Further details of the array and module connection schemes can be found in previously published papers [2] [3] [4].

D.c. electrical energy generated by the array is converted to 60 Hz a.c. in a 6 kW Omnion power converter. There is no battery storage at the site. Instead, the a.c. power is coupled directly into the campus electrical grid where it offsets the amount of power the campus load draws from the electric utility line. Although power from the array can theoretically be returned to the utility company during times of low campus usage, this has most likely never occurred because of the large campus load.

THE DATA ACQUISITION SYSTEM

The data acquisition system utilized at the campus was installed by Detroit Edison to monitor electrical performance of the PV system, capture relevant environmental parameters and process the results into a form that is readily analyzed. The heart of the system is a Campbell Scientific 21X Micrologger. Sensors connected to its input bring in d.c. array voltage and current, a.c. voltage and phase angle, global and plane-of-array insolation, ambient temperature and front and back surface temperatures of a representative module. In late spring of 1990, three experimental spectrum sensors were also installed at the site to assist in spectrum related efficiency studies. Although data have been collected from these, it is too early at the time of this writing to accurately correlate spectrum to performance.

The data collected in the micrologger is averaged over each hour and relayed via a telephone modem to a computer at Detroit Edison's Laboratory in Detroit. At that point, the data are stored in Lotus 1-2-3 spreadsheets and performance graphs are produced.

ENERGY PRODUCTION

In the 40 months of operation since system start-up in May, 1987 through August, 1990, the entire PV system has performed very reliably. No components of any type have failed, nor have any been replaced. Although a few modules have experienced water leakage from improper sealing during manufacture [4] [5], power generation is not measurably different from the other modules and, consequently, they have been left in the system to further build the base of long term reliability knowledge.

Figure 1 shows system availability of the Detroit Edison PV system over a 39 month period from June, 1987 to August, 1990. Availability in this figure is identified by positive net a.c. energy production at times when insolation is greater than or equal to 100 Watts/m². All but five months of the 39 have an availability of more than 90 percent. Total availability over the 39 months is 95.9 percent.

Availability on a 24 hour base, irrespective of insolation, is shown in Figure 2. Because winter

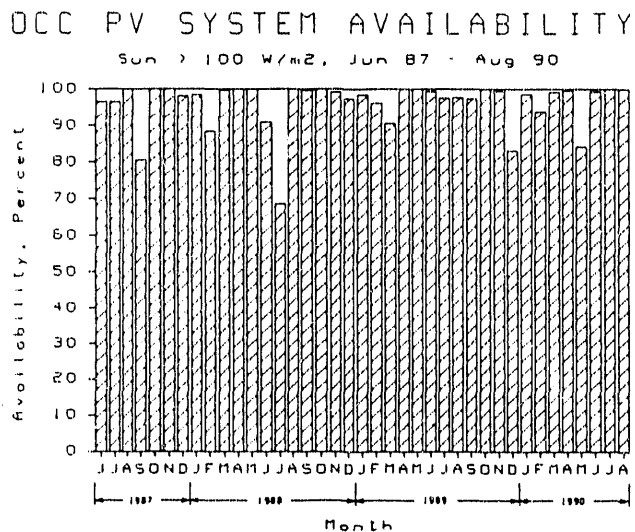


Fig. 1. Monthly PV system availability determined by positive a.c. power output during times of insolation greater than 100 Watts/m².

OCC PV SYSTEM AVAILABILITY
24 Hr base, Jun 87 - Aug 90

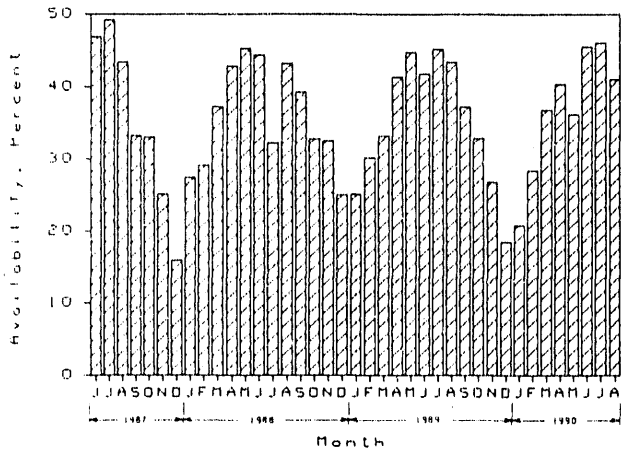


Fig. 2. Monthly PV system availability determined by positive a.c. power output on a 24 hour daily basis.

OCC PV MONTHLY DC ENERGY OUTPUT
(May 6, 1987 - August 31, 1990)

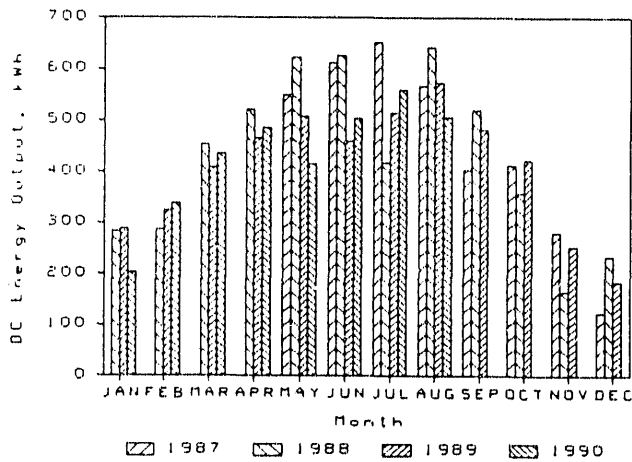


Fig. 3. Monthly PV system d.c. energy production.

days are short on sunlight and considerable cloud cover prevails in Michigan at that time of the year, 24 hour availability is considerably lower in winter than summer. Since system start-up, overall 24 hour availability is 35.8 percent.

Figure 3 shows the d.c. energy produced by the array during each of the 40 operational months (note that May, 1987 was only a partial month because of initial system start-up on May 6). As expected, energy generation is variable both monthly and seasonally. The best month's production was in July, 1987 when 652 kWh d.c. were produced. The lowest production occurred in December of that same year when only 124 kWh were generated by the array.

Capacity factor is the percentage of the actual electrical energy produced by a generating system compared with the theoretical energy production if the system were producing at full output at all times. Figure 4 shows the d.c. capacity factor for the Detroit Edison PV system over 39 months of operation. As with 24 hour availability, the months vary considerably with highs occurring in the summer and lows in the winter.

Overall capacity factor is 14.5 percent. Values during the first year reached almost 15 percent, whereas in the latter year they were just under 14 percent. This change, while reflecting the initial degradation of amorphous-silicon cells, would not be apparent if the power rating of the array at time of measurement were adjusted to represent the actual instantaneous maximum capacity of the array. For our graph, all computations were made at the design capacity of 4000 Watts d.c. A further discussion of array efficiency degradation is found in the following section.

OCC PV SYSTEM DC CAPACITY FACTOR
(June 1, 1987 - August 31, 1990)

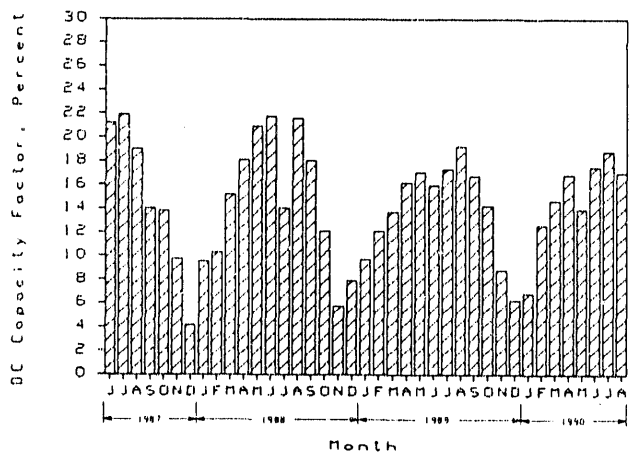


Fig. 4. Monthly PV system d.c. capacity factor based on a design size of 4 kW d.c.

DCC PV MONTHLY AC ENERGY OUTPUT
(May 6, 1987 - August 31, 1990)

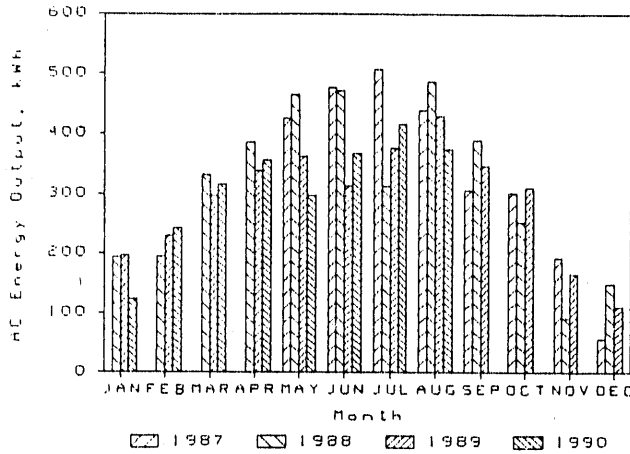


Fig. 5. Monthly PV system a.c. energy production.

A.c. energy delivered to the campus was less than the d.c. production each month because of losses in the inverter. Although instantaneous a.c./d.c. conversion efficiencies were in the range of 80 to 84 percent during times when the array was operating at 40 or more percent of capacity, the overall monthly net production was below that figure. This is due to the fact that the inverter becomes a consumer of a small amount of a.c. energy when the array d.c. production is very low (less than a couple hundred Watts) or when nighttime darkness occurs. Figure 5 shows the net a.c. energy delivered to the campus each month during the test period. In this graph, nighttime inverter energy consumption is subtracted from the daytime energy delivery to yield the net figures. In effect, it is the usable energy delivered over a month's time.

Because the seasonal variations of energy production obscure the actual production capability of the array, it is useful to analyze energy production using a "running year" computation. This is obtained by averaging the monthly productions over a complete 12 month period and sliding the beginning and ending months along each month to produce points on the curve that represent the year's data with the ending month specified (see Figure 6). If each year were identical in energy production, the graph's bar components would all be identical in height. Any variation sustained over a few months shows a trend in energy production.

It can be seen from Figure 6 that the general trend in our system has been to lower energy production

in the latter year and a half. While a number of factors can produce such a falloff in output, a significant cause has been a drop in the level of sunlight in southeastern Michigan since 1988.

Figure 7 shows the running year insolation measured at the site since system start-up. Figures 6 and 7 are quite similar. Individual variations in the energy output graph that are not seen in the insolation graph are mostly due to array downtimes. These have occurred on several occasions when lightning activity in and around the campus has caused power line surges throughout the campus grid. The inverter responds to severe surges by shutting down to protect its electronics from failure when it detects what it thinks may be a short circuit or severe overload. On occasion, the inverter has failed to automatically restart after such an event and has required manual restarting. Because performance data is not examined every day, system outages have not always been noticed quickly.

In one case (July, 1988) an outage resulted from a blown fuse in the campus grid during a severe storm. Because the event occurred at the beginning of a holiday and vacation period, the loss of generation went unnoticed for 10 days. The result was the loss of approximately a third of the month's potential energy production. Had it not been for this event, July, 1988 would probably have been the month of highest energy production because of its abundant insolation.

RUNNING YEAR ENERGY OUTPUT
Years Ending May 88 - August 90

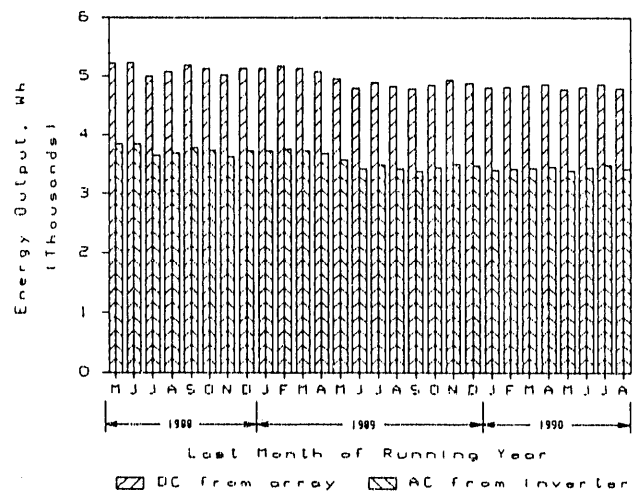


Fig. 6. Running year d.c. and a.c. energy production from the PV system.

RUNNING YEAR INSOLATION (45 DEGREE)

Year Ending May 88 - August 90

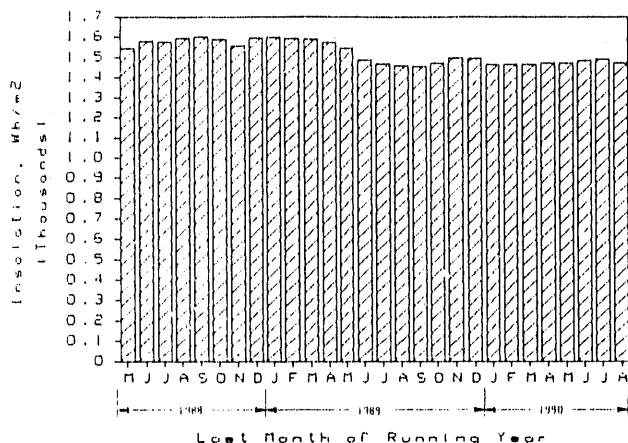


Fig. 7. Running year insolation at the plane of the array.

PV SYSTEM EFFICIENCY

Efficiency of the Detroit Edison 4 kW PV system was determined in several ways using a variety of analyses applied to the more than 1200 days of continuous data. The most straight-forward efficiency measurement is shown in Figure 8. All efficiency calculations were made using d.c. power output, plane-of-array insolation and physical constants of the array for each hour of data when the insolation was between 800 and 1050 Watts/m². While it would have been desirable to raise the lower limit to 900 or 950 Watts/m², that level of sunlight intensity is not generally found in November or December in southeast Michigan. In order to capture a reasonable number of sample points, the lower limit had to be reduced to 800 Watts/m².

In Figure 8, the seasonal cycling of efficiency is clearly seen. Efficiency lows occur during January and February and highs appear in August. There is also a noticeable downward slope to the curve in the first 250 days. This is the Staebler-Wronski Effect degradation observed in amorphous-silicon materials [1]. What is not certain in this curve is when the Staebler-Wronski Effect diminishes to insignificance and the seasonal cycle takes over as the predominant feature. Further it is not easily ascertained from Figure 8 whether the annual lows and peaks are retaining the same values from year to year or whether there is a continuing downward trend.

Figure 9 addresses these questions more clearly. This curve plots array d.c. efficiency versus calculated values of air mass over the entire 39 month period at insolation values between 800 and 1050 Watts/m². Because the Sovonics R100 modules exhibit performance variations related to the spectrum changes caused by air mass variations, and because air mass is an hourly and seasonally variable quantity, it was used in this curve in an attempt to correlate efficiency with a measurable and predictable parameter. Each point plotted in Figure 9 is an average of the 20 points preceding and following in the data base. This degree of smoothing was required to reduce the individual data variations to a more continuous curve.

By following the time markings in Figure 9, it can be seen that the efficiency of the array declined rapidly in the first few months, then rebounded during the following summer. The second year's efficiency generally tracks the same pattern as the first year, but is lower by approximately 0.1 percent absolute (2.8 percent relative). During the third year, the fall-to-winter efficiency decline showed values nearly identical to the second year, indicating that a point of stability had been reached in the modules. During the third winter and early spring, the array actually performed better than in the second year. The reason for this phenomenon is not evident from Figure 9.

DC PV ARRAY ENERGY EFFICIENCY

May 6, 1987 - August 31, 1990

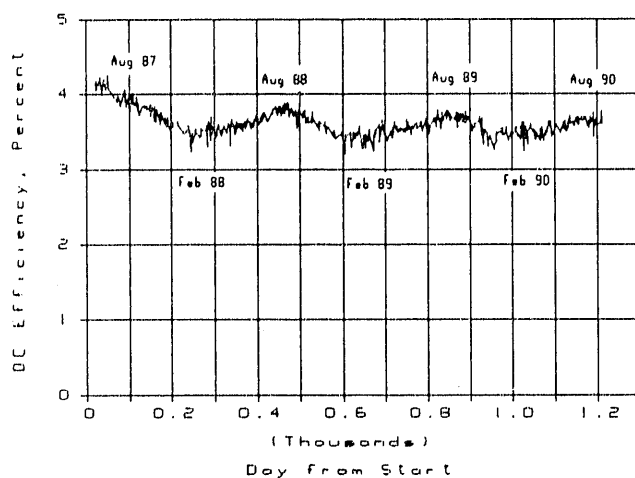


Fig. 8. Hourly array d.c. efficiency versus days since system start-up measured at insolation values between 800 and 1050 Watts/m². Data are shown as measured and are uncorrected for standard conditions.

OCC PV ARRAY ENERGY EFFICIENCY

(± 20 smoothed, 6/16/87 - 8/31/90)

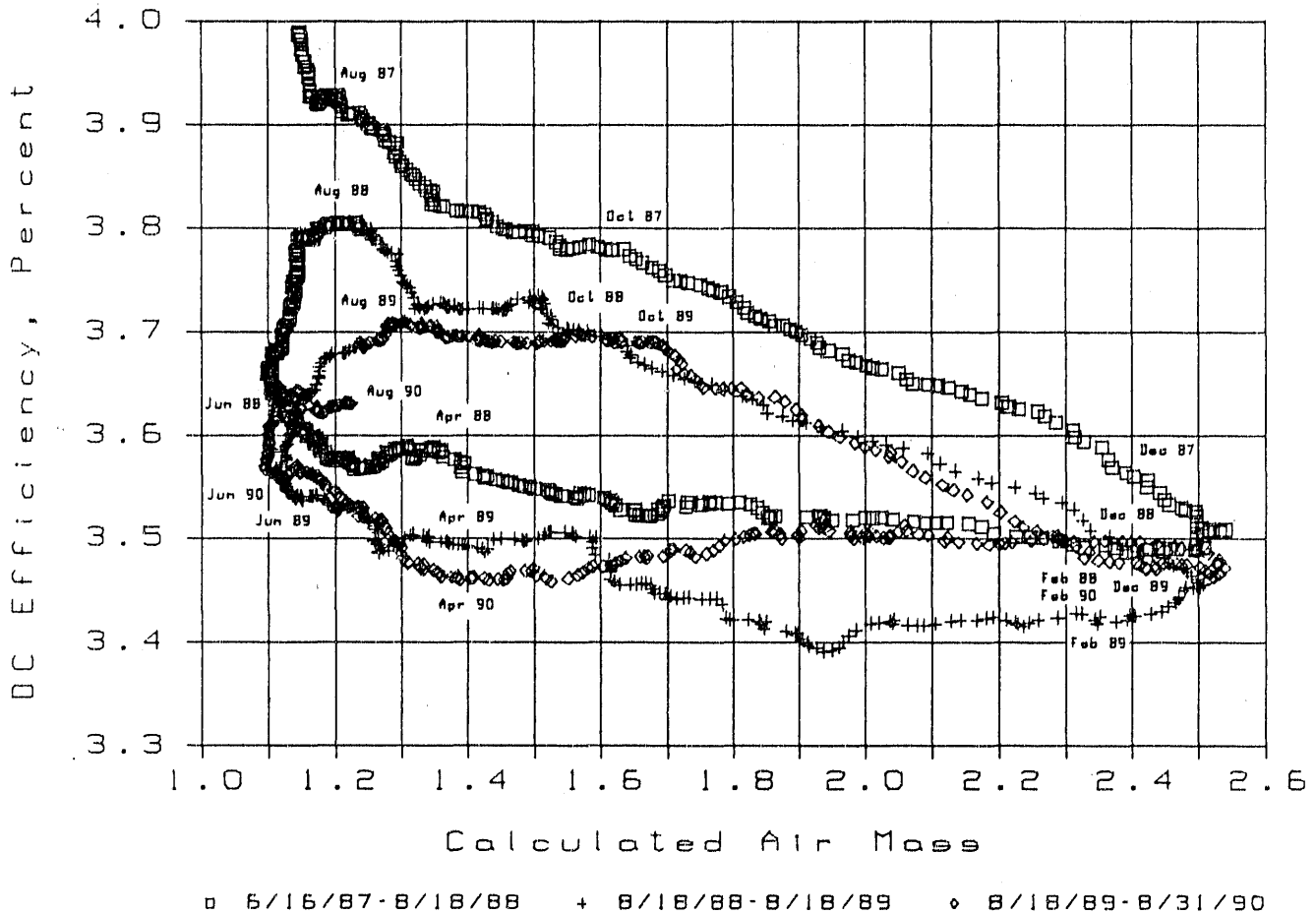


Fig. 9. Hourly array d.c. efficiency versus days since system start-up measured at insolation values between 800 and 1050 Watts/m². Data are shown as measured and are uncorrected for standard conditions.

It is interesting to note that the winter efficiency low does not necessarily occur in December, a time of the year when the air mass is highest. Further, the efficiency high occurs in August, almost two months after the air mass low. Although efficiency on an instantaneous basis is heavily influenced by air mass, it is clear that over the long term (several months or a season), there is another over-riding influence.

One such influence is temperature. The winter low temperatures are reached between December and February. During the summer, warm temperatures occur in June through August. The curve shows an efficiency drop during the fall and early winter with a minimum reached abruptly, then sustained for a

long period in the winter and spring. The hot days of summer, however, cause a slow but steady rise in the array efficiency until mid August. This is the summer heat soak that anneals the amorphous-silicon, raising its ability to deliver usable electrons from the photons striking its surface. The summer of 1988 shows an especially strong summer rise with the peak hitting 3.8 percent in August. This was an unusually hot and sunny summer. The rise that began in early summer of 1989 flattens out sooner and at a lower peak. That summer was much cooler with fewer sunny days. Further analysis of the efficiency versus temperature relationship can be seen in Figure 10. The data here is normalized over 39 months with each month's average plotted. While the actual

values are not important here, the trends are quite significant. For example, it is noted that the lowest efficiency usually occurs when the temperature is the lowest. Downward changes in temperature are usually the indicator of a similar change in efficiency. An upward change in temperature, however, begins the movement of efficiency in the upward direction, but the peak is usually reached a month or two later than the temperature peak. The summer annealing effect is evident in this delayed peak response.

While it is apparent from Figure 10 that there are changes in efficiency and temperature from one year to another, it is difficult to quantify such long term trends from this data presentation. Figure 11 resolves this problem by plotting a running year computation. Normalized values of both efficiency and ambient temperature are plotted with each point representing the average of a year's data. The individual point is the ending month of the running year. In this graph the seasonal variations are eliminated and only the last month's values from one year to the next are observed.

The first obvious feature of this curve is the sharp drop in efficiency seen on the left side. While giving the appearance of declining efficiency into the latter part of 1989, this is actually not the case. Because each point is looking backward over a year's time, the permanent loss in efficiency ceased its decline 11 months before September, 1989. The actual stabilization date of the PV array is near the end of September or the beginning of October,

MONTHLY TEMPERATURES AND EFFICIENCIES
June 1987 - August 1990

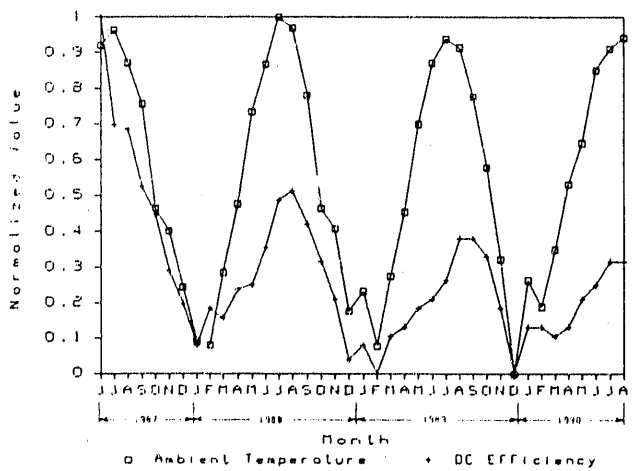


Fig. 10. Monthly average d.c. efficiency and ambient temperature.

RUNNING YEAR EFFICIENCY AND TEMPERATURE

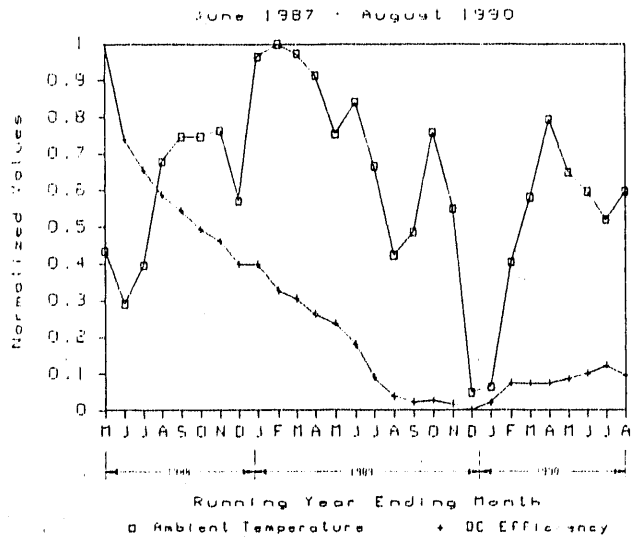


Fig. 11. Normalized running year d.c. efficiency and ambient temperature.

1988. The array was first exposed to light in April, 1987 and energized in May of that year. The Staebler-Wronski degradation then occurred over the initial 17 month period.

Further study of Figure 11 shows the subtle effect of temperature variations on the d.c. efficiency. While not a perfect match, it is evident that long term temperature variations cause similar changes in efficiency. Short term temperature effects on efficiency do not correlate well, however. A curve similar to Figure 9 with ambient temperature substituted for air mass was created earlier in the project and displayed scattered data points and much less of a direct relationship [4].

Figure 8 showed the actual instantaneous operating efficiency of the array over 39 months of operation. Figure 12 condenses that data into running year averages to eliminate the seasonal variations. Instead of showing the cyclic peaks and valleys, it displays a yearly average at each point. As in Figure 11, the early degradation period is clearly evident on the left half of the curve. The lowest portion of the curve corresponds to a period of lower average temperatures during the summer of 1989 and the succeeding early winter. When average temperatures became more normal in 1990, the array efficiency rose to a higher value and stabilized there. It should be remembered when viewing this graph that the efficiency figures are yearly averages, not individual monthly values.

RUNNING YEAR EFFICIENCY

June 1987 - August 1990

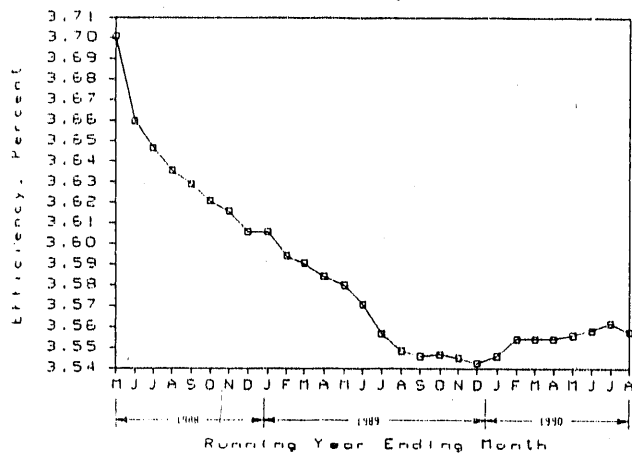


Fig. 12. Running year d.c. array efficiency

It is possible, using the efficiency data presented, to determine an amount of array degradation that has become permanent. It would not be correct to use Figure 12 to calculate that, however, since it represents annual averaged data and the majority of the degradation occurred during the first year. Using the earliest month of available efficiency data (4.16 percent in June, 1987) and comparing that to August, 1990 (3.64 percent), it can be seen that the degradation during that time was 12.5 percent relative. That is a minimum figure, however. The array was first exposed to sunlight in late April, 1987 and energized on May 6, 1987. Between one and two months passed from initial exposure until the solar sensors were installed at the site. It is certain that additional unmeasured degradation occurred during those early days.

CONCLUSIONS

The 4 kW amorphous-silicon alloy photovoltaic demonstration facility installed and operated by the Detroit Edison Consortium at Oakland Community College near Detroit, Michigan has proven to be durable and reliable within the solar regime of southeastern Michigan. It has performed largely as expected and has continued to deliver electrical energy to the campus on a daily basis.

Array efficiency varies monthly according to a seasonal pattern. Winter efficiency declines as ambient temperature drops. Summer efficiency improves, but on a delayed basis after a long period of warm summer temperatures which anneal the amorphous material. Instantaneous variations in efficiency are seen to be the result of changing solar

spectrum, calculated as air mass. The initial Staebler-Wronski Effect degradation, which resulted in a permanent efficiency reduction, occurred over an initial 17 month period, after which the array stabilized around an annual average efficiency of 3.56 percent.

ACKNOWLEDGEMENTS

This project is made possible through the work of many contributors. The author wishes to thank the members of the Consortium, as well as the following individuals for their planning, engineering and guidance in developing this project and making it the success that it is: L. Casey, W. Popravsky and T. Woodall (Detroit Edison); L. Boman, J. Burdick, L. Fatalaki, and D. Fillmore, (Energy Conversion Devices/Sovonics Solar Systems); S. Gozmanian, J. Mickelsen, D. Rowe and H. Templin (Oakland Community College); T. Anuskiewicz and J. Mogk (MERRA); M. Clevey (MERRA, formerly of Energy Conversion Devices); J. Reynolds (Consumers Power Company); R. Ophaug (Lansing Board of Water and Light); J. Schaefer (Electric Power Research Institute); T. Key and J. Stevens (Sandia National Laboratories); and S. Durand, C. Lashway and V. Risser (New Mexico Solar Energy Institute).

REFERENCES

- 1 D. L. Staebler, C. R. Wronski, "Reversible Conductivity Changes in Discharge-Produced Amorphous Silicon", *Applied Physics Letters*, Vol. 31, August, 1977
- 2 R. G. Pratt, "Construction and Evaluation of a 4 kW Amorphous-Silicon Photovoltaic System in Michigan", *Photovoltaic Thin Film Module Reliability Testing and Evaluation Workshop*, August 13-14, 1987, Lakewood, Colorado, SERI, 1987
- 3 R. G. Pratt, J. Burdick, "Performance of a 4kW Amorphous-Silicon Alloy Photovoltaic Array at Oakland Community College", *Proceedings of the Twentieth IEEE Photovoltaic Specialists Conference*, Las Vegas, Nevada, IEEE, September, 1988
- 4 R. G. Pratt, "Two Year Performance Evaluation of a 4 kW Amorphous-Silicon Photovoltaic System in Michigan", *Solar Cells*, February, 1990
- 5 J. Schaefer, H. Boyd, C. DeWinkel, D. Fagnan, R. Pratt, "Experiences with U. S. Line-Connected Amorphous Silicon Systems", *Proceedings of the 8th European Photovoltaic Solar Energy Conference*, Milan, Italy, May, 1988

PHOTOVOLTAIC CONCENTRATOR MODULE RELIABILITY:
FAILURE MODES AND QUALIFICATION

Elizabeth H. Richards
Sandia National Laboratories

Summary of Presentation Given
at the Photovoltaic Module Reliability Workshop

Denver, Colorado
October 25, 1990

Introduction

In the early 1980s, three first-generation photovoltaic (PV) concentrator systems were installed in Saudi Arabia, Phoenix, and Dallas. The systems in Phoenix and Saudi Arabia used passively cooled point-focus modules built by Martin Marietta, and the one in Dallas used actively cooled line-focus modules made by ENTECH (formerly E-Systems) [1,2,3]. Although some problems were encountered, especially with poor-quality solder bonds in the point-focus modules, the modules in these systems performed remarkably well for first-generation technology. (Additional problems with the balance-of-system components occurred, decreasing the overall reliability of the systems, but that subject is beyond the scope of this paper.)

Despite the success of the early module technology, there are still some concerns about the long-term reliability of PV concentrator modules. There are several reasons for this. First, energy-cost calculations generally assume a 20- to 30-year life in the field; the field experience with the first-generation systems is on the order of 6 to 9 years, considerably less than 30 years [4]. Second, relatively few (compared to flat-plate modules) concentrator modules have been deployed in the field, due mostly to the fact that the economics of concentrators are geared toward larger power markets that have not yet materialized. Third, concentrator module design has evolved and changed substantially since the first generation systems were installed. Most of these new designs have not been installed in fielded systems. And finally, although a lot of the reliability work on flat-plate modules applies to concentrator modules as well, there are some reliability issues with concentrator module designs that are different from those of flat-plate module designs.

The purpose of this paper is to discuss the current issues of interest in PV concentrator module reliability. Before describing in detail the reliability concerns about PV concentrator modules, it should be emphasized that, with proper design and attention to quality control, there is nothing to prevent concentrator modules from being as reliable as crystalline-silicon flat-plate modules have proven to be. Concentrator modules tested outdoors, as well as in the first-generation systems, have generally been reliable, and no degradation in cell output has been observed. Also, although they are not included in this paper, there are a few items currently of concern with the

Prepared by Sandia National Laboratories, Albuquerque, New Mexico 87185 and Livermore, California 94550, operated for the U. S. Department of Energy under Contract DE-AC04-76DP00789.

reliability of other PV module technologies that are not issues with PV concentrator technology, such as the stability of amorphous-silicon efficiencies and concerns about EVA encapsulation [5,6].

Differences in Reliability Concerns Between Concentrator and Flat-Plate Modules

The biggest difference, from a reliability standpoint, between concentrator modules and flat-plate modules is that concentrators have a much larger volume. This large volume means that concentrator modules cannot be hermetically sealed; that is, vents must be provided to equalize the pressure as the temperature changes. Vents allow air of different relative humidities to enter the modules, and, as the temperature changes, moisture condenses onto the interior surfaces of the modules. Any exposed electrical circuits inside the modules are therefore subject to contact with water, which provides paths for leakage currents and/or short-circuits. This situation, besides being potentially detrimental to reliability, also raises safety issues. Newer concentrator designs are addressing moisture intrusion by encapsulating the electrical circuits inside the modules.

Another difference between concentrator and flat-plate modules relates to heat transfer considerations. Having areas of concentrated sunlight means that there is a smaller area in which to remove a given amount of heat. Designing for heat removal, whether by passive or active means, would not be too difficult for PV concentrator modules except that the design is complicated by the conflicting requirement of high-voltage electrical isolation. Generally a metal heat sink of some sort (either a separate heat fin or a metal module housing) is used to keep the cells cool. This exposed metal piece must be grounded and therefore electrically isolated from the cell string. This leads to electrically isolating layers between the cell string and exposed ground that are often very thin to promote good heat transfer. This thinness can create reliability problems with the electrical isolation between the cell string and the heat sink, especially under wet conditions.

Both flat-plate and concentrator module designs must account for differential thermal expansion, but the main areas and materials of concern are different for the two technologies. The two major areas of concern in concentrators are the cell string with its associated relatively large-area solder bonds and the seal between the lens and the housing, which may join metal and plastic over a length of several feet.

Other significant differences between concentrators and flat plates include the possibility for off-track charring in the interior of concentrator modules, which must be accounted for in the module design, and possible differences in hot-spot response.

Failure Modes

Probably the most common source of problems with concentrator module reliability is moisture intrusion. Failures due to moisture intrusion can be put into three categories. The first is a temporary decrease in power due to a short circuit; when the water dries, power is restored. The power decrease is generally due to low-voltage short circuits across individual cell assemblies or cell strings within a module or modules. The second category of failure causes permanent damage and can occur when water causes a destructive

short or arc. The most likely place for this to happen is between a cell string and ground. Moisture intrusion can also create permanent open-circuit failures if water gets into a solder crack and freezes. The third type of failure due to moisture intrusion is caused by long-term degradation, such as corrosion. Examples of this type of failure include degraded cell metallization and deteriorated optical properties.

Modules under test both in the field and during qualification testing have exhibited several types of failures resulting from moisture intrusion. These include short circuits between cell strings and ground and between terminals and ground, high ground-fault currents which prevent the inverter from switching on, modules filling with water, corrosion, and degraded optics. The decrease in energy production of a system due to these failures is dependent on both the system configuration and the location of the failure. It can range from small short-term losses from individual cell assemblies to the entire system being shut down for a day or more after a rain storm.

Some other important failure modes in PV concentrator modules result from differences in thermal expansion coefficients. In particular, the solder bonds that connect the cells are susceptible to fatigue. Each cell typically carries a current on the order of 10 Amps, so the interconnects (usually copper) must be robust enough to carry the current. The coefficient of thermal expansion for silicon is much smaller than that of copper, so the joints between the interconnects and the cells must be designed to minimize stress on the solder bonds. The solder bonds joining cells to copper heat spreaders (if used) or other substrates must also be designed carefully to minimize the effect of differences in coefficients of thermal expansion.

If a metal housing is used with a plastic lens (as is frequently done), the difference in coefficient of thermal expansion between the metal and plastic must be accounted for in the design of the lens seal. If the seal is too weak, it will not survive thermal cycling. If the seal is too rigid, it will not allow relative movement between the lens and housing, and the lens will buckle.

Other types of failures are less frequently encountered, but are worth mentioning. The materials in the module must be able to withstand long-term ultraviolet (UV) light exposure. Some recent module tests have resulted in degraded or cracked lens seals, material embrittlement, and discoloration of glass secondary optical elements. The discolored glass secondaries ultimately cracked when they became dark enough to absorb significant amounts of light. Off-track concentrated sunlight can char materials (such as encapsulants or polymeric insulation) if the module is not properly designed. Improper design also occasionally results in lenses being pulled out of modules by high winds and failures due to hot-spot heating. And finally, no discussion of concentrator failure modes is complete without mentioning the importance of quality control during manufacture.

Current Issues in the Qualification of Concentrator Modules

Sandia has developed and published qualification specifications for PV concentrator modules [7,8]. The purpose of the tests is to screen new designs and new production runs for susceptibility to known failure mechanisms; however, there is insufficient information correlating accelerated testing with field exposure to establish field lifetimes. The tests include

ultraviolet radiation testing of materials, characterization of electrical performance, checks to assure safety and structural integrity of modules, and accelerated environmental aging or cycling. They are modelled after the Jet Propulsion Laboratories (JPL) Block V qualification specifications for flat plate modules [9]. In addition to testing complete modules, separate tests are conducted on cell assemblies and receiver sections because the receivers experience a more severe environment than the rest of the module.

The specifications are currently being revised to incorporate the latest information on failure mechanisms and the relationships between accelerated tests and field reliability. The major changes include an increase in the number of thermal cycles required for receiver assemblies and the addition of a wet insulation-resistance test.

The most critical components of a PV concentrator module are the cell assemblies. The cell assemblies, or receivers, collect the light transmitted by the module optics and convert it to electricity. Degradation of the cell assembly, in particular degraded or broken solder bonds, causes a corresponding decrease in electrical output as the resistance in the circuit increases. Complete breakdown of the cell assembly can result in loss of the solar cell altogether. Poorly designed cell assemblies can damage or break the cells.

In addition to being critical to module output, cell assemblies also see the most severe environment of any module component. Since the cell assemblies are exposed to concentrated sunlight, they undergo considerable thermal cycling as the sun rises and sets and the temperature of the assemblies changes from night-time ambient to 60°C or more. Thirty years encompass nearly 11,000 daily cycles. Intermittent clouds add additional thermal cycles.

Because cell assemblies are so crucial to module output and because they see the most severe environment, qualification of PV cell assemblies receives considerable attention in Sandia's reliability work. Tremendous progress has been made in this area: five years ago very few cell assemblies survived the accelerated 250-cycle qualification test; now most survive 1000 cycles. Our understanding of the correlation between field life and accelerated testing has also improved [10,11]. Accordingly, the revised qualification specifications will require survival of a minimum of 800 accelerated thermal cycles for cell assemblies and receiver sections; the current specifications require only 250 cycles. The cycling frequency may also be decreased, but this requirement must be balanced against the need to complete the test in a reasonable amount of time.

Testing in the field and in environmental chambers has established that moisture intrusion, especially condensation, must be addressed in the qualification of PV concentrator modules. This is important both for reliability and for personnel safety. Under contract to Sandia, JPL is developing a trial-use procedure for a wet insulation-resistance test. The test will be performed at 500 Vdc in each polarity. The interior surfaces of the module will be sprayed with water that contains a wetting agent, and the insulation resistance between the cell string and ground (or other appropriate locations) will be measured with a suitable high-impedance ohmmeter. This requirement may allow only one polarity (the circuit or ground) to be exposed

inside a module and could have a significant impact on future concentrator module designs. The latest concentrator modules are already being designed to pass this test [12].

A number of other less consequential changes to the qualification specifications are also being considered, such as increasing the number of modules required for testing, adjusting the allowable degradation levels, adjusting thermal cycling temperatures and frequencies for complete modules, and specifying tests for optical components, terminal robustness, and bypass diodes.

Summary

Despite the reliability concerns discussed above, all of the problems can be solved with proper design, manufacturing, and quality control; none of the problems require technical breakthroughs for solution. The reliability issues for concentrators are comparable in nature to many issues of concern in other PV technologies. Concentrator cell technology has proven to be very reliable, with no degradation in cell outputs observed in fielded modules.

In certain climates, concentrators still offer potential for producing PV-generated electricity at lower cost per kWh than flat-plate modules [13,14]. Concentrator modules use much less cell material than other PV options and do not require extremely sophisticated production facilities, making their production attractive to developing areas of the world. Most concentrator modules require two-axis tracking and accept only the direct-normal component of the incident sunlight, but these factors are offset by module efficiencies that are generally higher than those of other PV technologies.

The references below give more comprehensive discussions of the topics addressed in this paper. In addition to the references called out in the text, some papers on cell assembly design and quality control for concentrator module manufacturers are also included [15,16,17].

References

1. A.A. Salim, F. S. Huraib, N. N. Eugenio, and T. C. Lepley, "Performance Comparison of Two Similar Concentrating PV Systems Operating in the U.S. and Saudi Arabia," Proceedings of the 19th IEEE Photovoltaics Specialists Conference, New Orleans, Louisiana, 1987.
2. T. Lepley, Sky Harbor Photovoltaic Concentrator Project Phase III; First Forty-Two Months of Operation (Phoenix: Arizona Public Service Company, October 1986)
3. M. J. O'Neill, "Measured performance for the First Three Years of Operation of the DFW Airport 27-KW (Electric)/120KW (Thermal) Photovoltaic and Thermal (PVT) Concentrator System," Proceedings of the 18th IEEE Photovoltaics Specialists Conference, Las Vegas, Nevada, 1985.
4. Five Year Research Plan 1987-1991. Photovoltaics: USA's Energy Opportunity, DOE/CH10093-7 (Washington, D. C.: U. S. Department of Energy - National Photovoltaics Program, May 1987).

5. B. L. Stafford, "The Future of Amorphous Silicon Photovoltaics," Proceedings of the 1990 Annual American Solar Energy Society, Austin, Texas, 1990.
6. A. Czanderna, "Overview of Possible Causes of EVA Degradation in PV Modules," Proceedings of the Photovoltaic Module Reliability Workshop, Denver, Colorado, October 25-26, 1990.
7. R. S. Barlow and E. H. Richards, Qualification Tests for Photovoltaic Concentrator Cell Assemblies and Modules, SAND86-2743 (Albuquerque: Sandia National Laboratories, January 1988).
8. E. H. Richards and R. S. Barlow, "Qualification Testing of Photovoltaic Concentrator Modules," Proceedings of the 19th IEEE Photovoltaics Specialists Conference, New Orleans, Louisiana, 1987.
9. Block V Solar Cell Module Design and Test Specifications for Intermediate Load Applications - 1981, JPL Report #5101-161, (Pasadena: Jet Propulsion Laboratory, February 20, 1981)
10. C. J. Chiang and S. J. Blankenau, "Reliability Testing of Cell Assemblies for Photovoltaic Concentrator Modules," Proceedings of the 20th IEEE Photovoltaics Specialists Conference, Las Vegas, Nevada, 1988.
11. E. H. Richards and C. J. Chiang, "Reliability of Photovoltaic Concentrator Modules," Proceedings of the 21st IEEE Photovoltaics Specialists Conference, Orlando, Florida, 1990.
12. C. J. Chiang and M. Quintana, "Sandia's Concept-90 Photovoltaic Concentrator Module," Proceedings of the 21st IEEE Photovoltaics Specialists Conference, Orlando, Florida, 1990.
13. J. L. Chamberlin, "The Costs of Photovoltaic Concentrator Modules," Proceedings of the 20th IEEE Photovoltaics Specialists Conference, Las Vegas, Nevada, 1988.
14. E. H. Richards, J. L. Chamberlin, E. C. Boes, "Recent Progress in Photovoltaic Concentrator Module Technology," Proceedings of the 1990 Annual American Solar Energy Society, Austin, Texas, 1990.
15. C. J. Chiang and E. H. Richards, "Reliability Research and Cell Assembly Design for Photovoltaic Concentrator Modules," Proceedings of the 19th IEEE Photovoltaics Specialists Conference, New Orleans, Louisiana, 1987.
16. C. J. Chiang, "Design of Cell Mounts for Photovoltaic Concentrator Modules," Proceedings of the 20th IEEE Photovoltaics Specialists Conference, Las Vegas, Nevada, 1988.
17. V. S. Murty, A Generic Plan to Aid in the Preparation of Quality Assurance/Quality Control Manuals for the National Photovoltaic Concentrator Initiative Contractors, (Albuquerque: Sandia National Laboratories, draft).



**PV CONCENTRATOR
MODULE RELIABILITY:
FAILURE MODES AND QUALIFICATION**

Beth Richards

Sandia National Laboratories

October 25, 1990



**PV CONCENTRATOR
MODULE RELIABILITY**

Failures

- Moisture Intrusion
- Differential Thermal Expansion
- Plus UV Exposure
 - Wind Loading
 - Off-Track Charring
 - Hot-Spot

Qualification

- Wet Insulation Resistance Test
- Thermal Cycling Tests
- Other New Tests and Changes



Failures due to moisture intrusion can be put into three categories:

1. Temporary loss of power; when water dries, power is restored.
(Example: Short across one cell.)
2. Permanent failure; water causes destructive short.
(Examples: Short between cell string and ground; open circuit in cell assembly caused by freezing.)
3. Long-term degradation, such as corrosion.
(Examples: Open circuit in cell grid line; deterioration of optics.)

Safety is also a concern.



We have observed several types of failures resulting from moisture intrusion:

1. Cell strings shorting to ground.
2. Terminals shorting to ground.
3. High ground fault currents, preventing inverter from coming on.
4. Modules filling with water.
5. Corrosion.
6. Degradation of optics.

Decrease in energy production is dependent on system configuration and location of failure.



Differences in thermal expansion coefficients cause failures at material interfaces.

1. Cell to heat spreader
(solder bonds)
2. Cell to interconnect
3. Lens to housing
(glue bond)



Other types of failures are encountered less often.

1. UV degradation:
 - Seals degraded/cracked
 - Embrittlement
 - Solarization of glass secondaries
2. Lens failures due to wind
3. Off-track charring
4. Hot-spot failures



The purpose of the qualification tests is to screen new designs and new production runs for susceptibility to known failure mechanisms.

1. The tests do not establish field lifetimes.
2. Cell assemblies and complete modules are tested separately.
3. Specifications are currently being revised.



We are considering a Wet Insulation Resistance Test.

1. Response to the high percentage of failures due to moisture intrusion.
2. Test assumes water will, at some time, be present inside modules.
3. May require significant redesign of concentrator modules (already occurring).



JPL is developing Wet-IR test parameters:

- Perform the test at 500 V_{dc} in each polarity
- Maintain the temperature of the module and solution at $22 \pm 3^{\circ}\text{C}$ ($72 \pm 5^{\circ}\text{F}$)
- Wet all interior surfaces of the module thoroughly
- Use a non-ionic, non-corrosive surfactant, such as Triton X-100 (0.1% concentration), to wet the surface
- Measure the insulation-resistance between the shorted output terminations and ground plane (or solution) with a suitable high-impedance ohmmeter (Megohmmeter or Megger)
- Obtain readings after initial capacitive charging currents have subsided (approximately 2 minutes)



The number of thermal cycles for cell assemblies will be increased significantly.

- Current specifications require 250; new specifications will require at least 800.
- Thermal cycling frequency will likely be reduced from 36 cycles/day to no more than 24 cycles/day.
- Requirements for realistic test must be balanced against length of time required for test.



Several new tests will be added:

- Nonintrusive hot-spot
- UV exposure
- Terminal robustness
- Static loading
- Bypass diode qualification
- Twist

Also, other more minor changes in allowable degradation levels, number and frequency of cycling tests, and number of test modules required.

Results from the Field Surveys of First-Generation Systems have Demonstrated Concentrators to be a Reliable Technology

- No degradation in cell output has been observed.
- Vast majority of modules show no degradation in output.
- Power degradation is due mostly to discreet module failures caused by open circuits in solder bonds connecting cell assemblies.
- In general, the failures observed in the first-generation hardware can be avoided with better production quality control and improved designs.

The World is Ready for PV but Is PV Ready for the World?

**John Schaefer
Electric Power Research Institute**

**Photovoltaic Module Reliability Workshop
Lakewood, Colorado October 1990**

The World is Ready for PV

What emerges if we think globally?

- **Global climate change may be occurring now.**
- **It surely will occur if we increase carbon dioxide content.**
- **Growth of coal burning in developing nations will dwarf today's carbon dioxide production, so**
- **Race is between solar or nuclear development and industrialization of developing nations.**
- **If we win the race there is an enormous market for PV, among other benefits.**

The World Is Ready for PV

How large is the utility market for PV?

- All U.S. electricity can be supplied by about 1,000,000 MW
 - Assumes adequate storage and
 - Good sunshine (33% CF)
- This is a big enough electricity market that the PV industry can double every year for 15 years before saturating it.
- In the western U.S. (WSCC) utilities can take at least 30,000 MW without significantly altering system operation.
- But there is competition for this market:
 - Wind
 - Biomass
 - Solar thermal
 - Nuclear
 - Geothermal

but Is PV Ready for the World?

Utilities are the first big market for PV, but what will it take to reach them?

- Utilities are difficult to sell; they insist on a low risk product.
 - They have no incentive to take risks.
 - But they do respond to public pressure.
- Utilities want PV to be:
 - On time,
 - According to specification,
 - Reliable,
 - Backed by service, and
 - Low in cost.
- How are we doing in meeting these needs?

but
Is PV Ready for the World?

<u>Utilities' Needs</u>	<u>PV Manufacturers Consistently Satisfying Need</u>
On time	one
According to spec.	none
Reliable	one
Backed by service	one

but
Is PV Ready for the World?

Utilities look at power plant performance. Thanks to the foresighted efforts of government and private programs we have some results from PV power plants:

Phoenix-Sky Harbor	Austin PV 300
Hesperia-Lugo	Detroit
SMUD	Orlando
Carrisa Plains	PVUSA
Phoenix-John Long	

Each of these plants has taught us something of value.

but
Is PV Ready for the World?

Do PV power plants produce the power outputs their builders claim?

<u>Plant</u>	<u>Nameplate Rating (kW)</u>	<u>Measured Rating (kW)</u>
Phoenix-Sky Harbor	225	173
Hesperia Lugo 1	500	362
Hesperia Lugo2	500	367
SMUD PV1	1000	932
Carrisa Plains	6500	5100
Phoenix-John Long	200	166
SMUD PV2	1000	875
Austin PV 300	326	258
Detroit	4	4
Orlando	15	14

but
Is PV Ready for the World?

Utilities will look at these capacity factor data:

<u>Plant</u>	<u>1984</u>	<u>1985</u>	<u>1986</u>	<u>1987</u>	<u>1988</u>	<u>1989</u>
Phoenix-Sky Harbor	10	22	22	29	out of service	
Hesperia-Lugo1	32	35	23	28	33	36
Hesperia-Lugo2	34	35	24	30	33	37
SMUD PV1	na	23	25	7	0	13
Carrisa Plains	29	30	29	25	24	21
Phoenix-John Long			21	22	23	20
SMUD PV2			23	23	19	9
Austin PV300				22	25	23
Detroit				14	15	14
Orlando-Solar Progress					20	16

but
Is PV Ready for the World?

Utilities will look at these capacity factor data:

<u>Plant</u>	<u>1984</u>	<u>1985</u>	<u>1986</u>	<u>1987</u>	<u>1988</u>	<u>1989</u>
Phoenix-Sky Harbor	10	22	22	29	out of service	
Hesperia-Lugo1	32	35	23	28	33	36
Hesperia-Lugo2	34	35	24	30	33	37
SMUD PV1	na	23	25	7	0	13
Carrisa Plains	29	30	29	25	24	21
Phoenix-John Long			21	22	23	20
SMUD PV2			23	23	19	9
Austin PV300				22	25	23
Detroit				14	15	14
Orlando-Solar Progress					20	16

but
Is PV Ready for the World?

Utilities will look at these capacity factor data:

<u>Plant</u>	<u>1984</u>	<u>1985</u>	<u>1986</u>	<u>1987</u>	<u>1988</u>	<u>1989</u>	<u>MWh losses</u>
Phoenix-Sky Harbor	10	22	22	29	out of service		
Hesperia-Lugo1	32	35	23	28	33	36	697
Hesperia-Lugo2	34	35	24	30	33	37	514
SMUD PV1	na	23	25	7	0	13	4488
Carrisa Plains	29	30	29	25	24	21	9829
Phoenix-John Long			21	22	23	20	
SMUD PV2			23	23	19	9	1381
Austin PV300				22	25	23	
Detroit				14	15	14	
Orlando-Solar Progress					20	16	

but
Is PV Ready for the World?

What are the sources of poor performance?

- **Poor sunshine**
- **BOS components caused most outages:**
 - **PCUs, connections, switches, diodes, cables, fuses, contactors and trackers.**
 - **Losses total about 7000 MWh.**
- **Module degradation has emerged recently as a source of loss.**
 - **Brown cell at Carrisa Plains has cost about 9300 MWh.**

but
Is PV Ready for the World?

What does all this mean for us today in Lakewood?

- **We can learn from each other's experiences, and move on to new lessons rather than repeating the old ones.**
- **We will have to try new solutions to some problems.**
- **What we're doing here today involves difficult problems.**
- **What we're doing here is also very important.**

**Session 2:
Module Research and Testing**

THE USE OF INDOOR LIGHT SOAK DATA TO PROJECT
END OF LIFE OUTPUT POWER OF HYDROGENATED
AMORPHOUS SILICON SOLAR MODULES

D. Cunningham and J. Morris

Solarex, Thin Film Division
826 Newtown-Yardley Road
Newtown, PA 18940

Introduction

It is well known that the performance of hydrogenated amorphous silicon (a-Si:H) solar cells decreases when the cells are exposed to light [1]. Studies of this light induced degradation have shown that: (1) under constant illumination the normalized conversion efficiency of a solar cell decreases linearly with the log of time [1,2], and (2) for single junction solar cells the rate of light induced degradation increases with increasing i-layer thickness [1]. In addition it has been demonstrated that the rate of degradation for multi-junction solar cells is significantly lower than for their single junction counterparts [3,4].

Stability studies are typically carried out in the laboratory under controlled conditions, that is, under constant illumination intensity and constant temperature. The solar cell characteristics are measured at regular intervals to determine the effect of continuous light exposure on the performance of the cell. In contrast to well controlled indoor stability studies, modules placed outdoors are subject to wide variations in illumination intensity and temperature. In addition, unless extraordinary precautions are taken, it is likely that the spectral content of the light source used to degrade solar cells in the laboratory is significantly different than that experienced by modules placed outdoors. It is therefore not obvious that indoor light soak data can be used to project the performance of a-Si:H modules installed outdoors.

In this paper we compare projections of the normalized output power of a-Si:H modules based on indoor light soak data to the observed normalized output power of modules which have been degraded outdoors. The comparison is made for both single and tandem junction modules. We find that the normalized output power projected to 1000 hours of continuous illumination from indoor light soak data is in excellent agreement with that observed for modules which have undergone 1 year of outdoor exposure. For single junction modules comparison of measurements made at the end of the first and second years of outdoor exposure indicates that no detectable light induced degradation occurs during the second year of outdoor exposure.

Experimental Procedures

Module Fabrication

The single and tandem junction modules used in this study were fabricated on conductive tin oxide (CTO) coated glass by the dc glow discharge decomposition of silane and other gases. In all cases the i-layers were a-Si:H. The single junction modules had i-layers approximately 2600 Angstroms in thickness while the thicknesses of the front and back i-layers of the tandems modules were about 650 and 3000 Angstroms, respectively. The modules were all of monolithic construction; the single junction modules had 14 series connected segments and the tandem modules had 7 series connected segments.

Outdoor Exposure

Thirty seven single junction modules have been mounted outdoors for over two years. These modules were mounted at an angle of 35 degrees to the horizontal, facing due south in Newtown, Pennsylvania. The modules were held at open circuit voltage. In October of 1988 seventeen tandem junction modules were placed outdoors. Newtown is located northeast of Philadelphia, Pennsylvania with approximate latitude of 43 degrees. The climate is temperate, often with high humidity. Over the course of a year the air temperature may range from a low of about -20 degrees Centigrade to a high of about 35 degrees Centigrade. Each of the 37 single junction modules and the 17 tandem modules were taken indoors and (after the module temperature stabilized) measured on a calibrated solar simulator according to a fixed schedule. After the measurements were taken, the modules were returned to outdoors the same day.

Indoor Light Soak

To obtain data on the rate of degradation of modules which were continuously illuminated indoors, 46 single junction modules and 18 tandem junction modules were exposed to a constant illumination intensity using high pressure sodium vapor lamps. The modules were mounted above the lamps at open circuit and the lamp intensity was adjusted to 100 +/- 5 milliwatts per square centimeter using an appropriately filtered crystalline silicon reference solar cell. Good spatial uniformity of illumination was obtained by means of reflectors which had been coated with highly reflective paint [5]. The temperature of the modules during light soak was maintained at 45 +/- 3 degrees Centigrade by means of continuous running fans. The modules were under continuous illumination except when they were removed for testing. This typically occurred after 2, 20 and 168 hours of exposure.

All I-V measurements for the modules degraded indoors and outdoors were performed on a calibrated Spire Corporation solar simulator [6].

Results

Single Junction Modules

Figure 1 shows the normalized maximum output power plotted against the log of illumination time for the single junction modules degraded indoors. In figure 1 the data taken at 2, 20 and 168 hours is extrapolated out to 1000 hours of continuous exposure. In this and subsequent figures the error bars indicate the sample standard deviation of the normalized output power. An analysis indicates that the observed variation may be attributed to the repeatability of individual sample measurements.

Figure 2 shows the normalized maximum power output of the single junction modules degraded outdoors plotted against the log of the number of days of outdoor exposure. The average normalized output power at the end of one year and at the end of two years (approximately 730 days versus 365 days) of outdoor exposure is essentially the same, indicating that the modules have stabilized.

In the present case we wish to compare the normalized output power obtained by extrapolating the indoor light soak data out to 1000 hours with the normalized output power of the modules degraded outdoors after 1 year of exposure. Figure 3 is a histogram of the normalized output power of the thirty seven single junction modules after one year of outdoor exposure. For reference the best fit normal curve is superimposed on the histogram. The average normalized output power is 0.74, while the standard deviation of the sample is 0.04. Figure 4 is a histogram of the extrapolated normalized output power of the companion single junction modules which were degraded indoors. The best fit normal curve for this data is shown superimposed. The average extrapolated normalized output power for this sample is 0.76 which is in excellent agreement with the average normalized output power of 0.74 found for the modules degraded outdoors.

Figure 5 is a histogram of the normalized output power of the same 37 single junction modules after two years of outdoor exposure. As shown in the figure the average normalized output power of the modules is 0.74, with the sample standard deviation of 0.05. This is very similar to the results obtained after the first year of outdoor exposure.

Tandem Modules

Figure 6 shows the normalized output power plotted against the log of illumination time for the tandem modules degraded indoors, while Figure 7 shows the normalized output power of the tandem modules plotted against the log of the number of days of outdoor exposure.

Figure 8 is a histogram of the extrapolated normalized output

power of the 18 tandem junction modules which were light soaked indoors. For reference the best fit normal curve is superimposed on the histogram. The average extrapolated normalized output power for this group of tandem modules is 0.61, with a sample standard deviation of 0.04. Figure 9 is the histogram of the normalized output power of the 17 tandem modules light soaked outdoors for one year. In excellent agreement with the extrapolated result, the average normalized output power for this group of modules is 0.60, with a sample standard deviation of 0.03.

Discussion

In each of the histograms presented, the best fit normal curve was superimposed. In comparing the histograms generated from indoor and outdoor light soak data using companion samples, there is no evidence to indicate that there are significant differences in the average normalized output power of the indoor and outdoor samples or in the spread of the sample data. The comparisons indicate that indoor light soak data taken out to 168 hours (i.e., 1 week) and extrapolated to 1000 hours of continuous illumination may be used to project the expected normalized output power of solar modules degraded for one year outdoors.

Figure 3 and figure 5 are the histograms of the normalized output power of the single junction modules at the end of the first and second years of outdoor exposure. There is no significant difference in the average normalized output power or in the spread of the data. This indicates that by the end of the first year of outdoor exposure these modules have reached their stabilized efficiency.

The sodium vapor lamps used for indoor light soak emit strongly at wavelengths of 575 nm and 825 nm. The good agreement between the average projected normalized output power and the average observed normalized output power indicates that the spectral content of the light source used to degrade the a-Si:H modules is not an important consideration. This result is consistent with that reported by Bennett, et al[3].

Conclusions

We have compared the average normalized output power of single and tandem junction modules which have been placed outdoors for one year to that projected by extrapolation of indoor light soak data, taken in one week, out to 1000 hours. There is excellent agreement between the average normalized power projected from indoor data and the average normalized output power observed after one year of outdoor exposure for both single and tandem junction modules. Thus we are able to accelerate outdoor degradation by a factor of about 50. This is possible because light induced degradation of a-Si:H is not sensitive to the spectral content of the light used to degrade the solar cells and because of the low sensitivity of degradation rate over the temperature

range and time scales involved in this study. In addition, we find for single junction modules outdoor light-induced degradation effects occur during the first year of outdoor exposure, with no detectable additional degradation during the second year.

Acknowledgements

The authors wish to thank M. Bennett for useful discussions and critical review of this work, and the Engineering staff at Solar-ex, Thin Film Division. This work was partially supported by the Solar Energy Research Institute under contract number ZB-706033-2.

References

1. M.S. Bennett, J.L. Newtown and K. Rajan. Proc. 7th EC Photovoltaic Energy Conf (edit A. Goetzberger, W. Paiz and G. Willeke) Seville, Spain 1986 p.544
2. M.S. Bennett and J.C. Tu. Materials Research Society Proc. vol 192 (edit P.C. Taylor, M.J. Thompson, P.G. Lecomber, Y. Hamakawa, A. Madun) p. 45
3. M. Bennett and K. Rajan. Proc. IEEE PVSC, Las Vegas, NV, 1988, pg. 67
4. G. Nakamura, K. Sata, T. Ishihara, M. Usui, K. Okinawa, and Y. Yukimoto. J. Non-Cryst. Sol. 59&60 (1983) p. 1111
5. Kodak LabLEADERtm Analytical Standard White Reflectance Coating, Eastman Kodak Company, Rochester, NY
6. Spire Corporation, SPI-SUN SIMULATOR tm, Bedford, MA

LIGHT SOAK TEST SINGLE JUNCTION MODULES

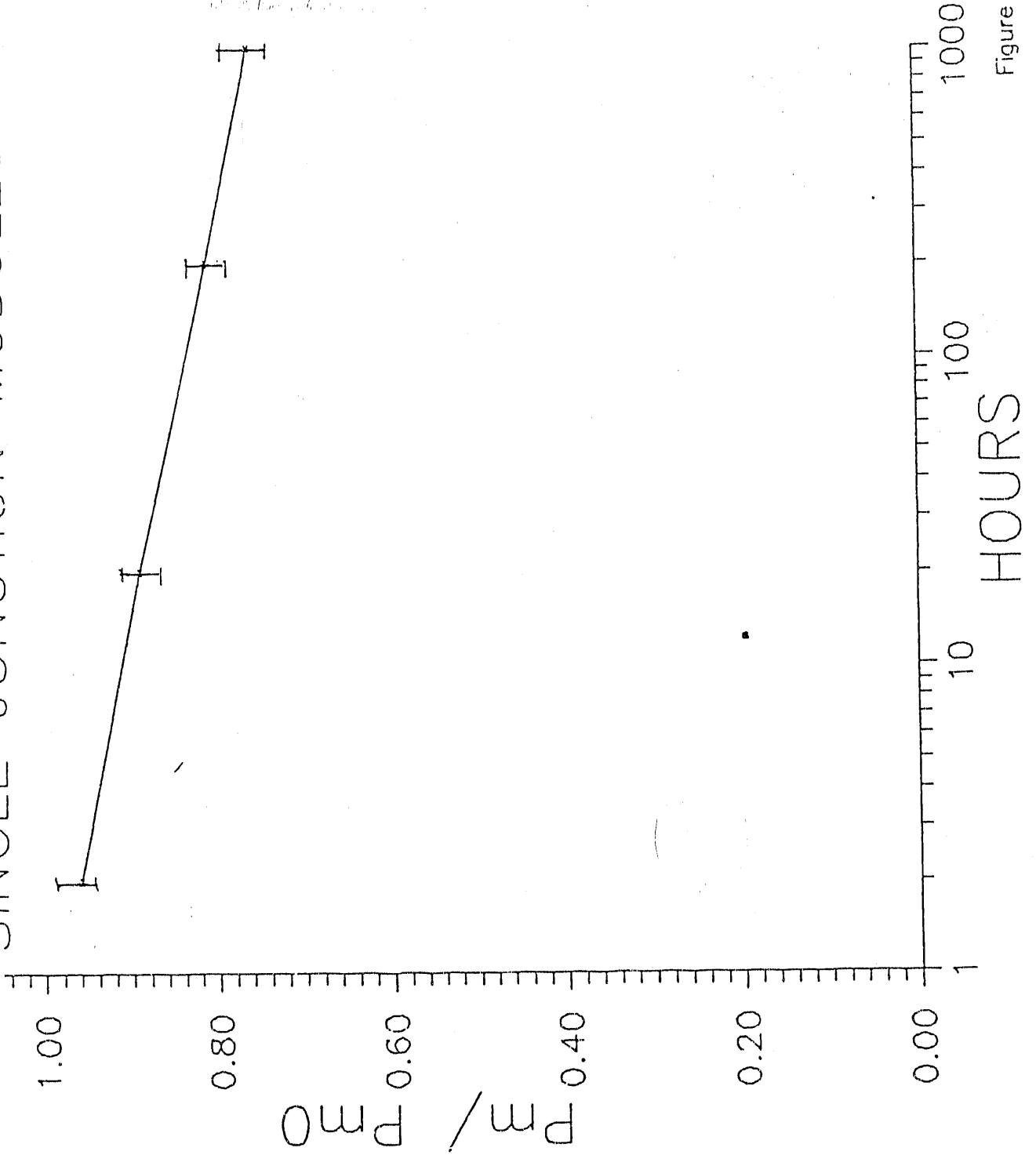


Figure 1.

OUTDOOR TEST SINGLE JUNCTION MODULES

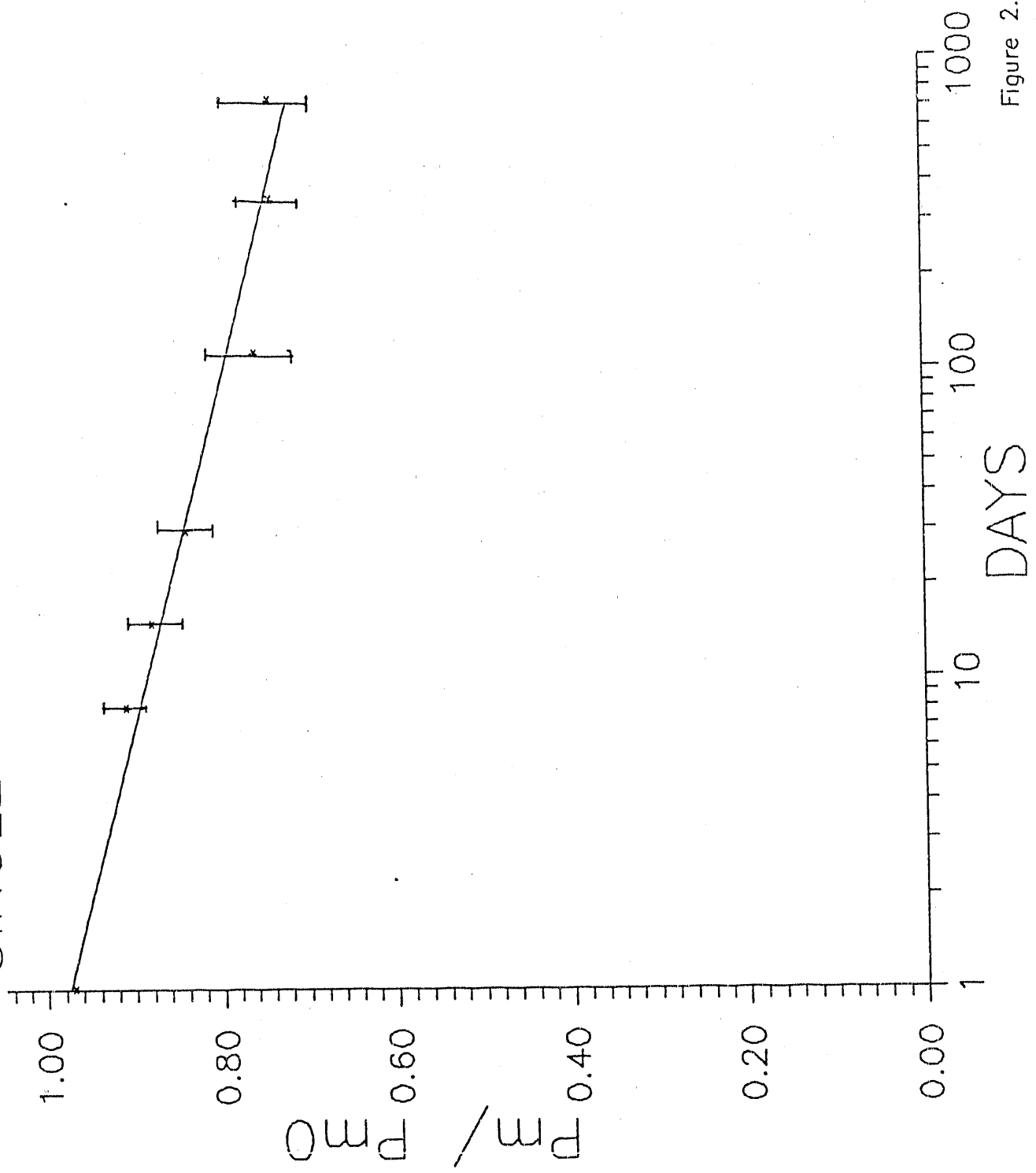


Figure 2.

Frequency Histogram

OUTDOOR DATA - ONE YEAR

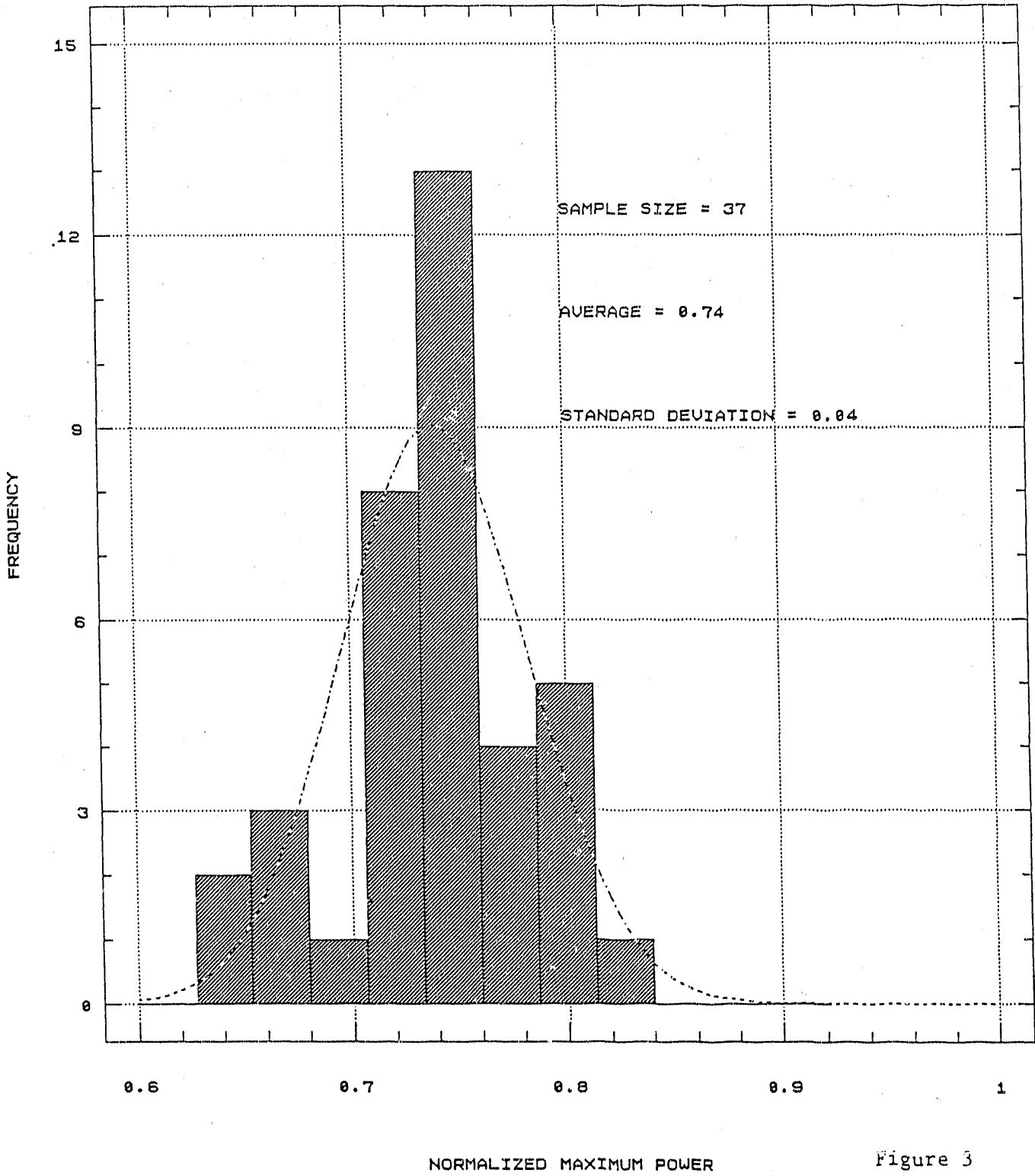


Figure 3

Frequency Histogram

EXTRAPOLATED INDOOR LIGHT SOAK DATA

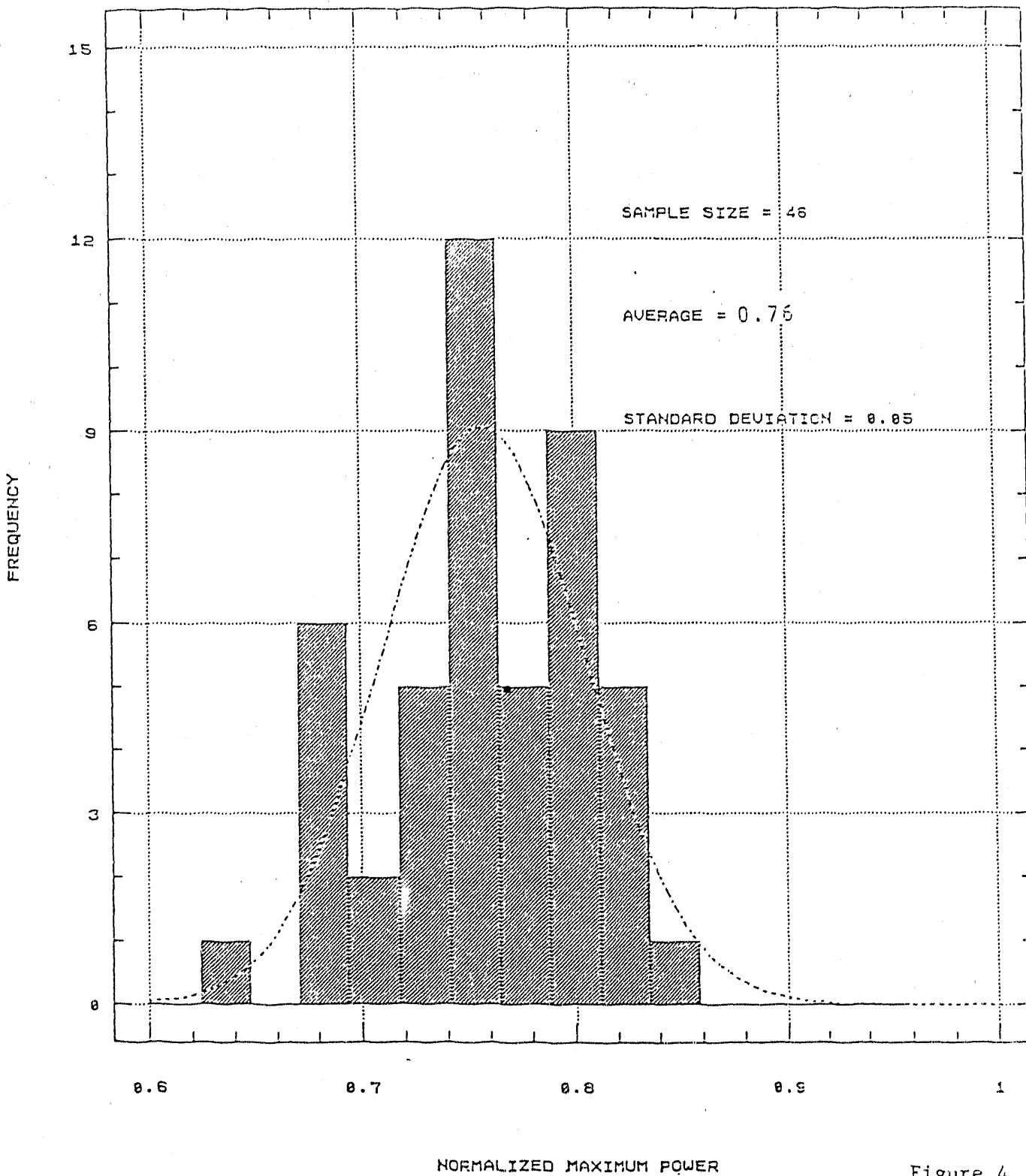


Figure 4

Frequency Histogram

OUTDOOR DATA - TWO YEARS

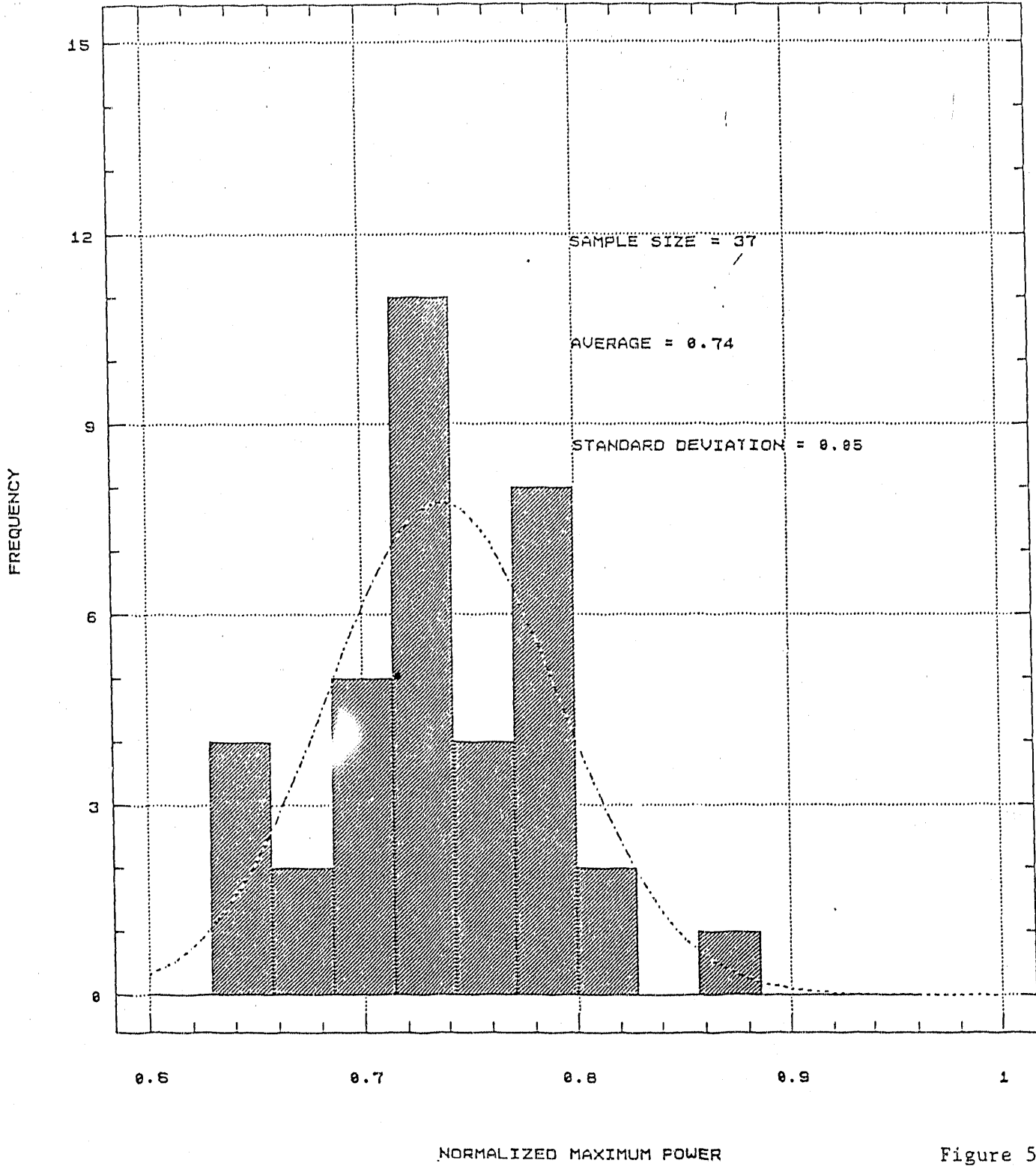


Figure 5

LIGHT SOAK TEST TANDEM JUNCTION MODULES

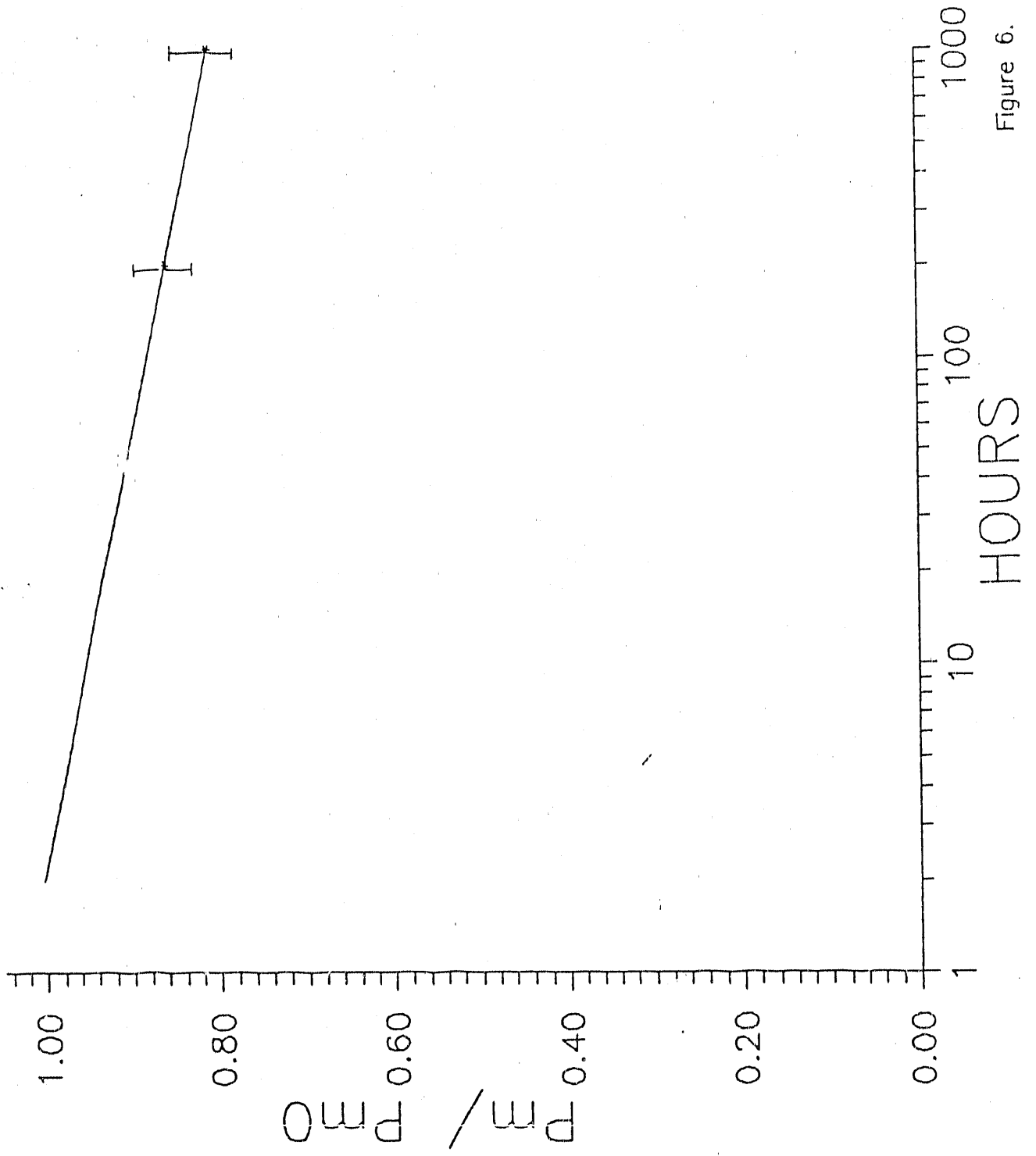


Figure 6.

OUTDOOR TEST TANDEM JUNCTION MODULES

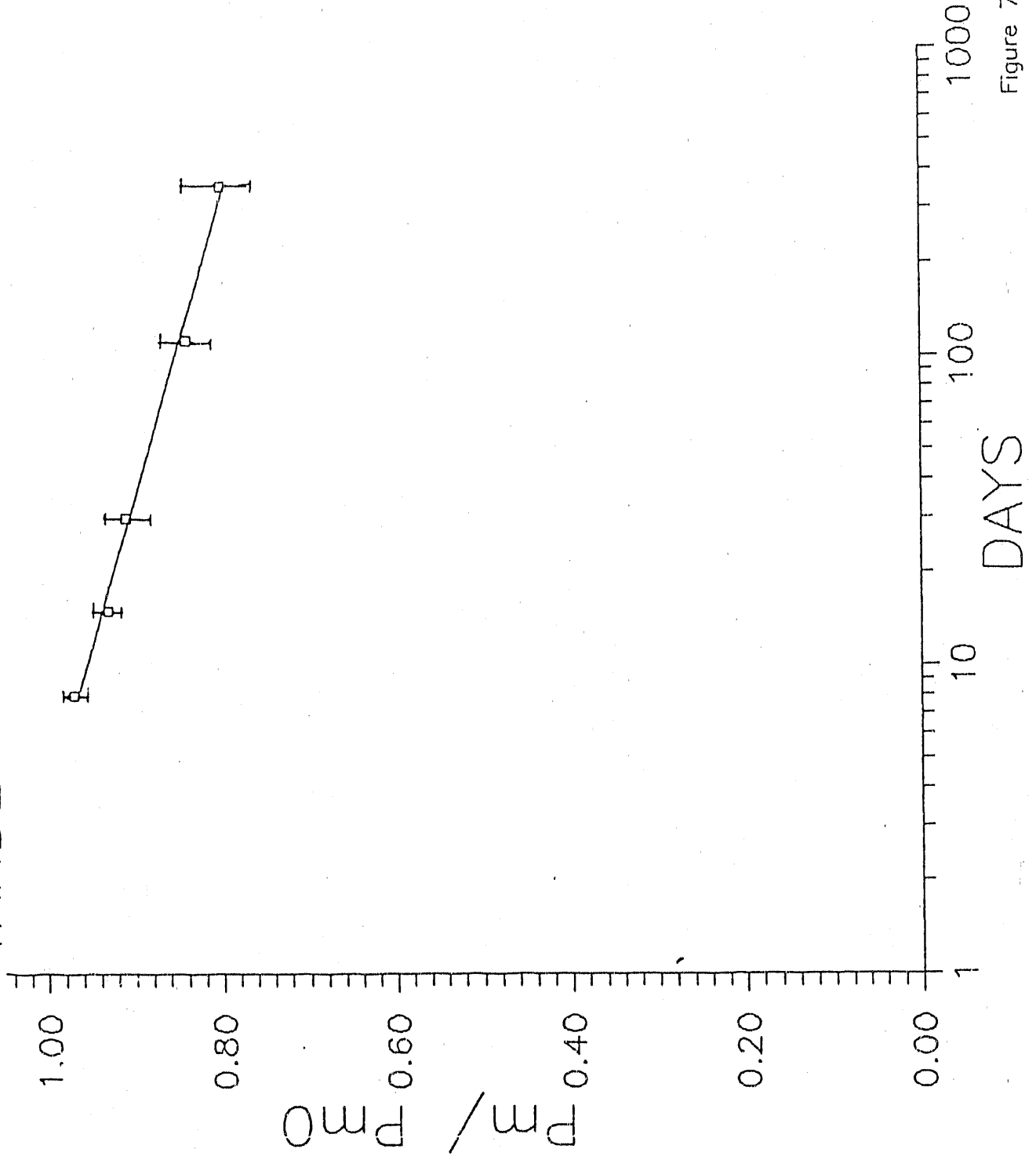


Figure 7.

Frequency Histogram

EXTRAPOLATED INDOOR LIGHT SOAK DATA

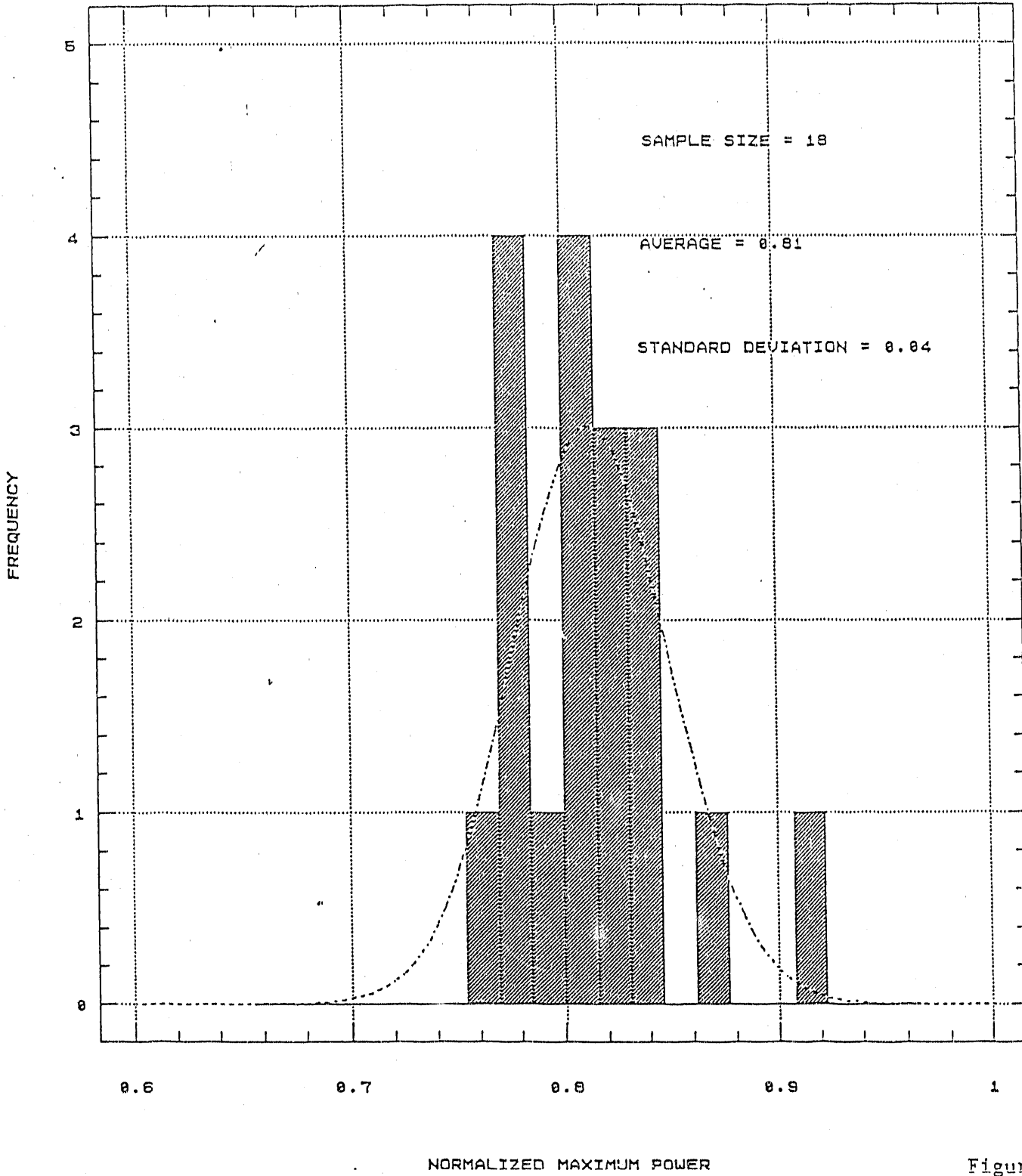


Figure 8

Frequency Histogram

OUTDOOR DATA - ONE YEAR

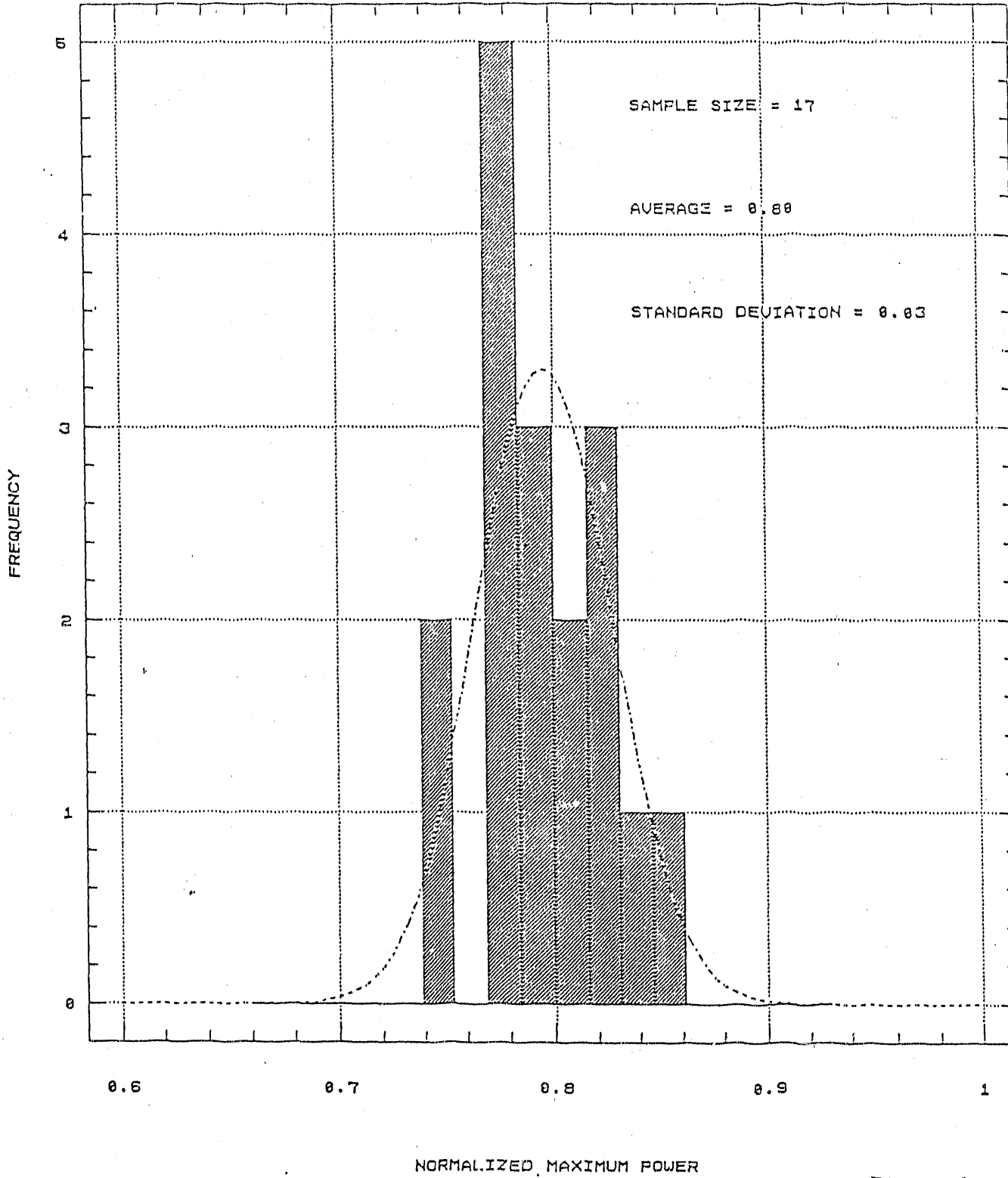


Figure 9

CuInSe₂ MODULE ENVIRONMENTAL RELIABILITY

Dale E. Tarrant, Robert R. Gay, Jean J. Hummel,
Cynthia Jensen, Al R. Ramos

Siemens Solar Industries
P.O. Box 6032
Camarillo, CA 93011

Summary

Environmental testing data are presented and discussed in relation to the qualification of CuInSe₂ (CIS) as a durable photovoltaic material and to the Interim Qualification Tests and Procedures for Terrestrial Photovoltaic Thin-Film Flat-Plate Modules (IQTP). Groups of modules having no significant change after 10 humidity-freeze cycles are reported. Heating during module packaging or during environmental testing to temperatures above those normally encountered by modules in outdoor service may introduce a temporary power loss; the power recovers with time to near the initial power. Data indicate that temperature alone, rather than temperature combined with humidity, causes the temporary power loss and that CIS is not inherently sensitive to humidity. Hermetic seals are not in general necessary for CIS materials. The IQTP may improperly indicate poor performance if the temporary power loss is not considered in electrical performance testing between different sections of the environmental test procedures and at the end of all environmental tests. Data are not available to validate accelerated testing as a means of predicting long term in-service performance; however, correlations between outdoor and accelerated testing are seen.

1. Introduction

Thin film CuInSe₂ (CIS) is a promising high power, low cost photovoltaic material, both as a stand alone single junction circuit and as the narrow band gap component in tandem junction circuits [1-3]. Research on CIS devices and modules has advanced the technology rapidly over the past five years. CIS technology is now moving from the research lab to the pilot production floor. The focus of CIS technology development is increasingly directed toward large areas, process uniformity, process reproducibility, and module durability. Prototype monolithic, integrated CIS submodules (unlaminated and unframed modules) with power densities greater than 100 W_p/m² have been fabricated on low cost, large area substrates using equipment and processing techniques compatible with commercial production.

We previously reported a 35.8 W, 0.4 m² submodule, fabricated in our research and development facility in Chatsworth, California

[4]. Since then, CIS fabrication activities were relocated to a new pilot production facility in Camarillo, California. Initial operation in this facility has produced a 37.8 W, 0.4 m² CIS submodule with 2.51 A short circuit current, 23.9 V open circuit voltage and 0.631 fill factor tested at 25°C under 1000 W/m² ASTM air mass 1.5 global illumination [5]. The electrical characteristics of the submodule average to 36.6 mA/cm² short circuit current density and 451 mV/cell V_{oc}, and equate to efficiencies of 9.7% on an aperture area of 3905 cm² and 10.4% on an active area of 3629 cm². The average interconnect width on the submodule is 0.041 cm.

As reported in reference 5, when the submodule aperture area efficiencies previously demonstrated on 0.1 m² areas are achieved on 0.4 m² areas, submodule power will increase to 43.6 W. Future 0.4 m² CIS submodule performance has been modeled using the junction characteristics of the 14.1% efficient 3.5 cm² CIS cell previously reported [4], and using interconnect widths and contact resistances typically measured on 0.1 m² submodules [5]. The model projects that the performance of 0.4 m² submodules will rise to 51.8 W when the junction efficiency previously demonstrated on small-area cells and the patterning routinely demonstrated on 0.1 m² submodules are realized on the larger area [5].

In this paper, accelerated environmental testing data (based on Block V [6] procedures) are presented and discussed in relation to the qualification of CIS as a durable photovoltaic material and to the new Interim Qualification Tests and Procedures for Terrestrial Photovoltaic Thin-Film Flat-Plate Modules (IQTP) [7]. Correlation between outdoor service and accelerated testing is also considered.

2. Submodule fabrication

The basic CIS cell structure includes a ZnO front transparent electrode, a thin (less than 50 nm) CdS layer, a CIS layer, a Mo back metal electrode, and a soda lime glass substrate. Gallium is added to the CIS layer in low concentrations to improve cell performance. A detailed description of the CIS cell structure and an analysis of CIS junctions are presented elsewhere [8,9].

Monolithic, integrated CIS submodules are fabricated on 4140 cm² glass substrates. The 32.2 cm × 128.6 cm substrate size is also used in Siemens Solar Industries' standard crystalline silicon and thin film silicon:hydrogen alloy (TFS) products. Thin film layers are deposited using equipment that is suitable for pilot production and capable of high effective deposition rates with high materials utilization efficiencies. Multibeam laser scribing and multitip mechanical scribing reduce the total patterning cycle time and provide narrow (0.025 to 0.041 cm) electrical interconnects across large submodule substrates.

Submodules are divided into 53 cells, each measuring 0.577 cm wide, including an interconnect (Fig. 1). The submodule interconnect region is shown in the expanded cross section of Fig.

1 and is discussed in detail elsewhere [4,10]. Approximately 240 cm² of substrate perimeter area is used for lead attachment. This perimeter area is subsequently covered by the module frame during packaging operations.

3. Module packaging

Submodules are encapsulated to mechanically protect the thin film layers and the encapsulated submodules are framed to strengthen the module package and provide for mounting. We have investigated a variety of module packages that were originally developed for Siemens Solar Industries' crystalline silicon and TFS products. These include glass/polymer and glass/metal sheet configurations used in crystalline silicon products, and glass/glass configurations used in TFS products. Recent efforts on CIS modules have emphasized the glass/glass package configuration.

Before submodules are laminated, electrical leads are soldered on each side of the circuit. A cover glass sheet is then laminated to the submodule plate with thermally cured ethylene vinyl acetate (EVA) to form a durable glass/EVA/thin film circuit/glass laminate. The cover glass is low iron, waterwhite glass, which reduces photocurrent loss due to absorption in the cover glass. The present design uses a 0.3 cm thick thermally tempered cover glass with approximately the same dimensions as the submodule substrate. A reaction injection molded (RIM) plastic frame provides additional mechanical support and finishes the prototype module package.

Heating the submodule during lamination causes a temporary power loss. With time the power returns to nominally the same power as before lamination. The improvement with time after heating has been called recovery and, as will be discussed, must also be considered during accelerated environmental testing since the submodules are heated to temperatures that would not normally be encountered in outdoor service. Figure 2 shows power recovery with time after lamination. Power changes are dominated by changes in the slope at open circuit component of the fill factor.

4. Environmental testing

Module stability is being evaluated under continuous outdoor exposure at test sites in Colorado and California (Fig. 3). Submodules laminated between a cover glass and a backing metal sheet with EVA have changed less than 6% after 17.5 months of continuous outdoor exposure at the SERI PV Outdoor Test Site in Golden, Colorado [11]. Similar stability has been observed on submodules laminated in glass/glass packages with EVA after 11 months of cumulative outdoor exposure at test sites in Chatsworth and Camarillo. This group of modules received 6.5 months of continuous outdoor exposure, followed by a 6.5-month period indoors, followed by an additional 4.5 months of continuous outdoor exposure. The interruption coincides with the relocation of Siemens Solar's CIS operations from Chatsworth to Camarillo.

Module durability is also being evaluated using test conditions defined in the 1981 JPL Block V standard test sequence [6]. The test sequence was developed to predict the durability of crystalline silicon modules, but has also been applied to thin film modules [12]. Initial tests on early prototype modules showed that the humidity-freeze (HF) portion of the environmental test sequence caused power losses ranging from 15% to 50% [5]. Evidence of moisture penetration and delamination was observed.

Recent module test groups include a variety of different edge seals at laminate edges. Before module test groups are laminated, adhesion measurements are made on representative samples using adhesive tapes with pull strengths of 1-90 oz/in. The stability of modules after 10 HF cycles is expressed as a ratio of the power P_{\max} after the test to the P_{\max} before the test. Distribution plots are used to identify trends within large test groups.

As reported in reference 5, data on recent test groups indicate that stability through 10 HF testing correlates strongly with adhesion at the CIS/Mo interface (Fig. 4). In module group A, the median module retained 93% of initial power after 10 HF cycles. All of the group A submodules passed tape adhesion tests at a minimum pull strength of 25 oz/in. In module group B, the median module retained only 58% of its initial power after 10 HF cycles. The group B submodules typically passed tape adhesion tests at a pull strength of only 1 to 5 oz/in. The impact of different edge sealing techniques was obscured by the strong dependence on film adhesion.

Modules from group A recovered with time and after about 30 days a significant number have nominally the same power as before HF cycling (Fig. 5). Group B modules did not recover significantly. Two subgroups are seen in the group A data: modules that recover to about the 98% of initial power and modules that recover to about the 92% of initial level. Differences between the subgroups have not been correlated with adhesion. This loss and recovery from 10 HF cycling is similar to the thermally induced loss during lamination.

Experiments were performed to distinguish between temperature alone and temperature combined with humidity effects during environmental testing. Temperature cycling with and without high humidity produces nominally the same temporary loss in power (Table 1). Temperature and humidity cycling defined by Block V procedures produces nominally the same temporary loss as the Block V cycles with the humidity eliminated and nominally the same effect as for the 50 temperature cycles section of the Block V environmental tests. The results after recovery are also nominally the same (the after recovery data include 200 rather than 50 temperature cycles).

Additional data support the findings of a solely thermal contribution to the temporary power loss during HF cycling and that CIS is relatively insensitive to moisture. Edge delamination of RIM-framed modules was previously reported [5]. This has been resolved by improvements in RIM framing. However, the performance

of delaminated modules after 10 HF cycles is nominally the same as for modules that did not delaminate. Insensitivity to moisture penetration in the delaminated modules is indicated. Insensitivity to moisture penetration is also indicated by tests on structures designed to prevent moisture penetration. A variety of moisture barrier edge seals and larger than normal vapor resistant perimeter areas have been tested through 10 HF cycling with no significant performance differences.

A solely thermal contribution to the temporary losses during HF cycling has been demonstrated and indicates that CIS is relatively insensitive to moisture. Therefore, a hermetic seal is not in general necessary for CIS materials. This does not imply that all CIS materials are inherently insensitive to moisture; the insensitivity to humidity has been demonstrated for only group A CIS materials.

In the IQTP, electrical performance tests between different types of environmental cycles and at the end of environmental cycles may improperly indicate poor performance if the temporary power loss and recovery are not considered. After environmental testing, time should be allowed for the power to stabilize. The IQTP calls for successful completion of electrical-performance tests after the thermal-cycle test and before proceeding to the humidity-freeze test. Time should be allowed for the power to stabilize between the thermal-cycle and humidity-freeze tests or an exception should be made for materials that are known to have a temporary power loss that is related to accelerated testing and not to outdoor in-service performance. For the data presented here, measurements after HF cycles are first made one to three days after 10 HF cycling. For the modules presented in Table 1, electrical performance tests, even after three days, would have improperly indicated poor performance. After recovery, the performance is excellent. Three days after HF cycles, modules from group A of Figures 4 and 5 recover to 93% of initial power. After recovery, a subgroup of modules recover to 98% of their initial power. It is possible that these modules would be rejected if measured immediately after HF cycles. Also, distinctions between the two subgroups (Fig. 5) would have been missed with only a pass/fail criteria. Without recovery most of the modules tested would have passed the IQTP criteria of losing less than 10% of initial power; however, distinctions between modules in the range from 90% to 100% of initial power would have been lost. Different CIS materials that pass the 90% pass/fail criteria may not perform equally well in service.

Data are not available to validate accelerated testing, such as IQTP, as a means of predicting long term in-service performance; however, correlations between outdoor and accelerated testing are seen in some cases. Figure 6 is a plot of power versus the number of days of outdoor exposure (at Siemens Solar Industries in Camarillo, California) for: the average power of 11 group A modules, two modules from group B, and the best performing module from group A. As for the HF cycle performance, modules from group

A are stable while modules from group B lose power. Differences in the processing of CIS can affect outdoor reliability and accelerated test results. For these two groups, short term (about 100 day) in-service performance follows the same trend as accelerated testing.

5. Conclusion

Recent significant improvements in CIS performance have been attributed to improved adhesion at the CIS/Mo interface. Groups of modules having no significant change after 10 HF cycles have now been demonstrated. Heating during module fabrication or environmental testing to temperatures above those normally encountered by modules in outdoor service may introduce a temporary power loss; the power recovers in time to near the initial power. Data indicate that temperature, rather than temperature along with humidity, causes the temporary power loss and that CIS is not in general sensitive to humidity. Hermetic seals are not inherently necessary for all CIS materials. The IQTP may improperly indicate poor performance if the temporary power loss and recovery are not considered in electrical performance testing between different sections of the environmental test and at the end of all environmental tests. Data are not available to validate accelerated testing as a means of predicting long term in-service performance; however, correlations between outdoor and accelerated testing are seen.

References

- 1 K.W. Mitchell, R.R. Potter, J. Ermer, R. Wieting, C. Eberspacher, D.P. Tanner, K. Knapp, R.R. Gay. *Proc. 19th IEEE PV Spec. Conf.*, pp. 13-18 (1987).
- 2 B.J. Stanbery, J.E. Avery, R.M. Burgess, W.S. Chen, W.E. Devaney, D.H. Doyle, R.A. Mickelsen, R.W. McClelland, B.D. King, R.P. Gale, J.C.C. Fan. *Proc. 19th IEEE PV Spec. Conf.*, pp. 280-284 (1987).
- 3 A. Rockett, R.W. Birkmire. "Current Status and Issues in Polycrystalline CuInSe₂ for Photovoltaic Applications." EPRI Research Project 2702-1. (1989).
- 4 J. Ermer, C. Fredric, K. Pauls, D. Pier, K. Mitchell, C. Eberspacher. *Proc. 4th Int. PV Science & Engr. Conf.*, pp. 475-480 (1989).
- 5 J. Ermer, C. Fredric, J. Hummel, C. Jensen, D. Pier, D. Tarrant, K. Mitchell. *Proc. 21st IEEE PV Spec. Conf.* (1990) (in press).
- 6 *Block V Solar Cell Module Design and Test Specification for Intermediate Load Applications.* Jet Propulsion Laboratory Technical Report JPL 5101-161; DOE/CS/31037-T1 (1981).
- 7 *Interim Qualification Tests and Procedures for Terrestrial Photovoltaic Thin-Film Flat-Plate Modules.* R. DeBlasio, L.

- Mrig, D. Waddington. SERI Technical Report SERI/TR-213-3624 (1990).
- 8 U.V. Choudary, Y. Shing, R.R. Potter, J. Ermer, V. Kapur. United States Patent 4,611,091 (1986).
- 9 K.W. Mitchell, H.I. Liu. *Proc. 20th IEEE PV Spec. Conf.*, pp. 1461-1468 (1988).
- 10 K. Mitchell, C. Eberspacher, J. Ermer, D. Pier. *Proc. 20th IEEE PV Spec. Conf.*, pp. 1384-1389 (1988).
- 11 Private Communication. Laxmi Mrig, Solar Energy Research Institute, Golden, Colorado (1990).
- 12 R.S. Sugimura, G.R. Mon, L. Wen, R.G. Ross Jr. *Proc. 20th IEEE PV Spec. Conf.*, pp. 1103-1109 (1988).

Table 1.
 Module recovery after temperature cycling. Power after environmental testing and recovery divided by power before environmental testing.

	Number of Modules	Average Standard Deviation	
		Partial Recovery	Full Recovery
Lot I			
50 temperature cycles	4	0.89 0.02	----- -----
200 temperature cycles	4	----- -----	0.97 0.06
Block V humidity-freeze cycles	8	0.86 0.04	0.93 0.03
Temperature cycles of Block V humidity-freeze cycles but without humidity	4	0.83 0.07	0.98 0.06
Lot II			
Temperature cycles of Block V humidity-freeze cycles but without humidity	4	0.92 0.02	1.03 0.02

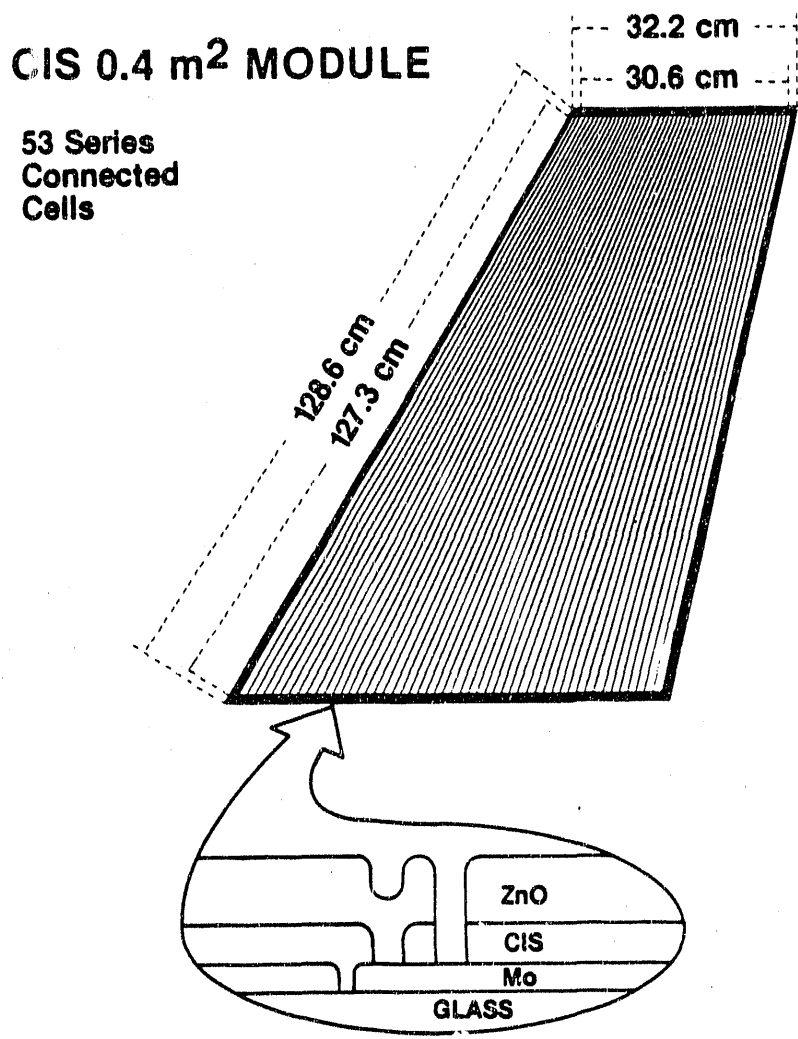


Fig. 1. Cross section of CIS module.

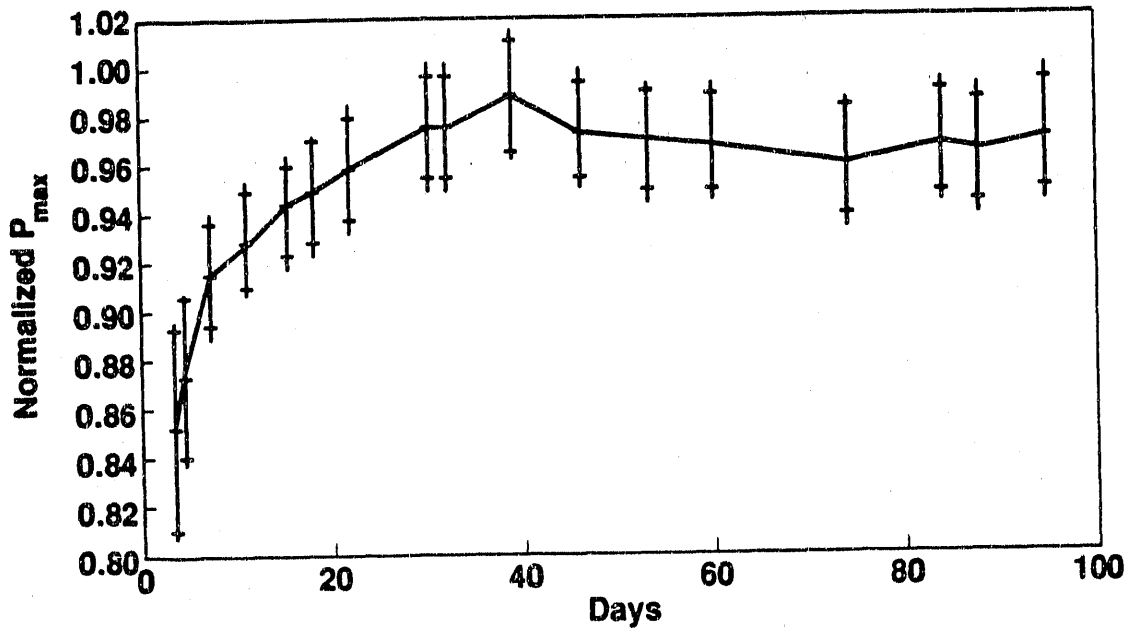


Fig. 2. Recovery from lamination.

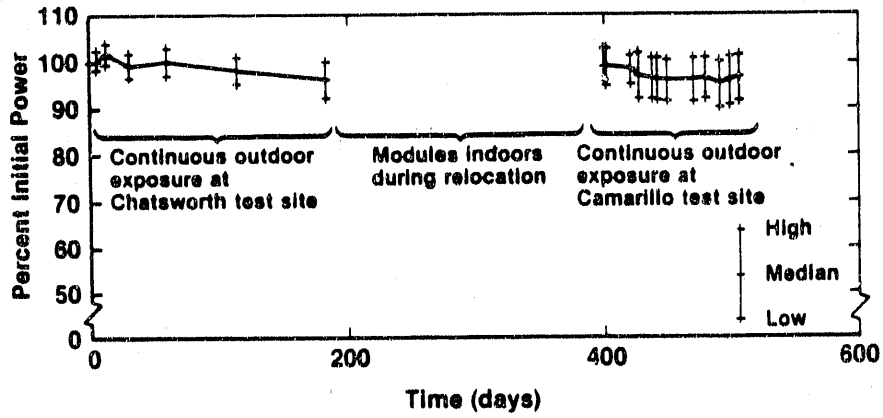
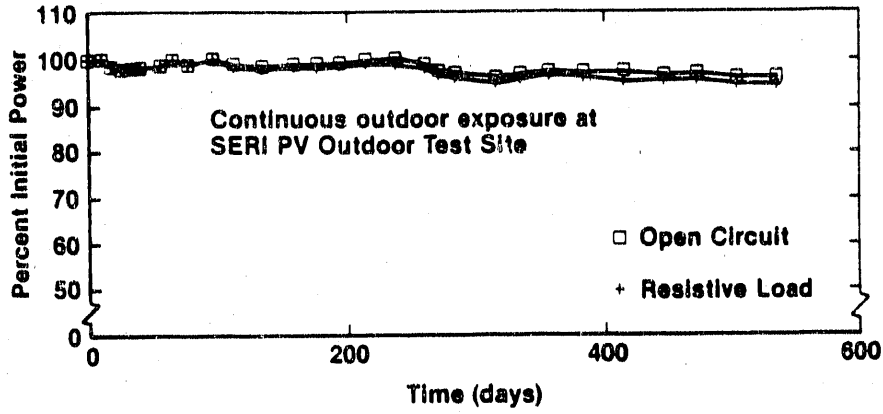


Fig. 3. CIS module stability outdoors.

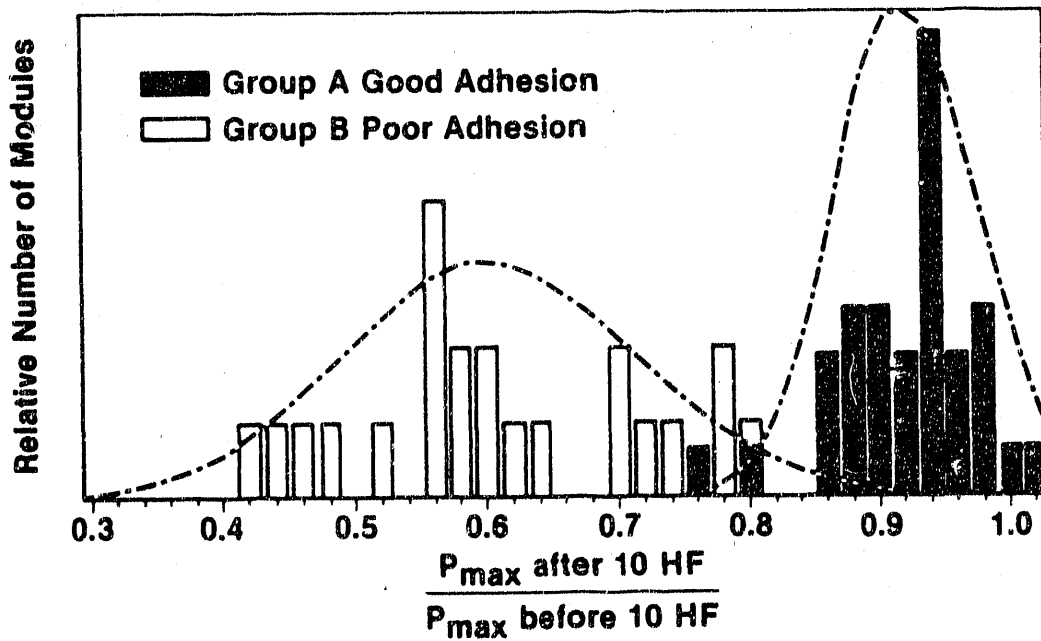


Fig. 4. CIS module stability after 10 humidity-freeze cycles.

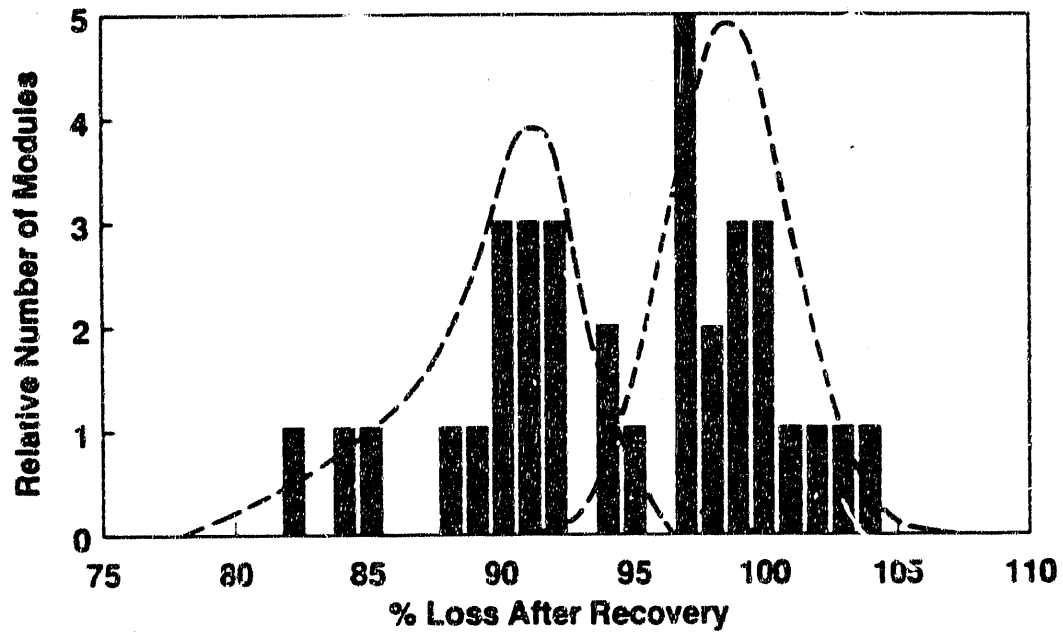


Fig. 5. CIS module stability after 10 humidity-freeze cycles and recovery.

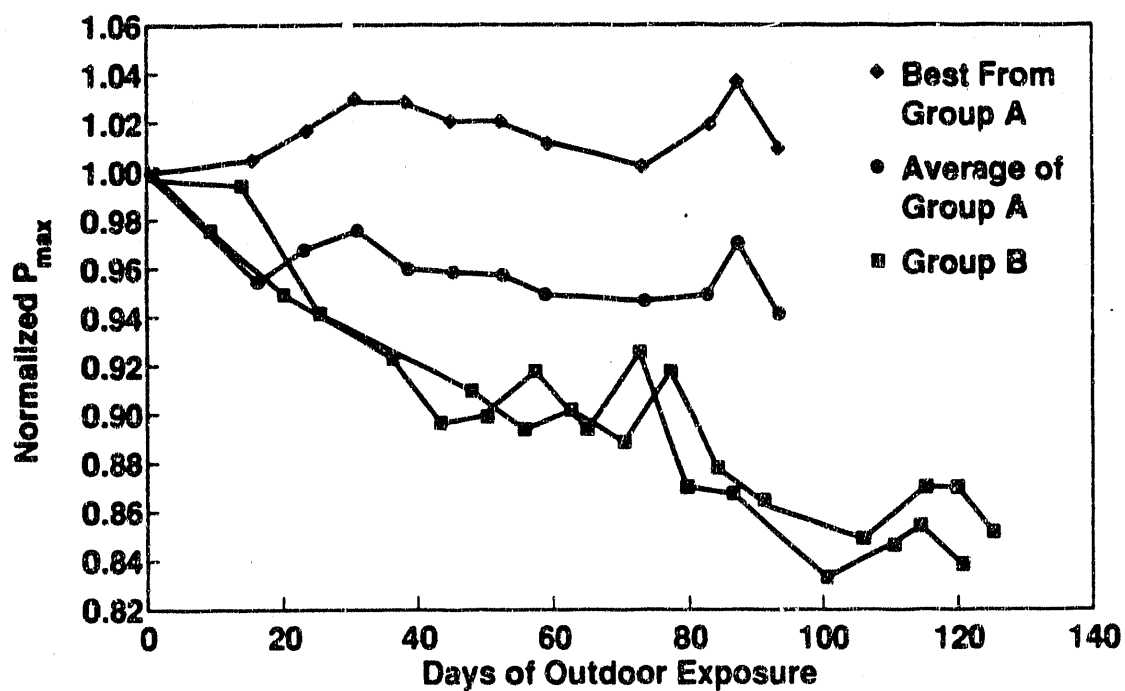


Fig. 6. Dependence of CIS stability outdoors on processing.

RELIABILITY STUDIES
OF
EUREKA MODULES

CHRONAR
CORPORATION

J. GREZ
J. KOLESAR
F. KAMPAS

**CHRONAR CO
ENCAPSULATION GROUP**

**M. GHERDAN
J. GREZ
J. KOLESAR
H. MATAS
G. MCCOMISKEY
P. SCHLAGEL**

EUREKA MODULE DESIGN FEATURES

a-Si Thin Film PV

31" x 61"

Glass/EVA/Glass Laminate

1/2" wide Border Isolation

Absence of Conducting Frame

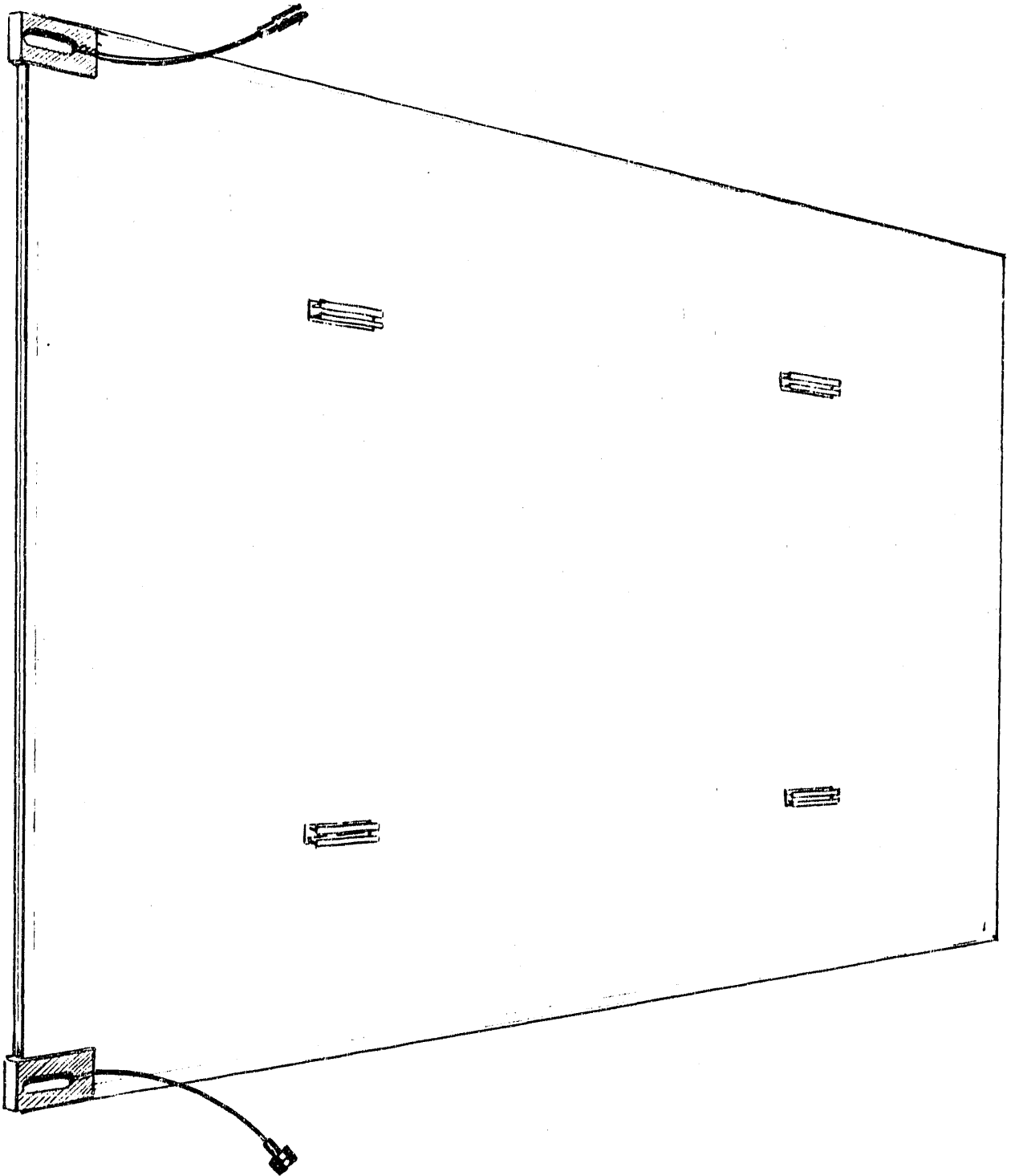
Mounts are interior to Module

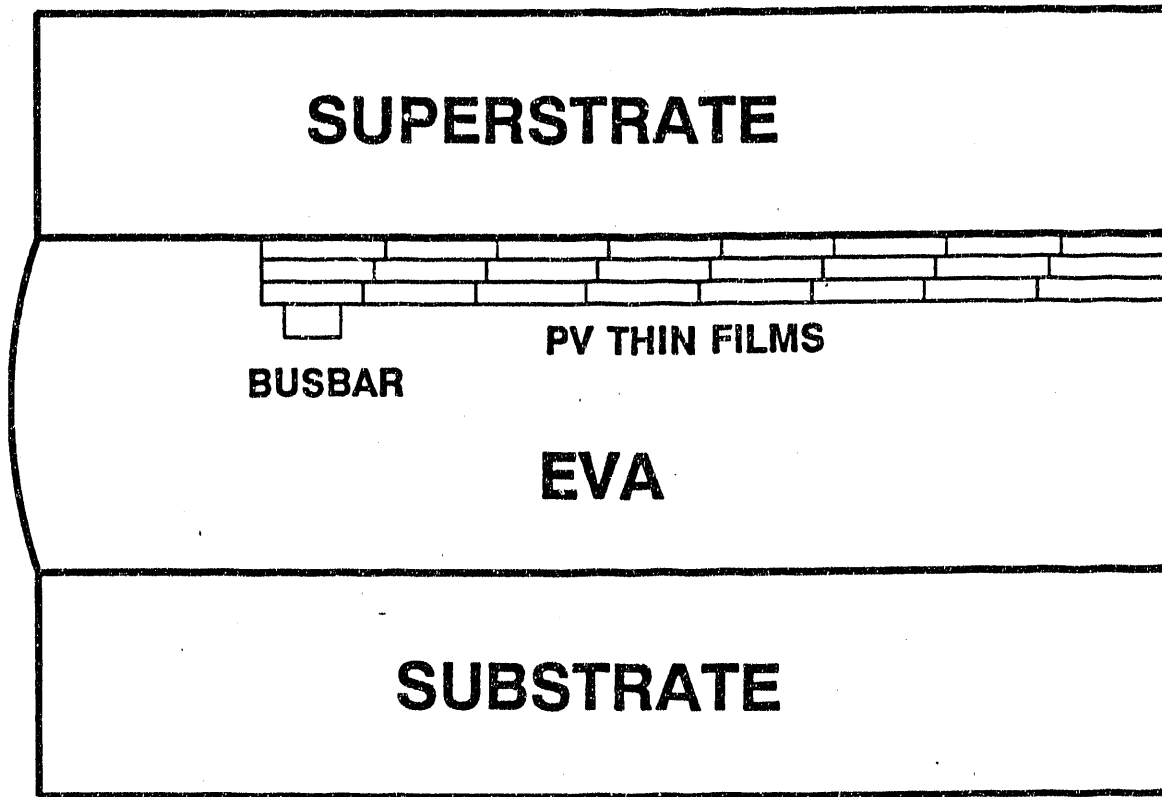
Sealed Connectors on Wires

Ultrasonically Bonded Busbars

Double Strength Glass

50 Watts Stabilized





EUREKA MODULE HOT SPOT TEST

A 1'x3' version of a Eureka Module went through the Hot-Spot test in UL 1703, performed at room temperature, with no change in efficiency and no visible damage.

A full size Eureka Module is currently being tested at 50 C.

EUREKA MODULE BYPASS DIODE THERMAL TEST

This test has not been carried
out at the present time.
The location of the bypass diode
has not been established.

EUREKA MODULE

HAIL IMPACT TEST

Two Eureka Modules were tested by Southern Electric International. They withstood without damage impact of 1" diameter ice balls at 52 mph. The modules were not damaged until corner target locations were struck with ice balls travelling at 120 mph.

EUREKA MODULE MECHANICAL LOADING TEST

This test is scheduled to
be performed in the next month.

EUREKA MODULE THERMAL CYCLING

Chronar has only one environmental chamber that can hold a full size Eureka Module, and it is being used for humidity/freeze cycling. A Eureka Module was cut in half and one of the halves thermally cycled 200 times in a smaller chamber. It showed a peak power drop of 5%.

EUREKA MODULE

HUMIDITY/FREEZE CYCLING

The average change in power output of a Eureka Module resulting from humidity/freeze cycling is -2%.

EUREKA MODULE

WET HI-POT TEST 1

In order to pass the Wet Hi-Pot Test and the Wet Insulation Test, we adopted a commercially available sealed connector. This connector can pass the Wet Hi-Pot test (completely immersed) after humidity/freeze cycling. Modules with this connector on them are currently undergoing humidity/freeze cycling.

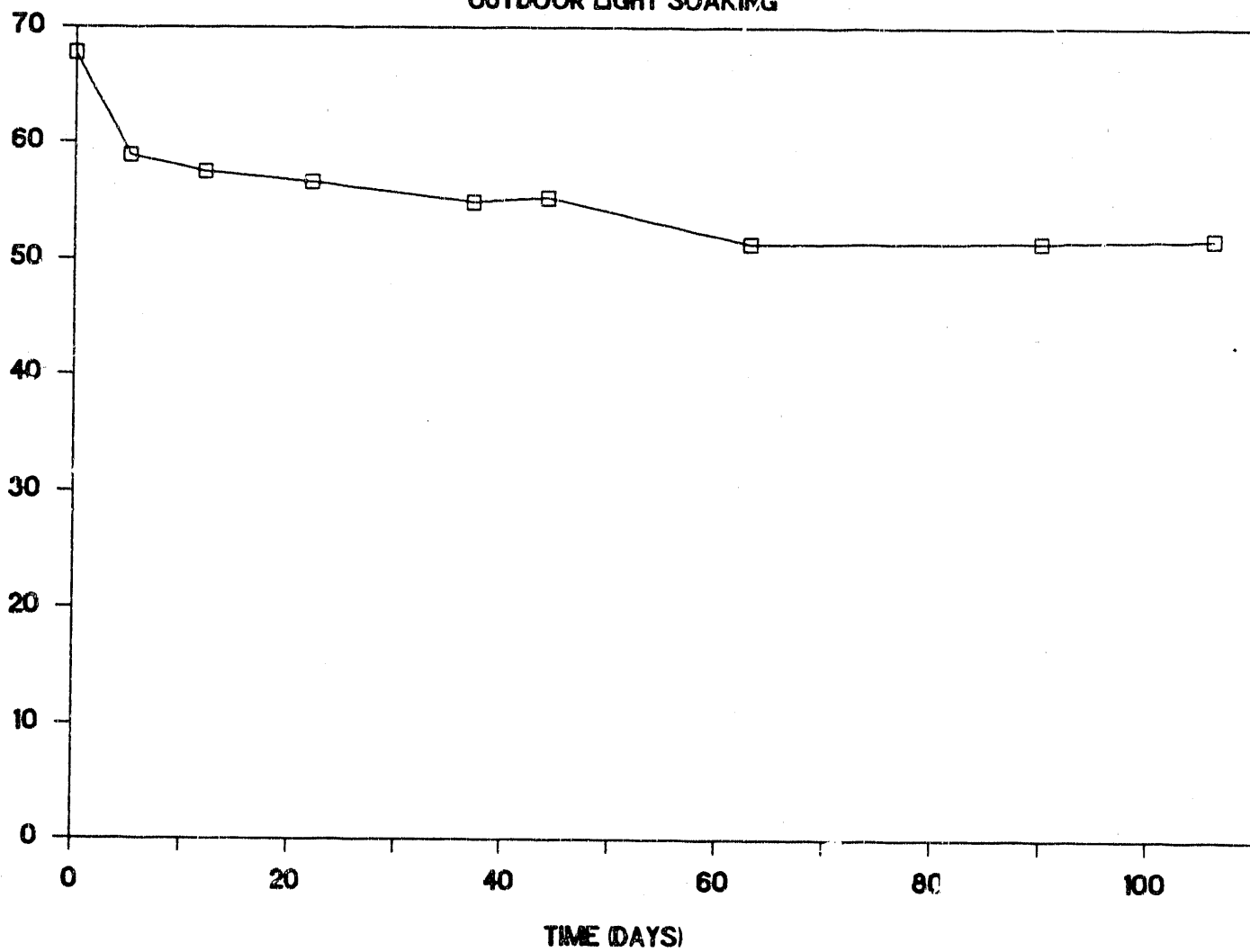
EUREKA MODULE

WET HI-POT TEST 2

Leakage currents from the long sides of Eureka Modules are typically about 4 microAmps and go up less than a factor of two on humidity/freeze cycling.

EUREKA MODULE

OUTDOOR LIGHT SOAKING



Encapsulation and Termination Processes for High
Reliability of Thin Film Modules

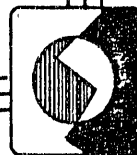
Gilbert Duran, UPG

Paper Not Available at Time of Printing

**Photovoltaic Power Systems
and
The National Electric Code®**

**A Handbook of Recommended
Installation Practices**

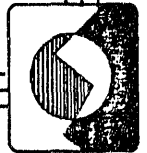
**John Wiles
Southwest Region Experiment Station
New Mexico State University
Las Cruces, New Mexico**



SOUTHWEST REGION EXPERIMENT STATION

Objectives

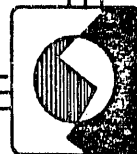
- **Safe, Reliable, Durable PV Systems**
- **Knowledgeable Manufacturers, Dealers, Installers, Consumers, and Inspectors**



SOUTH WEST REGION EXPERIMENT STATION

Method

- **Wide Dissemination of this Handbook**
- **Technical Interchange**
- **Seminars for Electrical Inspectors, Utilities, and Dealers/Installers**
- **Articles in Popular Magazines**



Contributing Factors

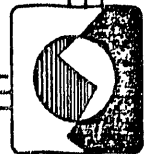
- Grass Roots Faction
- Code Applies for all Voltages—Even Less than 50V
- Inspectors not Familiar with DC or PV Systems
- DC Equipment is Hard to Find
- Advertising Says PV is Do It Yourself
- Few UL Tested Products
- Installers are not Familiar with PV or Code



SOUTHWEST REGION EXPERIMENT STATION

PV Problems

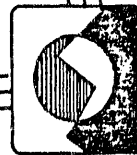
- **Unsafe Wiring Methods**
- **No Overcurrent Protection**
- **Misuse of UL Equipment**
- **Inadequate Disconnects**
- **No Short-Circuit Protection**
- **Use of Nonapproved Components**



SOUTHWEST REGION EXPERIMENT STATION

Unsafe Wiring

- Splices Outside Boxes
- Currents in Grounding Conductors
- Indoor Rated Cable Used Outdoors
- Single Conductor Cable Exposed
- "Hot" Fuses



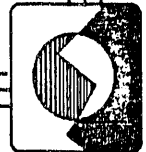
SOUTHWEST REGION EXPERIMENT STATION

No Overcurrent Protection

- Array Wiring
- Battery to Inverter Wiring

Misuse of UL Equipment

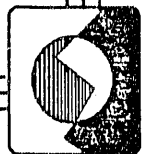
- Modules-Strain Reliefs/ Moisture
- BOS-Improper Connections



SOUTHWEST REGION EXPERIMENT STATION

Inadequate Disconnects

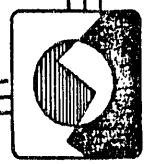
- No Way to Isolate Equipment
- Not Properly Rated—DC and Current
- Unmarked/Not Grouped
- Undervoltage



SOUTHWEST REGION EXPERIMENT STATION

No Short-Circuit Protection (Particularly in Systems with Batteries)

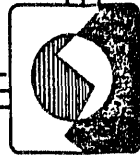
- **Switches, Fuses, Circuit Breakers Cannot Handle Short-Circuit Currents**
- **Possible Fire Hazard**



SOUTHWEST REGION EXPERIMENT STATION

Short-Circuit Currents

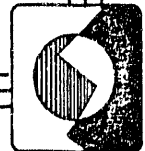
- 6 Volt 220 A-H Battery
 - 8,000 Amps - Fraction of Millisecond
 - 5-6,000 Amps - 2 to 10 Seconds
- Battery Bank—Larger Cells—?
- DC Rated Fuses and Circuit Breakers
 - 4,000-5,000 AIC
- Current Limiting Fuses Required
 - 125 VDC - 20,000 AIC - 100 Amp
 - Peak Let Through 3,500-4,500 Amps



SOUTH WEST REGION EXPERIMENT STATION

Nonapproved Components

- Auto Fuses
- AC Switches and Fuses
- Nonlisted Wire



Recommendations

- **PV Installers Use or Become Licensed Electricians**
- **Installers Learn the NEC**
- **PV Systems be Inspected by Authority**
- **Build Equipment to UL Standards**
- **Use Recognized Components**
- **PV Industry Educate Public and Upgrade Systems**
- **Inspectors Learn PV and DC**



SOUTHWEST REGION EXPERIMENT STATION

NEC CLARIFICATIONS

- Switching of Grounded Conductor
- Small System Requirements
- USE vs. UF Module Conductors
- Ampacity of Source and Inverter Conductors
- Current-Limiting Overcurrent Devices
- Multiple Voltage Systems



STABILITY RESULTS

ON

CdS/CdTe

SUBMODULES

By

Scot P. Albright, Rhodes R. Chamberlin

Under SERI Subcontract ZN-0-19019-1

AT

PHOTON ENERGY, INC.

***9650A Railroad Dr.
El Paso, TX 79924***

SUMMARY

The reliability of a large-scale photovoltaic module is probably the most important performance parameter related to any photovoltaic product. It is also the most difficult to extrapolate to a real time base from short term accelerated or real time reliability testing.

This paper attempts to describe a methodology utilized at Photon Energy Inc. (PEI) that forms an early basis for making reasonable reliability projections for a relatively new product. Many of the details have been given earlier.[1]

Utilizing both accelerated testing methods and real time outdoor life testing methods, the following statements can be made:

- * Thermal cycling experiments indicate there are no significant issues due to glass-metal bonding in the PEI design.
- * The humidity freeze thermal cycling testing regime indicates that further improvements can still be made in order to better insure the long-term reliability of the product.
- * Water permeability values into the modules of less than 50 mg per year per linear foot of edge are becoming the norm.
- * Early life testing results at SERI (and PEI) indicate no significant inherent stability problems with this technology.

INTRODUCTION

It has long been observed that thin film photovoltaics in general must be well encapsulated in order to withstand the extremes of humidity and temperature in the outdoor environment. Identification of the issues related to encapsulation techniques was primarily based on a review of Jet Propulsion Laboratory (JPL) papers and meetings with R. Ross's group at JPL[2-3]. A number of issues were defined during this period.

The objectives of the program at PEI are designed to :

- * Identify issues
- * Present and evaluate solutions
- * Insure that a viable product is being produced

Within this program, the general categories of experimental focus related to these objectives include:

* Accelerated life testing

1. Thermal cycling - structural integrity
2. Humidity freeze cycling - structural integrity and permeability
3. Permeability of water vapor

* Real Time Reliability Studies

1. Outdoor changes
2. Permeability of water vapor

EXPERIMENTAL

The categories outlined above will be reviewed. The thermal cycling and humidity-freeze cycling tests have been done primarily at the SERI Outdoor Reliability and Testing Laboratory.[4] The water permeability studies were begun by JPL and continued at PEI.

Accelerated Life Testing

The major issue for encapsulation is the rate of water permeability into the structure. A simple, low cost, highly illuminating means for determining leakage of water vapor is reviewed.

The test modules evaluated here were assembled by edge-sealing a metal backsheet to a 24" X 24" X 1/8" tin oxide coated glass substrate on a 0.5" border. For permeability studies of the various adhesive and techniques, smaller substrates were used (4" X 6" X 1/8"). Placed inside the internal volume was a Humiseal humidity indicator strip that had been dried completely at 65°C (completely blue in color). The indicator strip turns various shades of pink as the amount of water present increases.

The stripes contain a dessicant and will therefore absorb some water itself prior to indicating pink. Calibration of this strip to determine this limit of detection was undertaken. It was found that the limit of detection for water, from a completely dry state, increased the weight of the strip by 10 ± 5 mg. These strips respond within minutes to their surround.

The actual thermal cycling tests were done at JPL and SERI. Modules were cycled from -40°C to 90°C four(4) times per day for 200 cycles. At various times through the procedure the modules were removed from the chamber and visually inspected. The relative humidity(RH) during these cycles was <25% at the highest temperatures (ambient RH at room temperature).The only additional parameter for the humidity freeze thermal cycling tests was that the relative humidity was maintained at ~85% RH at the 85-90°C temperature.

The permeability to water vapor within a structure was determined using the 10 mg limit of detection to water vapor of the Humiseal strips and the time required to turn the strip pink in a specific environment. By observing the sample at regular intervals, one can determine the time it took to begin turning pink (the limit of detection) quite accurately. Since the indicator is known to absorb ≈ 10 mg of water at that point, the permeability is determined within roughly 100% of the value. That magnitude of error is quite accurate enough to allow for a number of determinates.

With techniques such as these in hand, one can easily address the major issues relating to encapsulation. Thermal cycling (both wet and dry) and permeability to water vapor can form a good basis for extrapolation.

Real Time Reliability Studies

The measurement of performance changes over time in the outdoor environment is the primary means for life testing. However, as extrapolation from accelerated permeability studies is often extremely difficult to do with satisfactory confidence, it is necessary to have some baseline studies based on real time for determining permeability.

Performance monitoring on submodules has been undertaken by SERI Outdoor Reliability Testing Lab under Laxmi Mrig. These submodules were all under load during exposure. Testing was done approximately monthly.

In addition to performance monitoring, the baseline studies for water permeability in the field in El Paso were done using 12" X 12" X 1/8" substrate encapsulated on to a 3/16" border with a humidity indicating strip placed inside. The glass was painted black so that a similar temperature would be reached by these test modules as by a photovoltaic(PV) CdTe module in operation. These 2 samples were left outdoors for over 14 months.

RESULTS, DISCUSSION, AND CONCLUSIONS

The samples sent to JPL and tested at 85°C, 85% RH showed a number of adhesives that passed ≥ 10 mg water after as few as 180 to 300 hours. This made an excellent screen for choice of adhesives. One particular choice of material, design and method went for over 2,000 hours passing less than 10 mg of water. The perimeter of the 4" X 6" sample was 20" permeability of the design was therefore < 30 mg per year per linear foot at 85°C, 85% RH.

Structural integrity was also a major issue with the presence of glass to metal bond. The expansion coefficient differences had to be addressed properly. Thermal cycling tests were the obvious means to improve the method and design. A number of samples of different design were thermally cycled for up to 200 cycles. Many failed. A number of good designs showed no failures after 200 full thermal cycles up to the 12" X 12" size at JPL. Substrates measuring 24" X 24" also were found to satisfactorily pass 200 Cycles with no delamination problems at

SERI. Less than 10 mg of water had entered the module after these 200 cycles. The same 24" X 24" modules were then subjected to the humidity freeze cycling. After roughly 40 such cycles a failure of part of the edge bond was observed. Though there was a small statistical sample size (2) and the humidity freeze cycles were done after a fair amount of stresses were already incurred, due to the previous cycling, modification of the edge design to minimize stresses due to formation of ice is presently being addressed.

The upper limit for the amount of water entering the modules during the humidity-freeze cycles can be approximated. In ~10 days approximately 10 mg of water had entered the structure. We might have used 40 since there were 40 cycles; We have also not included the contribution of the previous 200 cycles at 25% RH;; We have also not included the acceleration factor for diffusion at the 85 Celsius temperature that could be a factor of 8 to 16 over operating temperature. An incursion of 10mg water in 10 days is 3.7 g per year over 8 linear feet of bond line or .5 g water per year per linear foot.

Referring back to the outdoor permeability experiment noted earlier, it was found that after fourteen(14) months the pink color of the humidity sensor inside was apparent. This experiment started in August of 1989 and was extended over one winter and one summer prior to passing over 10 mg of water. The permeability calculated to be 2 mg per year per linear foot of edge. It should be noted that this experiment was done in El Paso where winter RH is often <10 % and the RH in the summer 40 to 70%. The permeability of such a design is, however, sufficiently low that reasonable lifetime may be extrapolated.

The results for real time life tests are given in Figure 1.[5] For the majority of submodules tested, the stability appears quite good. The initial differences in preparation between each of the submodules was one of a secondary type seal, (i.e. edging method). There does not appear to be any correlation between that initial experiment design and the observed life testing variations. The small degradations observed on some samples have therefore attributed to quality control and assurance issues.

In any event, it is apparent from this figure that CdTe based submodules do not have any significant inherent stability problem.

In summary, the highlights of the reliability testing done at JPL, SERI, and PEI are:

- * At JPL - 4" X 6" edge sealed modules survived over 200 thermal cycles from -40°C to 90°C without any signs of delamination (25% RH). No high humidity or freeze cycles were done at JPL.
- * At SERI - 24" X 24" edge sealed modules survived 200 thermal cycles from -40°C to 90°C without any signs of delamination and without passing 10 mg of water.

- * At SERI - Over 270 days of outdoor life testing has shown little, if any, degradation of the PEI modules tested.
- * At PEI - Permeability values into the modules of less than 50 mg per year per linear foot of edge are becoming the norm.
- * At SERI - Humidity freeze thermal cycling results indicate that further improvements can further extend the confidence of extrapolating lifetime.

REFERENCES

- 1 Ackerman, B.; Albright, S.P. "Encapsulation and Life Testing Issues for One Foot Square Cds/CdTe Modules" Presented at *Photovoltaic Thin Film Module Reliability Testing and Evaluation Workshop*, Sponsored by SERI, June 1989, Golden, Colorado; Published in *Solar Cells*.
- 2 G.Mon, L.Wen, and R.Ross, Jr., "Water-Module Interaction Studies", Presented at the 20th IEEE Photovoltaic Specialists Conference, Las Vegas, NV, Sept. 1988.
- 3 G. Mon, R.Ross, P.Willis, A.Garnica; JPL, Private Communication, 1987-89.
- 4 R. DeBlasio, Laxmi Mrig, SERI Outdoor Measurement and Reliability Testing Laboratory, Private Communication, 1989-1990.
- 5 Laxmi Mrig, SERI Outdoor Measurement and Reliability Testing Laboratory, Private Communication, 1989-1990.

OUTDOOR LIFE TESTING DATA MEASURED AT SERI

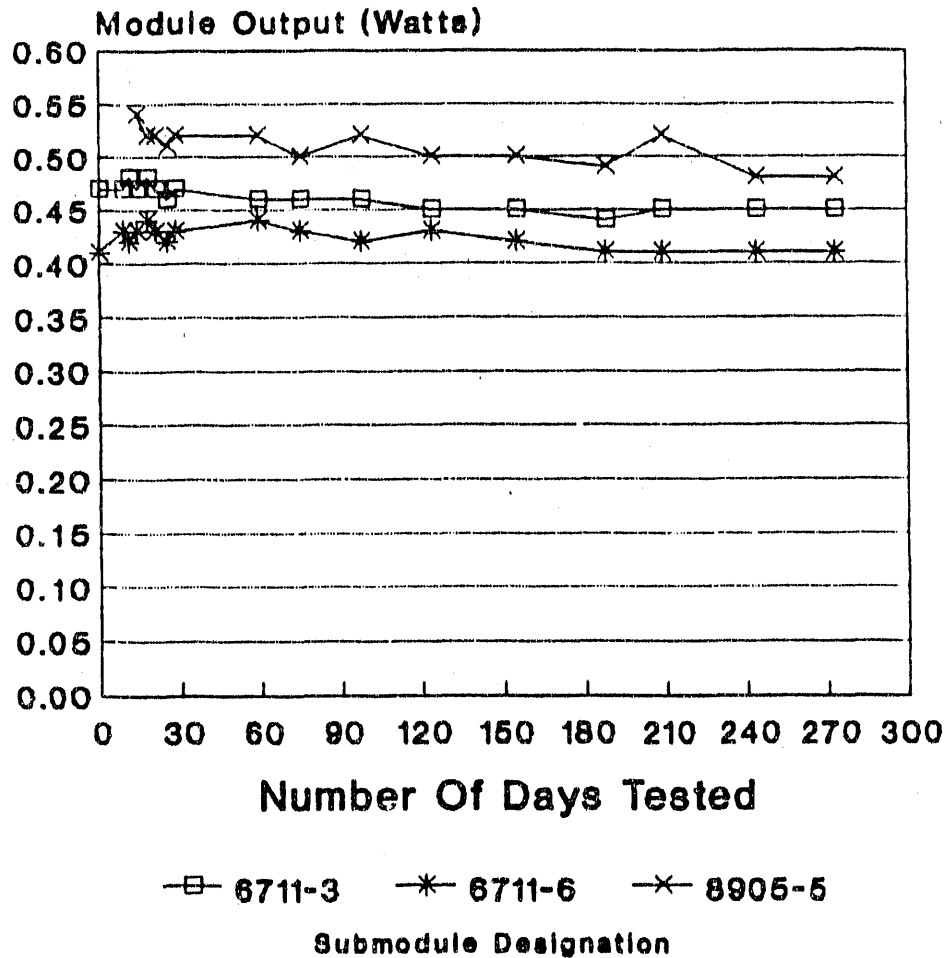


Figure 1: Outdoor Life Testing
Data Measured At SERI



Factory and Field Test Experience

- **Steve Hester — PG&E**
- **Walt Stolte — Bechtel**
- **Bill Clements — Bechtel**
- **Tim Townsend — Endecon**
- **Paul Hutchinson — Endecon**

PV Module Reliability Workshop

October 25, 1990



Factory and Field Test Objectives

- **Factory:**
 - **Demonstrate Compliance with Standards and Designs Criteria**
 - **Reliability/durability**
 - **Electrical performance**
 - **Mechanical strength**
 - **Safety**
 - **Corrosion resistance**



Factory and Field Test Objectives

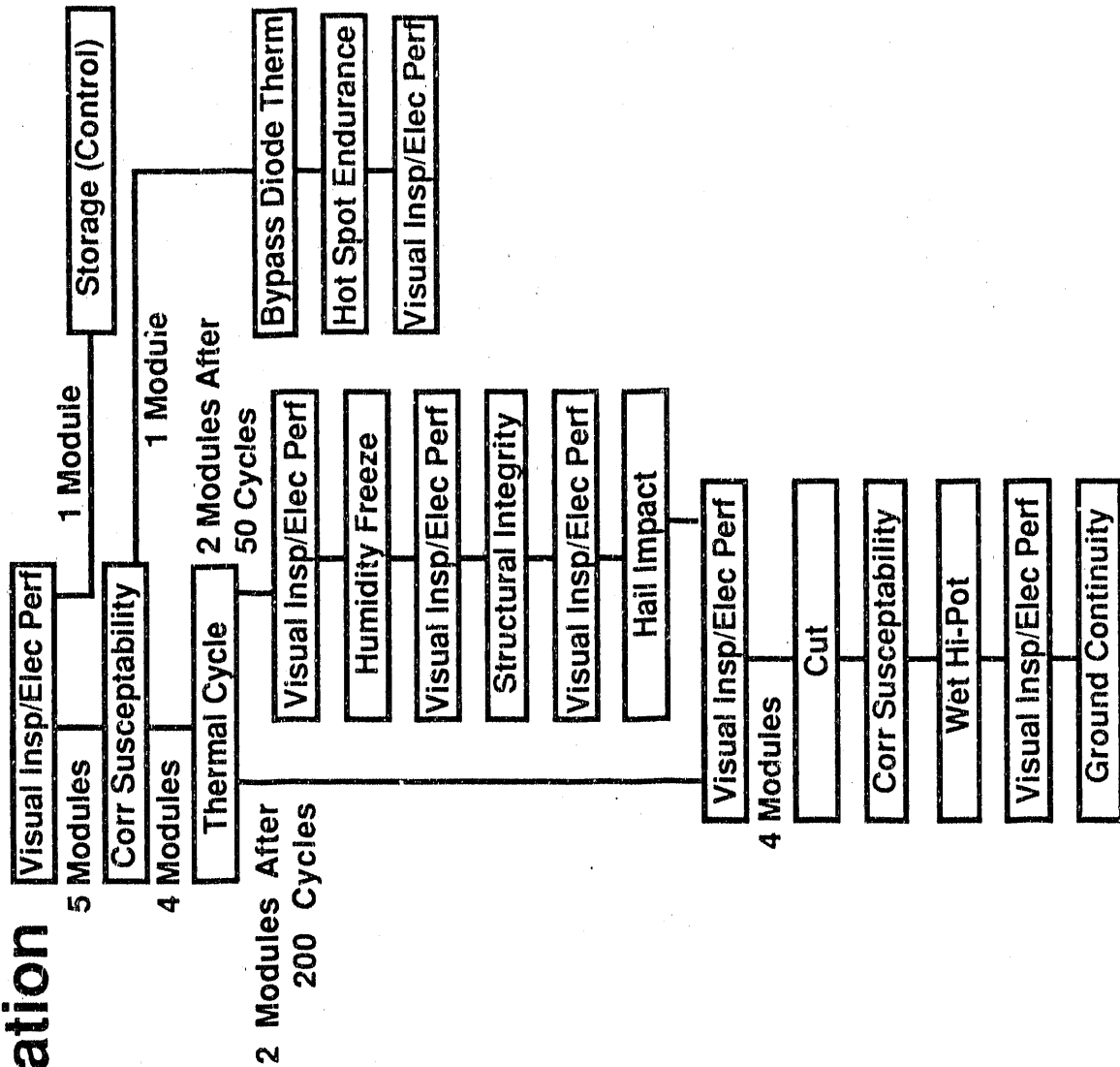
- **Field:**
 - **Demonstrate Satisfactory Shipping and Installation Practices**
 - **Engineering review**
 - **As-built inspection**
 - **Wet megger (electrical hi-pot) test**
 - **Field I-V curves**
 - **System protection functional check**
 - **Performance test period (payment)**



Factory Test Experience

- Qualifications Test Sequence
 - Based on JPL Block 5 and Sandia
- New "Wet" Portions Added
 - Wet hi-pot (ohmmeter)
- Few Small Companies Have All Equipment to Qual Test In-House
- Some Outside Labs Are Not Able to Do All Qual Test Steps
- "Tough" but "Necessary" Tests

PVUSA Qualification Test Sequence





Status

EMT-1

Siemens (ARCO) (Xtal-Si) — Operating Array

Sovonics (a-Si) — Operating Array

Utility Power Group (a-Si) — Operating Array

Solarex (Poly-Si) — Installed/Performance Test

ENTECH (concentrator) — Fabricating Modules



Status

EMT-2

Siemens (CIS) — In Qual Test

AstroPower (Thin Poly-Si) — Module Development

Photon Energy (CdS/CdTe) — Module Development



Status

US-1

Siemens (Xtal-Si) — Installing at Davis

IPC (Mobil Ribbon-Si) — In Qual Test

Chronar (a-Si) — Production Development



Field Wet Resistance Tests (Wet Megger Test)

- Siemens EMT-1 (400 modules)
 - Initial Test (12/88)
 - 3 modules failed (pinholes on back)
 - 2 bypass diodes failed
 - 12/89
 - No failures, modules or diodes
 - 9/90
 - No module failures
 - 5 bypass diodes failed



Field Wet Resistance Tests (Wet Megger Test)

- Sovonics (1200 modules)
 - Davis
 - Preliminary tests (9/88)
 - Prototype modules, (600, 2x4) significant failures
 - Initial tests (2/89) (1200 module, 1x4)
 - 4 modules failed
 - 1 module with bubble failed
 - 9/89
 - 12 modules with delaminations, no failures
 - 2/90
 - 25 modules with delaminations, no failures
 - Maui
 - (10/89 - 10/90) (1200 modules)
No wet megger tests conducted
 - 12 modules failed due to overheated junction box-electrical connection



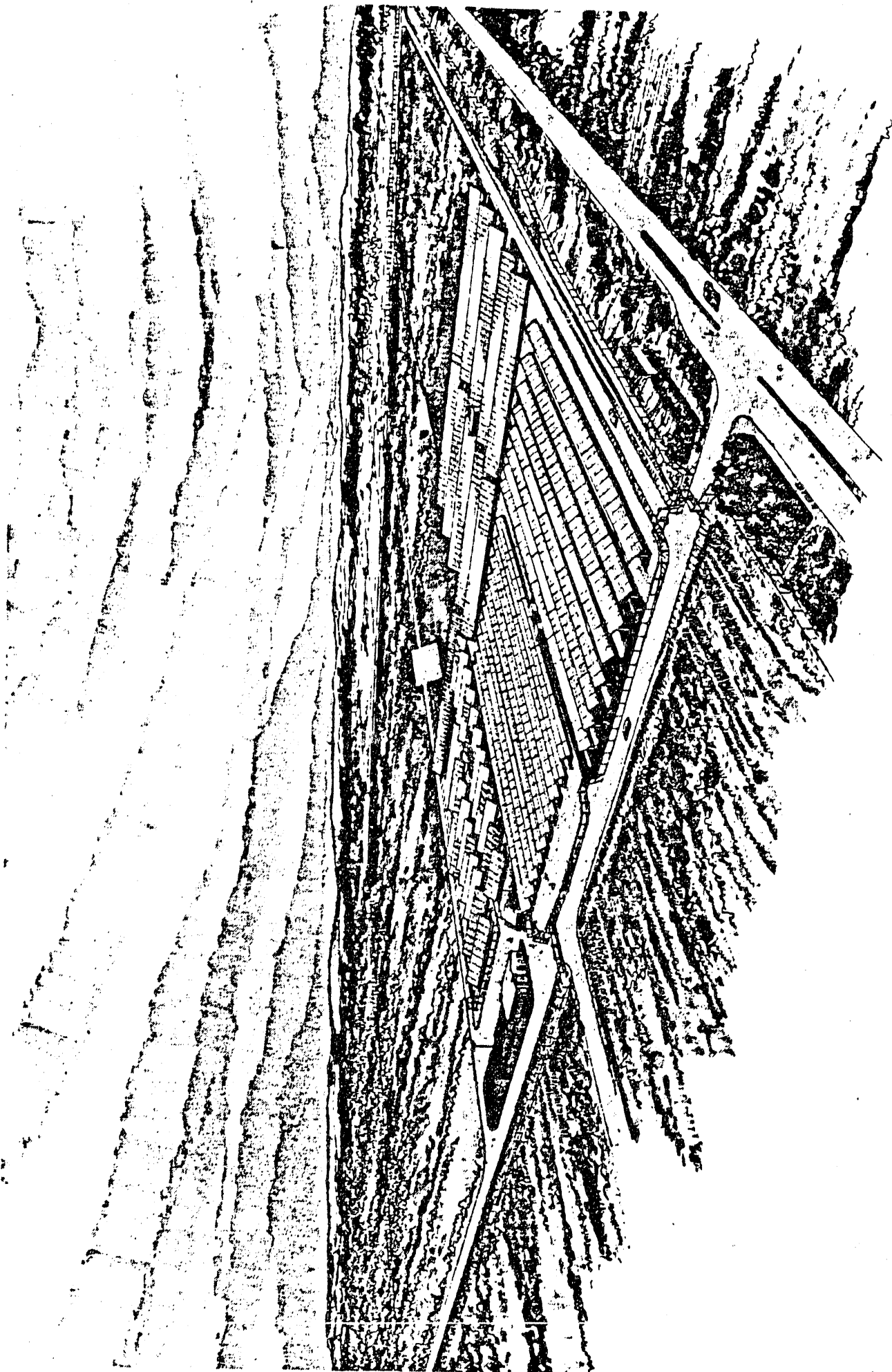
Wet Resistance Tests (Field Wet Megger Tests)

- UPG (4992 modules)
 - Initial tests (12/89)
 - 4 modules with glass cracked failed
 - 1 panel wiring failure
 - 2 unknown failures
- Solarex (336 modules)
 - Initial tests (4/90)
 - 75% of sample failed
 - Tefzel holes, solder bumps
 - Output wire entrance (potting)
 - Re-installation/passed field test



Wet Resistance Tests (Field Wet Megger Tests)

- US-1 Systems
 - Siemens
 - Preliminary (1/16 of array) (10/90)
 - Most bypass diodes fail
 - 2 cracked junction boxes failed
 - Diode repairs underway
- Chronar
 - Preliminary (7/90)
 - Wiring harness, module connections need better weather-proofing
 - Design improvements in progress



PHOTOVOLTAICS FOR UTILITY SCALE APPLICATIONS (PVUSA)

PACIFIC GAS AND ELECTRIC COMPANY

(ARTIST'S CONCEPT) DAVIS SITE



Session 3:
Module Design and Encapsulation Research

SERI
SERD

ENCAPSULATION
PV M&P BRANCH

Possible causes of EVA Degradation in PV Modules

A.W. Czanderna

PV Measurements and Performance Branch

Advanced Module Performance Testing and Reliability Research Group

SERI

October 26, 1990

OBJECTIVES: MODULE DESIGN AND ENCAPSULATION RESEARCH

- Bring together industry/SERI/DOE/other
 - Exchange information
 - Promote team work
 - Sharpen focus on industry's need
 - Report on recent SERI assistance
- Address questions about module materials problems with a major emphasis on EVA
 - How real or extensive is the EVA problem?
 - What is published and generic?
 - What is not published? Can it be discussed?
 - What research/testing is in progress? planned?
 - What are key research/technology issues?
 - What are suspected degradation mechanisms?
 - What are areas where SERI can further assist in requested cooperation, testing, analysis, and research?

OUTLINE

Module Encapsulation Stability - Generic

Polymer Stability in a Solar Environment

EVA Degradation and Yellowing - Literature

Polymer Protection from UV; General and EVA

Possible EVA Degradation Mechanisms

An Experimental Testing Approach for Securing a More Stable Pottant

ENCAPSULATION
PV M&P BRANCH

ABOUT SERI - EXPERIENCE RELATED TO MODULE DURABILITY

SERI
SERD

Agency	Years	Topical Study Area	Technology*
ST	5-8	Stabilizing polymers (e.g., PMMA)	Mirrors/Ag
ER	8	Polymer/metal (oxide) interface reactions	Cu, Ag, Au/P
ER	8	Corrosion at interfaces-multilayers	Ag/glass mirrors
ST	10	Accelerated testing/weather-Ometers, QUV	Mirrors; G and P
ST/ER	10	Accelerated testing/solar simulator, T, laser, impurities	Cu, Ag, Au/P
ST	2	Soiling, cleaning, "hard" covers	Mirrors/P
SB	5	Water vapor sorption by polymers	Dessicant P

*P = polymer

STABILITY OF INTERFACES IN SOLAR ENERGY MATERIALS*

A. W. CZANDIERNIA

*Materials Branch, Solar Energy Research Institute,
 Golden, CO 80401, U.S.A.*

Received 2 July 1981

This paper is a review of various methods for interface analysis and how they are or could be used for studying the stability of interfaces in solar energy materials. First, a brief overview is given that explains why interfaces are crucially important for developing long-life, cost-effective, multi-layer, polycrystalline-thin film stacks for solar energy conversion systems (SECS). Second, broad categories of characterization methods, approaches and processes in interface science are reviewed and related to studies required for components in SECS, in which the importance of compositional analysis of interfaces is emphasized. These include surface area, real and clean surfaces, structure and topography, interface composition or purity, surface thermodynamics, equilibrium shape, diffusion, amount adsorbed and nature of adsorbate/solid interactions. Third, an overview is given for the solar-related research needs and opportunities in various topical areas in interface science. These topics include thin films; grain, phase and interface boundaries; oxidation and corrosion; adhesion; chemisorption, catalysis and surface processes; abrasion and erosion; photon-assisted surface reactions and photoelectrochemistry; and interface characterization methods. Finally, a brief review will be given concerning interface methods being used to approach typical current problems with reflector, polymeric, absorber and PV cell interfaces.

4.1. Silver interfaces

Silver has the most desirable solar reflectance property of any element (~97%) and will therefore require the least concentrator area to collect a given amount of solar radiation. Although silver itself is relatively unreactive, a fractional monolayer of adsorbed oxygen enhances its reactivity to atmospheric gases, such as water, carbon dioxide, sulfur dioxide, nitric oxide, etc. [76]. At room temperature and atmospheric pressure, nearly one monolayer of oxygen always can be expected on silver. Therefore, chemisorption of atmospheric gases initiates corrosive reactions and a degradation of the reflectance. The results of these reactions have yielded visually transparent areas in mirrors used in demonstration heliostat fields in time spans ranging from several months to a few years.

The state-of-the-art mirror system now in use is a glass second-surface silver mirror backed with copper and paint, as shown in fig. 3. Interfacial degradation reactions may begin at the silver/glass interface because of impurities at the interface. These may be

Table 5
 Some current problems with solar materials

System or component	Material(s)	Problem (1981)
reflectors	silver/glass	degradation
encapsulants/coatings	polymers/metal (oxides)	photodegradation, interface degradation
solar cell material	Cu ₂ S	degrade in O ₂ and H ₂ O
absorbers	black chrome, black cobalt	degrade at elevated temperatures
thin film solar cells	numerous	interdiffusion at junction

residual impurities resulting from the method of preparation, or the impurities may accumulate there because of radiation-induced transport processes of various ions in the glass. Deterioration of the mirror material may also result from interdiffusion of copper and silver, and reaction of the copper and then the silver with atmospheric gases. The rate of permeation of the paint backing by atmospheric gases may increase as the paint weathers in the sun and elements. For this system, the characterization and study of the glass/silver, silver/copper and copper/paint interfaces before and after various stages of use are clearly required to understand the multilayer mirror stack shown in fig. 3. The methods of characterization outlined in section 2.4, especially those of ISS, XPS, AES and SIMS, are clearly applicable to this problem.

For solving the mirror degradation problem, it is important to prepare model mirror systems and secure commercially made mirrors now in use, and to elucidate the mechanisms of the reactions that result in deterioration of the reflectance of the mirror. Characterization of the systems will include using optical, diffraction, adhesion and corrosion resistance measurements in addition to various methods of interface analysis (ISS, XPS, AES, SIMS, SEM, IR, etc.). The mechanisms of reactions will be deduced by measuring the kinetics of pertinent surface reactions (e.g. Ag-O₂ + SO₂ (g) + H₂O (v) → Ag₂O, + other products), identifying the sources of contaminants that enhance the degradative reactions, and carrying out accelerated tests of the interfacial reactions. Both S/G and S/L interfacial reactions require study as well as

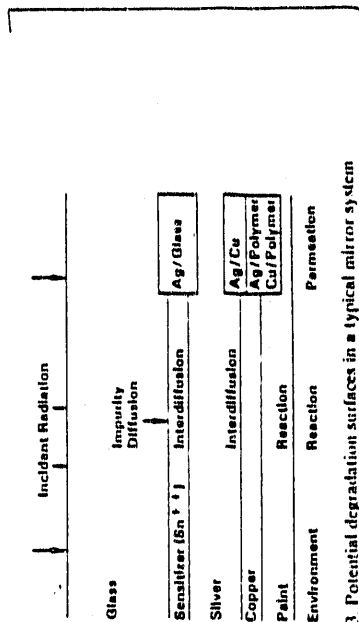


Fig. 3. Potential degradation surfaces in a typical mirror system

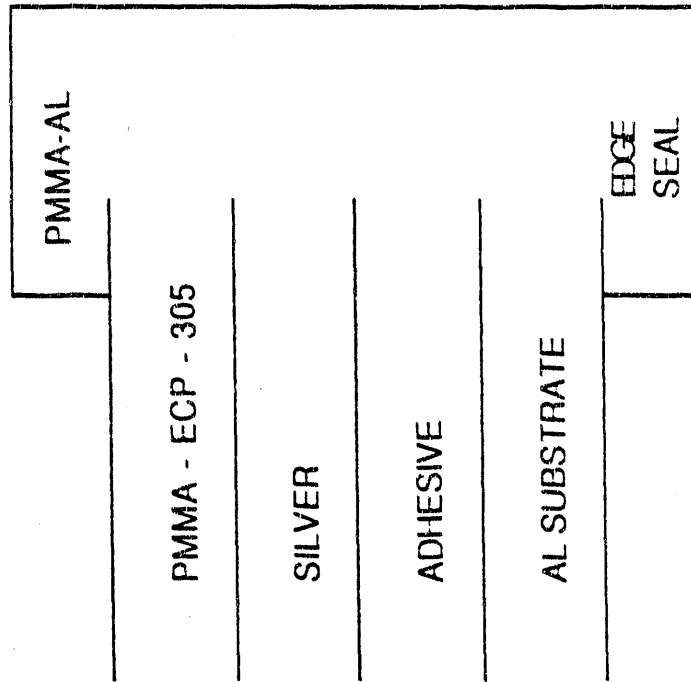
any interfacial degradation reactions at the polymer/copper (or other S/S) interface. Some of these approaches have been used and initial results were reported in a previous issue of this journal [77]. Important insight into the problem has been gained by using SEM, XPS, AES and SIMS by various authors. Extensive detailed study will be required to translate these initial results into an understanding of the degradation of reflectance in silver mirror systems. However, it is reasonable to anticipate that a significant improvement in mirror stability will result from using different glasses and/or backing materials and different fabrication processes. Modifications of materials and/or processes will follow once the cause of the degradation is understood.

Polymeric materials are important to solar technologies for use as protective coatings, encapsulants and backings for mirrors. In each of these cases, the "protected material" is known to degrade when exposed to the various parameters of a solar environment.

The problem is that the polymer/protected material interface may experience a degradative reaction. The protective value of the polymer may deteriorate because the UV and/or environmental parameters change the properties of the polymer.

SILVER/PMMA MIRROR EXPERIENCE

- Water Soak: Edge Seal; 10X Longer, R.T.
- Stress Causes Tunneling; Size >12"
- Tunneling is Always at PMMA/Ag
- Replace Al with Glass - No Tunneling (tests in progress)
- Stress May be from Water Sorption (~2 wt.%)
- PMMA/Ag/Adhes/Glass; Stable at 80°C, 80% R.H., Pollutants.
- Above plus UV; ALWAYS required for PMMA degradation



ACKNOWLEDGEMENTS

H. Chapman, Siemens Solar

M. Kardauskas, Mobil Solar

K. Mitchell, Siemens Solar

E. Tornstrom, Mobil Solar

J. Wohlgemuth, Solarex

J. Pem, SERI

R. DeBiasio, SERI

A. Nelson, SERI

S. Asher, SERI

J. Webb, SERI

P. Longrigg, SERI

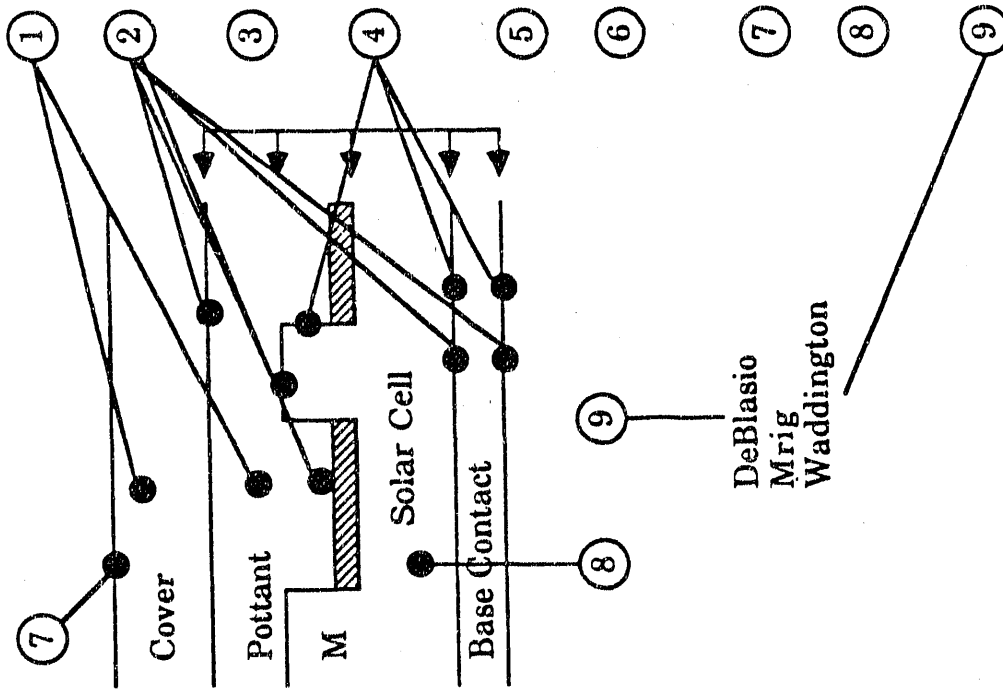
MAJOR POINTS

- Module durability is more than an EVA problem
- EVA degradation is not new
- What is not known about EVA degradation

OVERALL STRATEGY - EVA

- Understand why EVA is degrading
- Use/develop analytical capabilities
- Develop collaboration/cooperation with PV manufacturers
- Expand effort for securing a better pottant and more stable encapsulated module systems

SOME KEY RELIABILITY ISSUES: MODULE DEGRADATIVE REACTIONS/PROCESSES



1 Photo-thermal degradation of polymers (pottants, covers, screens, adhesives)

2 Catalyzed degradation polymers/M or oxides; interdiffusion.

3 Permeation of H_2O , O_2 , other G, into module.

4 Electrochemical corrosion, corrosion, E-induced or e-injected pottant degradation, delamination of M or other components.

5 Accelerated aging and lifetime prediction.

6 Electrical isolation of cell string and other module components.

7 Soiling of cover plate

8 Stability (e.g., $h\nu \rightarrow a-Si:H$) of cell materials

9 Plus, interim reliability qualification.

*Reliability issues of the solar cell materials themselves (e.g., light stability in a-Si:H) are not included above.

SERI
SERD

ENCAPSULATION
PV M&P BRANCH

ENCAPSULATION STABILITY

- Multilayer Stack on Either Side of Active Device Material
- Extremely Complex to Predict - Large Number of Variables
 - T Effects Including Cyclic T
 - Compositional Effects
 - Concentration of H₂O and O₂
 - Impurities
 - Electric Field Influences
 - UV Degradation
 - Slow Time Dependent Effects
 - Interface Reactions
 - Interdiffusion

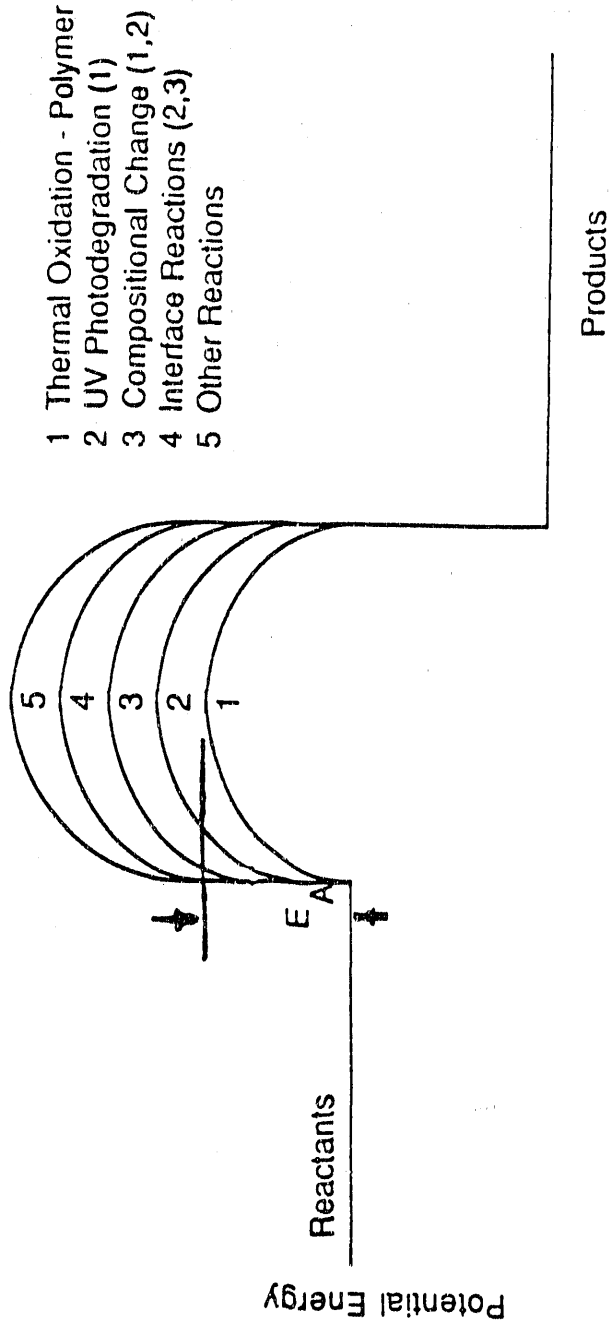
SERI
SERD

ENCAPSULATION
PV M&P BRANCH

POTTANT/INTERFACES:STABILITY?

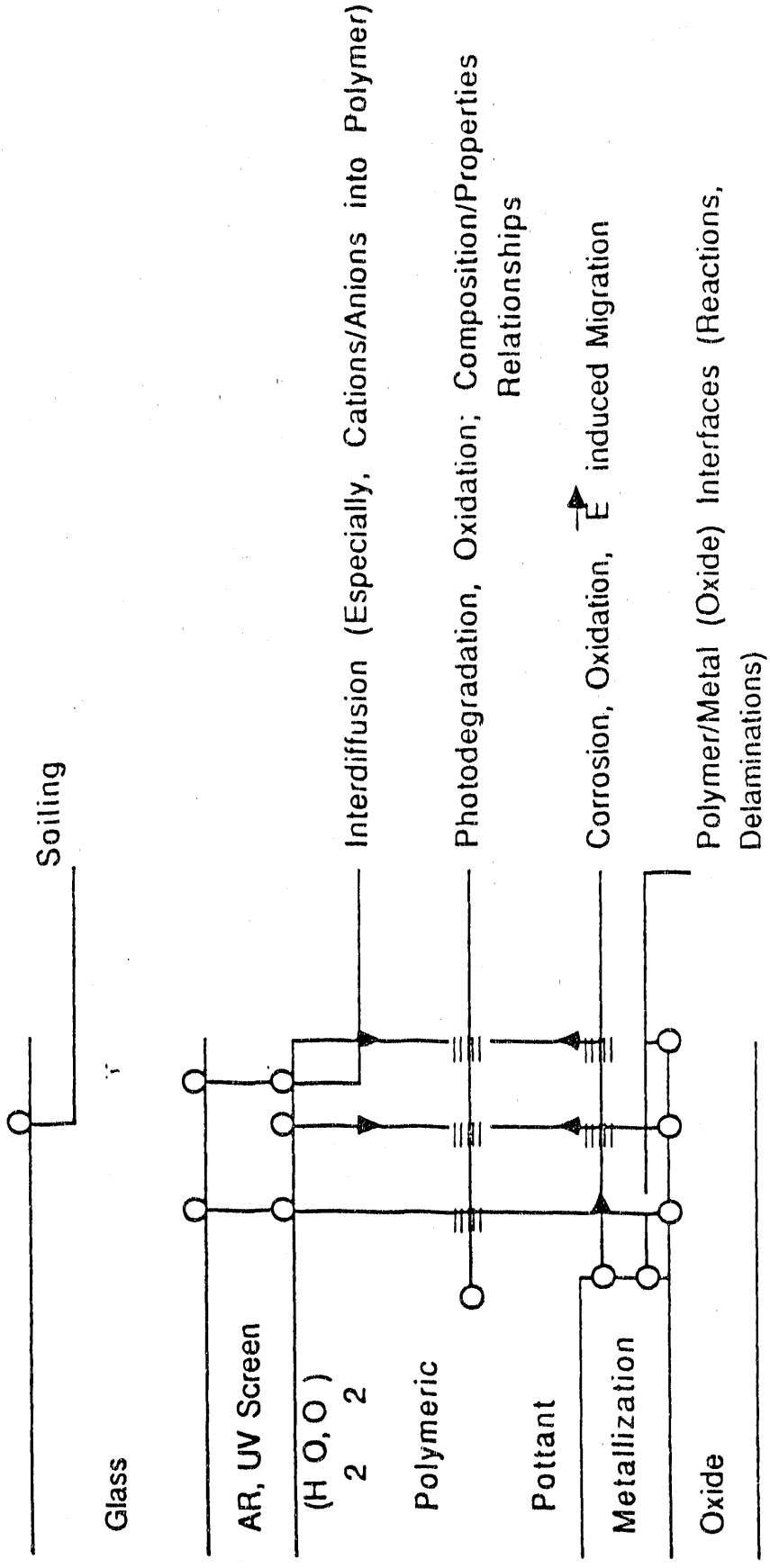
- Thermodynamically Unstable - Always in Higher G State
- Always Want a Lower Energy Surface
- "Stability" Depends on Kinetic Processes; Composition
- At Any T, One Reaction Usually Predominates
- Usually Many Reaction Paths with Different E_A .

POTANT/INTERFACES: EXAMPLES OF DEGRADATIVE REACTIONS

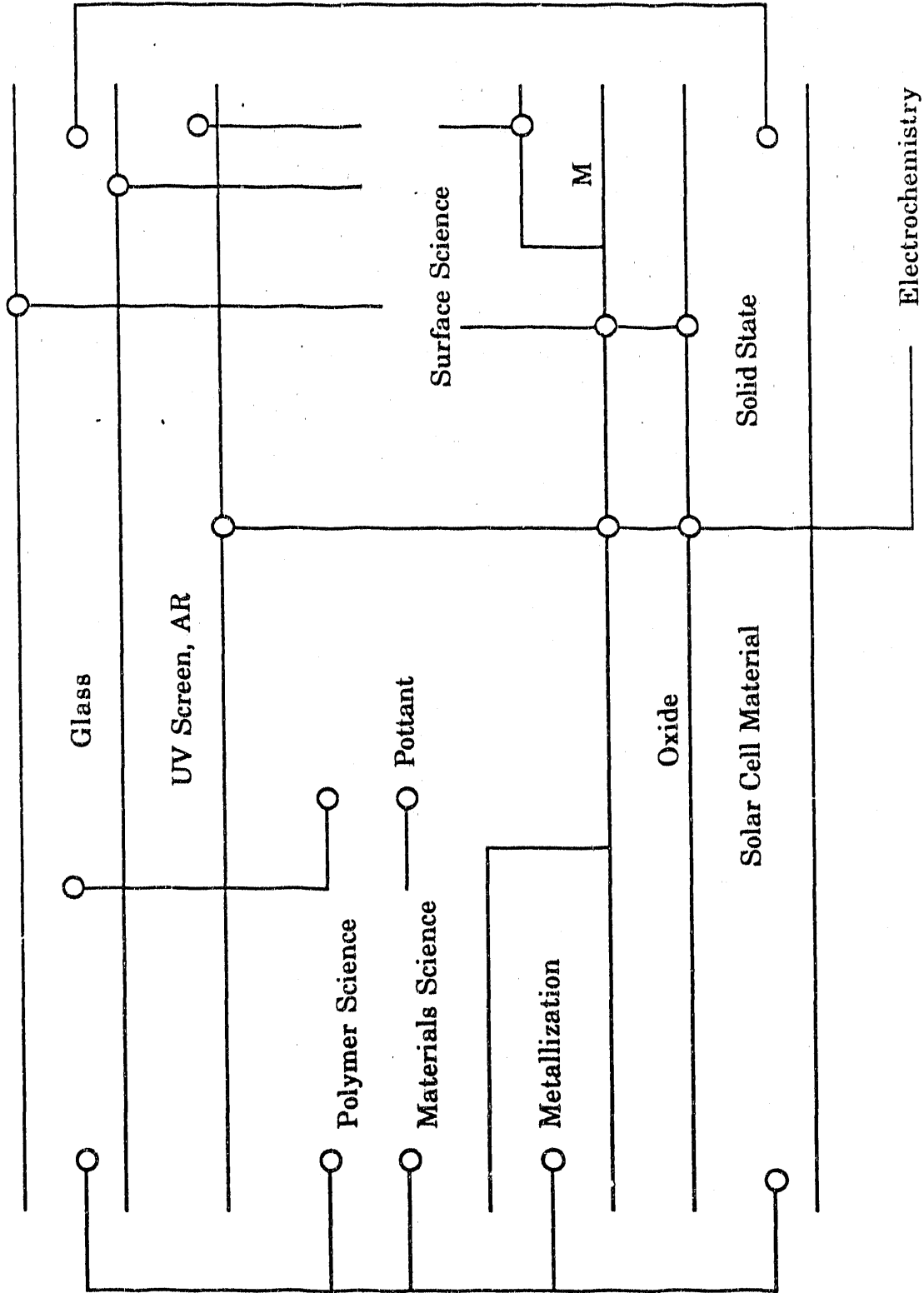


- Multidisciplinary:
 - Chemical Kinetics, Photochemistry
 - Polymer and Materials Science
 - Surface Science
 - Physics

REACTIONS/PROCESSES THAT LIMIT ENCAPSULANT DURABILITY
(Not Including Edge Seals)



ENCAPSULATION - SCIENTIFIC DISCIPLINES



SERI
SERD

ENCAPSULATION
PV M&P BRANCH

FAILURE MODES - EARLY WORK

- R • Delamination at Interfaces
- R • Penetration of Liquid Water -- Corrosion
- D • Soiling
- D • Weathering and Physical Degradation
- R • Short Circuiting/Arcing
- R • Cracking of Solar Cells - Differential Thermal Expansion
- R • Cell Interconnects Failure - Thermal Cycling
- R • Charring and Melting of Solder - Overheating

SERI
SERD

ENCAPSULATION
PV M&P BRANCH

PURPOSE - MATERIALS SYSTEMS

- Provide Mechanical Support for Solar Cells
- Provide Electrical Isolation for Solar Cells
- Provide Ancillary Electrical Circuitry for Solar Cells
- Permit Maximum Optical Coupling Between Sun and Solar Cell
- Isolate Solar Cells from Degrading Environmental Factors
(Hail, Solling, Reactive Elements/Compounds)
- Maintain Function for 30 Years
- Emphasize Low Cost
- i.e., All Necessary Functions Except that of the Solar Cell Itself.

POLYMERIC ENCAPSULANTS

- UV Stability
- Interfacial Reactions

Adhesion, Delamination

Structural Relationships of Laminates

- Permeation (Atmospheric Reactants)
- Adhesion (M/P, MO/P, SC/P)
- Surface Hardness (Abrasives)
- Surface Reactivity (Dust Air)

SERI
SERD

ENCAPSULATION
PV M&P BRANCH

TRANSPARENT POLYMERIC POTANTS - DEGRADATION MODES FROM WEATHERING

(All are permeable to oxygen and water vapor)

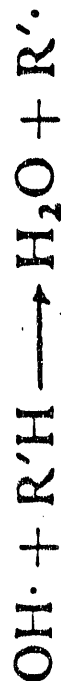
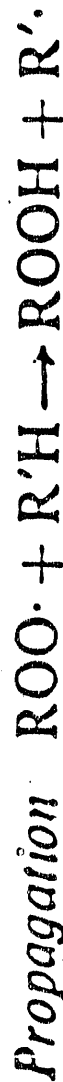
- UV Photo-oxidation
- Thermal Oxidation
- Hydrolysis

- Catalyzed Degradation by Metal Cations
 - (Reich and Stivala, (e.g., Cu⁺, Fe⁺⁺, Co⁺⁺⁺, Mn⁺⁺), 1969)
 - (Hansen, 1972).

Table 2. Specifications and Requirements for Compounded Pottant Materials

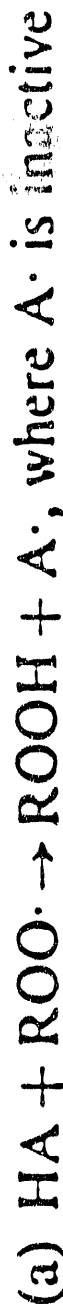
Characteristic	Specification or Requirement
Glass transition temperature (T_g)	< -40°C
Total hemispherical light transmission through 20-mil-thick film integrated over the wavelength range from 0.4 μm to 1.1 μm	> 90% of incident
Hydrolysis	None at 80°C, 100% RH
Water absorption	< 0.5 wt % at 20°C/100% RH
Resistance to thermal oxidation	Stable up to 85°C
Mechanical creep	None at 90°C
Tensile modulus as measured by initial slope of stress-strain curve	< 3000 lb/in. ² at 25°C
Fabrication temperature	\leq 170°C for either lamination or liquid pottant systems
Fabrication pressure for lamination potants	\leq 1 atm
Chemical inertness	No reaction with embedded copper coupons at 90°C
UV absorption degradation	None at wavelength > 0.35 μm
Hazing or clouding	None at 80°C, 100% RH
Minimum thickness on either side of solar cells in fabricated modules	6 mils
Odor, human hazards (toxicity)	None

10/86 JPL



Termination Decrease in number of participating species by:

(1) Action of antioxidant



(b) Heterolytic hydroperoxide decomposition

(2) Disproportionation

(3) Combination

(4) Depletion of accessible material

Hansen, 1972

Fig. 6. Oxidation of polymers:

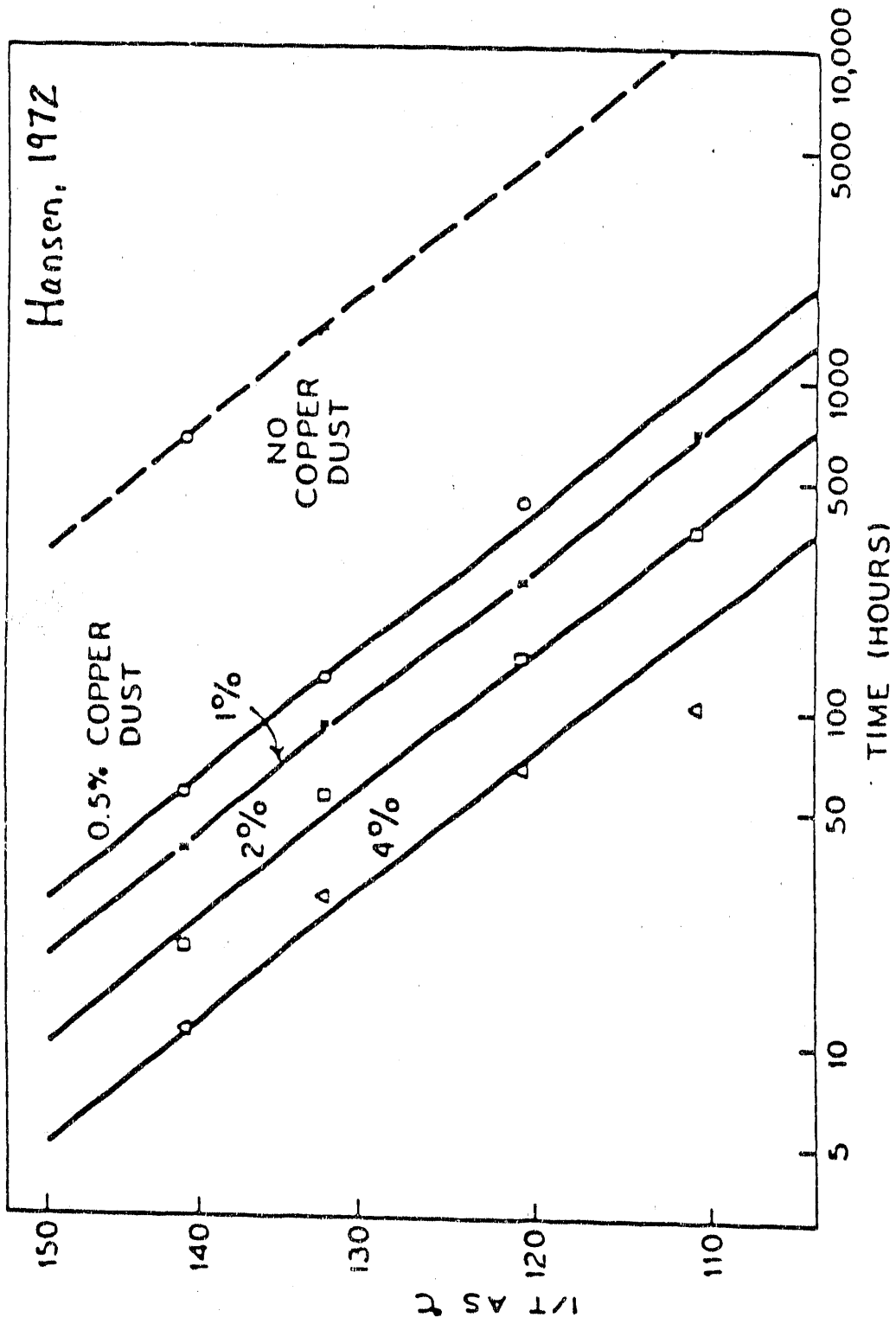


Fig. 24. Effect of copper dust concentration on oxidative stability of a commercial polypropylene composition.

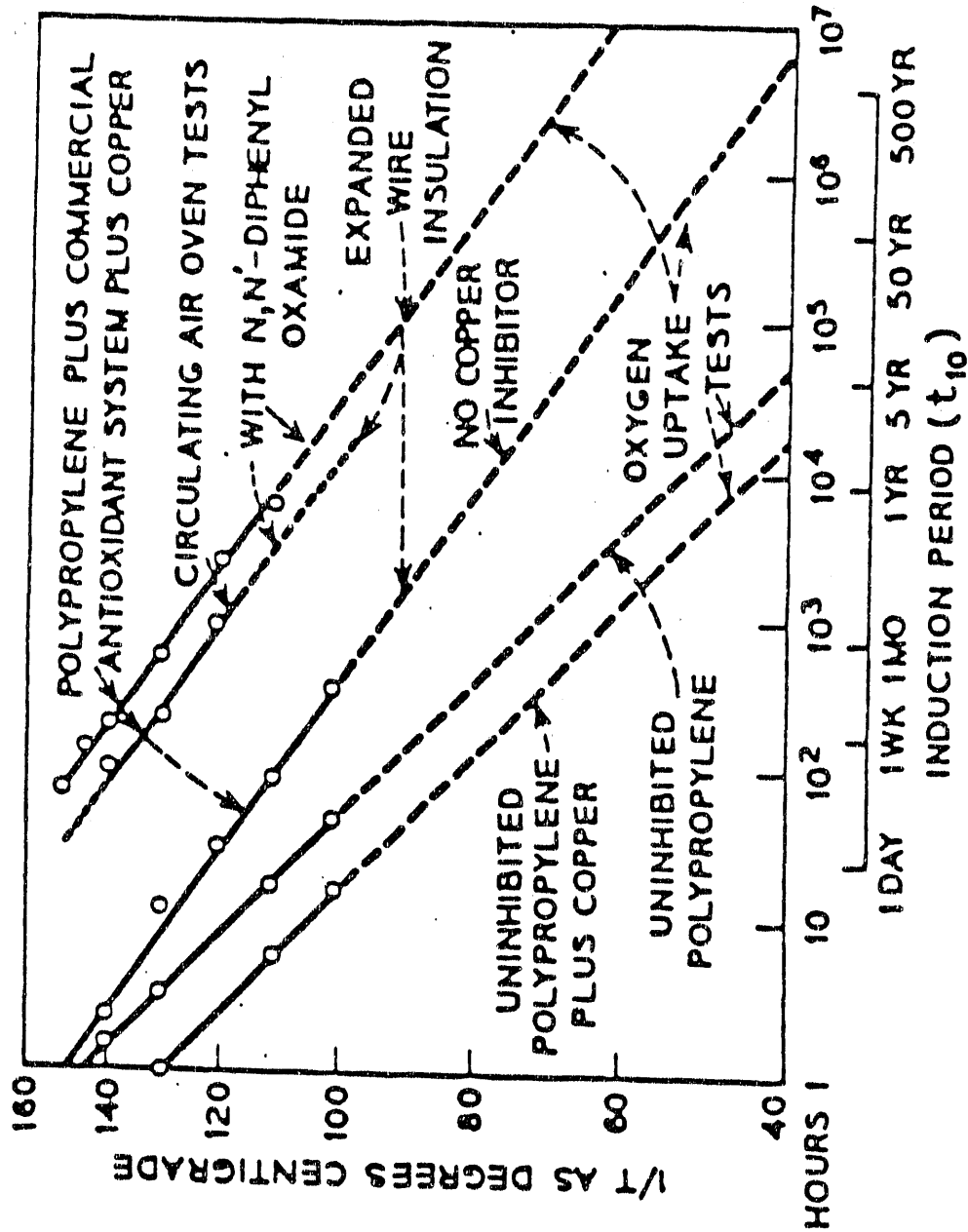
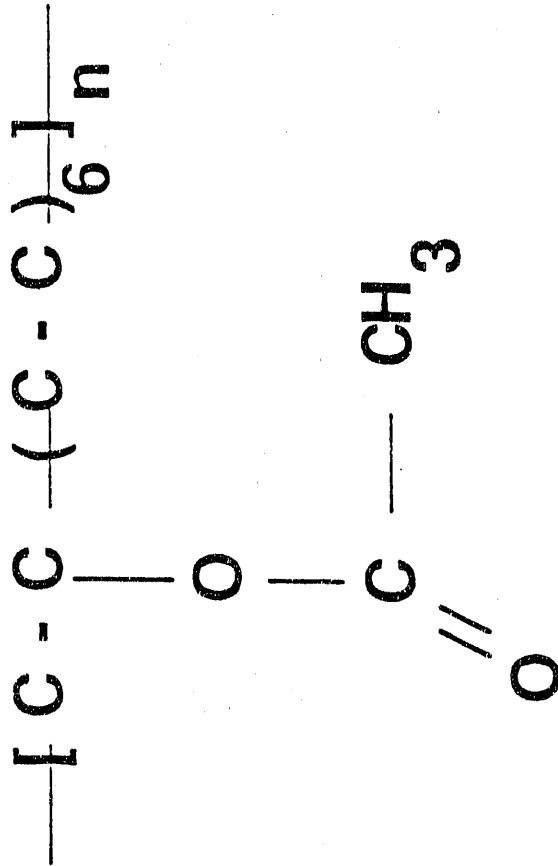


Fig. 20. Arrhenius plots showing effectiveness of oxanilide as a copper inhibitor. Circulating air oven tests were based on onset of brittleness; other tests were based on isothermal oxygen uptake tests.

SERI
SERD

ENCAPSULATION
PV M&P BRANCH

DU PONT ELVAX 150; SPRINGBORN A - 9918; EVA



SERI
SERD

ENCAPSULATION
PV M&P BRANCH

FORMULATION/STABILIZATION OF EVA

- Curing agent [Lupersol 101 or TBEC]
- UV absorber [Cyasorb UV 531]
- Anti-photo oxidant [Tinuvin 770]
- Anti-thermal oxidant [Naugard P]
- Also, use a UV screen between cover/EVA.

CYASORB 531 (UV Stabilizer)



UV Absorption ~ 270 - 280 nm

~ 350 - 450 nm

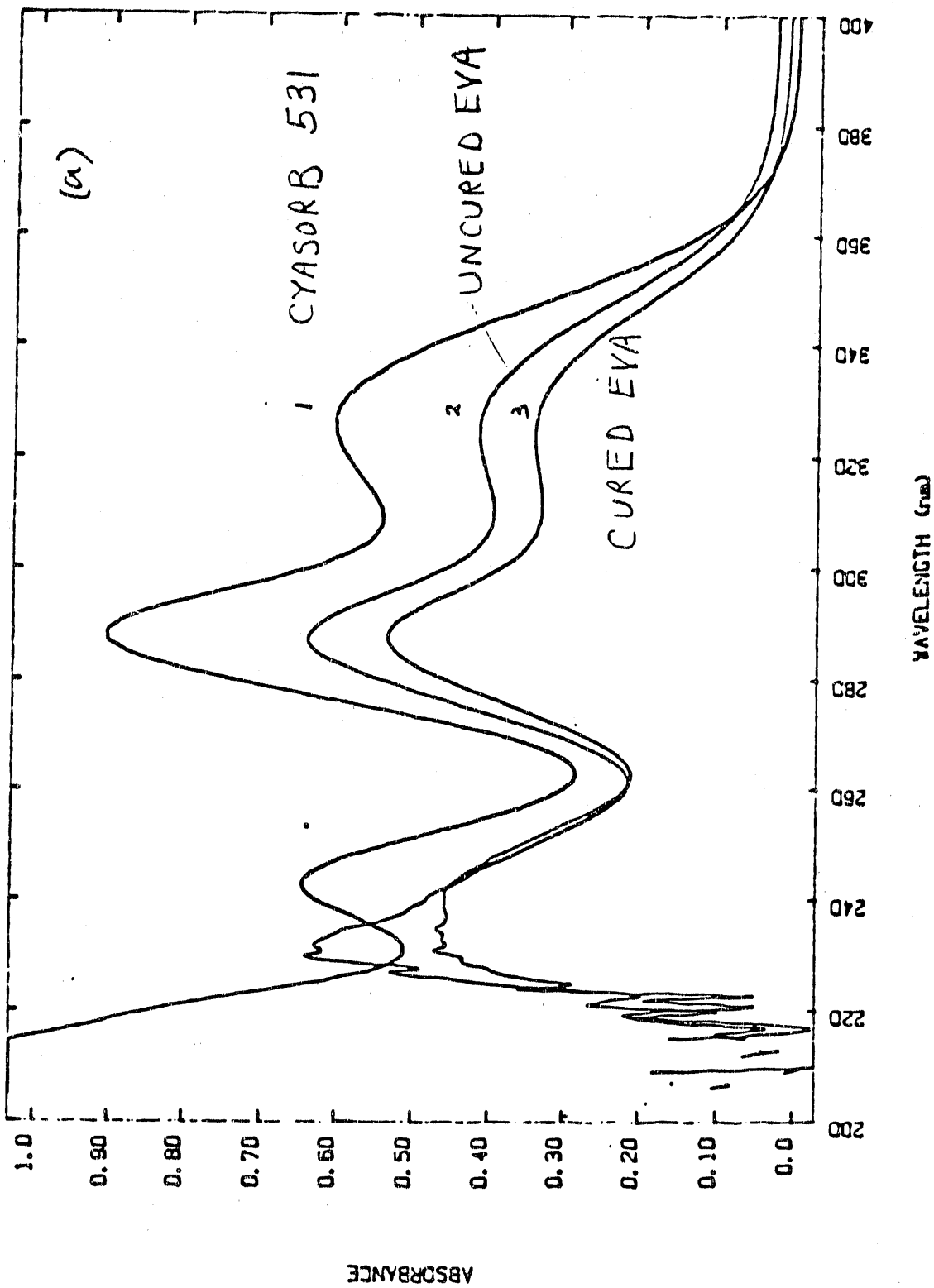
Polar Molecule, permanent dipole

Can be leached from EVA — 105°C, 6 suns — 800 h

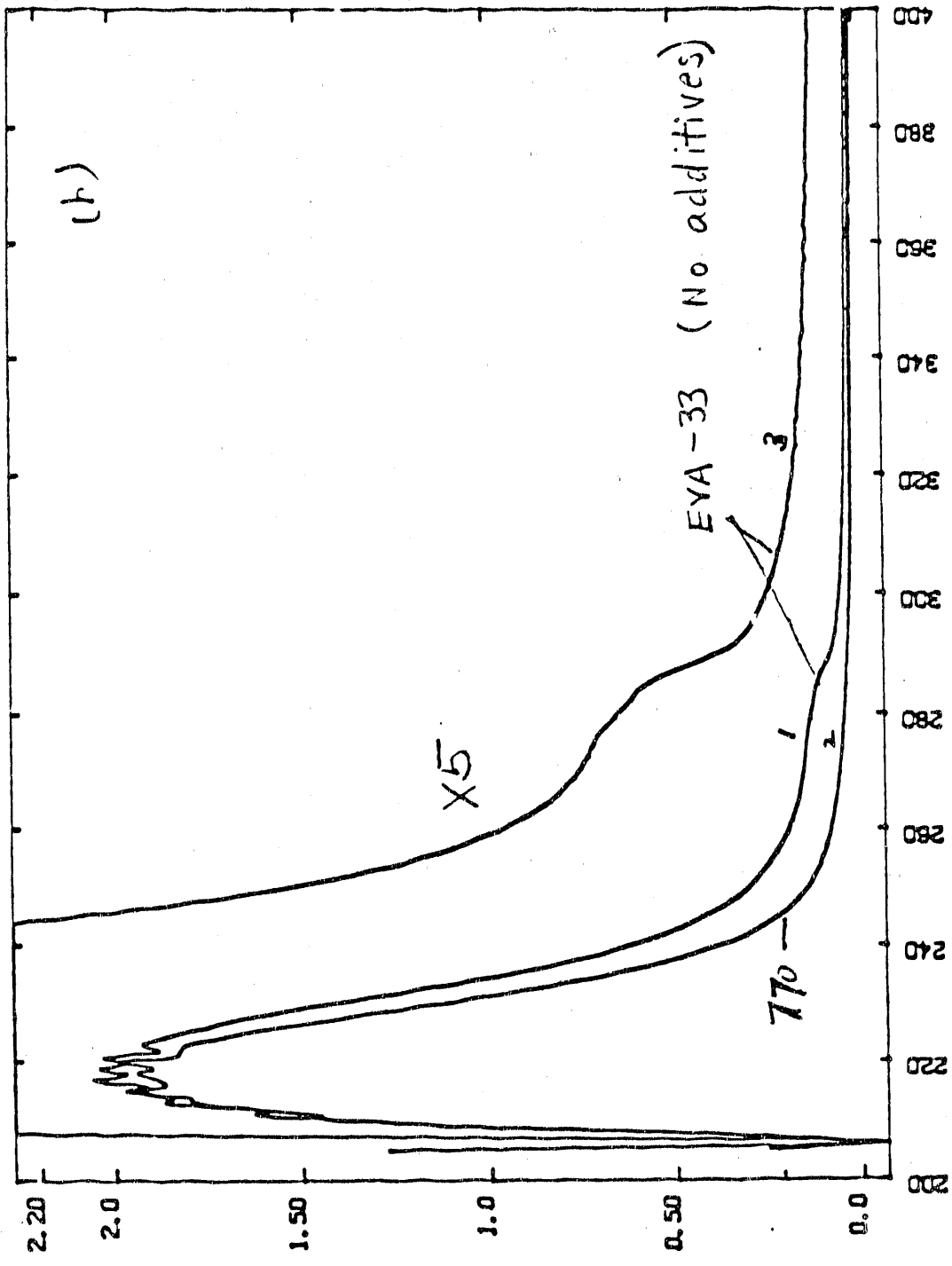
(wt. loss ~1 - 1.5%) EA ~7 Kcal/mol (physical process).
Gupta, Liang, et al., 1983

Absorbs ~ 90% of incident UV energy (Gupta, 1983).

CYASORB UV531 / THF 2/12/1990



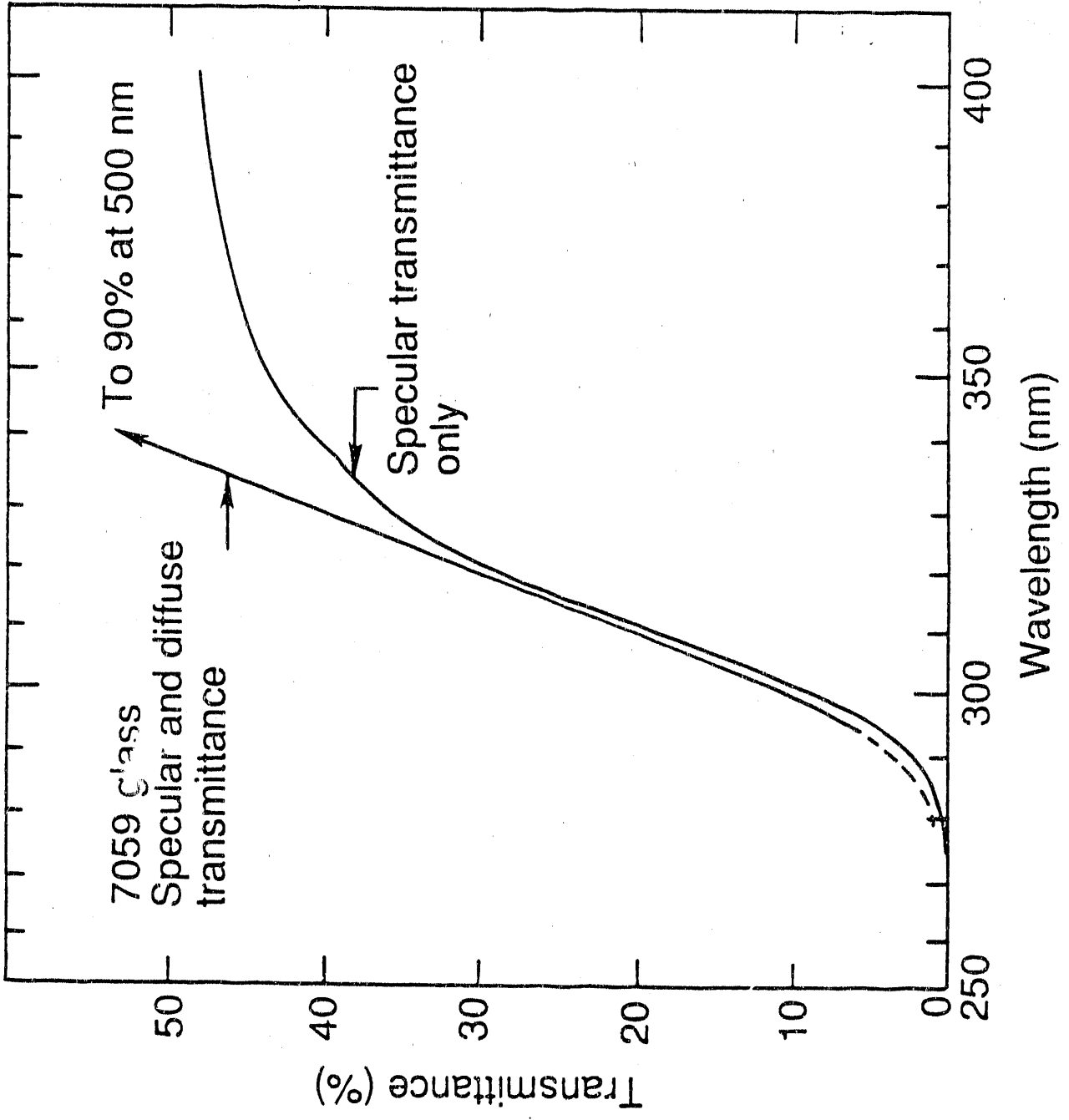
1. EVA-33
2. Tinuvin 770 /THF 2/12/1890



1. EVA-33
2. Tinuvin 770
3. 1, 5x

ABSORBANCE

BA-G0684701



POTTANTS: CANDIDATES/STRATEGY

- Teflon FEP, PMMA, Silicones (as a class) meet above criteria
- All others (including EVA) are subject to above weathering reactions
- Strategy: Provide a level of UV shielding (UV cut-off 350 nm)
Pottant must be intrinsically resistant to hydrolysis and T_{ox}
- Materials by Design (Taguchi)

LITERATURE: EVA DEGRADATION

Gupta, 1980 Polymer Preprints

Liang, et al., 1983, in Polymer Science Technology

Lewis and Megerle, 1983, in Polymers, S.E. Utilization

JPL 11 Years of Progress, Cuddihy, et al., 1986

Russian, Japanese, Romania Abstracts

DEGRADING EVA: WHAT HAPPENS TO IT? LITERATURE

- Degradation initiation; hydroperoxides, acids, alcohols (Russian)
- Leaching/evaporation of additives (Liang, et al.) 1983.
- CH_3COOH volatile (Liang, et al.), 1983; others.
- $-\text{C} = \text{C}-$ formed in main chain (Russian) - D. Initiation
- Cross linking \Rightarrow mechanical changes, structural changes (many)
- Cured, dense, partially degraded \Rightarrow polyenes — yellowing (some).
- Reaction products promote more degradation (few)

Therefore — expect to find changes in

- bonding (IR), transmittance (UV-vis), mass (some losses, some gains), composition (surface, bulk), MW, conductivity, mechanical properties, structure, other, losses of additives.

SERI
SERD

EVA YELLOWING: Lewis/Megerle, 1983

- Oven heated to 150°C - No UV
- More pronounced over metallization
- Oxidative degradation, catalyzers
CuO_x/NiG, VO_x, SbO_x greatest accelerators.

1983

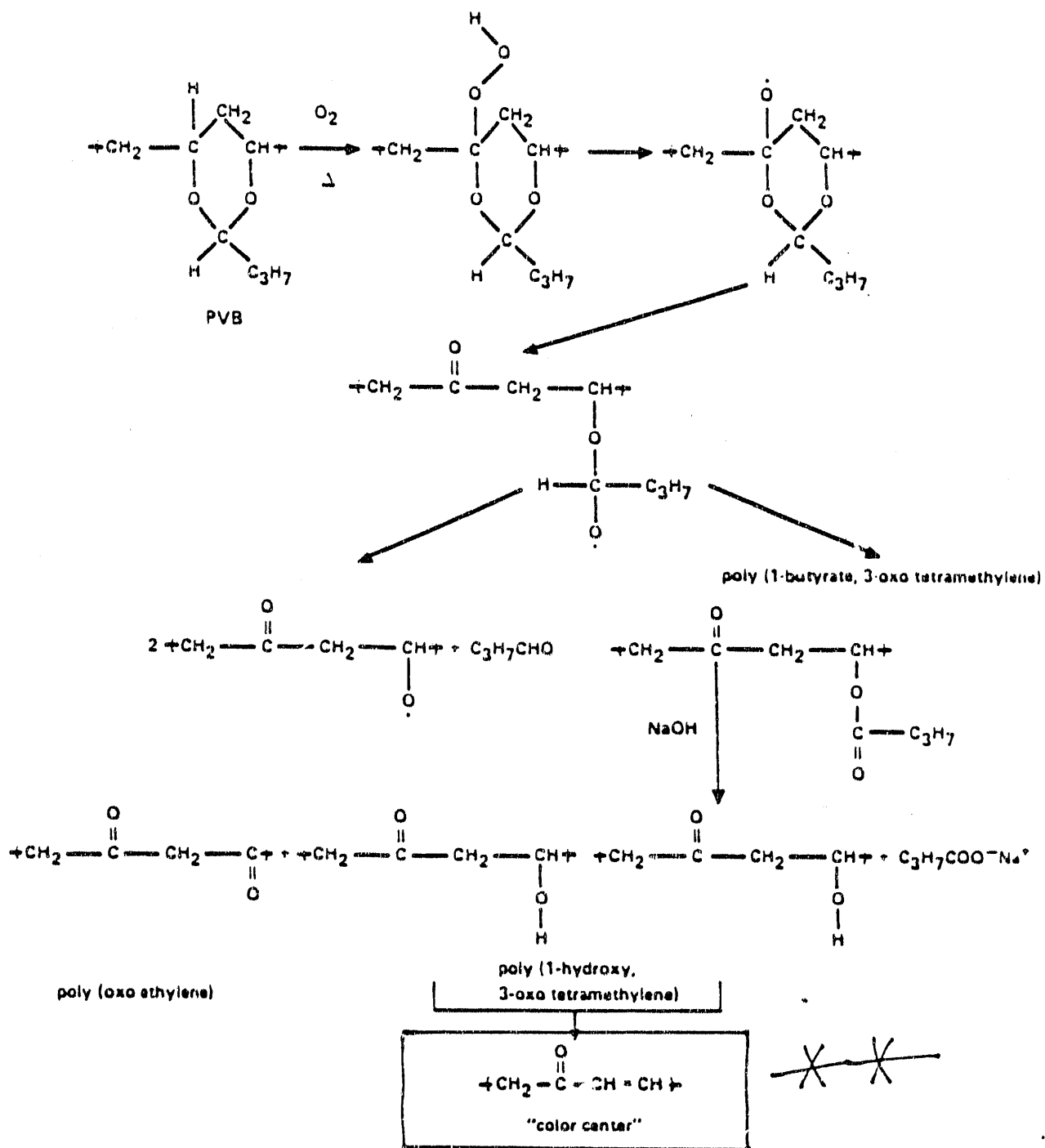
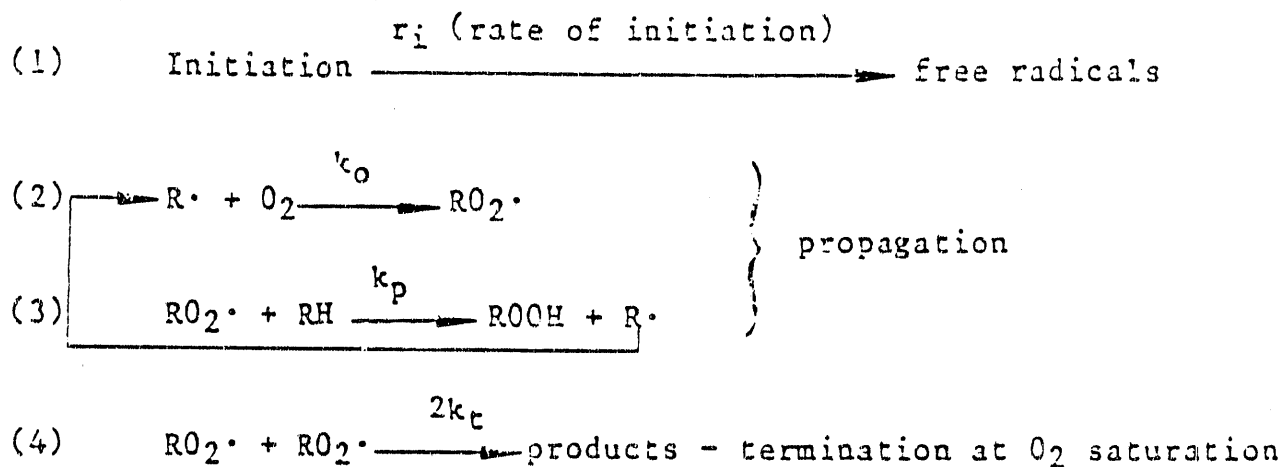


Figure 8. Possible PVB Browning Mechanism.

basic mechanism of this process, identified over 35 years ago by Bolland and Gee (2), is as follows:



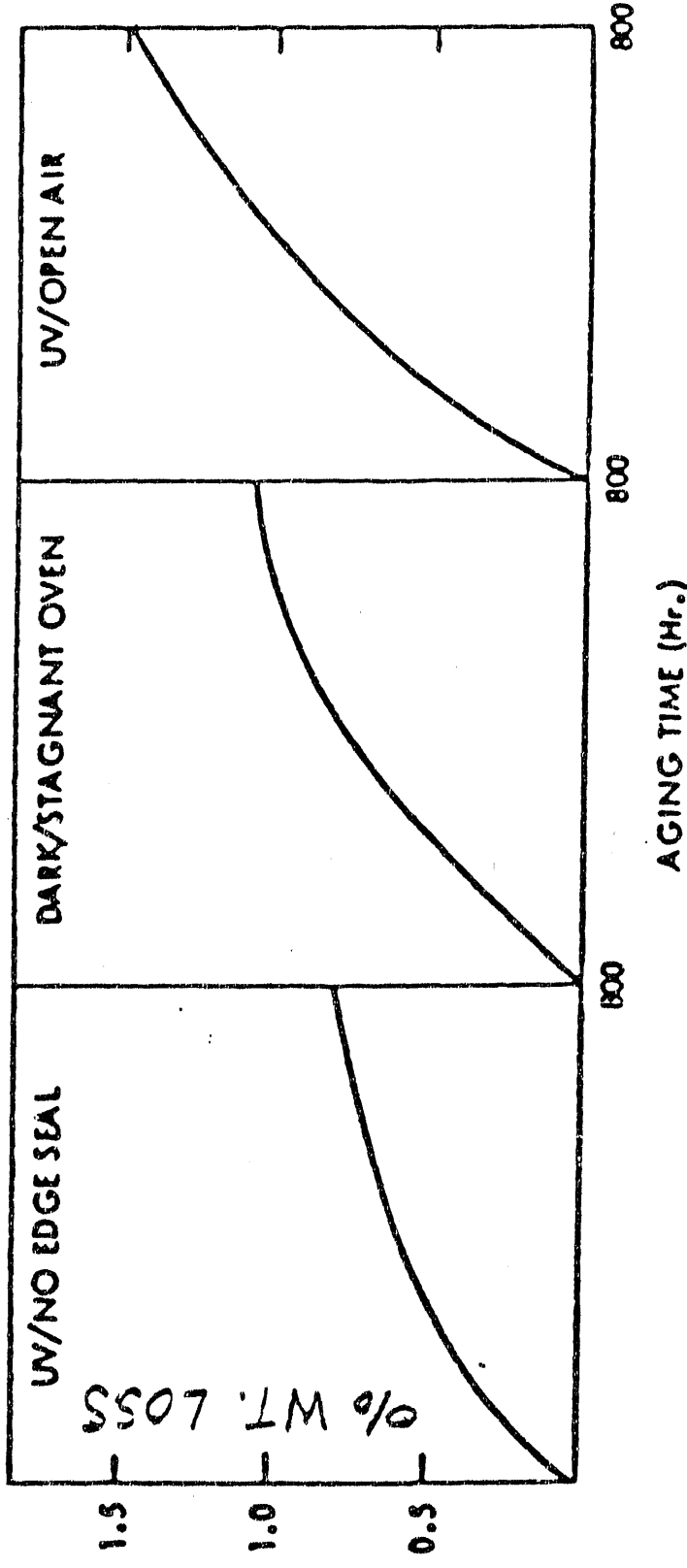


Figure 8. Weight Losses of EVA Films (A9918) as a Function of Photothermal Aging at 105°C and 6 Suns

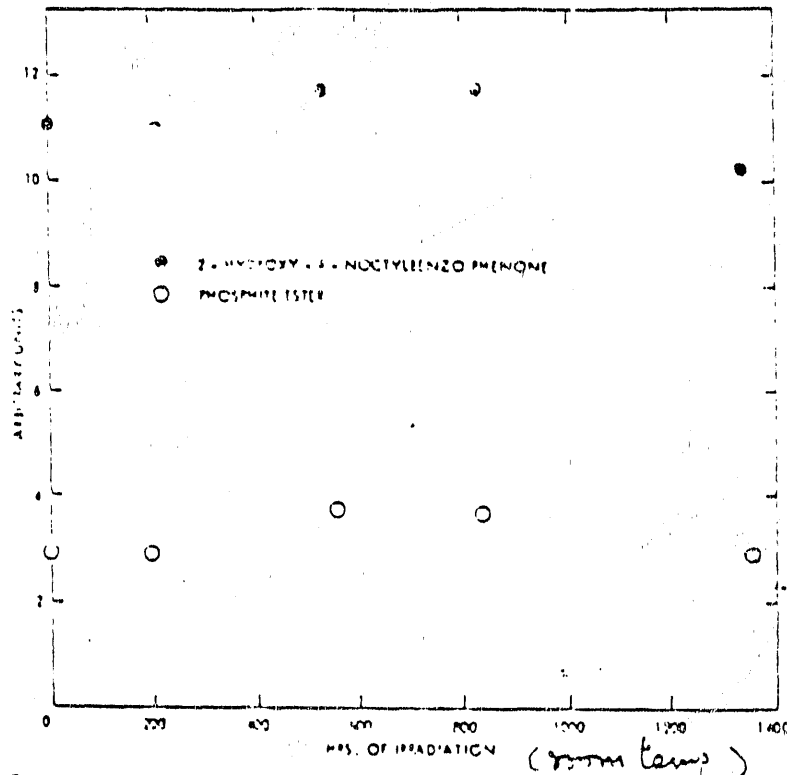


Figure 2. Concentration of UV Absorber and Antioxidant of (A9918) as a Function of Photoaging as Detected

PHOTOTHERMAL DEGRADATION

271
Liang,
et.al.

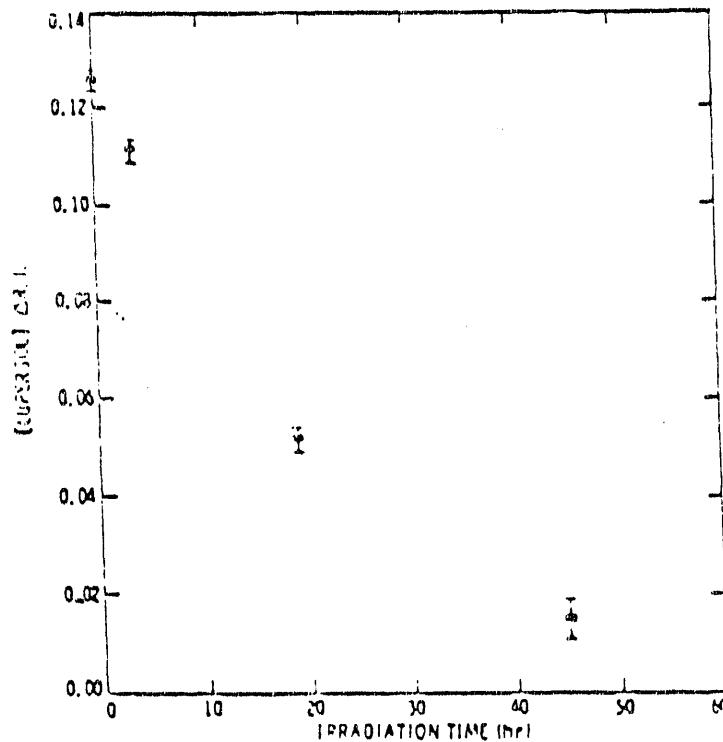


Figure 3. Concentration of Residual Curing Agent of EVA (A9918) as a Function of Photoaging at 30°C as Detected by HPLC

is a definite increase in absorption at wavelength longer than 400 nm for the dark over-aged samples, which causes the samples to appear yellow. Transmission at 360 nm and shorter λ also shows a

SERI
SERD

ENCAPSULATION
PV M&P BRANCH

POTTANT - IMMEDIATE CONCERN

- Yellowing (Conjugated bonds; Carbonyl Groups)
- Metallization Corrosion - Water Ingress
- Leakage Currents - Water Content, etc.

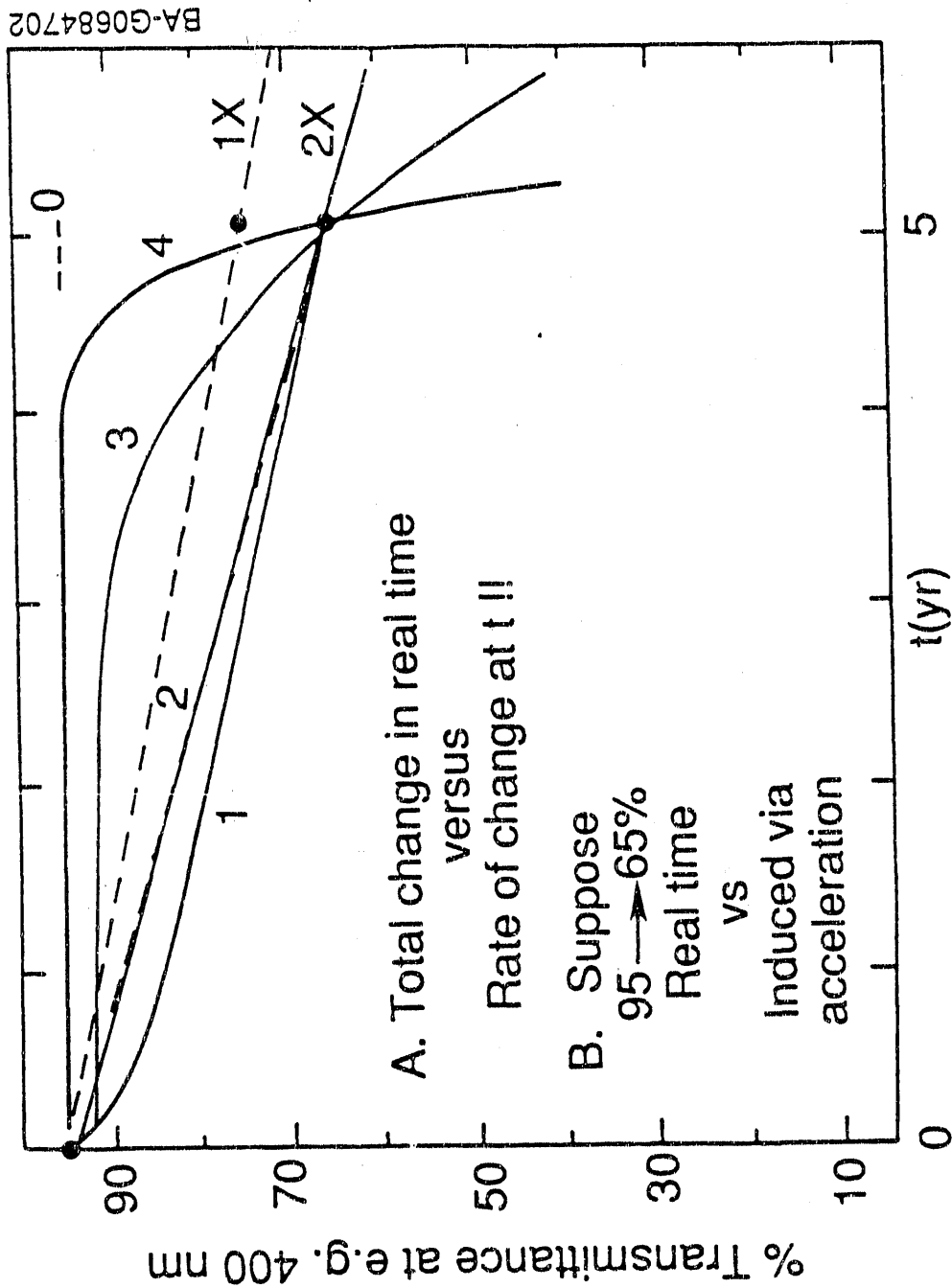
SERI
SERD

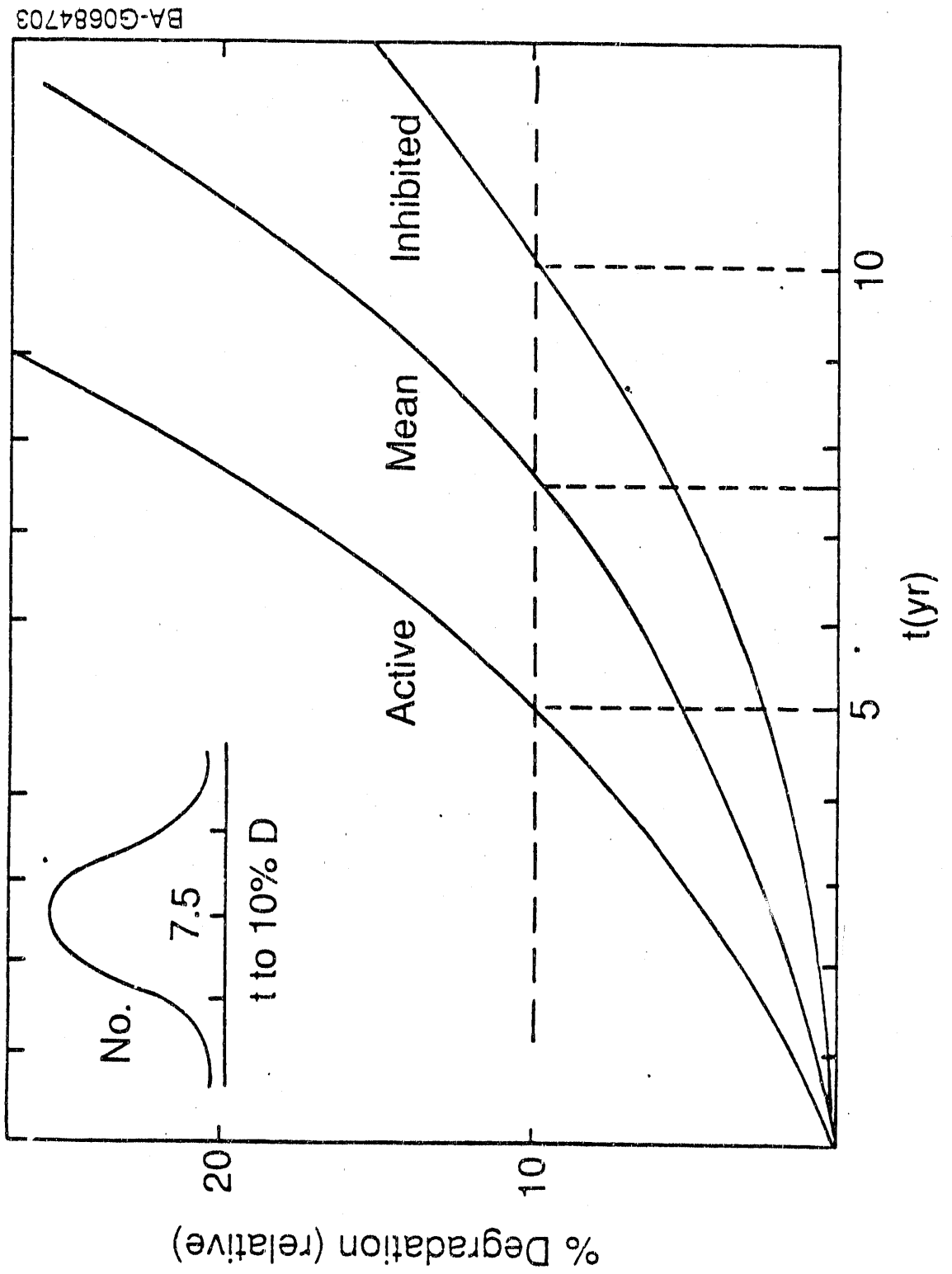
ENCAPSULATION
PV M&P BRANCH

MODULES - CARISSA SITE

- Yellowing
 - Enhanced Over Metallization
 - Enhanced with 2X Exposure
 - Occurs Throughout Entire Module
- Performance Losses: Efficiency Drops to % (1X) and % (2X)
- Ag Alloy Metallization; Sn over Cu Conduits
 - EVA, Elvax 150
 - XPS, SIMS, ATR-IR Results

Yellowing vs Time (hypothetical)





BA-G0684703

SERI
SERD

ENCAPSULATION
PV M&P BRANCH

Glass	
yellow	yellow-brown
clear	yellow-brown EVA
clear	yellow-brown
Grid	Cell Material

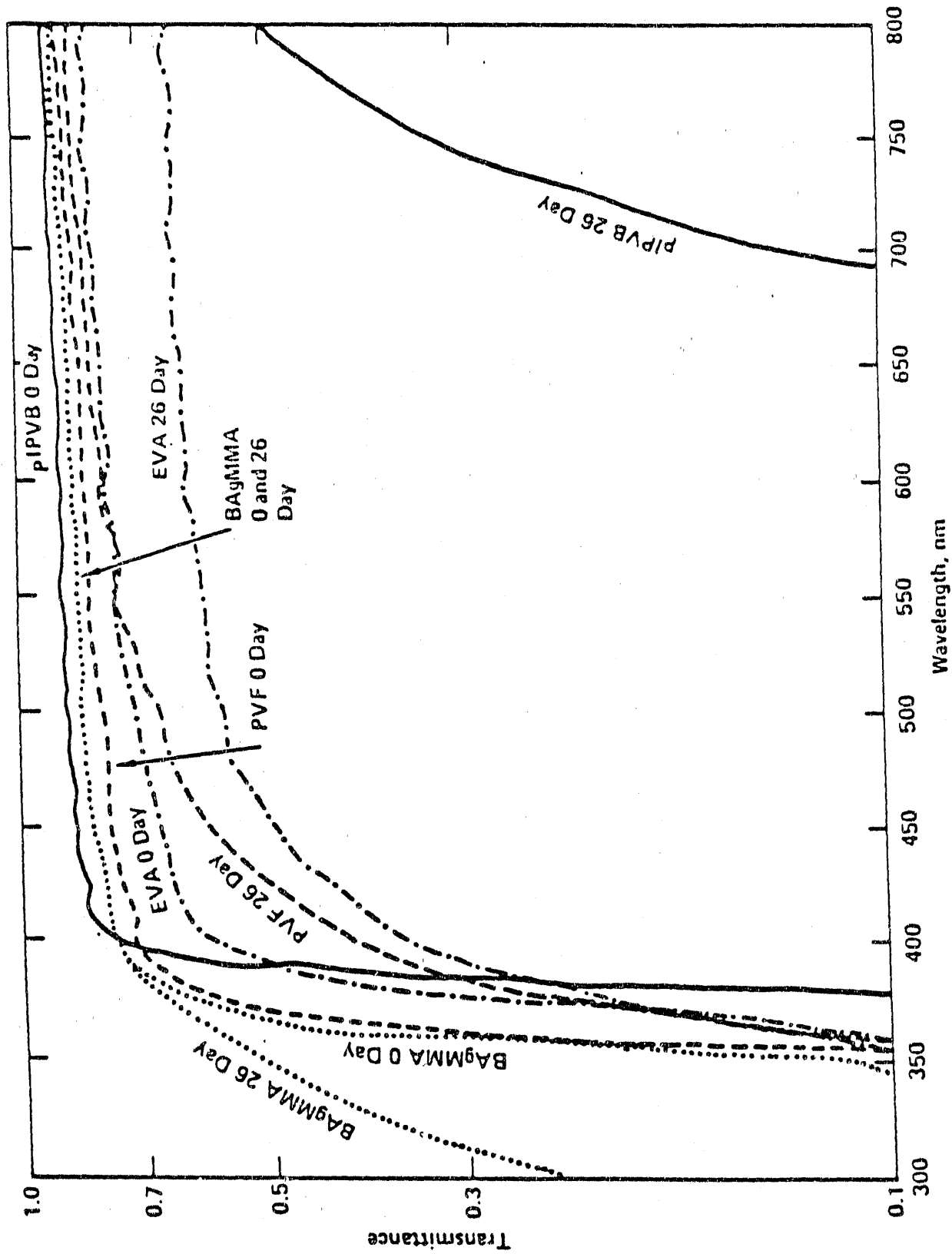
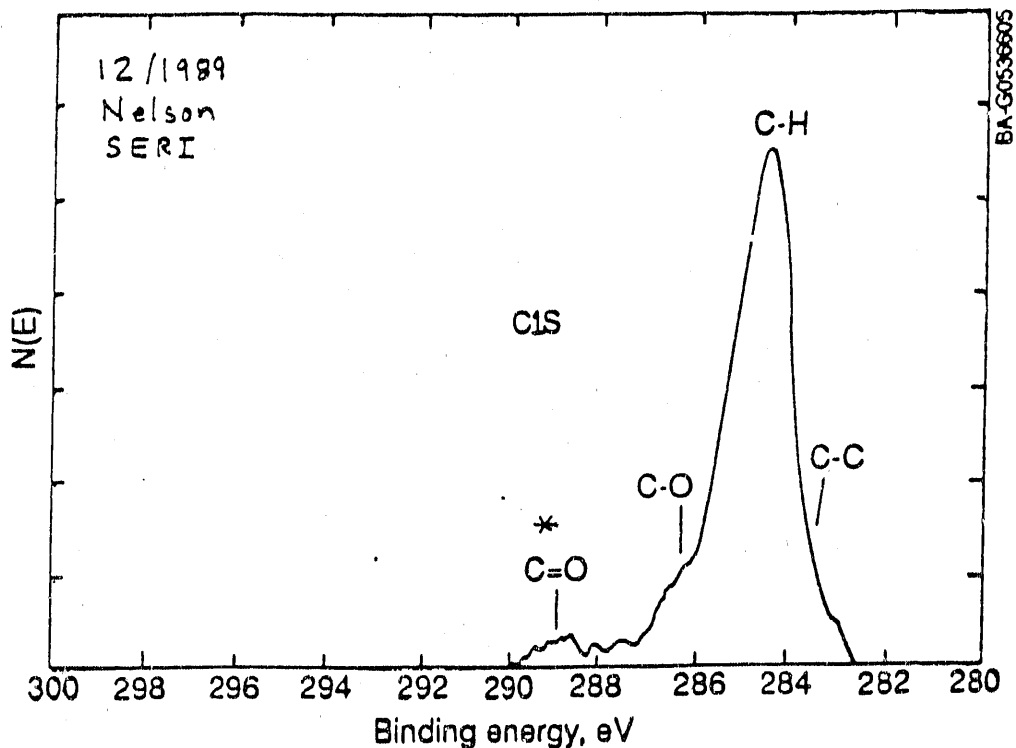
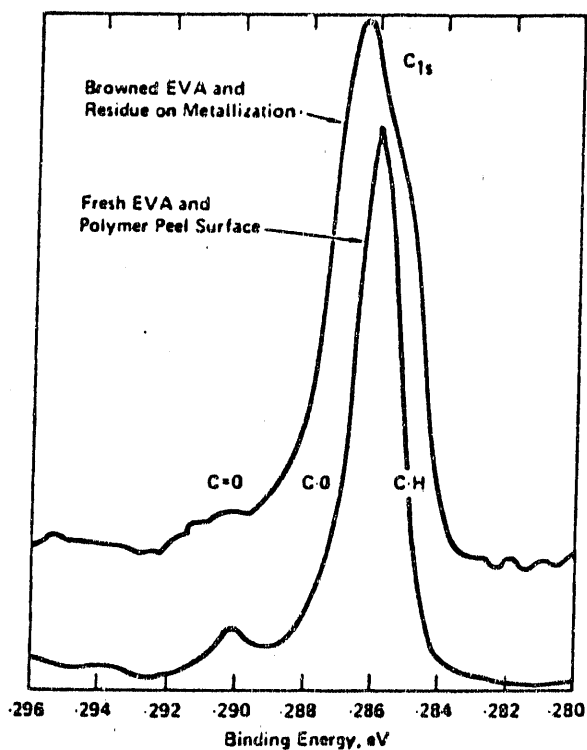


Figure 2. Degradation of Optical Transmission.

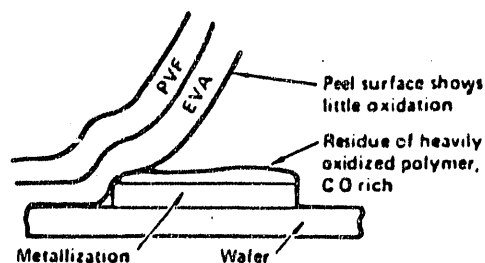
EVA Sheet as received



* C=O is lost in degraded EVA (Carissa Site)

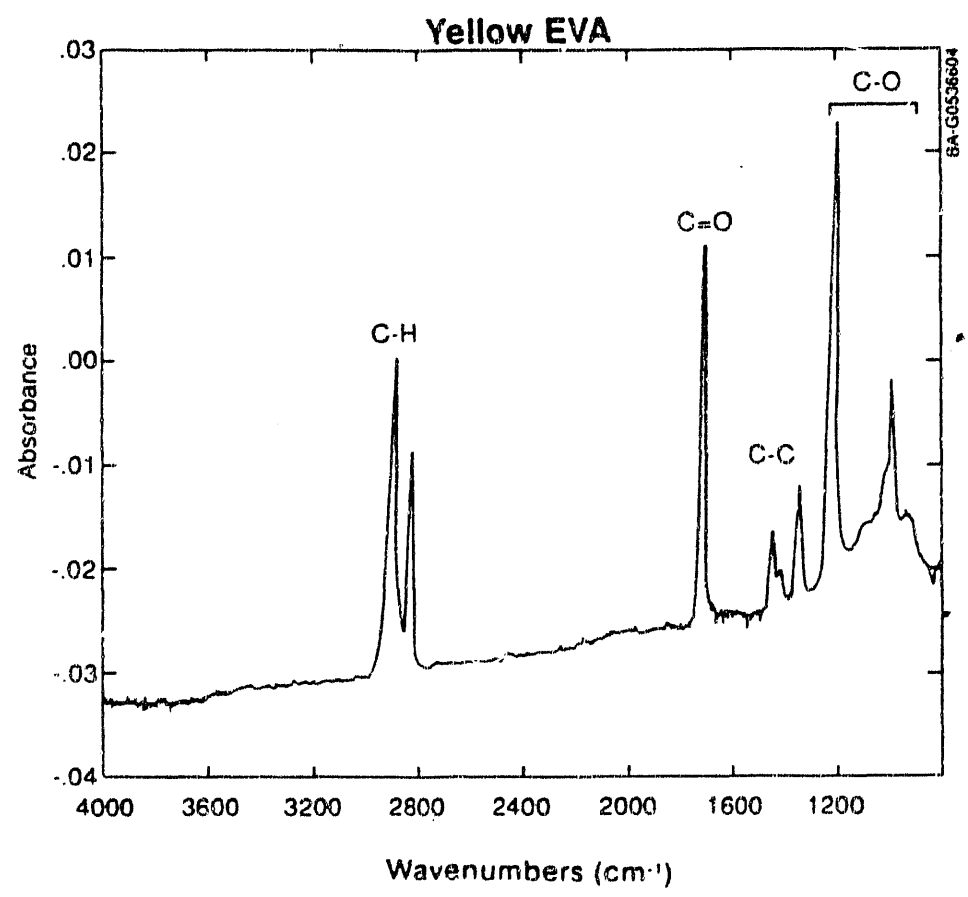
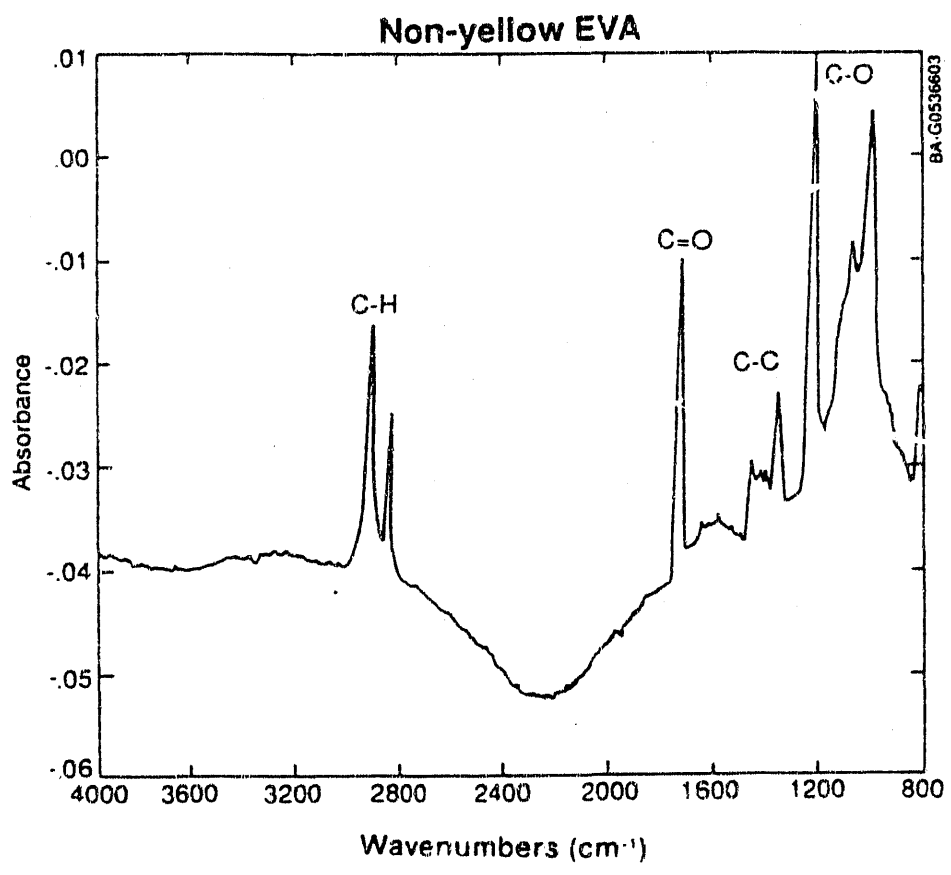


- ESCA & MIR-IR show an increase in C O in browned EVA
- Accelerated oxidation of EVA occurs at metallization surface. A layer of polymer, several thousand Angstroms thick, was oxidized.
- Upon peeling EVA from cell, tear occurs at reaction interface between heavily and lightly oxidized EVA layers.



LEWIS AND MEGERLE *Encapsulant Degradation* Figure 9. ESCA Analysis of EVA.

1983



EVA DEGRADATION MECHANISMS

Variables	Mechanism or Possible Mechanism	Well-studied
1. T, [O ₂ , H ₂ O]	Thermal oxidative degradation	Well-studied
2. UV, T, []	Photothermal oxidative degradation	Few studies
3. M ⁺ , T, []	Metal-ion-catalyzed thermal oxidative degradation	Not studied*
4. M ⁺ , UV, T, []	Metal-ion-catalyzed photothermal oxidative degradation	Not studied*
5. M _g ⁺ , UV, T, []	Surface-M ⁺ -catalyzed thermal of PT oxidative degradation	Not studied
6. i flow in M plus 1-5	E induced migration or e ⁻ injection plus other mechanisms 1-5	Not studied
7. [O ₂ , H ₂ O] effects	1.-6 but [] dependence	Minimal in 1. and 2.
8. [Original formulation]	1.-7 but [] additives	Minimal in 1. and 2.
9. Electrochemical processes plus 1-6	Related to 6. and [H ₂ O]	Not studied
10. As 1. 2. but Hot T	Any part of 1.-6. but initiated at hot spots	Isolated studies
11. Effect of pin-holes or areas of high resistance		

DISCUSSION QUESTIONS

1. Do past and present fabrication procedures include using a fluorocarbon UV screen between the glass and EVA?
2. What is the formulation of the EVA (% co-polymers, and concentrations of UV screens, stabilizers, anti-oxidants, cross-linking agents, etc., hand processing impurities)? We, of course, know the generic formulation of EVA, but also realize these may have been modified for proprietary reasons.
3. What temperatures are reached in EVA processing? In what atmospheres? For how long? In contact with what materials?

DISCUSSION QUESTIONS (CONT'D)

4. What is the formulation of the metallization and how is it applied to the silicon? at what temperatures? How has the composition of the initially-used slurry varied over the years? Does it contain organics as vehicles for applying the "silver" contacts?
5. What is the meaning of %T or "Degree of Yellowing" from:
 - Real-time
 - Simulation
 - Isolated bulk vs. EVA in a module?
6. What is the value of T/UV degradation of EVA? of E_A from this mechanism?
7. What other polymers are used? Europe, Japan? PVB?

SERI
SERD

ENCAPSULATION
PV M&P BRANCH

POTTANTS: TECHNICAL APPROACH

- Selection of polymers.
- Accelerated/real time testing conditions.
- Characterization before/during/after testing.
- Mechanisms of degradation that must be isolated/considered.

SERI
SERD

ENCAPSULATION
PV M&P BRANCH

TECHNICAL APPROACH · POLYMER SELECTION

- Bulk Pottant Materials
 - EVA, A-9918, 15295 - Supplier
 - EVA, 18170 - Springborn
 - GE-PALS - Springborn
 - Other (EMA, PMMA, etc.) - TBD
- Ingredients in Polymer
 - UV stabilizers
 - Anti-oxidants
 - Curing agent
 - Primer

TECHNICAL APPROACH

- Utilize EVA in Module (operating) Configurations
 - Accelerated Testing
 - Monitor Measures of Degradation (Non-destructive)
 - Monitor Measures of Degradation (Destructive)
- Utilize EVA in Designed Experiments - "Separate Variables"
 - Photothermal - Bulk - UV Screens, Absorbers, Anti-oxidants
 - M^+ and M_S^+ Catalyzed Thermal
 - M^+ and M_S^+ Catalyzed Photothermal (PT)
 - \bar{E} and/or $e^- \rightarrow$ Induced/Photothermal
- Combined $PT/M_S^+/E^-$ Oxidative Degradation

Reality

Coordinate These

Sub-divide Reality

• ACCELERATED TESTING OF COMPLETE MODULES: LIFETIMES

- Gain Insight as to What Parameters Induce Degradation for Particular Configuration
- Failure of a particular test (e.g., excessive T) may be unimportant.
- May or may not correlate with field experience
- Gain Relative Ranking of Durability based on THAT Test
- Would like on-line NDT monitor
- Does test/monitor relate to reality?
- Does not Provide Insight into Detailed Mechanisms
- Mechanisms may change for different test conditions
- Mechanism (materials, T, ΔT , UV, % R.H., gases, interfaces, E, etc.)

TECHNICAL APPROACH: REALITY?

Parameter	Reality	What is the Acceleration?
UV	AM 1.5	10-50 Suns <u>Simulate control</u>
T	85°C - ΔT	T > 85°C - ΔT
ΔT	40 - 50°C	With T
M*	Ag, Al ₂ O ₃	M* as "Impurities"
(Near M) E	10 ⁴ V/cm	10 ⁵ V/cm, accelerate; or 10 ³ V/cm - Decelerate
[O ₂ , H ₂ O, other]	TBD	Increased [] of I, in particular, where I may be impurity or degradation, products
t	Real time	None

M* may be metallization, simulation (Au, Cu), or glass or SiO₂ surfaces plus impurities on them.

TECHNICAL APPROACH - CHARACTERIZATION
BEFORE, DURING, AFTER VARIOUS STAGES OF TESTING POLYMERS

- | | |
|--|--|
| • UV-Vis spectrophotometer | Ingredients present |
| • FT-IR-ATR, -RA, -microscopic/microtome | Bonding changes |
| • Gel content | Cross linking amount |
| • GPC, HPLC | MW changes |
| • XPS, SIMS, ISS, EPMA | Surface/near surface comp. |
| • TGA-weight loss | Stability changes |
| • Microbalance | Permeation rate changes |
| • LCR | Impedance changes
(catalyzed effects) |
| • Conductivity | |

EVA DEGRADATION: SERI CAPABILITIES

EQUIP/TECH	Usefulness for Polymer Photodegradation	
FT-IR-ATR	Transmission and near surface	----- Intermediates & chemical bonding
FT-IR-RA/CEEC	Controlled PTM _s ⁺ or PTE _{Ind} degradation	----- Interface reactions
UV-vis Spectro.	Transmittance, absorbance	----- Optical properties
XPS, SIMS, ISS,	Surface compositional analysis	----- Surface comp. effects
TGA (DTA, DSC)	Decomposition T in controlled environment	----- Weight loss, other
GPC, HPLC	Chromatographic analysis	----- MW changes
QCM, Beam Balance	Controlled "reactions/processes"	----- Mass changes: permeation
Conductivity M.	Conductivity changes [t]	----- Ion concentration
EPMA	Near surface (~10 μm) comp.	----- Metallization composition
Env. Test Chambers	Accelerated testing (WOM, QUV, Tenney, BMA)	----- Collective effects
Light Sources/ Simulators	Accelerated UV exposures - (Solar Furnace)	----- Accelerated test
LCR, ESR, SEM, NMR, Optical, Visual, Hot Spot, Other Analytical	Variable, other compositional (bulk) effects including additives.	----- E, effects - Free radicals Topography

APPENDIX I - SERI Module Materials Needs

Specific Needs for Assisting our Future Work Aside from the "new" EVA and other polymer formulations SERI is securing from Springborn and other laboratories, the following samples of as-manufactured units, samples, and information will be extremely helpful for our comparison and analysis:

1. Samples of solar cells without metallization.
2. Identification of materials and the metallization method used.
3. Mini-modules (4x4") that operate at expected efficiencies.
4. Samples of unused cover materials (glass, Crane glass, Tefzel).
5. Any reference spectra you have on pure materials. We can obviously generate a partial data base from the materials you send.
6. Information about any departure from using "Ag metallization" (and ITO) over the cell material.
7. About one square foot cut from field-deployed modules so that the cover materials, EVA, solar cells, etc. remain intact.
8. Sheets 0.1 mm-thick (or thinner) of plain, cured and uncured EVA (surface textured sheets are undesirable for UV-vis and ATR measurements).
9. Raw material of your metallizations, samples of your grid-line metallizations, and thin films of your metallization on a substrate (quartz or 7059 glass materials are preferred).

SERI recognizes some of the above may involve proprietary information. It will perform services on a business confidential basis.

FIELD TEST RESULTS FOR THE 6-MW CARRIZO SOLAR PHOTOVOLTAIC POWER PLANT

Andrew L. Rosenthal
Cary G. Lane

Southwest Technology Development Institute
P.O. Box 30001, Dept. 3SOL
New Mexico State University
Las Cruces, New Mexico 88003-0001

ABSTRACT

Testing of subgroups, trackers, and laminates was performed at the Carrizo Solar Photovoltaic Power Plant. Testing was performed to characterize the effects of EVA degradation at the plant. EVA degradation is believed to have been accelerated by the high operating temperatures accompanying the use of mirrors to concentrate sunlight. Testing of 128 laminates revealed that degradation is highly non-uniform. Measured laminate peak power values ranged from 8.6 W to 47.8 W with an average value of 32.6 W. This average was 35.9 % below the installed laminate rating at similar conditions. Mismatch between laminates contributed an additional power loss of 11.1 %. Mismatch was found to increase with laminate temperature. One tracker was tested with and without mirror enhancement. It produced 3046.5 W with mirrors and 3275.9 W when the mirrors were covered. Preliminary results indicate that removal of the mirrors would increase the plant's peak power output on hot days.

INTRODUCTION

The world's largest photovoltaic (PV) power plant, the Carrisa Plains PV Power Plant, came on-line in late 1983. The facility was owned by Arco Solar, Inc. until late 1989 when it was purchased by Carrizo Solar Corporation. The plant consists of ten segments, nine of which utilize 60-degree angled mirrors in a "v-trough" shape to increase the total radiation on the surface of the laminates to a nominal two-suns. Segment 10 (added to the plant in 1985) does not utilize mirrors for irradiance enhancement.

Though the plant has demonstrated high availability, energy production efficiency has declined linearly at the rate of 8-12 % per year since 1986

[1]. In 1984, plant ac efficiency was 10.3 %. The 1989 plant ac efficiency was 6.9 %. The primary cause of the decline in plant efficiency has been attributed to thermal degradation of the Ethylene Vinyl Acetate (EVA) encapsulant by the high operating temperatures associated with sunlight concentration [2]. The most notable outward evidence of EVA degradation has been a browning of the laminates in the mirrored segments.

To gain insight into the nature of this degradation, members of the staff of the Southwest Technology Development Institute (TDI) under contract with the Electric Power Research Institute (EPRI) performed I-V (current-voltage) testing at the plant in June 1990.

EXPERIMENTAL

I-V curves were taken with portable equipment capable of testing systems with operating parameters up to 600 V and 125 A. Irradiance was monitored with a silicon pyranometer. This pyranometer is cosine corrected for accurate readings up to incident angles of 80 degrees. Temperatures were measured with Type K thermocouples affixed to the backs of the laminates.

Each mirrored segment is organized into seven 12-tracker groups. The groups are designated by the letters A through G. Electrically, three trackers in series are designated as one subgroup. There are 28 subgroups in parallel per segment. Each two-axis tracker consists of eight panels in series. Panels contain 16 laminates (modules): 4 laminates per parallel block with 4 blocks in series.

TDI tested several subgroups and trackers. Tracker 7G6 (the sixth tracker of Group G in Segment 7) was chosen for testing down to the panel and laminate level. This tracker was selected because it was in a convenient location and not because of any known characteristic in its performance history.

I-V curves were taken of components with mirrors (two-sun irradiance) and without mirrors (one-sun irradiance). Throughout the test period, the trackers continued to follow the sun in two axes. One-sun illumination conditions were achieved by covering the mirrors with opaque plastic.

RESULTS

Figure 1 shows the I-V characteristic for Tracker 7G6 in its normal operating state with the tracker following the sun and all mirrors in place.

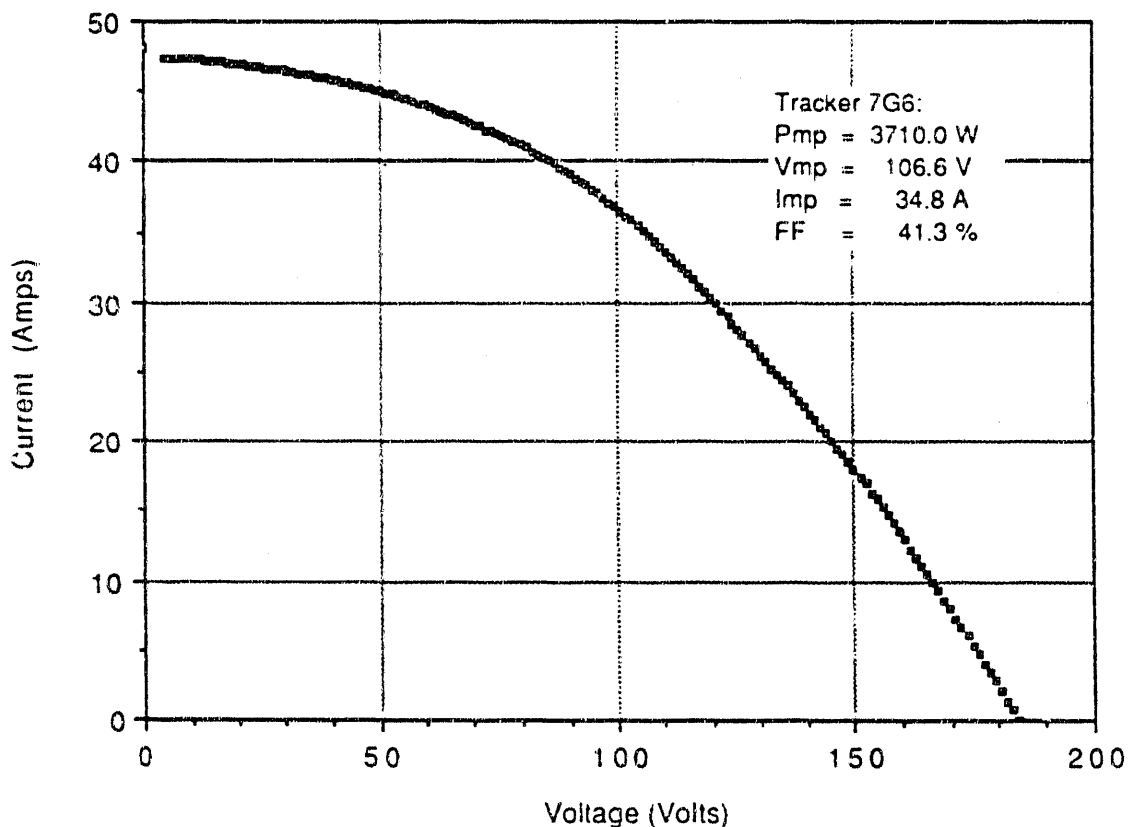


Figure 1. Tracker 7G6 (With Mirrors).

The tracker I-V curve has a fill factor of 41.3 percent and a maximum power of 3.71 kW. This curve was taken when the average laminate temperature was 74 °C.

After this curve was taken, the series connections between the eight panels of tracker 7G6 were broken. I-V curves were taken of each of the eight panels. During this time, the tracker continued to track normally and all of the mirrors remained in place. Figures 2 and 3 show the I-V curves for Panels 1-4 and 5-8, respectively

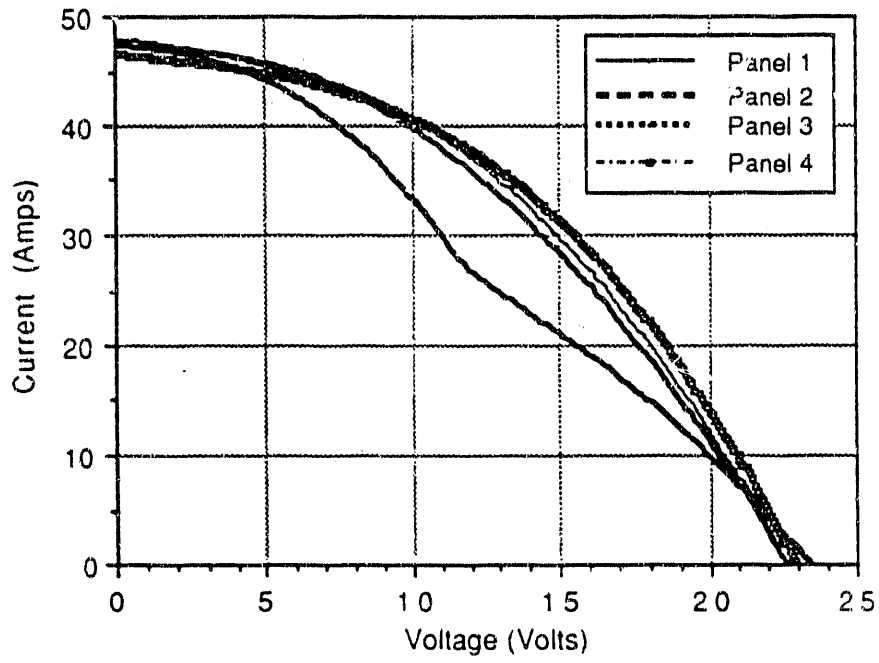


Figure 2. Panels 1-4 of Tracker 7G6.

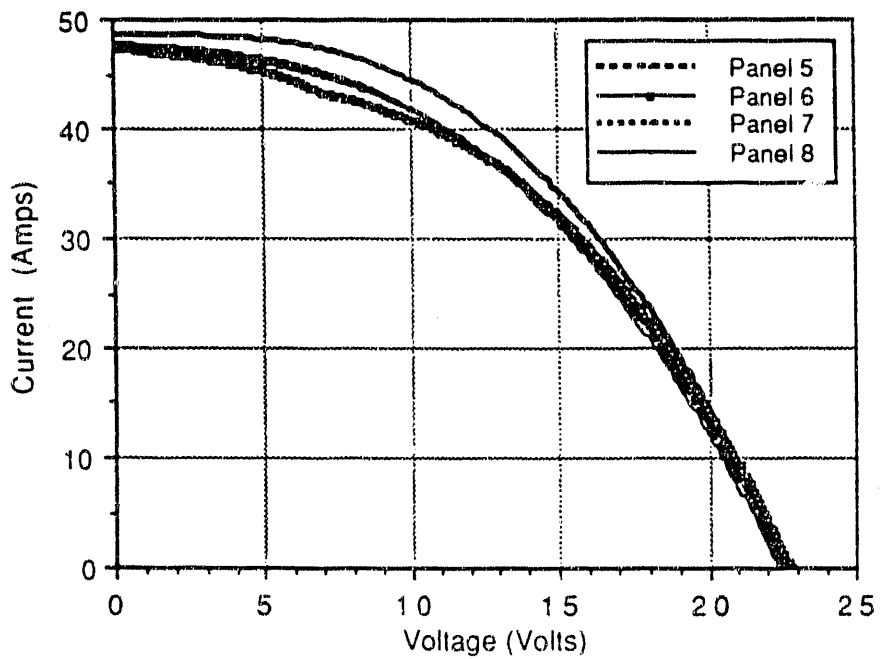


Figure 3. Panels 5-8 of Tracker 7G6.

Open circuit voltages and short circuit currents were closely matched for all 8 of the panels. Panel 2, however, produced a maximum power much less than the other seven panels. The seven similar panels operated with an average maximum power and fill factor of 475.6 W and 44.2 percent, respectively. Panel 2 produced a maximum power of 333.7 W with a fill factor of 30.2 percent.

Panel 6 I-V curves were taken at two different temperatures to quantify the effects of temperature on panel performance. These curves are presented in Figure 4. Panel 6 had performance characteristics typical of the majority of the panels tested.

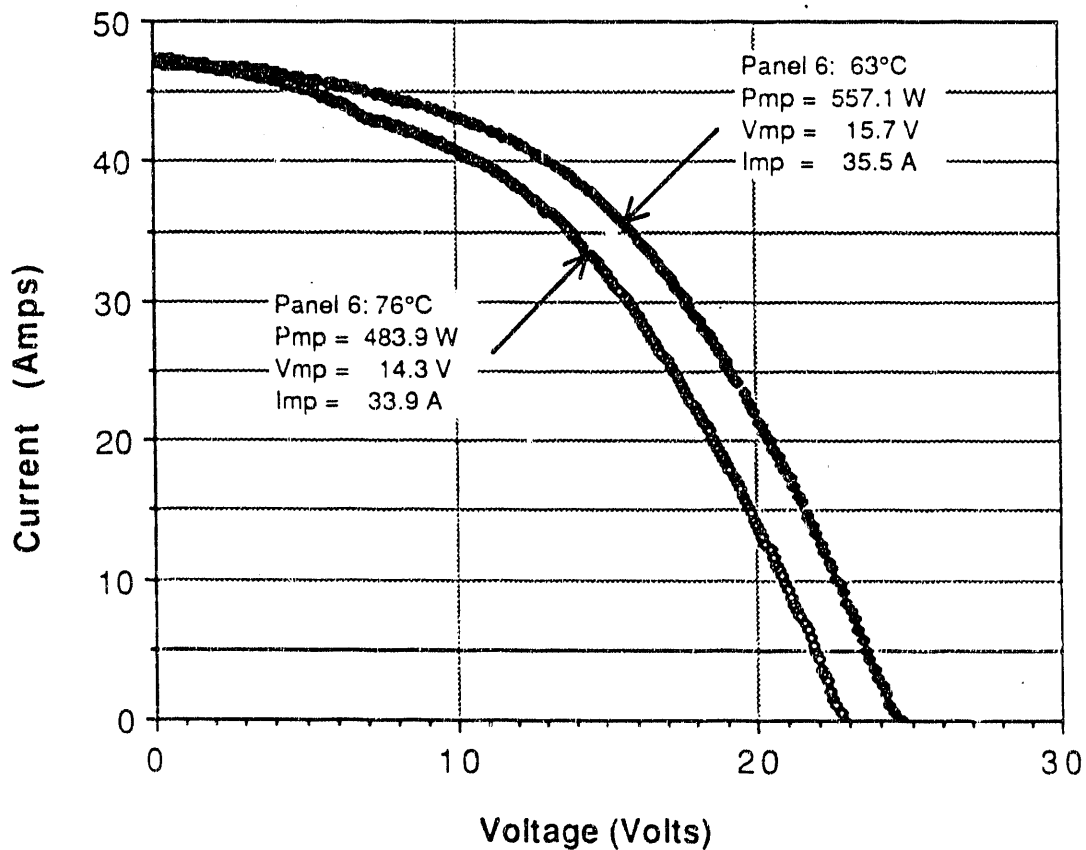


Figure 4. Panel 6 at 76°C and 63°C (With Mirrors).

For Panel 6, the open circuit voltage increased 1.9 V as the temperature dropped 13.2 °C. This represents 0.14 V/°C or 0.57 percent/°C. The series resistance, estimated as the negative reciprocal of the slope of the curve at the open circuit condition, remained unchanged at 0.2 ohms. Fill factor for the curve at 76 °C was 44.8 percent. At 63°C, the fill factor was 47.7 percent.

I-V curves were taken of all 128 laminates (mirror enhanced) of tracker 7G6. Table 1 presents a summary of the peak power values determined for these laminates.

Table 1
PEAK POWER VALUES FOR 128 LAMINATES

Sum of 128 Peak Power Values	4171.0 W
Average	32.6 W
Minimum	8.6 W
Maximum	47.8 W
Standard Deviation	6.9 W

At this point, the mirrors of Panel 6 were covered. I-V curves were again taken on this panel and its laminates. Figure 5 compares I-V curves of Panel 6 operating with and without mirror enhancement.

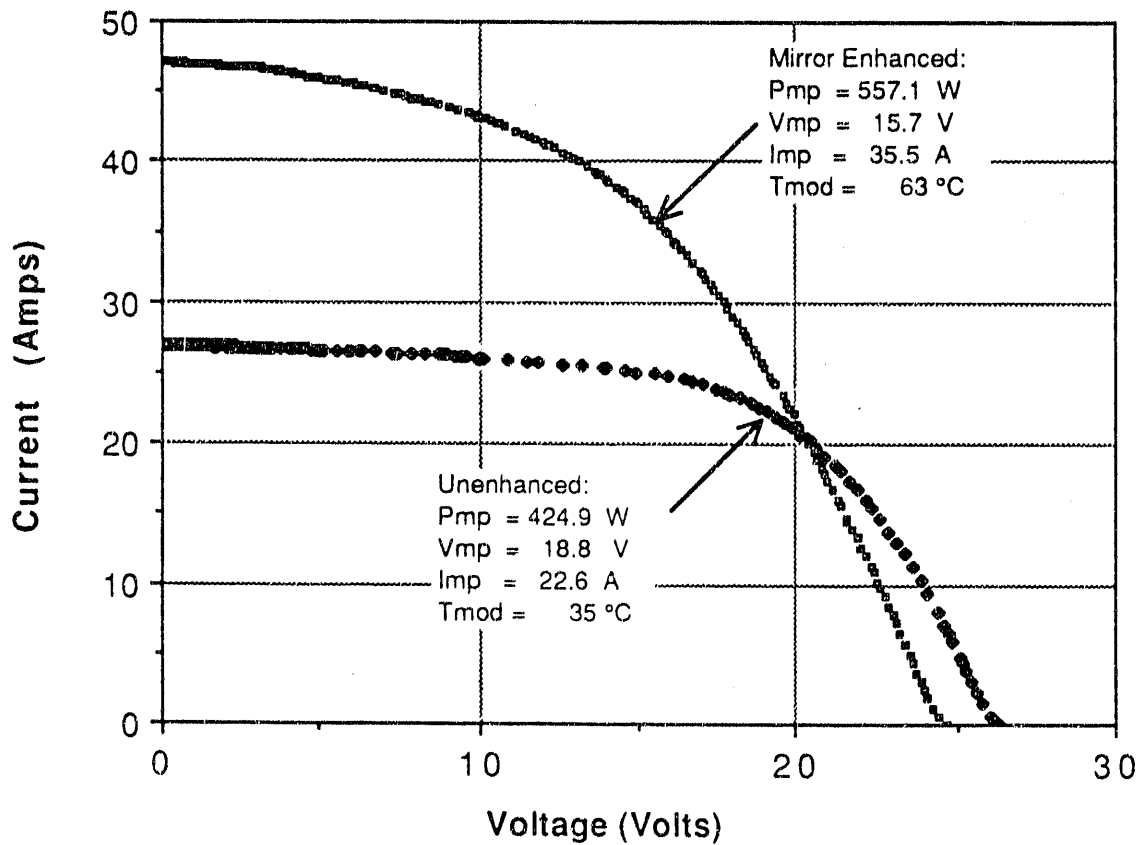


Figure 5. Panel 6 (With and Without Mirrors).

Without mirrors, Panel 6 operated with a fill factor of 59.7 percent and maximum power of 424.9 W. With mirror enhancement, Panel 6 operated with a fill factor 47.7 percent and a maximum power of 557.1 W. Use of mirror enhancement increased the maximum power of Panel 6 by 132.2W (31.1 percent).

Figure 6 compares the I-V curves taken on Laminate 11 of Panel 6 with and without mirror enhancement. This laminate had performance characteristics typical of the majority of the laminates of Panel 6.

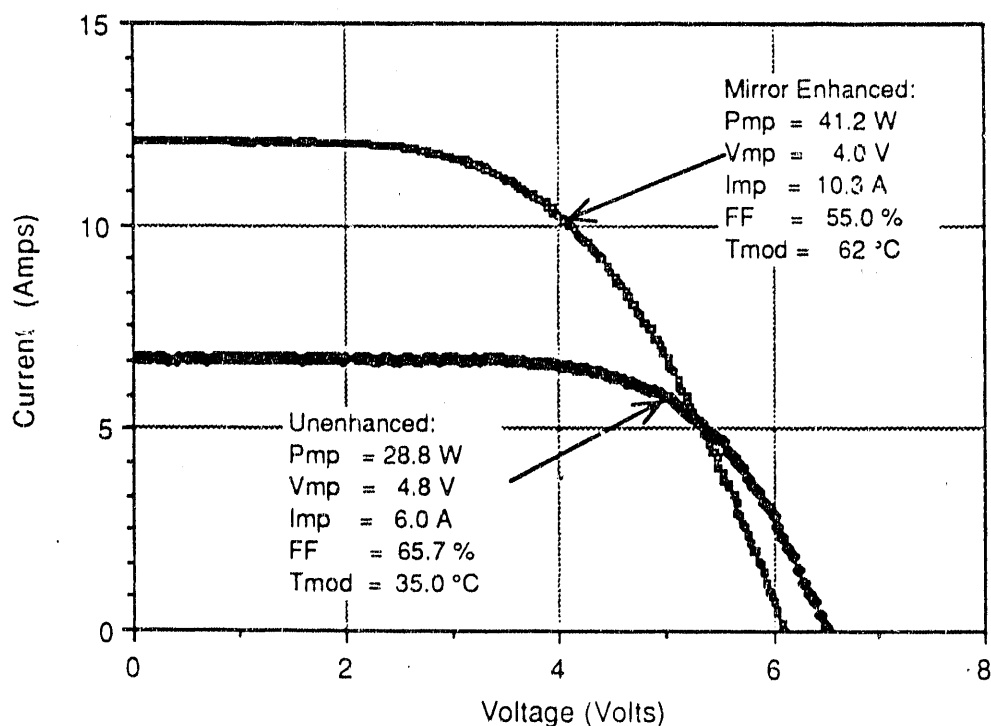


Figure 6. Laminate 11 (With and Without Mirrors).

Under mirror enhancement, Laminate 11 had a fill factor of 55.5 percent and maximum power of 41.2 W. With the mirrors covered, Laminate 11 had a fill factor of 65.7 percent and a maximum power of 28.8 W. Use of mirror enhancement increased the maximum power of Laminate 11 by 12.4 W (43 percent).

Table 2 presents the performance values for the 16 laminates of Panel 6 measured with and without mirror enhancement.

Table 2
 PANEL 6 LAMINATE PERFORMANCE DATA

WITHOUT MIRRORS

Laminate	Module Temp. (°C)	Irrad. (W/m ²)	Voc (V)	Isc (A)	Max. Power (W)	Fill Factor (%)
T6P6L16	36	1040	6.6	6.5	29.2	67.9
T6P6L15	35	1046	6.7	7.0	32.1	68.8
T6P6L14	35	1046	6.6	7.3	29.8	62.0
T6P6L13	35	1046	6.5	6.2	27.7	68.7
T6P6L12	34	1036	6.5	6.3	23.8	58.3
T6P6L11	35	1050	6.5	6.7	28.9	65.7
T6P6L10	35	1050	6.5	6.1	24.0	60.3
T6P6L09	35	1054	6.6	6.8	29.8	66.6
T6P6L08	34	1054	6.6	6.7	27.1	61.4
T6P6L07	33	1057	6.5	6.7	29.3	67.0
T6P6L06	33	1057	6.5	7.0	27.5	61.0
T6P6L05	34	1058	6.4	6.1	22.3	56.7
T6P6L04	35	1066	6.7	7.2	22.5	47.1
T6P6L03	35	1066	6.6	7.1	28.9	61.5
T6P6L02	35	1066	6.4	6.2	20.9	52.8
T6P6L01	35	1069	6.4	6.3	26.2	64.9
Average	34.7	1053.8	6.5	6.6	26.9	61.9
Max	36	1069	6.7	7.3	32.1	68.8
Min	33	1036	6.4	6.1	20.9	47.1

WITH MIRRORS

Laminate	Module Temp. (°C)	Irrad. (W/m ²)	Voc (V)	Isc (A)	Max. Power (W)	Fill Factor (%)
T6P6L16	60	2005	6.2	11.0	40.2	69.4
T6P6L15	60	2019	6.2	12.3	43.4	57.1
T6P6L14	60	2027	6.1	12.7	39.3	50.4
T6P6L13	60	2027	6.2	11.1	39.6	57.9
T6P6L12	62	2010	6.1	10.9	32.4	48.4
T6P6L11	62	2016	6.1	15.1	41.2	55.5
T6P6L10	63	2005	6.1	10.7	30.8	47.1
T6P6L09	64	2005	6.1	12.4	40.4	53.6
T6P6L08	64	2009	6.1	11.8	34.2	47.1
T6P6L07	64	2001	6.1	12.1	39.2	53.6
T6P6L06	64	2007	6.0	12.2	34.7	47.0
T6P6L05	65	2007	6.0	10.8	29.4	45.2
T6P6L04	63	2011	6.3	10.4	20.7	31.7
T6P6L03	64	2011	6.2	12.4	37.8	49.4
T6P6L02	65	1977	6.1	10.7	27.7	42.3
T6P6L01	65	2004	6.1	11.1	37.5	55.5
Average	62.8	2008.8	6.1	11.5	35.5	50.1
Max	65	2027	6.3	12.7	43.4	59.4
Min	60	1977	6.0	10.4	20.7	31.7

In going from a nominal irradiance of one-sun (unenhanced) to two-suns (mirror enhanced), the average power of the laminates increased from 26.9 W to 35.5 W, an increase of 32.2 percent. In all cases, laminate fill factors increased when the mirrors were covered. The average fill factor increased from 50.1 percent to 61.9 percent. At two-suns, the laminate I-V curves show a degree of flattening that indicates a rise in series resistance.

Of importance is the range over which the different laminates encounter their maximum power points. Under one-sun conditions, the 16 laminate maximum power points showed a standard deviation of 3.1 W. Under two-suns, the standard deviation was 5.8 W. This larger standard deviation suggests that mismatch between laminates will occur more at two-sun than one-sun conditions. For the one-sun condition, the sum of the 16 laminate peak power values was 430.0 W while the I-V curve (shown in Figure 4) displayed a maximum power of 424.9 W. This indicates loss due to mismatch was 5.1W (1.2 percent). Under two-suns, the sum of the 16 individual laminate maximum power values was 568.5 W. The I-V curve for the panel (using the 63°C curve) had a maximum power of 557.1 W, a loss due to mismatch of 11.4 W (2.0 percent).

Further testing of trackers and subgroups indicated that the number of severely degraded panels and laminates may be greater in the plant at large than in tracker 7G6.

I-V curves were taken on Tracker 8A7 in its normal operating condition with all mirrors exposed to the sun and later with all of the tracker's mirrors covered by opaque plastic. Figure 7 presents these I-V curves for Tracker 8A7.

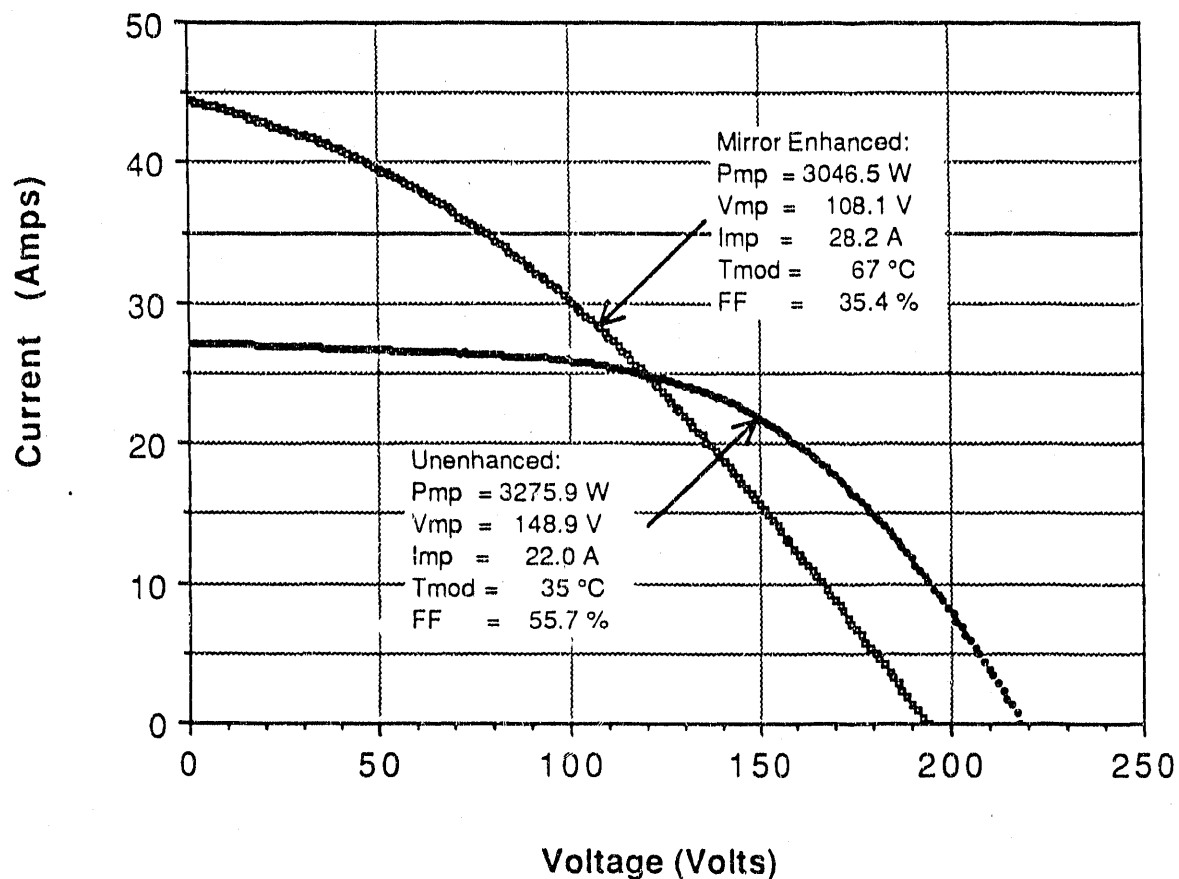


Figure 7. Tracker 8A7 With and Without Mirrors.

Of interest is the fact that the maximum power increased when the mirrors were covered. As observed above, mismatch increases with temperature, particularly in panels with severely degraded laminates. The presence of degraded laminates is indicated by the low fill factor of the mirror enhanced I-V curve (35.4 percent).

Tracker 8A7's greater maximum power production without mirror enhancement is not unique. I-V curves were taken on Trackers 8A1 through 8A9. Three of these trackers, 8A4 through 8A6, have been operating for several months with their mirrors permanently removed. Table 3 presents performance data for these nine trackers.

Table 3
TRACKER PERFORMANCE DATA

WITHOUT MIRRORS

Tracker	Module Temp. (°C)	Irrad. (W/m ²)	Voc (V)	Isc (A)	Max. Power (W)	Fill Factor (%)
8A4	35	1080	204.0	26.3	3221.5	60.0
8A5	35	1080	202.0	26.3	3122.3	58.8
8A6	35	1080	202.0	27.3	2746.1	49.3
Average	35	1080	203.3	26.6	3030.0	56.0
Max	35	1080	204.0	27.3	3221.5	60.0
Min	35	1080	202.0	26.3	2746.1	49.3

WITH MIRRORS

Tracker	Module Temp. (°C)	Irrad. (W/m ²)	Voc (V)	Isc (A)	Max. Power (W)	Fill Factor (%)
8A1	70	1900	168.0	43.9	2692.4	36.5
8A2	70	1900	192.0	46.1	2773.5	31.3
8A3	70	1900	190.0	44.0	3372.7	40.3
8A7	70	1900	193.0	43.3	2895.3	34.6
8A8	70	1900	193.0	42.4	3433.0	42.0
8A9	70	1900	192.0	42.1	3531.3	43.7
Average	70	1900	188.0	43.6	3116.4	38.1
Max	70	1900	193.0	46.1	3531.3	43.7
Min	70	1900	168.0	42.1	2692.4	31.3

In this small population there were two trackers (8A1 and 8A2) that showed performance similar to 8A7: low fill factor and low maximum power.

Figure 8 compares the I-V curves taken for the mirror enhanced Subgroup 8A1-8A3 and the unenhanced Subgroup 8A4-8A6.

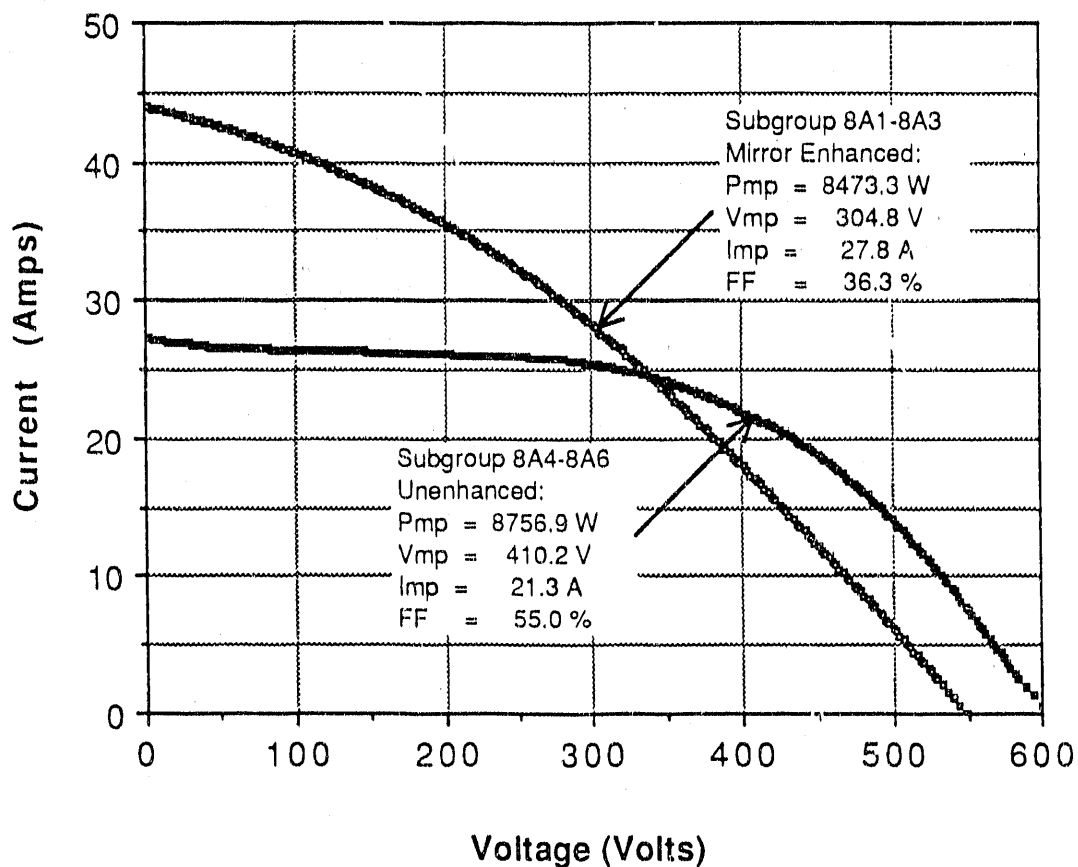


Figure 8. Subgroups 8A1-8A3 and 8A4-8A6.

The maximum power of the unenhanced subgroup exceeded the maximum power of the mirror enhanced subgroup by 283.6 W. Unlike the comparison presented for tracker 8A7, it must be remembered that these curves compare different subgroups.

DISCUSSION

When installed, the laminates of the first nine segments were rated at 39.75 W at standard test conditions (STC, 1000 W/m², 25 °C cell temperature, air mass 1.5) [2]. The 60-degree mirrors have been calculated to add an additional irradiance (received at the surface of the cells) of 60 percent [1]. Hence, at STC, the original rating for the mirror-enhanced laminates was 63.6 W. If we assume a voltage-temperature coefficient of 0.5 percent/°C, the rating at 65°C would be 50.9 W. The 128 laminates of tracker 7G6 had an average peak power (mirror-enhanced) of 32.6 W. Hence, peak power per laminate has declined 18.3 W (35.9

percent) due to degradation. The sum of the 128 laminate peak power values was 4171.0 W. The tracker's measured peak power was 3710.0 W. This represents 461 W (11.1 percent) of power lost due to mismatch.

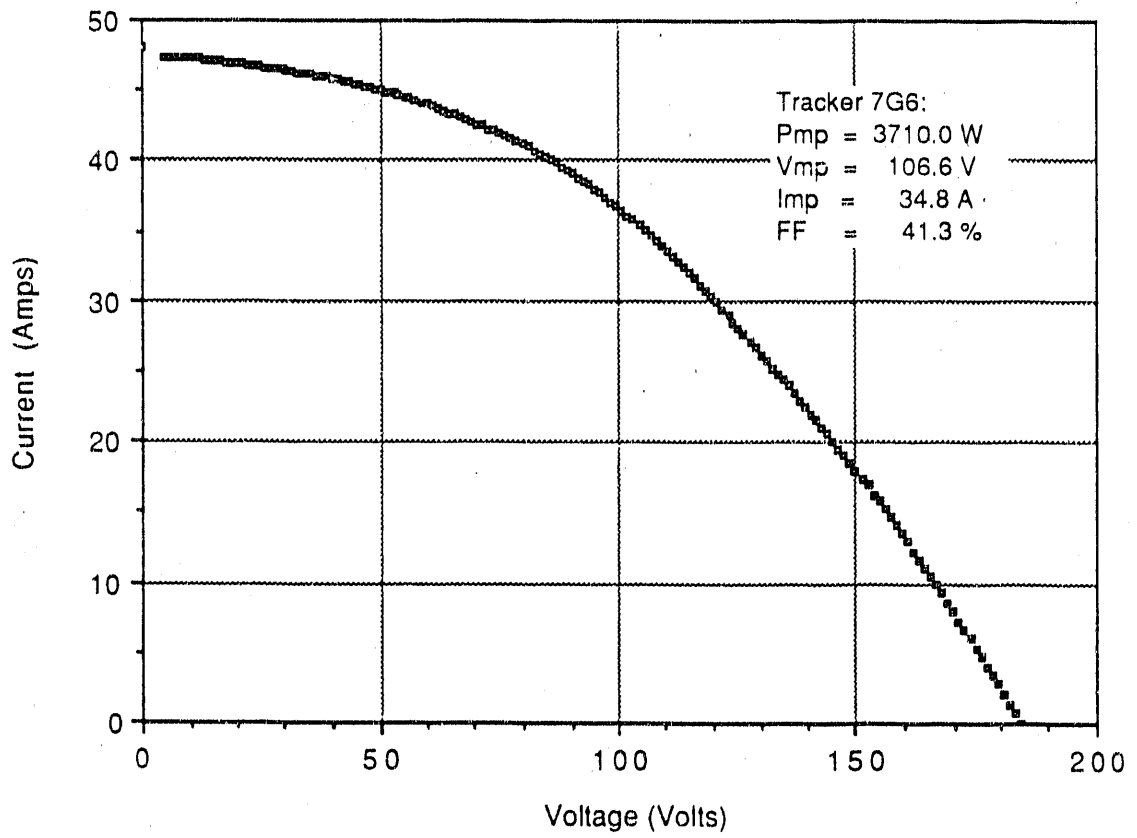
Comparison of laminate performance with and without mirror enhancement indicates that the increased operating temperatures associated with the use of the mirrors increase mismatch losses. For the 16 laminates of Panel 6 of Tracker 7G6, mismatch increased from 1.2 percent without mirrors to 2.0 percent when the mirrors were used. Results of testing other trackers indicate that these data may represent better than average performance for the plant. In some cases, the increase in mismatch losses results in lower power output for operation with mirror enhancement than without. Tracker 8A7 was tested with and without mirror enhancement. With mirror enhancement, the tracker produced 3046.5 W while operating at a temperature of 67°C. Without mirror enhancement, the tracker produced 3275.9 W while operating at a temperature of 35 °C. Other trackers operated with performance characteristics similar to Tracker 8A7.

ACKNOWLEDGMENTS

The authors would like to thank the following individuals for their hard work and assistance: John Schaefer (EPRI), Howard Wenger and Daniel Shugar (PG&E), and Mike Kelly and Lance Pierson (Carrizzo Solar Corp.).

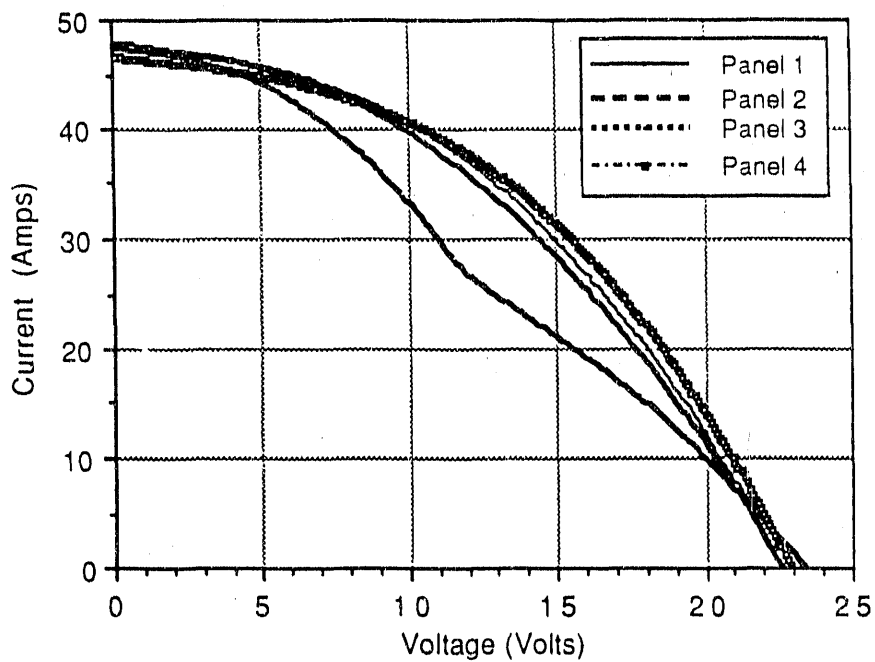
REFERENCES

1. H. J. Wenger, C. Jennings, and J. J. Iannucci. Proceedings of the 21st IEEE PV Specialists Conference (1990).
2. D. D. Sumner, C. M. Whitaker, and L. E. Schlueter, Proceedings of the 20th IEEE PV Specialists Conference (1990) 1289.



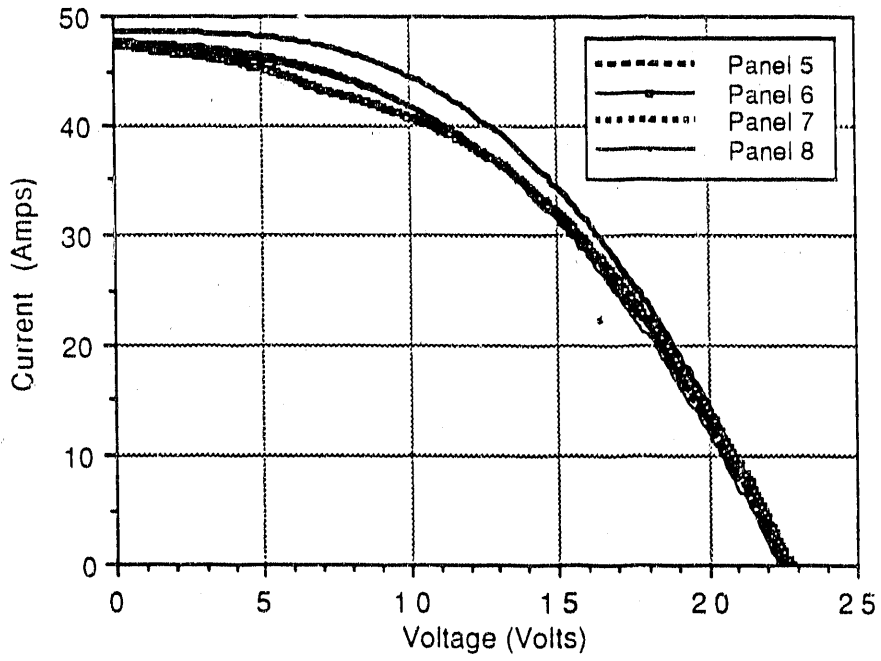
FIELD TEST RESULTS FOR THE 6-MW CARRIZO SOLAR
PHOTOVOLTAIC POWER PLANT

Andrew L. Rosenthal



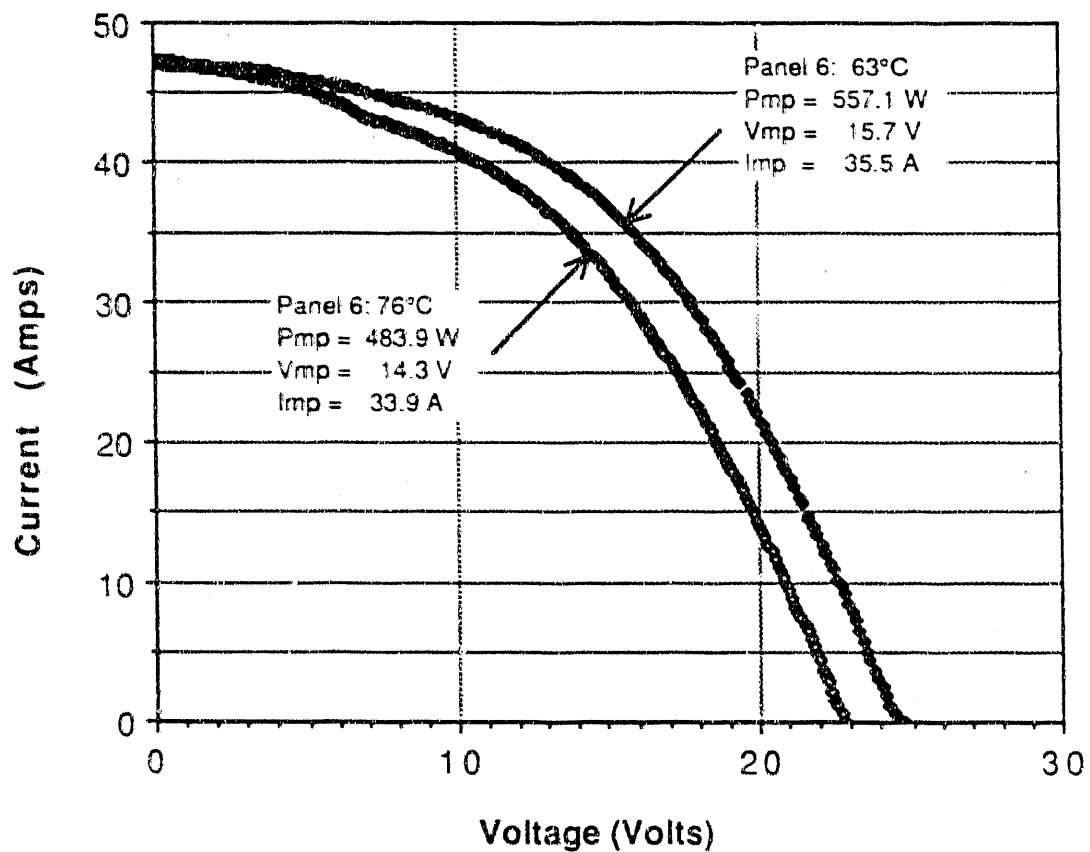
FIELD TEST RESULTS FOR THE 6-MW CARRIZO SOLAR
PHOTOVOLTAIC POWER PLANT

Andrew L. Rosenthal



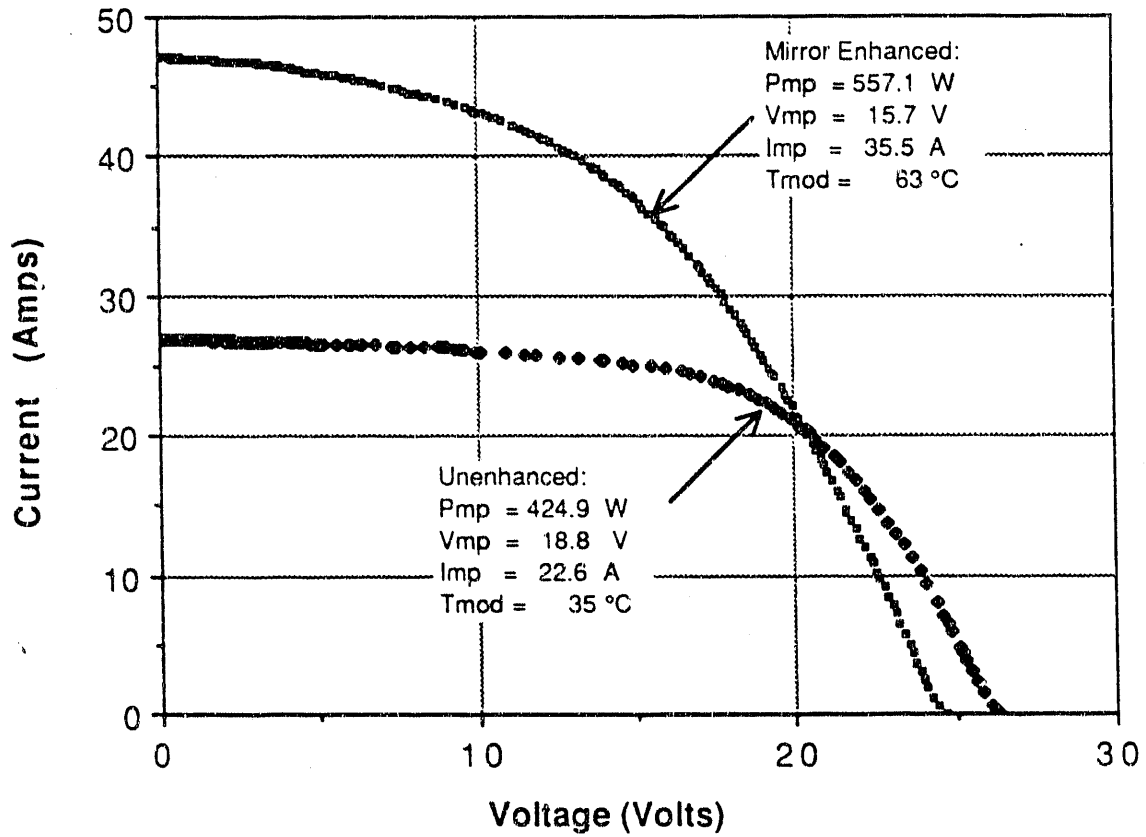
FIELD TEST RESULTS FOR THE 6-MW CARRIZO SOLAR
PHOTOVOLTAIC POWER PLANT

Andrew L. Rosenthal



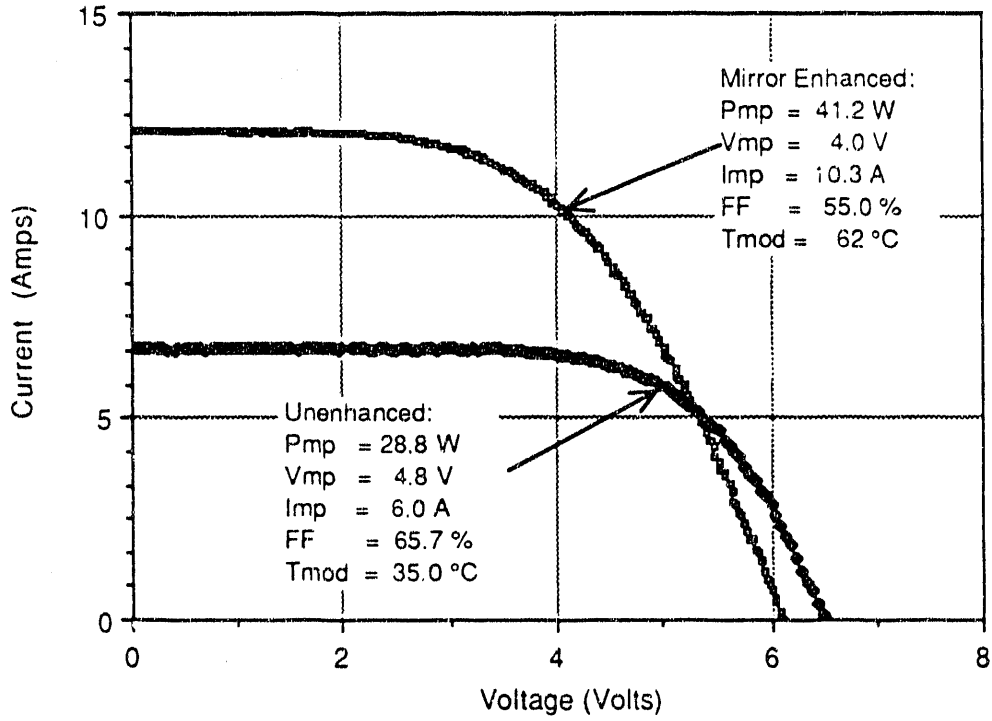
FIELD TEST RESULTS FOR THE 6-MW CARRIZO SOLAR PHOTOVOLTAIC POWER PLANT

Andrew L. Rosenthal



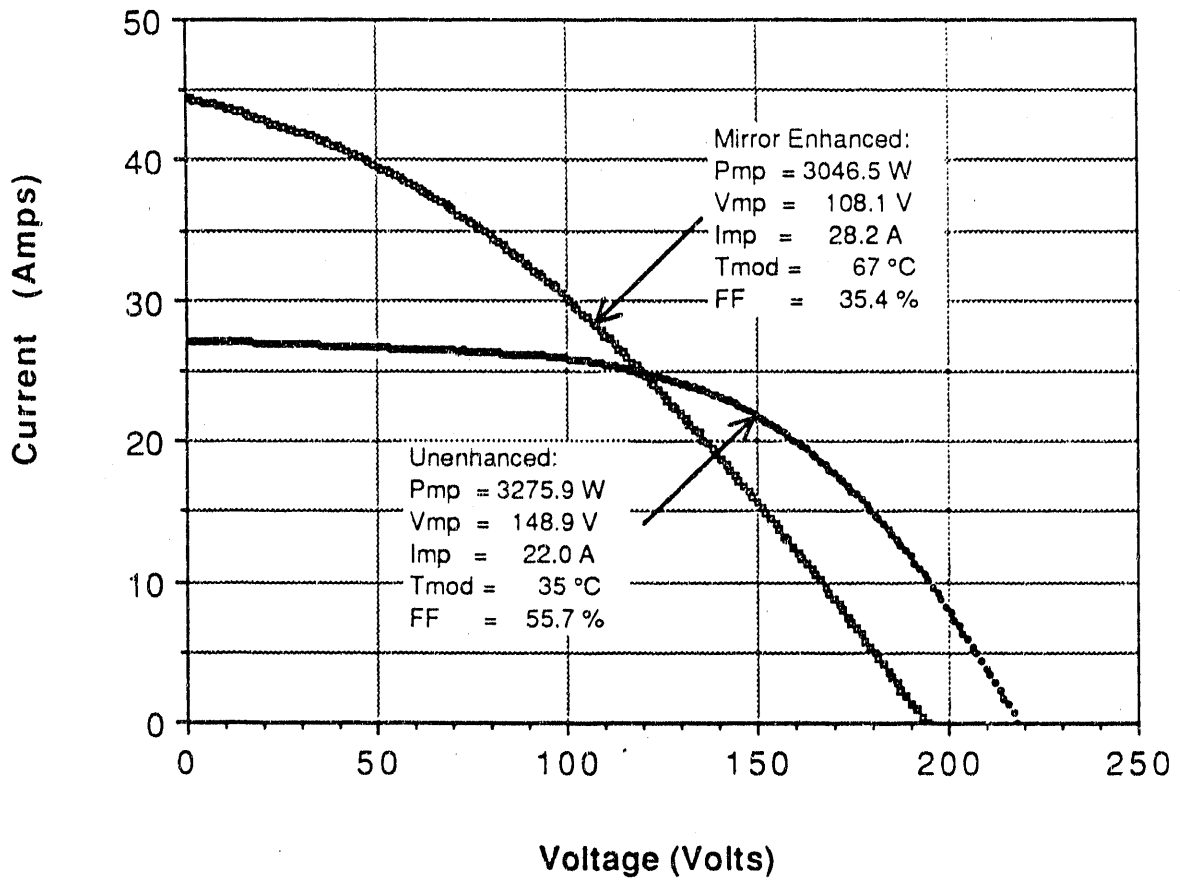
FIELD TEST RESULTS FOR THE 6-MW CARRIZO SOLAR
PHOTOVOLTAIC POWER PLANT

Andrew L. Rosenthal



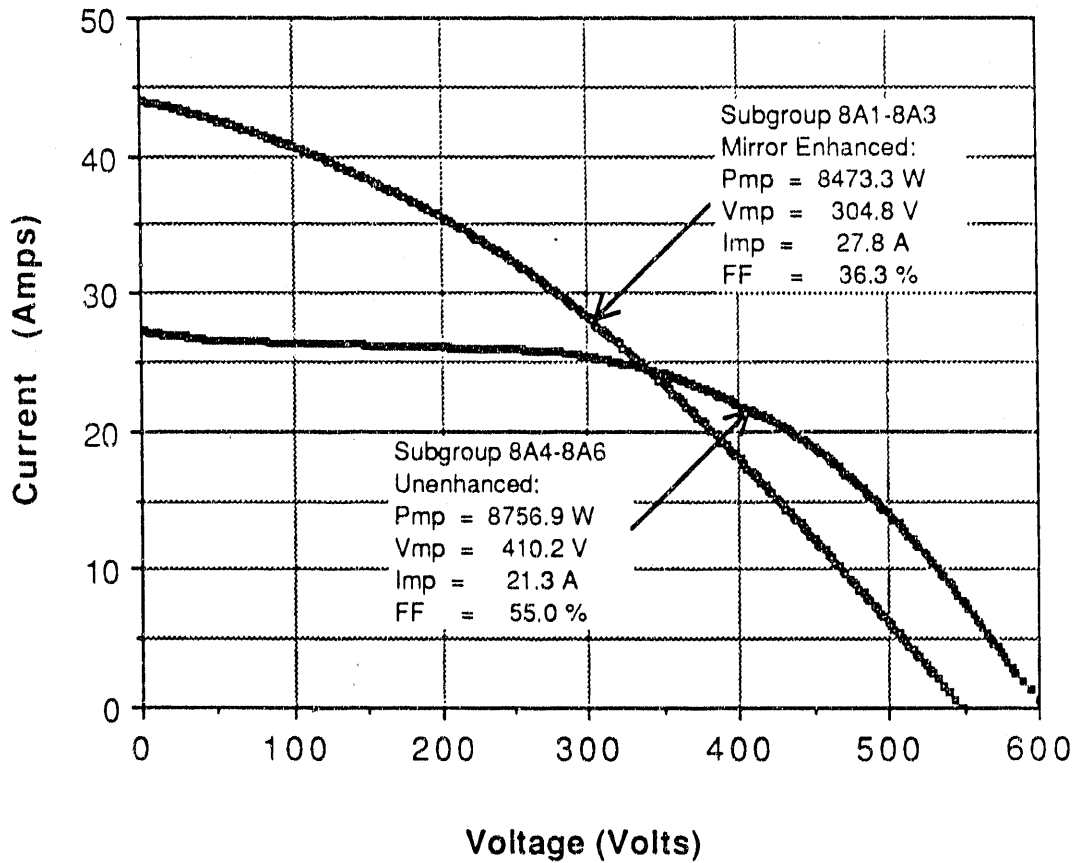
FIELD TEST RESULTS FOR THE 6-MW CARRIZO SOLAR PHOTOVOLTAIC POWER PLANT

Andrew L. Rosenthal



FIELD TEST RESULTS FOR THE 6-MW CARRIZO SOLAR
PHOTOVOLTAIC POWER PLANT

Andrew L. Rosenthal



FIELD TEST RESULTS FOR THE 6-MW CARRIZO SOLAR
PHOTOVOLTAIC POWER PLANT

Andrew L. Rosenthal

Table 1
PEAK POWER VALUES FOR 128 LAMINATES

Sum of 128 Peak Power Values	4171.0 W
Average	32.6 W
Minimum	8.6 W
Maximum	47.8 W
Standard Deviation	6.9 W

FIELD TEST RESULTS FOR THE 6-MW CARRIZO SOLAR
PHOTOVOLTAIC POWER PLANT

Andrew L. Rosenthal

Table 2
 PANEL 6 LAMINATE PERFORMANCE DATA

WITHOUT MIRRORS

Laminate	Module Temp. (°C)	Irrad. (W/m ²)	Voc (V)	Isc (A)	Max. Power (W)	Fill Factor (%)
T6P6L16	36	1040	6.6	6.5	29.2	67.9
T6P6L15	35	1046	6.7	7.0	32.1	68.8
T6P6L14	35	1046	6.6	7.3	29.8	62.0
T6P6L13	35	1046	6.5	6.2	27.7	68.7
T6P6L12	34	1036	6.5	6.3	23.8	58.3
T6P6L11	35	1050	6.5	6.7	28.9	65.7
T6P6L10	35	1050	6.5	6.1	24.0	60.3
T6P6L09	35	1054	6.6	6.8	29.8	66.6
T6P6L08	34	1054	6.6	6.7	27.1	61.4
T6P6L07	33	1057	6.5	6.7	29.3	67.0
T6P6L06	33	1057	6.5	7.0	27.5	61.0
T6P6L05	34	1058	6.4	6.1	22.3	56.7
T6P6L04	35	1066	6.7	7.2	22.5	47.1
T6P6L03	35	1066	6.6	7.1	28.9	61.5
T6P6L02	35	1066	6.4	6.2	20.9	52.8
T6P6L01	35	1069	6.4	6.3	26.2	64.9
Average	34.7	1053.8	6.5	6.6	26.9	61.9
Max	36	1069	6.7	7.3	32.1	68.8
Min	33	1036	6.4	6.1	20.9	47.1

WITH MIRRORS

Laminate	Module Temp. (°C)	Irrad. (W/m ²)	Voc (V)	Isc (A)	Max. Power (W)	Fill Factor (%)
T6P6L16	60	2005	6.2	11.0	40.2	69.4
T6P6L15	60	2019	6.2	12.3	43.4	57.1
T6P6L14	60	2027	6.1	12.7	39.3	50.4
T6P6L13	60	2027	6.2	11.1	39.6	57.9
T6P6L12	62	2010	6.1	10.9	32.4	48.4
T6P6L11	62	2016	6.1	15.1	41.2	55.5
T6P6L10	63	2005	6.1	10.7	30.8	47.1
T6P6L09	64	2005	6.1	12.4	40.4	53.6
T6P6L08	64	2009	6.1	11.8	34.2	47.1
T6P6L07	64	2001	6.1	12.1	39.2	53.6
T6P6L06	64	2007	6.0	12.2	34.7	47.0
T6P6L05	65	2007	6.0	10.8	29.4	45.2
T6P6L04	63	2011	6.3	10.4	20.7	31.7
T6P6L03	64	2011	6.2	12.4	37.8	49.4
T6P6L02	65	1977	6.1	10.7	27.7	42.3
T6P6L01	65	2004	6.1	11.1	37.5	55.5
Average	62.8	2008.8	6.1	11.5	35.5	50.1
Max	65	2027	6.3	12.7	43.4	59.4
Min	60	1977	6.0	10.4	20.7	31.7

Table 3
TRACKER PERFORMANCE DATA

WITHOUT MIRRORS

Tracker	Module Temp. (°C)	Irrad. (W/m ²)	Voc (V)	Isc (A)	Max. Power (W)	Fill Factor (%)
8A4	35	1080	204.0	26.3	3221.5	60.0
8A5	35	1080	202.0	26.3	3122.3	58.8
8A6	35	1080	202.0	27.3	2746.1	49.3
Average	35	1080	203.3	26.6	3030.0	56.0
Max	35	1080	204.0	27.3	3221.5	60.0
Min	35	1080	202.0	26.3	2746.1	49.3

WITH MIRRORS

Tracker	Module Temp. (°C)	Irrad. (W/m ²)	Voc (V)	Isc (A)	Max. Power (W)	Fill Factor (%)
8A1	70	1900	168.0	43.9	2692.4	36.5
8A2	70	1900	192.0	46.1	2773.5	31.3
8A3	70	1900	190.0	44.0	3372.7	40.3
8A7	70	1900	193.0	43.3	2895.3	34.6
8A8	70	1900	193.0	42.4	3433.0	42.0
8A9	70	1900	192.0	42.1	3531.3	43.7
Average	70	1900	188.0	43.6	3116.4	38.1
Max	70	1900	193.0	46.1	3531.3	43.7
Min	70	1900	168.0	42.1	2692.4	31.3

FIELD TEST RESULTS FOR THE 6-MW CARRIZO SOLAR
PHOTOVOLTAIC POWER PLANT

Andrew L. Rosenthal

MIRROR MADNESS

by John Kusianovich

Carrizo Solar Corp.

Star Box 105, Santa Margarita, CA 93453

Introduction: This paper discusses some of the aspects of the time exposure of photovoltaic panels in a power plant during six years of commercial operation.

The World's largest PV module destructive tester is located at California Valley, CA, and has been in operation since 1984. To date it has successfully destroyed several hundred PV modules under actual operating conditions. Some of these were completely burned by current overloads while many others were only lightly toasted by high cell temperatures. The latter are the subject of this report.

The toasted look is apparently caused by the EVA sealant behind the cover glass turning a lovely golden color after exposure to high cell temperatures over a long time period. This has reduced the light transmission by about ten per cent. This is based on flash testing of some of the modules in the LAPPS at Siemens Solar. (figure 1)

The peak power output of the plant has dropped to 4 megawatts from the theoretical 6.5 MW. Therefore, reduced light transmission is not the whole story.

In June 1990, a team from New Mexico State University did field testing for EPRI and discovered other aspects of the problem.

The discoloration of the EVA also may help raise the cell operating temperatures to the point that the IV curves are depressed to the extent that severe voltage mismatches occur.

The paper presented by Andrew Rosenthal (Field Test Results for the 6-MW Carrizo Solar Photovoltaic Power Plant) just prior to this explained these effects in great detail, thus cleverly saving me the trouble.

When the mirrors are covered or removed the IV curves jump back to a normal shape, just as if a great weight had been lifted from their shoulders.

This seems to indicate that the laminates are not permanently damaged by the browning other than the reduced light transmission mentioned above. See attached IV curves referred to above.

As we disassemble trackers into 16 laminate panels and then break them down in the warehouse into individual laminates for shipment to customers, we run an IV curve on each of them. They are sorted into 3 categories: above 32 watts, 20-31 watts, and below 20 watts. The outcome from segment 6 is shown in the table.(figure 2). This is our worst segment (84 trackers, 128 laminates each) for power output, 125kw vs 260kw for our best segment.

Interestingly, we have tried with no success to guess by looking at the laminates to tell their power output. There is no correlation between how badly browned they are with the wattage. Some with the cell edges crinkled put out 38 watts, while some that are barely tan put out 18 watts. The original manufacturing spec is 40 watts. By the way, these are all ARCO single crystal silicon cells.

Three trackers with the mirrors removed a year ago are now producing as much power as a typical set of trackers with mirrors. The mirrors produce a nominal 2 X concentration. When they were removed a year ago the power output was about 12% less than a mirrored array. The voltage for the non-mirrored trackers is higher also which makes the inverters work better. 360V vs 400V, for example.

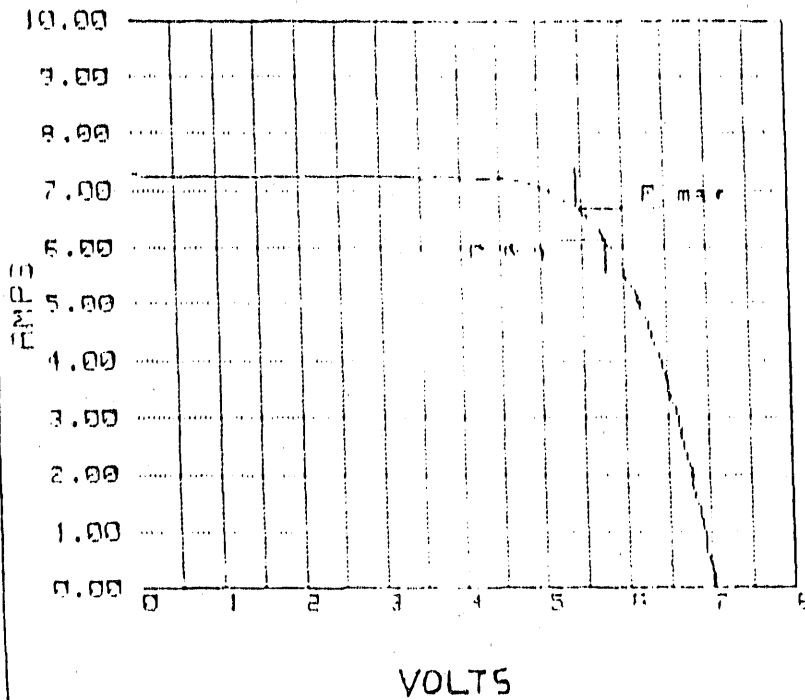
So you ask, why not just remove the mirrors instead of the laminates and continue to operate for ever? Very simple, no one wants to buy 16 foot mirrors. Plenty of people want to buy cheap PV modules. PG&E doesn't want our electricity enough to allow us to pass on the cost of any plant improvements. Isn't the price for our electricity going up with the price of oil? No, PG&E's avoided cost is tied to natural gas and has actually gone down since the unpleasantness in Kuwait!

Photos received from Bill Cerrito at Photocomm indicate that similar ARCO laminates that they are removing from a solar pumping plant exhibit the same browning after 6 years in the sun as ours even though they were exposed to only one sun not 2x.

They also exhibit an interesting behavior that we have noticed, namely the browning disappears over time if the cover glass is broken. We have deliberately broken two laminates and are photographing them over time to confirm this on a controlled basis.

ARCO SOLAR LAPSS (V3.2)

IV CURVE



SERIAL NO. 711
 MODEL EVALUATION
 DATE 11/29/89
 OPERATOR --1135

MODEL ---- M52L
 PART NO. --- 014504
 REVISION -- A

Isc ---- 7.274 AMPS
 Voc ---- 7.04 VOLTS
 V_{Ratd} --- 5.730 VOLTS
 I_{QVr} --- 6.150 AMPS
 P_{QVr} --- 35.51 WATTS
 I_{emp} --- 6.593 AMPS
 V_{emp} --- 5.49 VOLTS
 P_{max} --- 36.15 WATTS
 Fill --- 71.19

TRANSLATION: MSEA
 REF CELL: ASI145

STC AIR MASS 1.50
 STC IRR. 100 MW/CM²
 STC TEMP. 25 DEG C

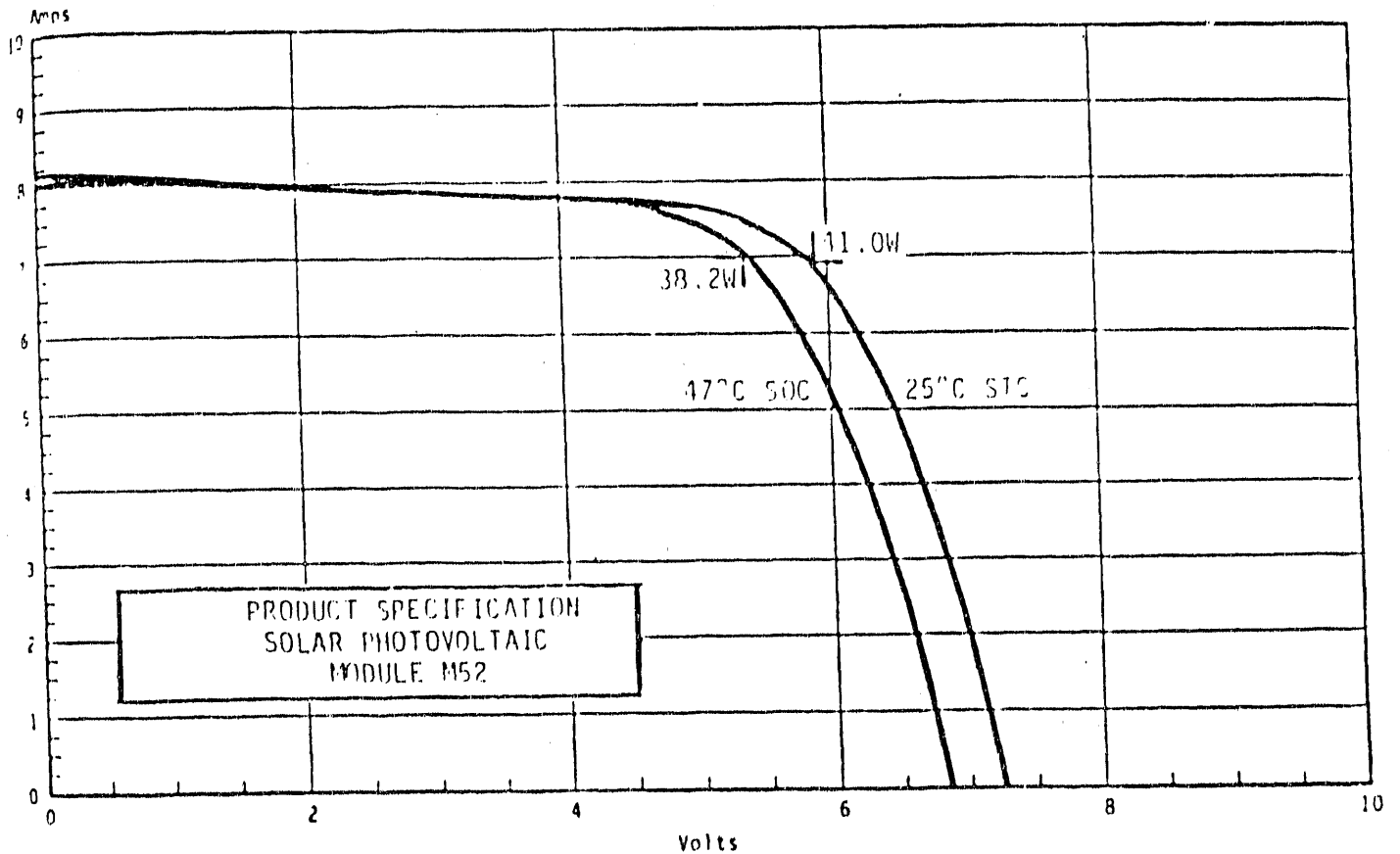


FIGURE 1 FLASH TEST OF TYPICAL GARRIZO BROWNED LAMINATE (TOP) VS ORIGINAL MANUFACTURING SPEC.

CARRIZO SOLAR
LAMINATE WATTAGE TOTALS

TRACKER	FACTORY RATING AMPS	LAMINATE RATING				PANEL TOTAL
		32+ WATTS	32-27 WATTS	27-20 WATTS	20-10 WATTS BURNT/BUBBLE	
6A1	8.0	103	24	*	1	128
6A2	8.0	82	44	*	2	128
6A3	8.0	68	51	*	9	128
6A4	8.0	105	23	*	0	128
6A5	8.0	108	15	*	5	128
6A6	8.0	119	9	*	0	128
6A7	8.1	92	32	*	4	128
6A8	8.1	107	18	*	3	128
6A9	8.1	106	4	NEED	2	112
6A10	8.1	107	18	TO	3	128
6A11	8.1	114	13	RETEST	1	128
6A12	8.1	114	11	*	3	128
7G5	N/A	69	54	*	5	128
6B1	7.4	65	51	*	12	128
6B2	7.4	38	84	*	6	128
6B3	7.4	46	78	*	4	128
6B4	7.6	97	23	*	8	128
6B5	7.6	103	25	*	0	128
6B6	7.6	77	46	*	5	128
6B7	7.6	47	49	*	16	112
6B8	7.6	40	56	NEED	32	128
6B9	7.6	56	50	TO	6	112
6B10	8.1	70	21	RETEST	21	112
6B11	8.1	107	17	*	4	128
6B12	8.1	58	57	*	13	128
6C1	7.5	49	50	*	13	112
6C2	7.5	65	58	*	5	128
6C3	7.5	56	66	*	6	128
6C4	7.5	98	19	*	11	128
6C5	7.8	55	46	*	11	112
6C6	7.8	44	74	*	10	128
6C7	7.8	88	30	*	10	128
6C8	7.8	97	27	*	4	128
6C9	7.8	91	30	3	4	128
6C10	N/A	25	50	16	21	112
6C11	N/A	32	71	13	12	128
6C12	N/A	28	70	30	0	128
6D1	N/A					0
6D2	N/A					0
6D3	N/A					0
6D4	6.7					0
6D5	6.7	15	88	11	14	128
6D6	6.7	31	82	9	6	128
6D7	6.9	14	76	11	11	112
6D8	7.8					
6D9	7.8					
6D10	7.8					
6D11	7.8					
6D12	7.8	48	35	12	17	112
TOTALS		2934	1745	105	320	5104
PERCENT		0.57	0.34	0.02	0.06	

FIGURE 2 TEST RESULTS

245/246

SOLAREX EXPERIENCE WITH EVA ENCAPSULATION

BY

**JOHN H. WOHLGEMUTH
&
RAYMOND C. PETERSEN**

**SOLAREX CORPORATION
CRYSTALLINE DIVISION**

OUTLINE

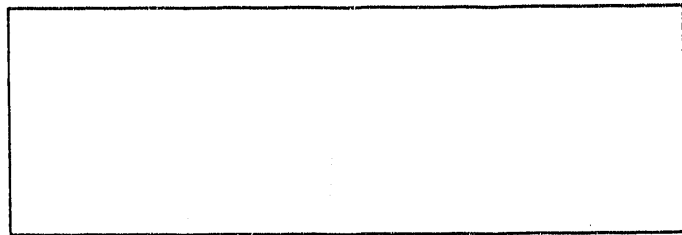
- **HISTORY**
- **MODULE CONSTRUCTION**
- **EVA FORMULATIONS**
- **LAMINATION PROCESS**
- **ACCELERATED TESTING**
- **FIELD EXPERIENCE**
- **CONCLUSIONS**

HISTORY

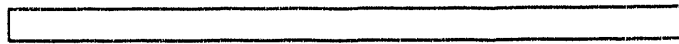
- **BLOCK IV - 1979**
- **DOE SPONSORED DEMONSTRATIONS**
 - Solarex house at Northeast Residence
 - MIT house at Northeast Residence
 - Solarex house at Southwest Residence
 - Carlisle house
 - Block V
- **QUALIFIED TO BLOCK IV & V**
- **POSITIVE FIELD EXPERIENCES**
- **COMMERCIAL MODULE PRODUCTION
BEGUN IN 1982**
- **TODAY ALL SOLAREX TERRESTRIAL
MODULES ENCAPSULATED USING EVA**

MODULE CONSTRUCTION

- **LOW IRON TEMPERED GLASS
SUPERSTRATE**
- **CLEAR EVA ABOVE CELL MATRIX**
- **INTERCONNECTED MATRIX OF CELLS**
- **EVA WITH CRANGLAS BEHIND CELLS**
- **BACKSHEET OF
POLYETHYLENE-MYLAR-TEDLAR**



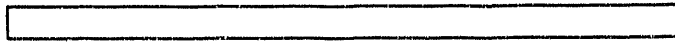
GLASS



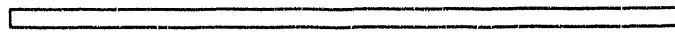
EVA



MATRIX

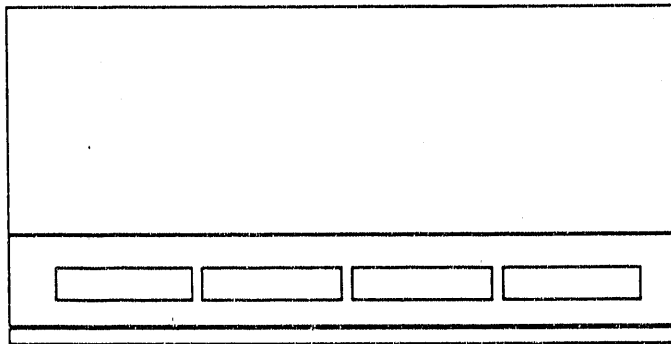


EVA



BACKSHEET

LAMWICH LAYERS



GLASS

MATRIX / EVA

BACKSHEET

**LAMWICH
AFTER
LAMINATION**



EVA FORMULATIONS

- **SPRINGBORN A9918 -
DUPONT ELVAX 150 WITH**
 - 0.2% Uniroyal Naugard antioxidant
 - 0.1% Ciba-Geigy Tinuvin 770 UV Stabilizer
 - 0.3% American Cyanamid Cyasorb UV-531 UV Stabilizer
 - 1.5% Lupersol 101 organic peroxide curing agent

- **IN 1987 SWITCHED TO SPRINGBORN FORMULATION # 1 5 2 9 5**
 - Lupersol TBEC replaces Lupersol 101
 - Reduces temperature-time cycle

- **PRIMER**
 - Not in EVA formulation
 - Apply directly to glass
 - Better assurance of primer at interface
 - No problem with evaporation from film
 - No unwanted chemical reactions with excess primer

- **SPRINGBORN SOLAREX'S ONLY QUALIFIED VENDOR**
- **MIXING COMPLETED & EXTRUSION BEGUN RAPIDLY OR MATERIAL BEGINS TO CURE**
- **EXTRUSION PERFORMED SLOWLY OR RESULTANT FILM WILL SHRINK EXCESSIVELY DURING LAMINATION**

LAMINATION PROCESS

- **REQUIRES SPECIFIED TIME AT CURE TEMPERATURE**
- **INADEQUATE CURE RESULTS IN**
 - Flow of encapsulant at operating temperatures
 - Delamination during use and during humidity - freeze test
- **SOLAREX PERFORMS ENTIRE PROCESS IN LAMINATOR**
 - Easier to ensure proper cure
 - Volatile by-products of Lupersol decomposition are removed from laminate

- **DO NOT USE METALLIC BARRIER IN BACKSHEET**
 - Do not want to trap by-products of Lupersol decomposition

- **USE LUPERSOL TBEC INSTEAD OF 101**
 - More efficient cross-linking reaction
 - Process at lower temperature for shorter time
 - Fewer volatile by-products to remove from laminate


FIELD EXPERIENCE

- **NO FIELD FAILURE OF SOLAREX PRODUCT DUE TO DEGRADATION OF EVA**
- **9 YEARS EXPOSURE - SOUTHWEST RES**
 - Power same as before shipment
 - No delaminations or other signs of mechanical problems
 - Visual browning which goes away when textured glass is covered with alcohol
 - Metallization pattern is yellowed
- **CONCENTRATOR SYSTEMS**
 - Higher operating temperatures & possibly increased UV cause EVA darkening & loss of module power like at Carrisa Plains
 - Consistent with accelerated test results

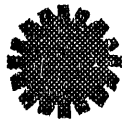
CONCLUSIONS

- **UNDER NORMAL FLAT PLATE OPERATING CONDITIONS ($T < 75^{\circ}\text{C}$)**
 - No reported power loss
 - No reported mechanical degradation
 - Accelerated tests would predict only slight yellowing of encapsulant
 - Field experience for 9 years (in worst case conditions) confirms accelerated test results

- **QUESTIONS LEFT TO ANSWER**
 - What causes yellowing?
 - Will the process ultimately degrade module performance and if so when?
 - Are today's modules as susceptible as the early modules to yellowing (TBEC vs 101)?
 - What changes can be made in the formulation to eliminate or retard the yellowing?



SPIRE'S EXPERIENCE WITH EVA LAMINATION/CURING



spire

M. J. Nowlan
Spire Corporation
Patriots Park, Bedford, MA 01730

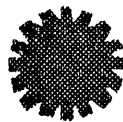
SERI/DOE
PV Module Reliability Workshop
October 26, 1990





EVA R&D AT SPIRE

- 1979 R & D begins with EVA formulation A9918.
- 1979-82 Modules developed for JPL Block IV program. Modules pass Block IV environmental tests.
- 1981 First Spire commercial laminator shipped.
- 1983-85 Modules developed for JPL Block V program. Modules pass Block V environmental tests.
- 1985 R & D begins with EVA formulation 15295.
- 1990 55th Spire laminator shipped.



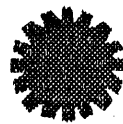
spire





PRESENTATION OUTLINE

- 1. Equipment for EVA Encapsulation**
- 2. Module Design & Processing with EVA**
- 3. QA Testing for EVA Encapsulation**

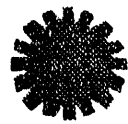


spire



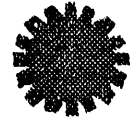
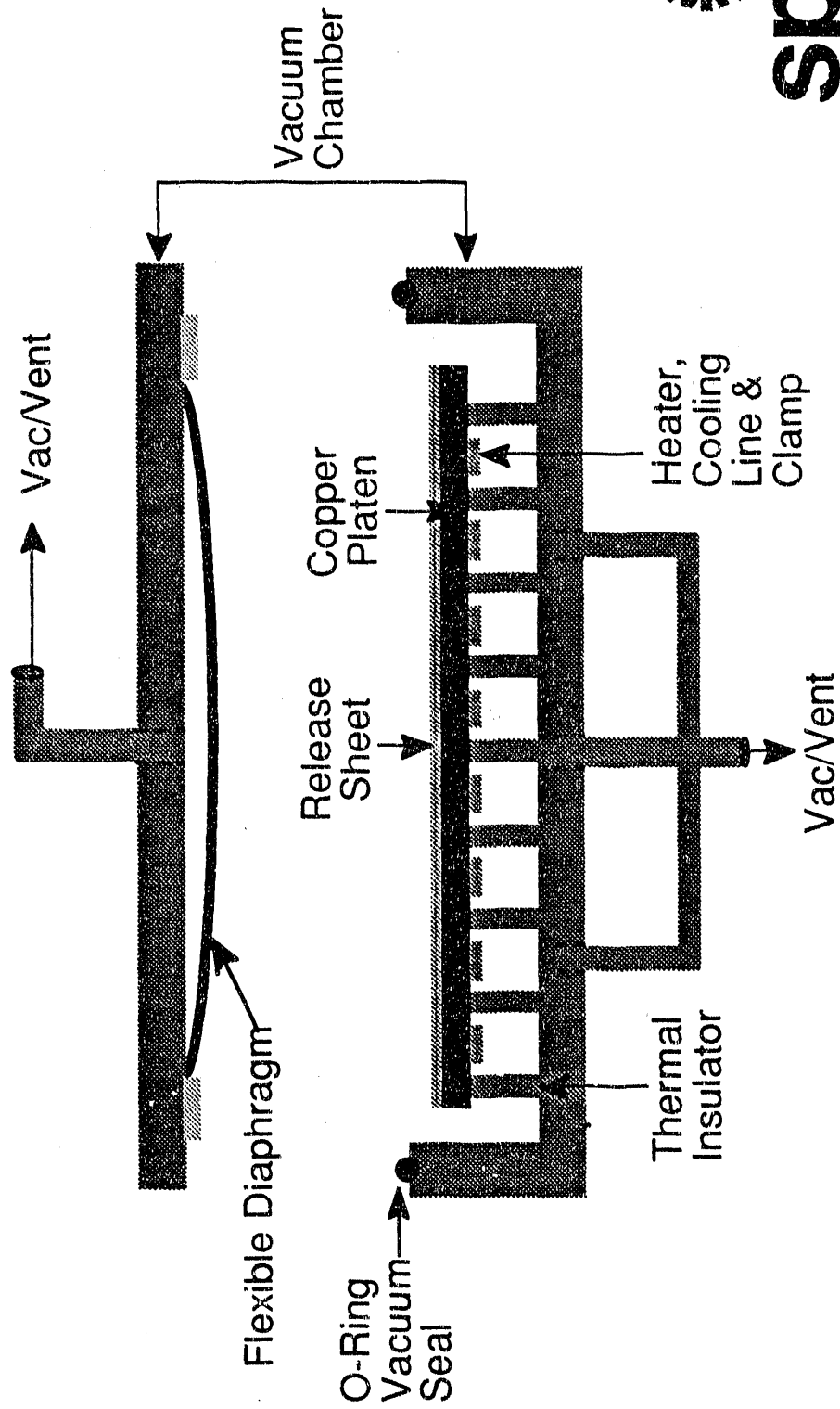
EQUIPMENT REQUIREMENTS FOR EVA ENCAPSULATION

- ▶ **VACUUM SYSTEM**
 - Good pumping speed
 - High conductance between module & pump
 - Chamber P of 0.5 to 1 torr
- ▶ **HEATING SYSTEM**
 - Uniform T across the plane of the module
 - Heat source/load/T sensor balanced for control
- ▶ **PRESSING SYSTEM**
 - Uniform P across the module
- ▶ **CONTROL SYSTEM**
 - Automated, programmable sequence
for reliability



spire

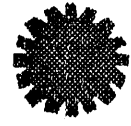
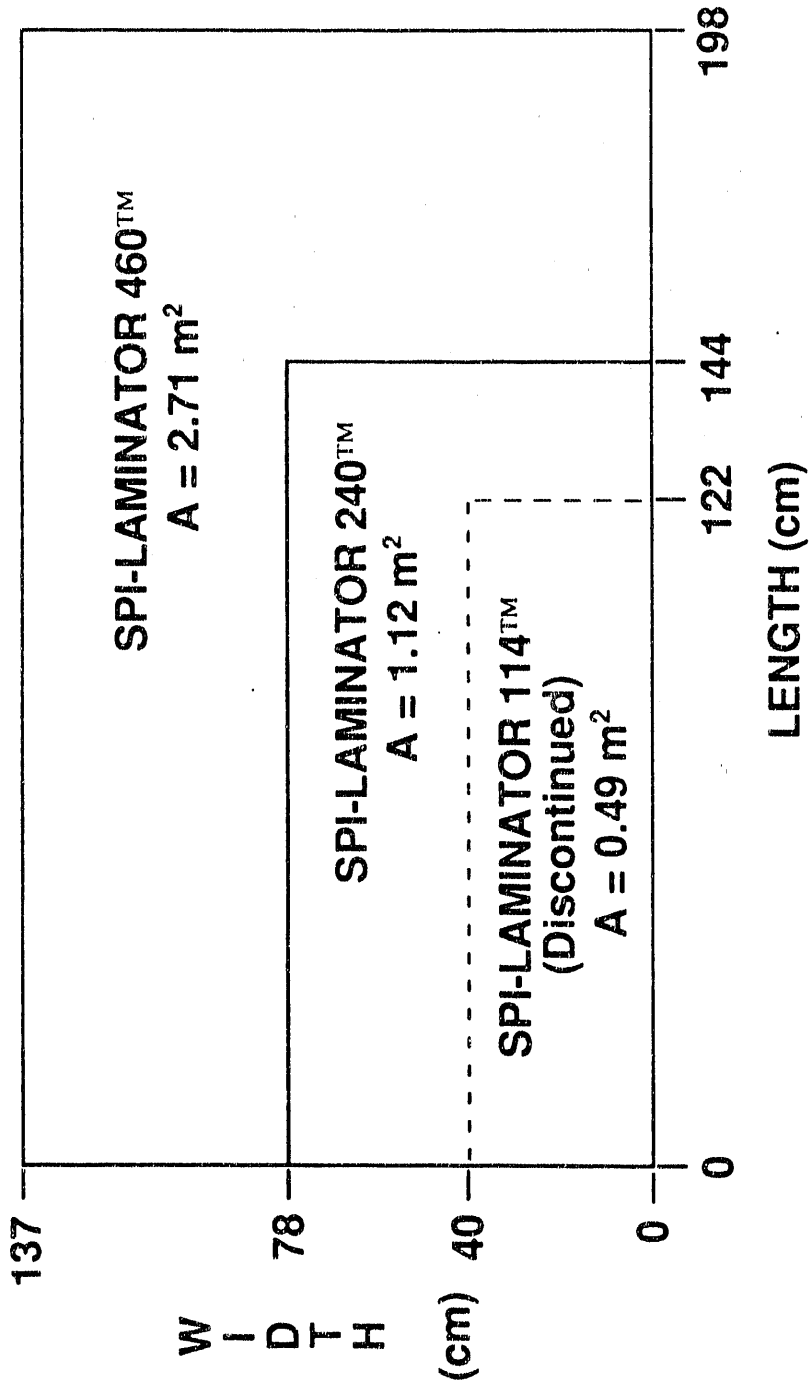
PROCESS CHAMBER - SPI-LAMINATOR



spire

SPIRE LAMINATOR TYPES

Axes show maximum module(s) dimensions



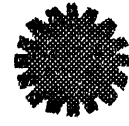
spire

SPIRE LAMINATOR LOCATIONS

October 1990

Region	Laminator Model			Total
	114	240	460	
USA & Canada	1	6	3	10
Europe	2	8	1	11
Japan	1	10	0	11
Other Asia	2	12	0	14
Other Worldwide ^a	3	6	0	9
Total	9	42	4	55

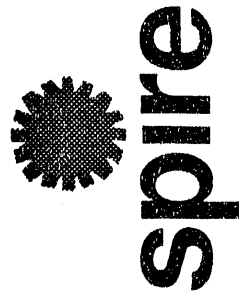
^aIncludes Africa, Australia, and South America



spire

SECTION 2

Module Design & Processing with EVA





MODULE DESIGNS PRODUCED WITH SPIRE'S LAMINATORS

▶ CELL MATERIALS

- x-Si, poly x-Si, ribbon Si, a-Si

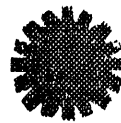
▶ MODULE TYPES

- superstrate, substrate, flexible, double rigid

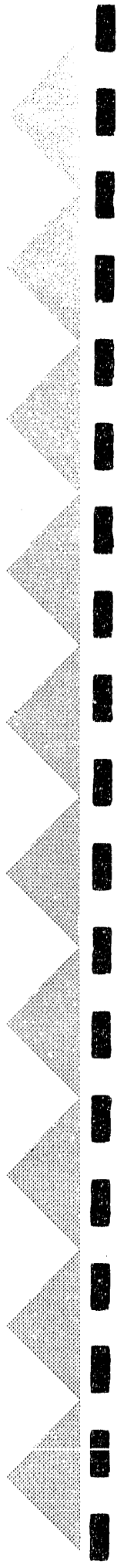
▶ MODULE MATERIALS

- glass, polycarbonate, Tefzel^a, PVF,
polyester film, Al foil, fiberglass, etc.

^aTM of E.I. duPont de Nemours

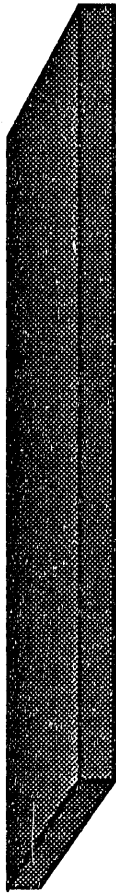


spire

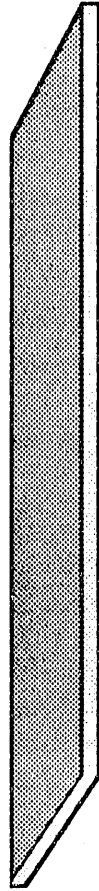


SUPERSTRATE MODULE DESIGN

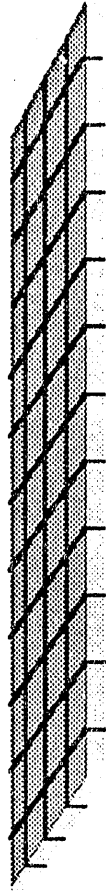
MATERIAL



Glass, low Fe_2O_3



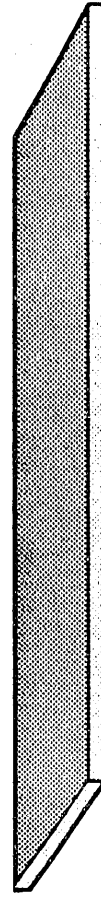
EVA Film



Solar Cells



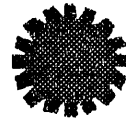
Fiberglass Cloth



EVA Film



PVF or Other Back
Cover Film



spire





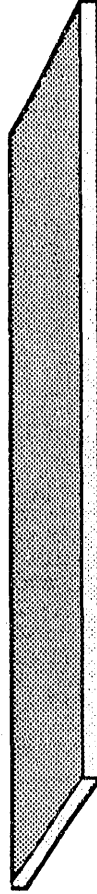
SUBSTRATE MODULE DESIGN

MATERIAL

Tefzel™ or PVF
Cover Film



EVA Film



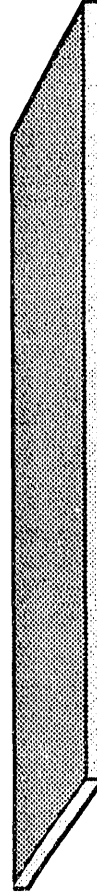
Fiberglass Cloth



Solar Cells



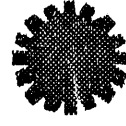
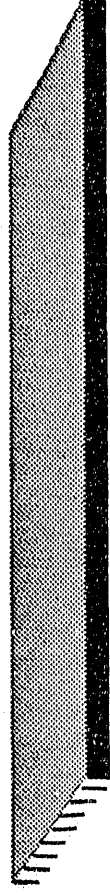
EVA Film



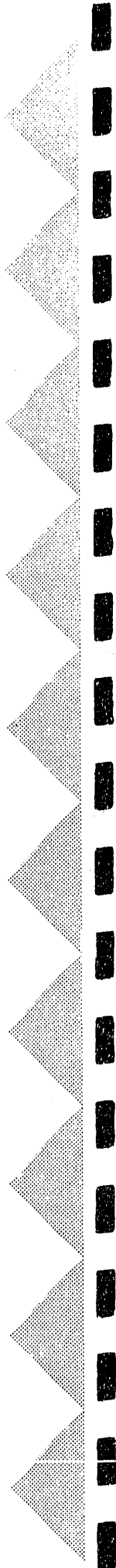
PVF or Polyester
Insulator Film



Rigid Substrate

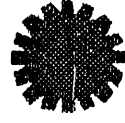


spire



EVA ENCAPSULATION PROCESS

1. Assemble materials in a stack
2. Remove air from within the stack's layers
3. Heat the materials to melt the EVA
4. Press the materials to fill voids with EVA
5. Cure the EVA (T,t)
 - Stabilize the EVA via cross-linking
 - Adhere EVA to other materials

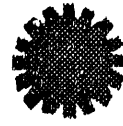


spire

PROCESSING TIME FOR VARIOUS EVA FORMULATIONS

EVA Types	Description	Process	Process Time in SPI-LAMINATOR™ (minutes)
A9918	Standard EVA	Laminate	5 to 7
A9918-P	Standard EVA with Primer	Laminate & Cure	25 to 30
15295	Fast-cure EVA	Laminate	5 to 7 ^a
15295-P	Fast-cure EVA with Primer	Laminate & Cure	25 to 30 ^a
		Laminate & Cure	5 to 7
		Laminate & Cure	5 to 7 ^a

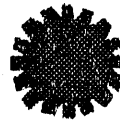
^aNo priming step required.



spire

SECTION 3

QA Testing for EVA Encapsulation



spire



QA TESTING FOR EVA ENCAPSULATION

1. STANDARDIZED MODULE ENVIRONMENTAL TESTING

Purpose: To indicate module lifetime.

Frequency: For each module design.

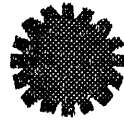
Examples: JPL (Blocks IV & V), ASTM, UL, USCG, IEC.

2. EVA PHYSICAL TESTING

Purpose: To maintain consistent product quality.

Frequency: For each batch of EVA.

Examples: Gel content, Peel strength.



spire

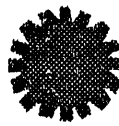
EVA GEL CONTENT TEST

Springborn Laboratories/JPL Method

1. Laminate & cure EVA at desired conditions.
Temperature & pressure cycles, thermal resistances.
2. Weigh cured EVA and filter paper.
3. Soak EVA in 60° C toluene, 4 hrs.
4. Pour EVA/toluene through filter paper.
5. Dry paper & EVA gel fraction at 60° C, 4 hrs. (odor-free).
6. Weigh gel & paper.
7. Calculate gel content:

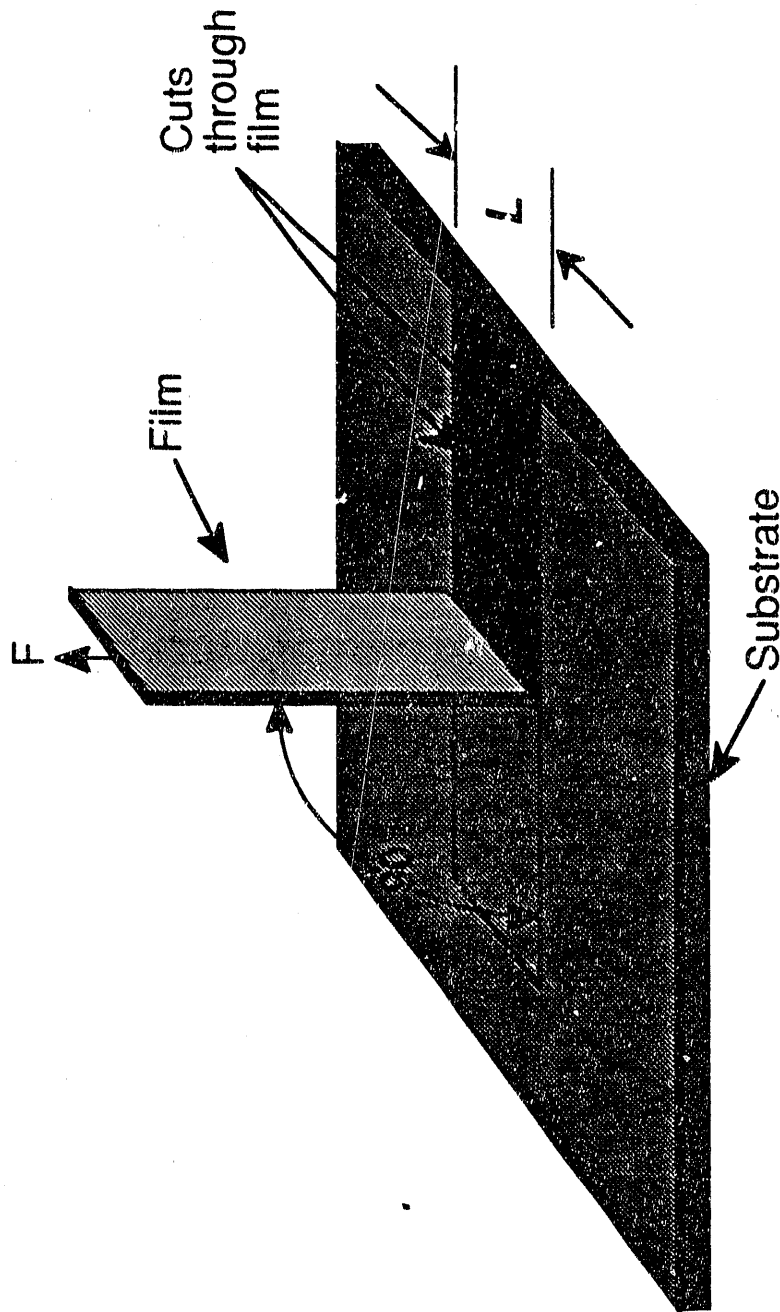
$$\text{gel fraction} = \frac{(\text{Wt of gel}) - (\text{Wt of paper})}{(\text{original Wt of EVA})}$$

8. Acceptance Level: 65%

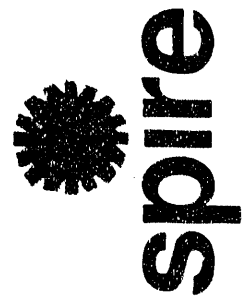


spire

PEEL TEST METHOD

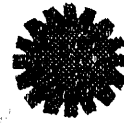


$$\text{Peel strength} = \frac{F}{L} \quad (\text{lbs/inch) or (g/cm)}$$



EVA GEL FRACTION AND PEEL STRENGTH

Run No.	Pump Time (min)	Total Time (min)	Temp (°C)	Gel Fraction (%)	Peel Strength (lbs/in)	Comments
59	t_0	5.0	T_0	78	1.81	Good gel, Weak peel strength
				85	1.53	
60	t_0	5.0	$T_0 + 5$	81	6.78	Good gel, Trapped air, Weak peel strength
				83	5.13	
64	$t_0 + 1.0$	5.0	$T_0 + 10$	100	>20.7	Good gel, Excellent peel strength
				87	>24.4	



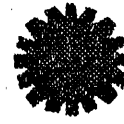
spire

- ▶ EVA age: 1 month
- ▶ Peel interface: EVA/glass
- ▶ EVA type 15295-P (fast cure)
- ▶ Laminated in the SPI-LAMINATOR™

EVA GEL FRACTION AND PEEL STRENGTH

Run No.	Pump Time (min)	Total Time (min)	Temp (°C)	Gel Fraction (%)	Peel Strength (lbs/in)	Comments
Peel interface: EVA/glass						
2B	$t_o + 1$	5.0	$T_o + 10$	83	10.3	Good gel, Moderate peel strength
					13.0	
3B	$t_o + 1$	7.0	$T_o + 10$	82	21.0	Good gel, Excellent peel strength
					31.6	
Peel interface: EVA/PVF						
3A	$t_o + 1$	7.0	$T_o + 10$	82	26.8	Good gel, Excellent peel strength
					31.2	

- ▶ EVA age: 6 months
- ▶ EVA type: 15295-P (fast cure)
- ▶ Laminated in the SPI-LAMINATOR 240™



spire

Recent Generic Studies of

Ethylene Vinyl Acetate (EVA)

Degradation

279

John Pern

Group Leader: Dick DeBlasio

Sub-Task Leader: Al Czanderna

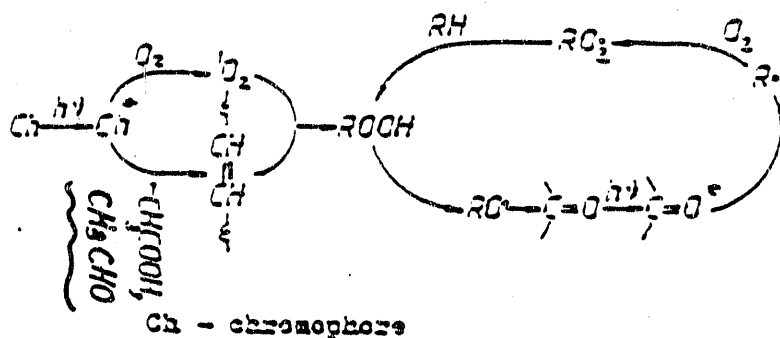
Outline

1. Introduction -- Encapsulant
2. Degradation and Stabilization of EVA
3. Analysis of EVA Before and After Degradation
 - Structural Effects of Thermal Processing
 - Degradation of EVA: EVA Yellowing, [UV Absorber] and [% Cross-linking]
4. Conclusions

Photodegradation of Unstabilized EVA

- C. Andrei, I. Hogeia and V. Dobrescu,
 1. Proc. IUPAC Macromol. Symp. 28 (1982) 329
 2. Rev. Roum. Chim., 33 (1988) 53-58

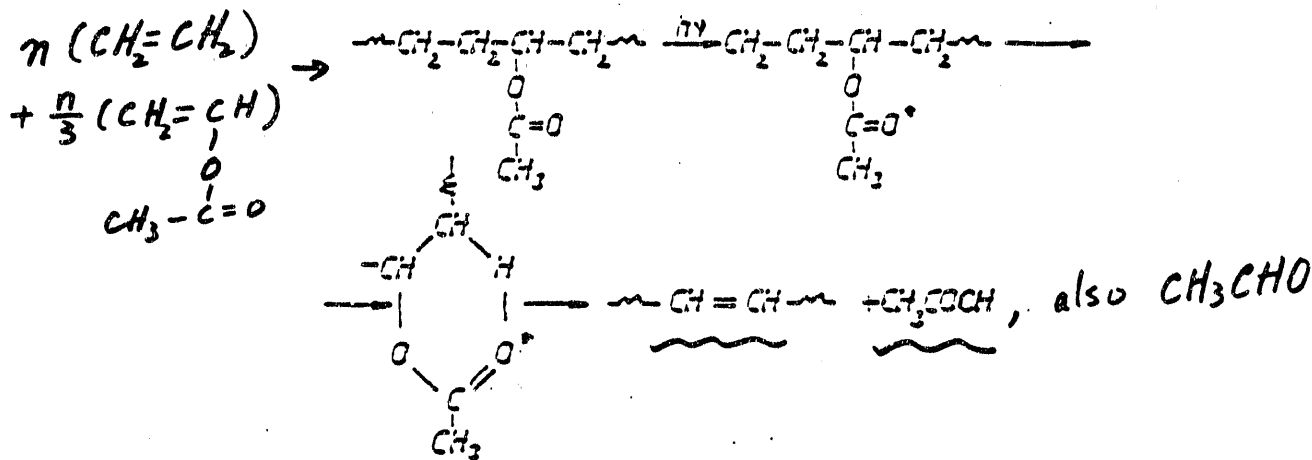
Photodegradation Mechanisms



Degrading factors:

- UV light,
 O₂, heat,
 $-C=C-\overset{O}{\parallel}$,
 $-C=O$, etc.

The formation of double bonds with acetic acid elimination by a mechanism comprising a transition state, with the formation of a six membered ring:



Compounds Resulted From Irradiation of EVA Copolymer at 27°C for Three hours

Compound	% g ± 10%
CH ₃ COOH	72.82
CH ₃ CHO	22.80
CH ₄	4.15
CO ₂	0.19
CO	0.04

Formulation and Stabilization of EVA

1. Add curing agent [Lupersol 101 or TBEC]
 - => to produce cross-linked polymer chains (65-70% Gel)
 - => to render desired mechanical properties

2. Add UV absorber [Cyasorb UV 531] (0.3 wt%)
 - => to absorb UV light (light --> heat)
 - => but, itself is photodecomposable

3. Add photo-antioxidant [Tinuvin 770]
 - => to intercept the chain-breaking radicals
 - => itself is regeneratable

4. Add thermo-antioxidant [Naugard P]
 - => to block thermal oxidation by O₂
 - => hygroscopic, hydrolyzable

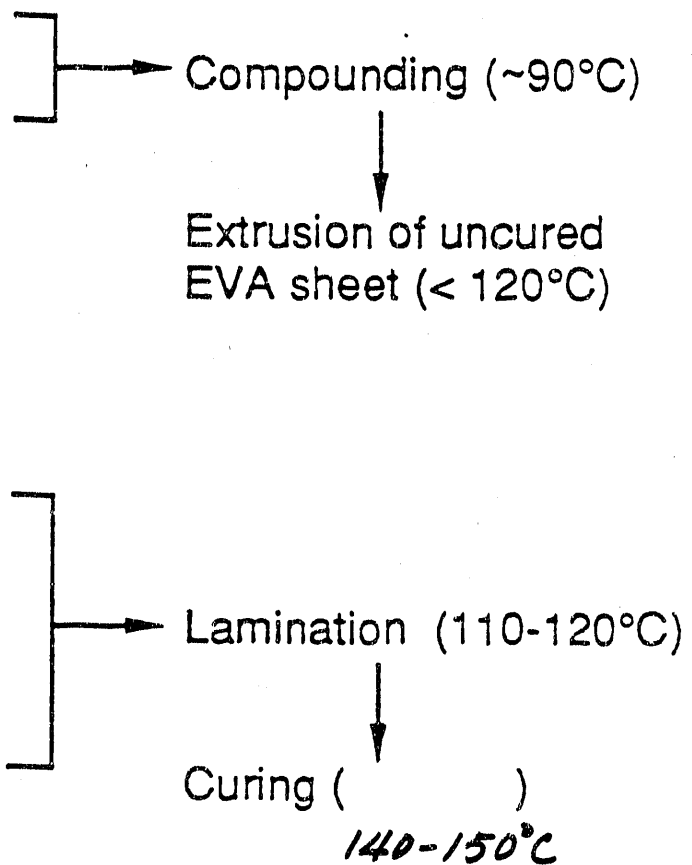
Formulation

Elvax 150 (Du Pont)
+
Pre-mixed additives
(UV absorber, curing
agent, anti-oxidants)

Encapsulation

- Cover glass (7059)
- Uncured EVA sheet
- Metallized cells and interconnections
- Uncured EVA sheet
- Teflon back sheet

Thermal Processing



Photothermal Degradation of Stabilized EVA

Liang et. al. (JPL), Polym. Sci. & Tech. 20 (1982) 267-278

★ Increased cross-linking (gel content) on the EVA

Table 3. Percentage of Extractable, Molecular Weight Distribution (M_w) of the Extract and Crosslinking Density of EVA as a Function of Photothermal Aging

TEMPERATURE °C	TIME OF TEST (HOURS)	TEST CONDITIONS	% EXTRACTABLE	M_w	CROSSLINKING DENSITY (mole/cm ³)
85	800	AS RECEIVED	48	206,000	1.12×10^{-6}
		OVEN	35	168,000	2.79×10^{-6}
		UV/AMBIENT AIR	33	118,000	4.32×10^{-6}
105	800	UV/NO EDGE SEAL	29	75,000	7.60×10^{-6}
		OVEN	37	174,000	1.33×10^{-6}
		UV/AMBIENT	33	91,000	5.86×10^{-6}
		UV/NO EDGE SEAL	34	44,000	10.10×10^{-6}

Analysis of EVA Degradation

Analytical Methods

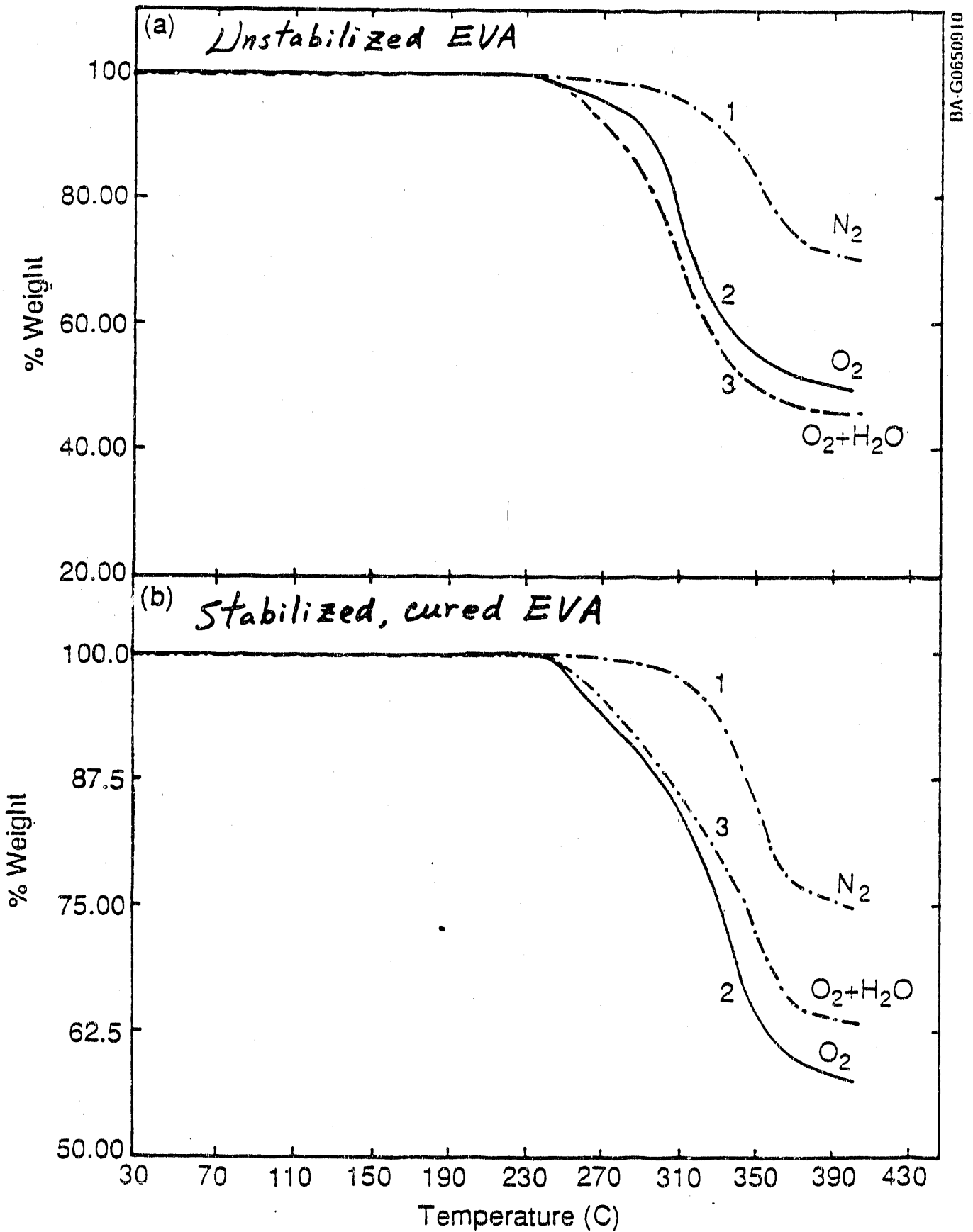
1. **Net chemical** : separation & quantification
2. **Fluorescence** : structure, chromophores
3. **UV-visible** : molecular identification & quantification
4. **FTIR-ATR** : molecular structure (surface)
5. **XPS (ESCA)** : surface analysis
6. **Thermogravimetry (TGA)**: thermal stability

Analytical Objects

1. Quality of EVA raw material (EIVax 150)
2. Effects of thermal processing on EVA structure (FA)
3. UV absorber (Cyasorb UV 531) concentration
4. Gel content (degree of cross-linking)
5. Structural change (via FTIR-ATR, UV-vis, FA, XPS)

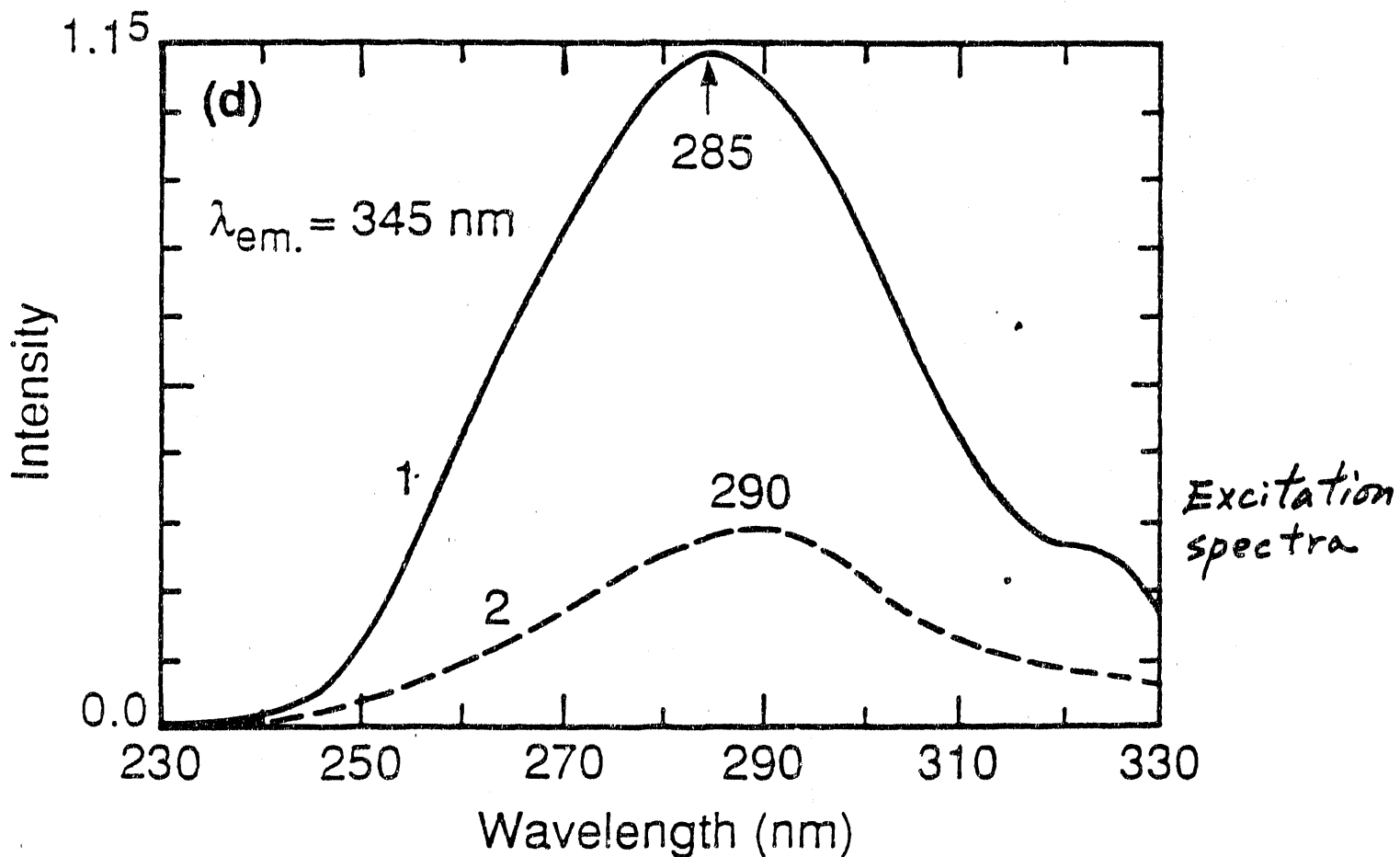
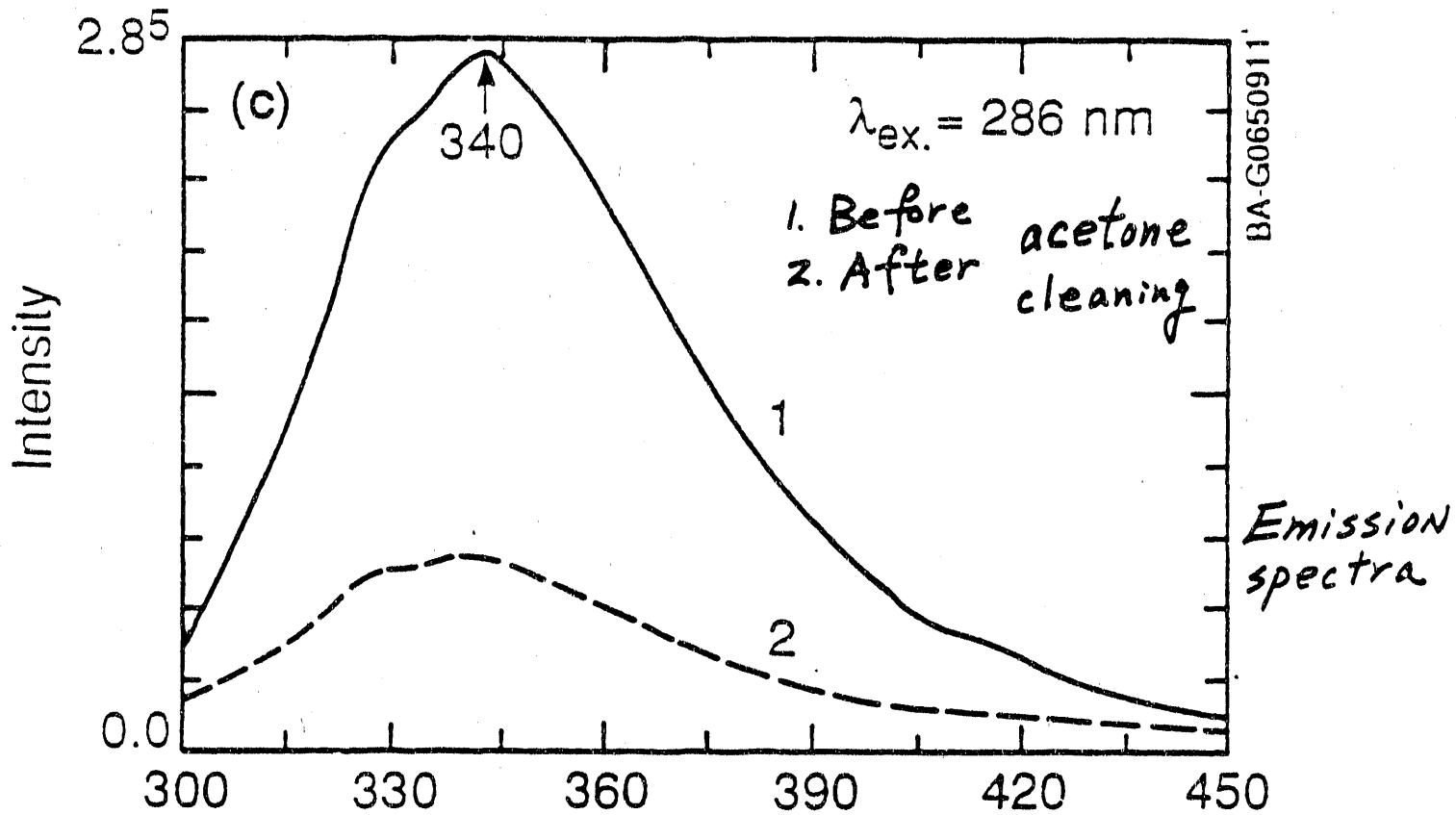
Analytical Procedure

TGA Profiles (5°C/min)



⇒ O₂ and H₂O reduce EVA's thermal stability.

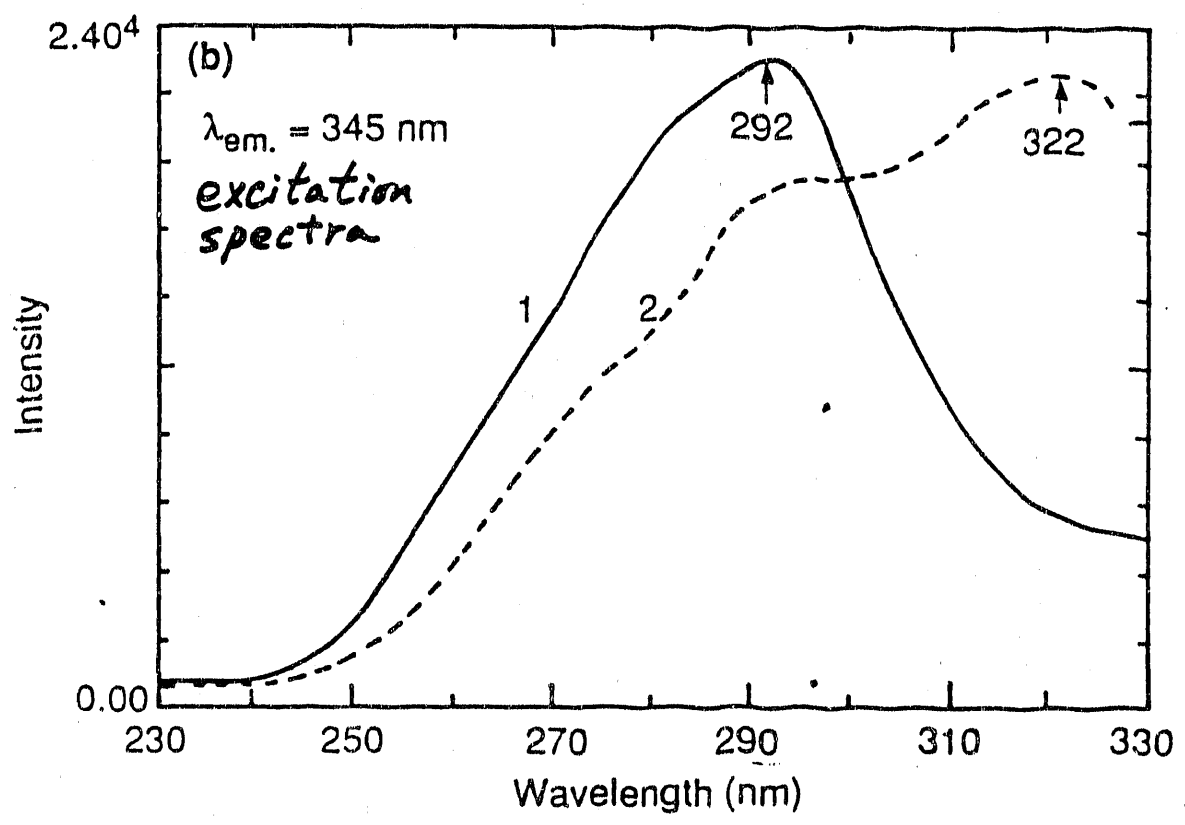
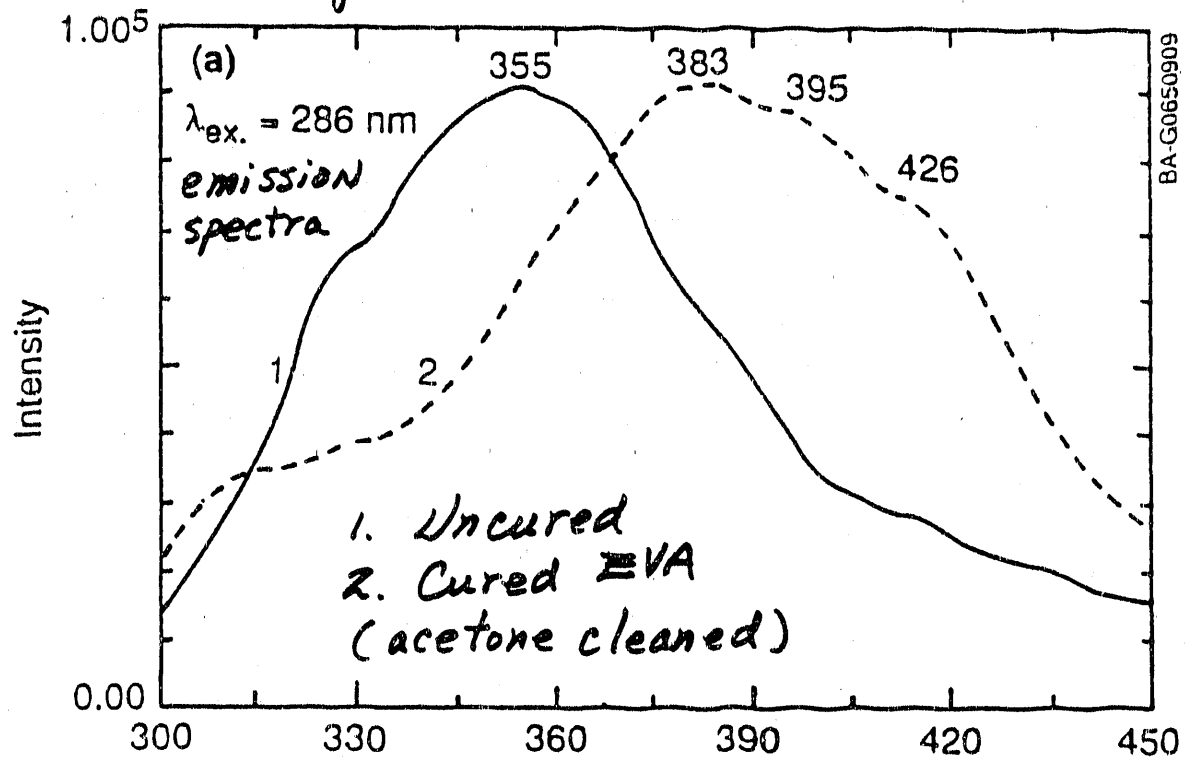
Raw EVA material (Elvax 150)



⇒ Presence of photosensitizer & benzophenone)

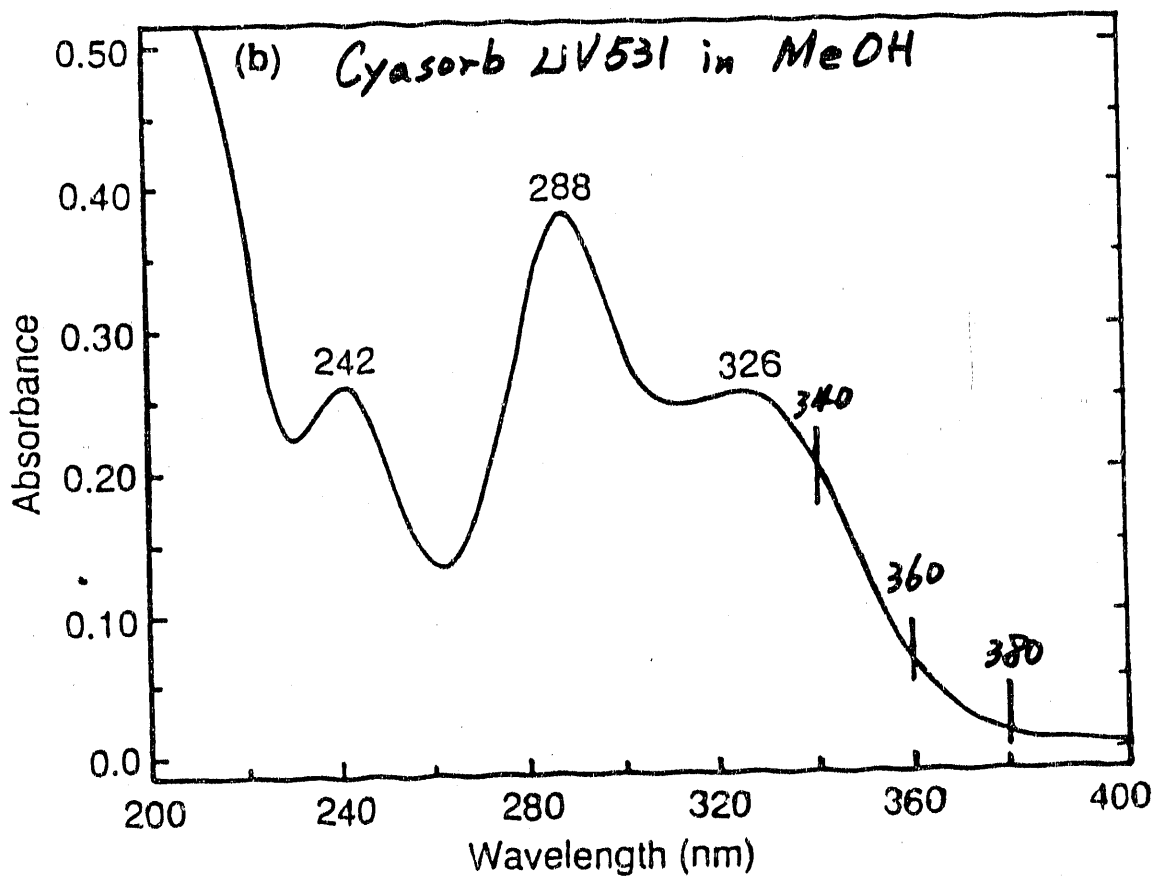
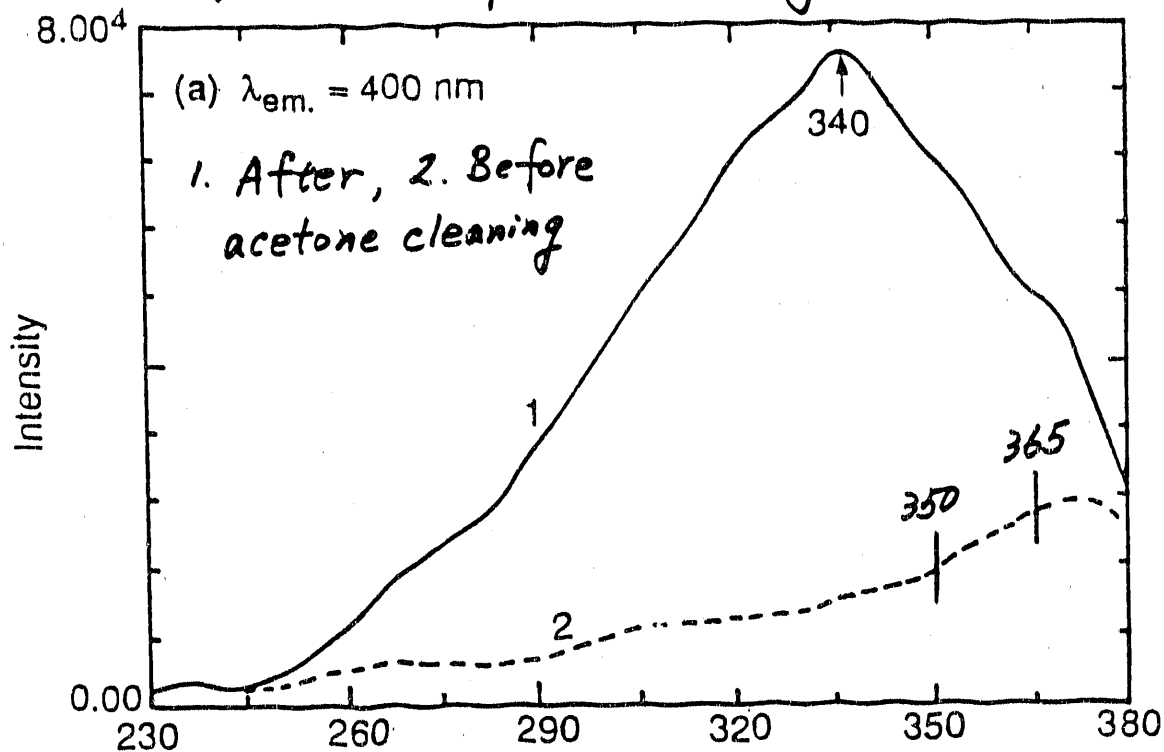
⇒ $-C=C-\overset{287}{\underset{||}{C}}-$ chromophores on EVA

Curing effect on the EVA structure



⇒ New chromophores developed upon curing at $\sim 150^\circ\text{C}$.

Excitation spectra of virgin cured EVA



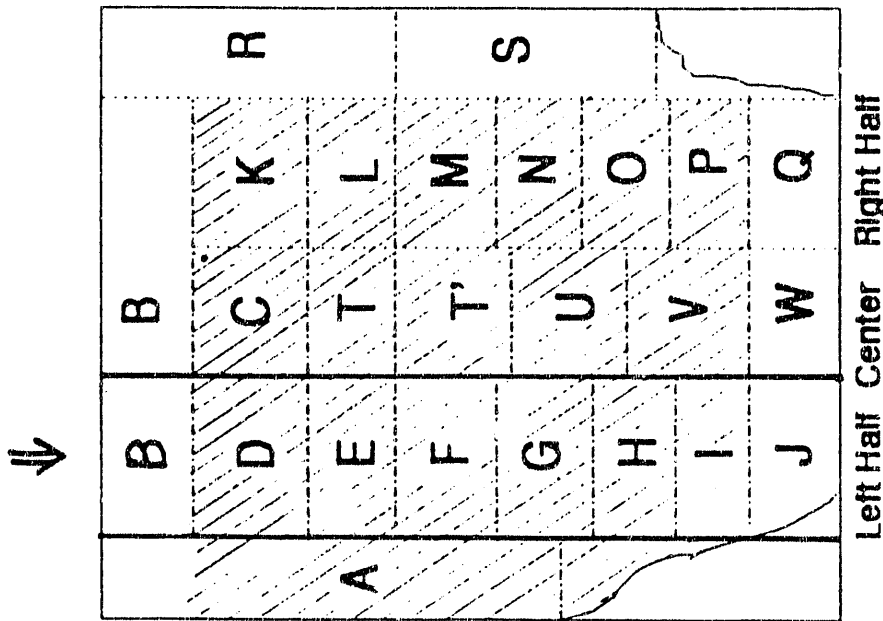
- ⇒ New chromophores on cured EVA absorb light $\geq 380 \text{ nm}$ (near-visible).
- ⇒ Insufficient shielding of the chromophores by Cyasorb in $\geq 370 \text{ nm}$ range.

On an EVA partially degraded PV module:

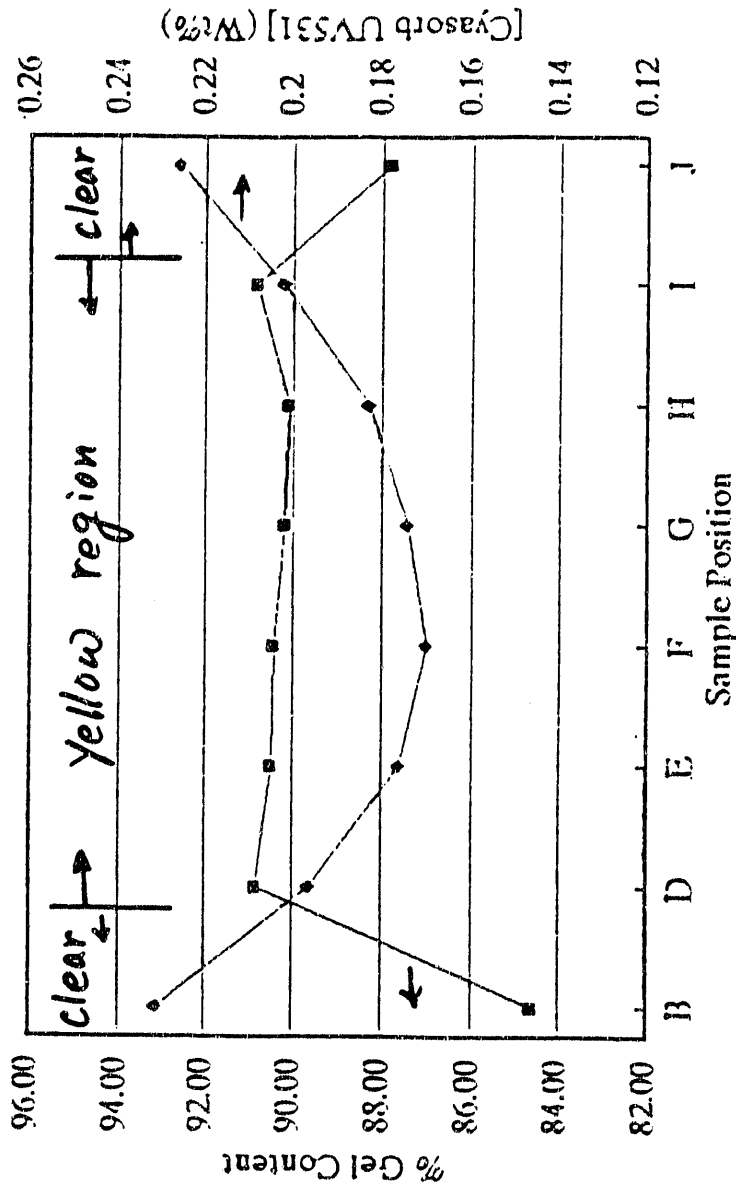
1. EVA Yellowing on the front side
2. Strong Acetic acid smell
3. Other volatile organic compounds
4. Relatively low power output

Effects of EVA Yellowing

1. Reduced optical transmission on EVA
2. Reduced power output of PV modules
3. Acidic corrosion of metallic circuits
4. Acidic corrosion of solar cells
5. Enhanced M^{n+} -catalyzed photodegradation
6. Reduced service life of PV modules



Gel Content and [Cyasorb UV531] Analysis



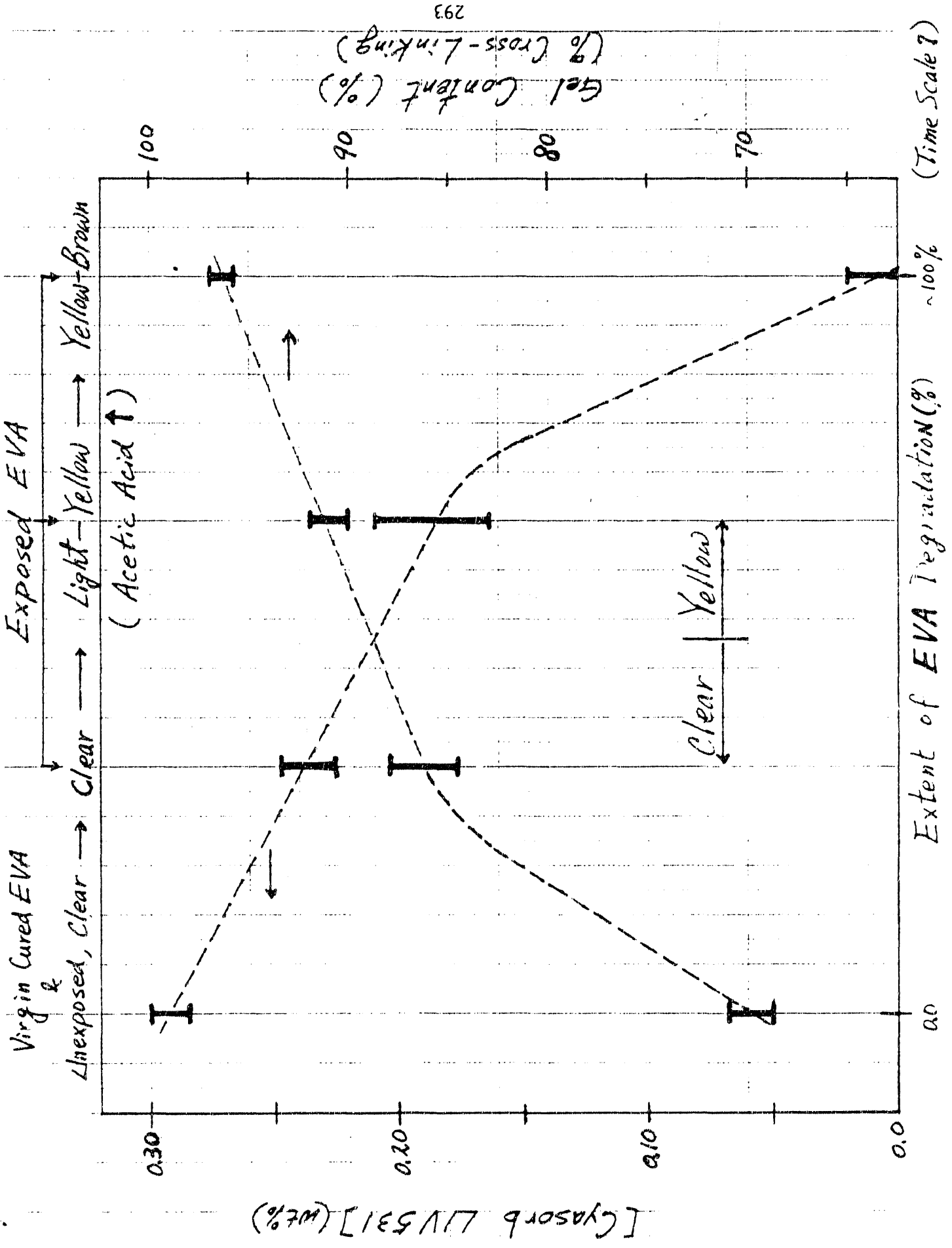
-■- % Gel Content -◆- [Cyasorb] (Wt%)
 (Wt%: calculated from absorbance at 326 nm)

A Partially Degraded EVA Film Mapping

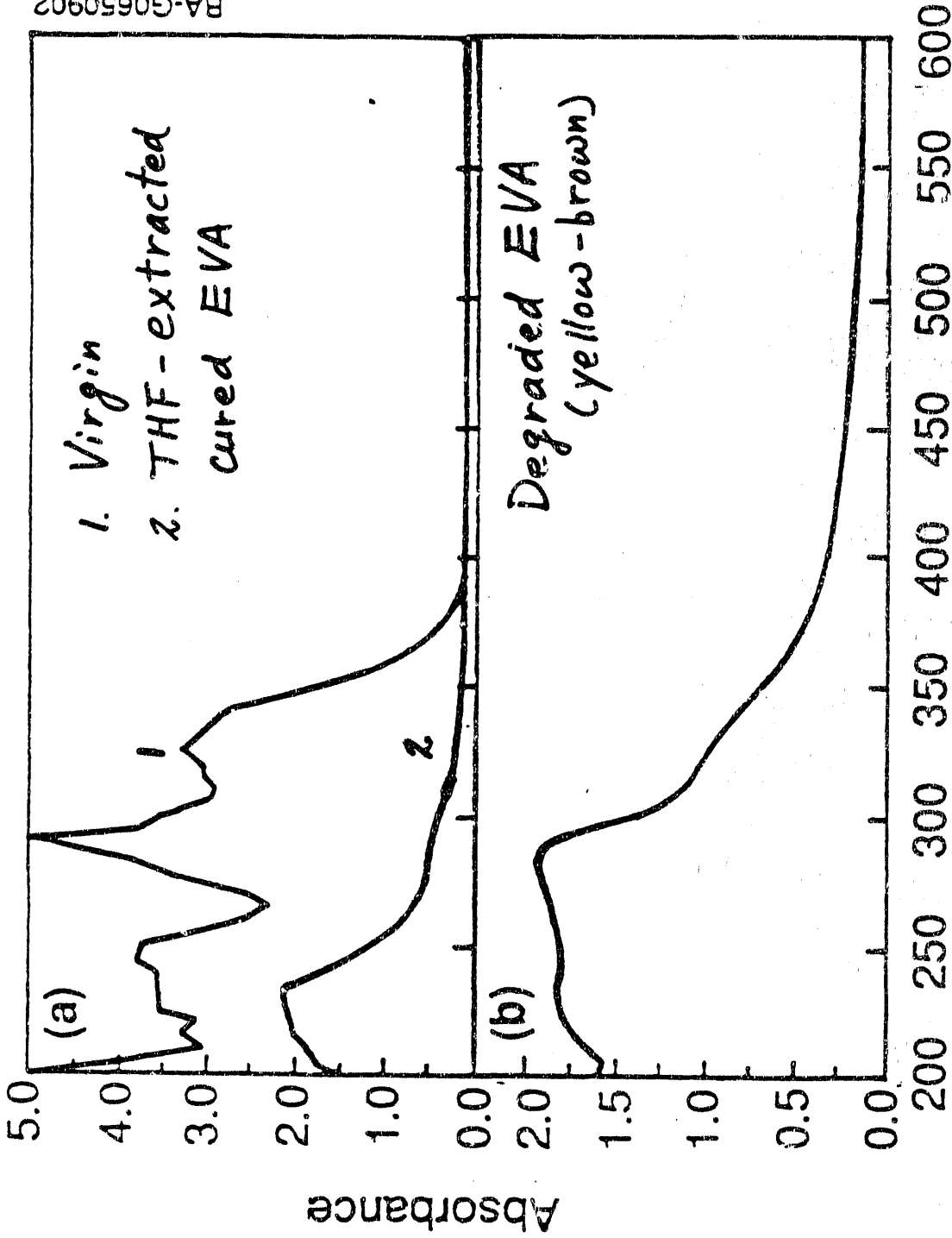
(4x4" EVA film)
(Acetic acid smell)
(Yellow layer on the front side)

by J. PERN

10/23/90



BA-G0650902



Wavelength (nm)

⇒ Polyconjugated $-(C=C)_n$, $n > 3$. (Polyenes)

⇒ Luminescence in 450 - 700 nm range

*Spectral Response Measurements
using a x'tal Si reference solar cell.*

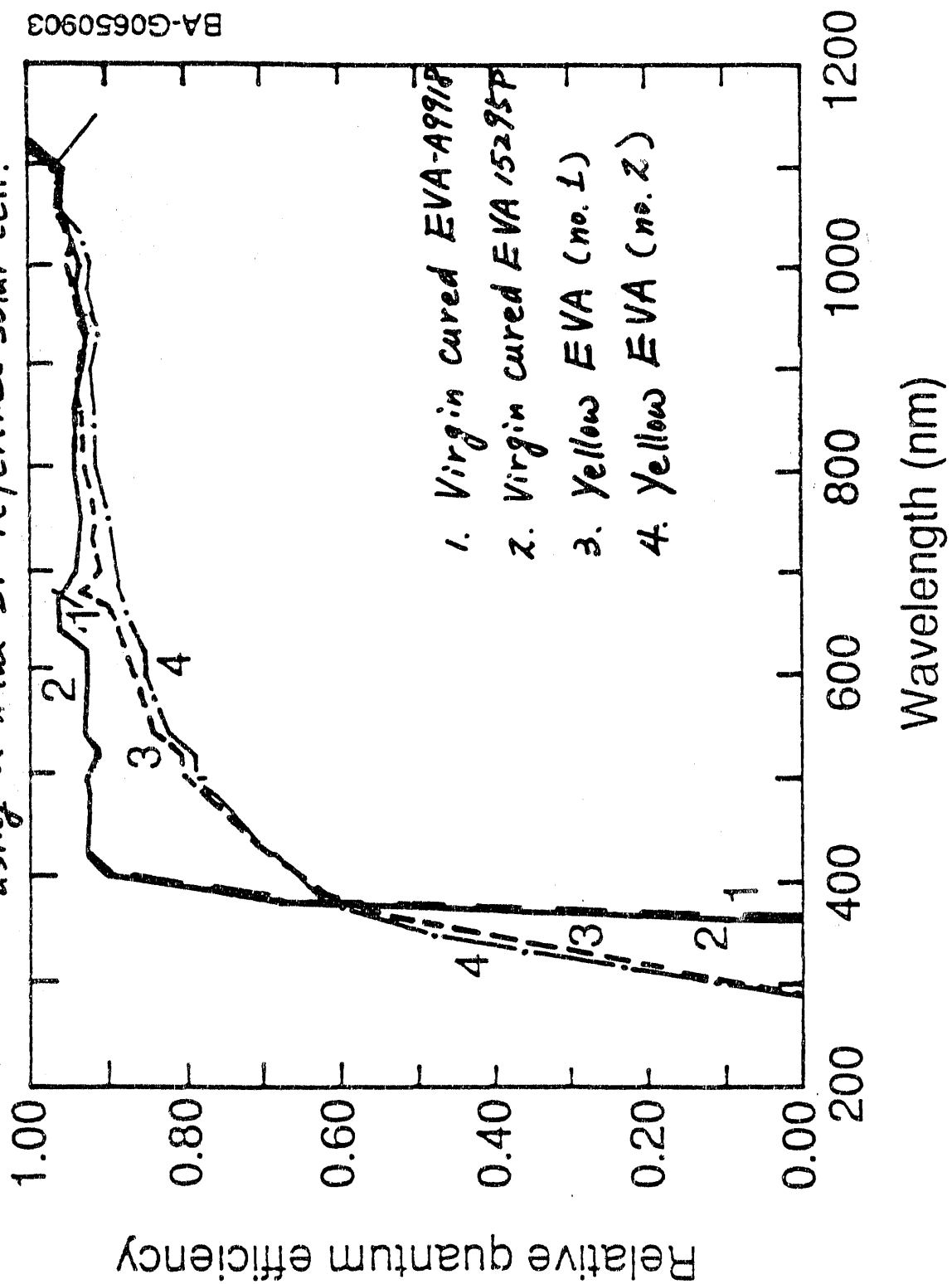


Table 1: ISC of NASA4 S1 Standard Solar Cell^a

EVA Type	ISC (mA)	Ratio	Loss%
No EVA over cell	13.733	1.000	----
Virgin EVA A9918	12.824	0.934	----
Virgin EVA 15295P	12.808	0.933	----
Degraded EVA no.1	12.087	0.880	5.68%
Degraded EVA no.2	11.861	0.864	7.39%

a: An aperture ~ 0.35 cm² was used. The EVA film was placed over the aperture. No cover glass was placed on top of the cell or EVA, hence allowing the UV component of the light to produce current. The loss would be larger if the UV light was cut off.

Summary of Results

- ==> O₂ and H₂O reduce EVA's thermal stability
- ==> Presence of photosensitizer in Elvax 150
- ==> Chromophores absorbing near-visible light developed upon curing of EVA
- ==> Insufficient shielding of Cyasorb over the chromophores
- ==> No physical loss of Cyasorb by natural diffusion
- ==> No weathering, no degradation
- ==> Large or total loss of Cyasorb from EVA in PV modules deployed outdoors for 5-6 years
- ==> Gel content (% cross-linking) increased as [Cyasorb] decreased (Cross-linking >> scission)
- ==> Acetic acid and volatile organics are produced
- ==> Yellowing of EVA occurred after Cyasorb was depleted
- ==> Yellowing is due to formation of polyconjugated (C=C)_n bonds, where n > 3, on the EVA polymeric chains
- ==> The polyconjugation is a mixture of various (C=C)_n length
- ==> The front side degraded more than the grid side
- ==> Strong luminescence of the degraded EVA compensates partially for the module's power loss due to EVA absorption
- ==> Electrical measurement of PV modules cannot truly indicate or reflect the extent of EVA degradation

Conclusions

- ==> Current EVA encapsulant formulation is NOT optimal
- ==> EVA degradation in weathered PV modules is significant
- ==> Degradation of EVA took place even when the film appears clear
- ==> Degradation of EVA includes
 1. Decomposition (produces CH_3COOH , CH_3CHO , $-\text{HC}=\text{CH}-$, etc.)
 2. Increase in %cross-linking of polymeric chains
 3. Loss of UV absorber [Cyasorb UV531]
 4. Yellowing after Cyasorb UV531 was depleted

Acknowledgement

SPEX Fluorolog II : Mike Himmel (Biotechnology Branch)
HP 8450A UV-visible : Art Frank, Mike Seibert (Photoconversion)
EVA transmission/Cells: Keith Emery
EVA FTIR-ATR analysis : John Webb
EVA UV-vis absorption : Cheryl Kennedy, Ramesh Dhere
EVA surface analysis : Art Nelson, Amy Franz
Module Hot Spot Analy.: Paul Longrigg
Module IV & Efficiency: Steve Rummel
Gridline EPMA analysis: Alice Mason
Thermogravimetry (TGA): Yvonne Shinton, Dick Burrows
Cell Impedance/Resist.: Larry Roybal